



**CONTRIBUTION OF CORTICOMUSCULAR  
SYNCHRONY TO HUMAN MOVEMENT AND ITS  
POTENTIAL USE IN NEUROPROSTHETIC  
CONTROL**

**VOLUME 1**

**VASILEIOS G. STAMATOPOULOS**

**JUNE 2005**



Declaration of author's rights:

“The copyright of this thesis belongs to the author under the terms of the United Kingdom Copyright Acts as qualified by University of Strathclyde Regulation 3.51. Due acknowledgement must always be made of the use of any material contained in, or derived from, this thesis”.

## ***ABSTRACT***

The growing interest in the development of robust methods of intention detection for use in the activation and regulation of prosthetic devices and communication aids for people with motor impairments has led to the examination on synchronous rhythmic activity of the nervous system as a source of signals for use in the activation and control of neuroprosthetic devices. It has been reported that EMG activity during movement shows high spectral power and high intermuscular coherence in the 8-12Hz range. During posture, the EMG is modulated in the 15-30Hz band and this activity is correlated to localised beta activation of the motor cortex measured by EEG.

This thesis further investigates these task dependencies using multichannel EEG and EMG recording. Robust detection and interpretation of movement dependent features will create the prospects for efficient neuroprosthetic devices driven by patients activating brain or muscle components associated with the motor behaviour replicated by the prosthesis.

Beta (15-30Hz) EEG power, intracortical coupling, corticomuscular coupling, and intermuscular coupling showed the most consistent task dependent features during posture. The cortical activity, underlying the beta corticomuscular coherence was localised in the area over the contralateral motor cortex. During movement the beta modulation was suppressed while agonist antagonist intermuscular coherence was replaced by 8-12Hz features likely to have a central origin. Changes in attention state and simultaneous cognitive activity did not affect the robustness of the corticomuscular and intermuscular features.

This thesis provided useful insights on the involvement of central oscillatory activity in motor control and its manifestations in the periphery. Despite the not clear functional significance of the identified features, and the subject variability it was concluded that the examined signals and associated task dependent characteristics have a significant potential for use in neuroprosthetic control.

# ACKNOWLEDGEMENTS

First of all I would like to thank my family, my parents George and Ekaterina and my brother Sotiris, for their help and support throughout the duration of my studies.

I would also like to thank my supervisor Dr. Bernie A. Conway for his support and encouragement during this project. His input and advice contributed enormously to the production of this thesis.

I would also like to thank Professor J.C. Barbenel, Professor J. Courtney and Professor A.C. Nicol for allowing me to work and study at the Department of Bioengineering as well as the departmental staff for facilitating my research.

I owe gratitude and thanks to all the willing subjects that went through the time consuming and often uncomfortable experiments.

Finally I would like to thank my friends Christos and Calliope for their help.

I would like to acknowledge the European Commission (through the Neuros Network) and the Wellcome Trust that funded this project.



*“Men ought to know that from the brain and from the brain only arise our pleasures, joys, laughter and jests, as well as our sorrows, pains, grieves and tears”*

Hippocrates (460-400 B.C.)



*στους γονείς μου Γιώργο και Αικατερίνη*

*to my parents George and Ekaterina*



*στον ξάδελφο μου Πάνο και στον φίλο μου Άντυ  
που θα αποφοιτούσαν αν ήταν μαζί μας  
ας είναι αυτή η δική τους διατριβή*

*to my cousin Panos and my friend Andy  
who would be also graduating if they were with us  
let this be their thesis*



# LIST OF ABBREVIATIONS-ACRONYMS

1DI	First Dorsal Interosseous Muscles
2DI	Second Dorsal Interosseous Muscles
AP	Action Potential
APB	Abductor Pollicis Brevis
BBLH	Biceps Brachii, Long Head
BCI	Brain Computer Interface
CL	Cognitively Loaded
CME	Continuous Movement Extension
CMF	continuous Movement Flexion
CNS	Central Nervous System
DFT	Discrete Fourier Transform
DP	Dedicated Performance
ECoG	Electrocorticogram
ECRL	Extensor Carpi Radialis Longus
EEG	Electroencephalogram
EMG	Electromyogram
EPSP	Excitatory Post Synaptic Potentials
EPT	Enhanced Physiological Tremor
ERD	Event Related Desynchronisation
ERP	Event Related Potentials
ERS	Event related Synchronisation
FCR	Flexor Carpi Radialis
FES	Functional Electrical Stimulation
FFT	Fast Fourier Transform
fMRI	functional Magnetic Resonance Imaging
HA	High Attention
IME	Intermittent Movement Extension
IMF	Intermittent Movement Flexion
INB	Ischemic Nerve Block



IPE	Intermittent Posture Extension
IPF	Intermittent Posture Flexion
IPSP	Inhibitory Post Synaptic Potential
ISI	Interspike Interval
LA	Low Attention
M1	Primary Motor Cortex
MEG	Magnetoencephalogram
MPE	Maintained Posture Extension
MPF	Maintained Posture Flexion
MRI	Magnetic Resonance Imaging
PET	Positron Emission Tomography
PM	Premotor Cortex
PMA	Premotor Cortex
PNS	Peripheral Nervous System
PSD	Power Spectral Density
pSMA	preSupplementary Motor Area
SMA	Supplementary Motor Area
TMS	Transcranial Magnetic Stimulation
TRCoh	Task Related Coherence

## LIST OF FIGURES

Fig.5.1	Segment of raw rectified EMG, EEG and wrist angle records from Subject 5. 7 from a total of 28 recorded EEG channels are displayed. ....	123A
Fig. 5.2	EMG bursting during movement.....	124A
Fig. 5.3	Frequency characteristics of ECRL, FCR and BBLH EMGs, during movement flexion. ....	125A
Fig. 5.4	Cumulant plots for ECRL\FCR EMGs during movement flexion.....	126A
Fig. 5.5	Cumulant plots for FCR\BBLH EMGs during movement flexion. ....	126A
Fig. 5.6	Example of delay estimation from the 7-13Hz FCR\BBLH phase curve, based on weighted least squares regression.....	127A
Fig. 5.7	Cumulant plots for ECRL\BBLH EMGs during movement flexion.....	127A
Fig. 5.8	Frequency characteristics of ECRL, FCR and BBLH EMGs, during posture flexion.....	130A
Fig. 5.9	Cumulant plot for ECRL\FCR EMGs during posture flexion. ....	131A
Fig. 5.10	Example of delay estimation from the 13-28Hz ECRL\FCR phase curve, based on weighted least squares regression.....	131A
Fig. 5.11	Cumulant plots for FCR\BBLH EMGs during posture flexion.....	132A
Fig. 5.12	Cumulant plots for ECRL\BBLH EMGs during posture flexion.....	132A
Fig. 5.13	Frequency characteristics of ECRL, FCR and BBLH EMGs, during movement extension. ....	133A
Fig. 5.14	Cumulant plot for ECRL\FCR EMGs during movement extension.. ...	134A
Fig. 5.15	Cumulant plot for FCR\BBLH EMGs during movement extension.....	134A
Fig. 5.16	Cumulant plot for ECRL\BBLH EMGs during posture flexion. ....	135A
Fig. 5.17	Frequency characteristics of ECRL, FCR and BBLH EMGs, during posture extension. ....	135A
Fig. 5.18	Cumulant plots for ECRL\FCR EMGs during posture extension.....	136A
Fig. 5.19	Cumulant plots for FCR\BBLH EMGs during posture extension.....	137A
Fig. 5.20	Cumulant plot for ECRL\BBLH EMGs during posture extension. ....	137A
Fig. 5.21	Monopolar (A) and bipolar (B) multichannel EEG montages showing the main motor anatomical motor areas.....	140A
Fig. 5.22	EEG monopolar power spectral difference map between movement flexion and posture flexion; pooled power spectral maps.....	143A



Fig. 5.23 EEG monopolar power spectral difference map between movement flexion and posture flexion; pooled power spectral maps.....	143A
Fig. 5.24 EEG monopolar power spectral difference map between posture flexion and movement extension, pooled power spectral maps.....	144A
Fig. 5.25 EEG bipolar power spectral difference map between posture flexion and movement extension, pooled power spectral maps. ....	144A
Fig. 5.26 EEG monopolar power spectral difference map between movement extension and posture extension, pooled power spectral maps. ....	145A
Fig. 5.27 EEG bipolar power spectral difference map between movement extension and posture extension, pooled power spectral maps.....	145A
Fig. 5.28 EEG monopolar power spectral difference map between posture extension and movement flexion, pooled power spectral maps.....	146A
Fig. 5.29 EEG bipolar power spectral difference map between posture extension and movement flexion, pooled power spectral maps. ....	146A
Fig. 5.30 EEG monopolar spectral power (A-D) and changes in power (E-H) within 8-12Hz band visualised as topographic maps of a scalp data field in a 2-D circular view using interpolation on a fine cartesian grid.....	148A
Fig. 5.31 EEG bipolar spectral power (A-D) and changes in power (E-H) within 8-12Hz band visualised as topographic maps of a scalp data field in a 2-D circular view using interpolation on a fine cartesian grid.....	149A
Fig. 5.32 EEG monopolar spectral power (A-D) and changes in power (E-H) within the 17-23Hz band visualised as topographic maps of a scalp data field in a 2-D circular view using interpolation on a fine cartesian grid.....	150A
Fig. 5.33 EEG bipolar spectral power (A-D) and changes in power (E-H) within 17-23Hz band visualised as topographic maps of a scalp data field in a 2-D circular view using interpolation on a fine cartesian grid.....	151A
Fig. 5.34 Pooled coherence map of all subject data, between right wrist ECRL EMG and multiple monopolar EEG channels during flexion movement.....	154A
Fig. 5.35 Pooled cumulant map of all subject data, between right wrist ECRL EMG and multiple monopolar EEG channels during flexion movement.....	154A
Fig. 5.36 Pooled coherence map of all subject data, between right wrist ECRL EMG and multiple bipolar EEG channels during flexion movement.....	155A



Fig. 5.37 Pooled cumulant map of all subject data, between right wrist ECRL EMG and multiple bipolar EEG channels during flexion movement.....	155A
Fig. 5.38 ECRL\FC2 coherence and corresponding cumulant plot during posture flexion. ....	156A
Fig. 5.39 ECRL\FC5-FC3 coherence and corresponding cumulant plot .....	156A
Fig. 5.40 ECRL\FZ-FCZ coherence and corresponding cumulant plot . ....	156A
Fig. 5.41 Pooled coherence map of all subject data, between right wrist FCR EMG Aand multiple monopolar EEG channels during flexion movement.....	158A
Fig. 5.42 Pooled cumulant map of all subject data, between right wrist FCR EMG and multiple monopolar EEG channels during flexion movement.....	158A
Fig. 5.43 Pooled coherence map of all subject data, between right wrist FCR EMG and multiple bipolar EEG channels during flexion movement.....	159A
Fig. 5.44 Pooled cumulant map of all subject data, between right wrist FCR EMG and multiple bipolar EEG channels during flexion movement.....	159A
Fig. 5.45 FCR\FC2 coherence and corresponding cumulant plot .....	161A
Fig. 5.46 FCR\C2-C4 coherence and corresponding cumulant plot .....	161A
Fig. 5.47 Pooled coherence map of all subject data, between right BBLH EMG and multiple monopolar EEG channels during flexion movement. ....	162A
Fig. 5.48 Pooled cumulant map of all subject data, between right BBLH EMG and multiple monopolar EEG channels during flexion movement. ....	162A
Fig. 5.49 Pooled coherence map of all subject data, between right BBLH EMG and multiple bipolar EEG channels during flexion movement. ....	163A
Fig. 5.50 Pooled cumulant map of all subject data, between right BBLH EMG and multiple bipolar EEG channels during flexion movement. ....	163A
Fig. 5.51 BBLH\FZ coherence and corresponding cumulant plot .....	165A
Fig. 5.52 Pooled coherence map of all subject data, between right wrist ECRL EMG and multiple monopolar EEG channels during flexion posture.....	166A
Fig. 5.53 Pooled cumulant map of all subject data, between right wrist ECRL EMG and multiple monopolar EEG channels during flexion posture.....	166A
Fig. 5.54 Pooled coherence map of all subject data, between right wrist ECRL EMG and multiple bipolar EEG channels during flexion posture.....	167A

Fig. 5.55 Pooled cumulant map of all subject data, between right wrist ECRL EMG and multiple bipolar EEG channels during flexion posture.....	167A
Fig. 5.56 ECRL\FZ coherence and corresponding cumulant plot .....	168A
Fig. 5.57 ECRL\FZ coherence and corresponding cumulant plot .....	168A
Fig. 5.58 ECRL\CP3 coherence and corresponding cumulant plot .....	168A
Fig. 5.59 ECRL\FC1-C1 coherence and corresponding cumulant plot .....	169A
Fig. 5.60 ECRL\FC1-C1 coherence and corresponding cumulant plot .....	169A
Fig. 5.61 Pooled coherence map of all subject data, between right wrist FCR EMG and multiple monopolar EEG channels during flexion posture.....	170A
Fig. 5.62 Pooled cumulant map of all subject data, between right wrist FCR EMG and multiple monopolar EEG channels during flexion posture.....	170A
Fig. 5.63 Pooled coherence map of all subject data, between right wrist FCR EMG and multiple bipolar EEG channels during flexion posture.....	171A
Fig. 5.64 Pooled cumulant map of all subject data, between right wrist FCR EMG and multiple bipolar EEG channels during flexion posture.....	171A
Fig. 5.65 FCR\FZ coherence and corresponding cumulant plot .....	172A
Fig. 5.66 FCR\CP3 coherence and corresponding cumulant plot .....	172A
Fig. 5.67 FCR\FC1-C1 coherence and corresponding cumulant plot . .....	172A
Fig. 5.68 Pooled coherence map of all subject data, between right wrist BBLH EMG and multiple monopolar EEG channels during flexion posture.....	173A
Fig. 5.69 Pooled cumulant map of all subject data, between right BBLH EMG and multiple monopolar EEG channels during flexion posture. ....	173A
Fig. 5.70 Pooled coherence map of all subject data, between right BBLH EMG and multiple bipolar EEG channels during flexion posture. ....	174A
Fig. 5.71 Pooled cumulant map of all subject data, between right BBLH EMG and multiple bipolar EEG channels during flexion posture. ....	174A
Fig. 5.72 BBLH\FZ coherence and corresponding cumulant plot .....	175A
Fig. 5.73 BBLH\CP3 coherence and corresponding cumulant plot . .....	175A
Fig. 5.74 BBLH\FC1-C1 coherence and corresponding cumulant plot . .....	175A
Fig. 5.75 Pooled coherence map of all subject data, between right wrist ECRL EMG and multiple monopolar EEG channels during extension movement.....	177A



Fig. 5.76 Pooled cumulant map of all subject data, between right wrist ECRL EMG and multiple monopolar EEG channels during extension movement.....	177A
Fig. 5.77 Pooled coherence map of all subject data, between right wrist ECRL EMG and multiple bipolar EEG channels during extension movement.....	178A
Fig. 5.78 Pooled cumulant map of all subject data, between right wrist ECRL EMG and multiple bipolar EEG channels during extension movement.....	178A
Fig. 5.79 ECRL\Cz coherence and corresponding cumulant plot during movement extension.....	179A
Fig. 5.80 ECRL\CP1 coherence and corresponding cumulant plot during movement extension.....	179A
Fig. 5.81 Pooled coherence map of all subject data, between right wrist FCR EMG and multiple monopolar EEG channels during extension movement.....	180A
Fig. 5.82 Pooled cumulant map of all subject data, between right wrist FCR EMG and multiple monopolar EEG channels during extension movement.....	180A
Fig. 5.83 Pooled coherence map of all subject data, between right wrist FCR EMG and multiple bipolar EEG channels during extension movement.....	181A
Fig. 5.84 Pooled cumulant map of all subject data, between right wrist FCR EMG and multiple bipolar EEG channels during extension movement.....	181A
Fig. 5.85 FCR\CP2 coherence and corresponding cumulant plot during movement extension. The blue plot represents the 14-17Hz cumulant component while the blue dashed lines represent the estimated upper and lower 95% confidence limits for the cumulant component. ....	183A
Fig. 5.86 FCR\Cz-CPz coherence and corresponding cumulant plot during movement extension. ....	183A
Fig. 5.87 Pooled coherence map of all subject data, between right BBLH EMG and multiple monopolar EEG channels during extension movement. ....	184A
Fig. 5.88 Pooled cumulant map of all subject data, between right BBLH EMG and multiple monopolar EEG channels during extension movement. ....	184A
Fig. 5.89 Pooled coherence map of all subject data, between right BBLH EMG and multiple bipolar EEG channels during extension movement. ....	185A
Fig. 5.90 Pooled cumulant map of all subject data, between right BBLH EMG and multiple bipolar EEG channels during extension movement. ....	185A

Fig. 5.91 Pooled coherence map of all subject data, between right wrist ECRL EMG and multiple monopolar EEG channels during extension posture.....	187A
Fig. 5.92 Pooled cumulant map of all subject data, between right wrist ECRL EMG and multiple monopolar EEG channels during extension posture.....	187A
Fig. 5.93 Pooled coherence map of all subject data, between right wrist ECRL EMG and multiple bipolar EEG channels during extension posture.....	188A
Fig. 5.94 Pooled cumulant map of all subject data, between right wrist ECRL EMG and multiple bipolar EEG channels during extension posture.....	188A
Fig. 5.95 ECRL\Fz coherence and corresponding cumulant plot during posture extension.....	189A
Fig. 5.96 ECRL\Fz coherence and corresponding cumulant plot during posture extension.....	189A
Fig. 5.97 ECRL\CP3 coherence and corresponding cumulant plot during posture extension.....	189A
Fig. 5.98 FCR\FC1-C1 coherence and corresponding cumulant plot during posture flexion.....	190A
Fig. 5.99 ECRL\FC1-C1 coherence and corresponding cumulant plot during posture extension.....	190A
Fig. 5.100 Pooled coherence map of all subject data, between right wrist FCR EMG and multiple monopolar EEG channels during extension posture.....	191A
Fig. 5.101 Pooled cumulant map of all subject data, between right wrist FCR EMG and multiple monopolar EEG channels during extension posture.....	191A
Fig. 5.102 Pooled coherence map of all subject data, between right wrist FCR EMG and multiple bipolar EEG channels during extension posture.....	192A
Fig. 5.103 Pooled cumulant map of all subject data, between right wrist FCR EMG and multiple bipolar EEG channels during extension posture.....	192A
Fig. 5.104 FCR\Fz coherence and corresponding cumulant plot during posture extension.....	193A
Fig. 5.105 FCR\Fz coherence and corresponding cumulant plot during posture extension.....	193A
Fig. 5.106 FCR\CP3 coherence and corresponding cumulant plot during posture extension.....	193A



Fig. 5.107 FCR\FC1-C1 coherence and corresponding cumulant plot during posture extension.....	194A
Fig. 5.108 FCR\FC1-C1 coherence and corresponding cumulant plot during posture extension.....	194A
Fig. 5.109 Pooled coherence map of all subject data, between right BBLH EMG and multiple monopolar EEG channels during extension posture. ....	195A
Fig. 5.110 Pooled cumulant map of all subject data, between right BBLH EMG and multiple monopolar EEG channels during extension posture. The green horizontal line represents the 95% confidence interval.....	195A
Fig. 5.111 Pooled coherence map of all subject data, between right BBLH EMG and multiple bipolar EEG channels during extension posture. ....	196A
Fig. 5.112 Pooled cumulant map of all subject data, between right BBLH EMG and multiple bipolar EEG channels during extension posture. ....	196A
Fig. 5.113 BBLH\Fz coherence and corresponding cumulant plot during posture extension.....	197A
Fig. 5.114 BBLH\CP3 coherence and corresponding cumulant plot during posture extension.....	197A
Fig. 5.115 BBLH\FC1-C1 coherence and corresponding cumulant plot during posture extension. ....	197A
Fig. 5.116 EEG monopolar corticomuscular coherence topographic maps within 17-23Hz band for during movement flexion, posture flexion, movement extension, posture extension. ....	199A
Fig. 5.117 EEG bipolar corticomuscular coherence topographic maps within 17-23Hz band for during movement flexion, posture flexion, movement extension, posture extension. ....	201A
Fig. 5.118 Topographic maps of 17-23Hz cumulant components topographic maps for ECRL, FCR, BBLH EMGs with monopolar electrodes and vertical bipolar electrodes during posture flexion.....	202A
Fig. 5.119 Topographic maps of 17-23Hz cumulant components topographic maps for ECRL, FCR, BBLH EMGs with monopolar electrodes and vertical bipolar electrodes during posture extension.....	203A



Fig. 5.120 Monopolar and bipolar cumulant topographic maps for ECRL, FCR and BBLH EMGs during posture flexion and posture extension at -7ms of the cumulant estimate..	205A
Fig. 5.121 Pooled EMG spectrograms for ECRL, FCR, BBLH are displayed together with averaged wrist angle and audio cue triggers.....	208A
Fig. 5.122 Pooled EMG spectrogram of BBLH muscle, displayed together with averaged wrist angle and audio cue triggers.....	209A
Fig. 5.123 Grid consisting of the pooled monopolar EEG spectrograms during the move-hold sequence. ....	211A
Fig. 5.124 Grid consisting of the pooled bipolar EEG spectrograms during the move-hold sequence.....	212A
Fig. 5.125 Grid consisting of the pooled intracortical EEG time dependent coherences between monopolar electrodes on the vertical axis, during the move-hold sequence.....	213A
Fig. 5.126 Grid consisting of the pooled intracortical EEG time dependent coherences between monopolar electrodes on the horizontal axis, during the move-hold sequence. ....	214A
Fig. 5.127 Pooled EEG spectrograms for monopolar FC1, monopolar C1 and bipolar FC1-C1 channels are displayed together with averaged wrist angle and audio cue triggers.....	216A
Fig. 5.128 Pooled intermuscular time dependent coherence and cumulant estimates displayed together with averaged wrist angle and audio cue triggers. ....	217A
Fig. 5.129 Grid consisting of the pooled time dependent coherences between ECRL EMG and monopolar EEG spectrograms during the move-hold sequence...	219A
Fig. 5.130 Grid consisting of the pooled time dependent coherences between ECRL EMG and bipolar EEG spectrograms during the move-hold sequence.....	220A
Fig. 5.131 Pooled ECRL\Fz, ECRL\CP3, ECRL\FC1-C1 corticomuscular time dependent coherence and cumulant estimates displayed together with averaged wrist angle and audio cue triggers. ....	221A
Fig. 5.132 Grid consisting of the pooled time dependent coherences between FCR EMG and monopolar EEG spectrograms during the move-hold sequence..	222A

Fig. 5.133 Grid consisting of the pooled time dependent coherences between FCR EMG and monopolar EEG spectrograms during the move-hold sequence. .	223A
Fig. 5.134 Pooled FCR\Fz, FCR\CP3, FCR\FC1-C1 corticomuscular time dependent coherence and cumulant estimates displayed together with averaged wrist angle and audio cue triggers. ....	224A
Fig. 5.135 Grid consisting of the pooled time dependent coherences between BBLH EMG and monopolar EEG spectrograms during the move-hold sequence. .	225A
Fig. 5.136 Grid consisting of the pooled time dependent coherences between BBLH EMG and bipolar EEG spectrograms during the move-hold sequence. ....	226A
Fig. 5.137 Pooled BBLH\Fez, BBLH\CP3, BBLH\FC1-C1 corticomuscular time dependent coherence and cumulant estimates displayed together with averaged wrist angle and audio cue triggers. ....	227A
Fig. 5.138 EMG frequency characteristics during Intermittent Movement Flexion (IMF), Continuous Movement Flexion (CMF).....	232A
Fig. 5.139 Pooled coherence map of all subject data, between right wrist ECRL EMG and multiple bipolar EEG channels during flexion movement (Intermittent Movement Flexion (IMF), Continuous Movement Flexion (CMF)).....	232A
Fig. 5.140 Pooled coherence map of all subject data, between right wrist FCR EMG and multiple bipolar EEG channels during flexion movement (Intermittent Movement Flexion (IMF), Continuous Movement Flexion (CMF)).....	232A
Fig. 5.141 Pooled coherence map of all subject data, between right BBLH EMG and multiple bipolar EEG channels during flexion movement (Intermittent Movement Flexion (IMF), Continuous Movement Flexion (CMF)).....	232A
Fig. 5.142 EMG frequency characteristics during Intermittent Posture Flexion (IPF), Maintained Posture Flexion (MPF). ....	233A
Fig. 5.143 Pooled coherence map of all subject data, between right wrist ECRL EMG and multiple bipolar EEG channels during flexion posture (Intermittent Posture Flexion (IPF), Maintained Posture Flexion (MPF)). ....	233A
Fig. 5.144 Pooled coherence map of all subject data, between right wrist FCR EMG and multiple bipolar EEG channels during flexion posture (Intermittent Posture Flexion (IPF), Maintained Posture Flexion (MPF)). ....	233A



Fig. 5.145 Pooled coherence map of all subject data, between right BBLH EMG and multiple bipolar EEG channels during flexion posture (Intermittent Posture Flexion (IPF), Maintained Posture Flexion (MPF)). .....233A

Fig. 5.146 EMG frequency characteristics during Intermittent Movement Extension (IME), Continuous Movement Extension (CME). .....234A

Fig. 5.147 Pooled coherence map of all subject data, between right wrist ECRL EMG and multiple bipolar EEG channels during extension movement (Intermittent Movement Extension (IME), Continuous Movement Extension (CME)).....234A

Fig. 5.148 Pooled coherence map of all subject data, between right wrist FCR EMG and multiple bipolar EEG channels during extension movement (Intermittent Movement Extension (IME), Continuous Movement Extension (CME)).....234A

Fig. 5.149 Pooled coherence map of all subject data, between right BBLH EMG and multiple bipolar EEG channels during extension movement (Intermittent Movement Extension (IME), Continuous Movement Extension (CME)).....234A

Fig. 5.150 EMG Frequency characteristics during Intermittent Posture Extension (IPE), Maintained Posture Extension (MPE).....235A

Fig. 5.151 Pooled coherence map of all subject data, between right wrist ECRL EMG and multiple bipolar EEG channels during extension posture (Intermittent Posture Extension (IPE), Maintained Posture Extension (MPE)). .....235A

Fig. 5.152 Pooled coherence map of all subject data, between right wrist FCR EMG and multiple bipolar EEG channels during extension posture (Intermittent Posture Extension (IPE), Maintained Posture Extension (MPE)). .....235A

Fig. 5.153 Pooled coherence map of all subject data, between right BBLH EMG and multiple bipolar EEG channels during extension posture (Intermittent Posture Extension (IPE), Maintained Posture Extension (MPE)). .....235A

Fig. 5.154 Pooled power spectra of right ECRL (a) and APB (b), intermuscular coherence (c) and intermuscular cumulant during low motor attention and high attention. ....240A

Fig. 5.155 Pooled corticomuscular coherence map for the right ECRL with bipolar EEG recordings during the precision task during low and high motor attention. ....241A



Fig. 5.156 Pooled corticomuscular coherence map for the right APB with bipolar EEG recordings during the precision task during low and high motor attention. .....	241A
Fig. 5.157 Pooled power (a, b), intermuscular coherences (c, d) and cumulant plots (e, f) of homologues ECRL and APB muscles during dedicated performance of the elastic band precision extension task and the same task during simultaneous performance of mental arithmetic task .	243A
Fig. 5.158 Pooled corticomuscular map of right ECRL coherences with bipolar EEG recordings during the dedicated and cognitively loaded performance of the band extension task.....	244A
Fig. 5.159 Pooled corticomuscular map of right APB coherences with bipolar EEG recordings during the dedicated and cognitively loaded performance of the band extension task.....	244A
Fig. 5.160 Pooled corticomuscular map of left ECRL coherences with bipolar EEG recordings during the dedicated and cognitively loaded performance of the band extension task.....	245A
Fig. 5.161 Pooled corticomuscular map of left APB coherences with bipolar EEG recordings during the dedicated and cognitively loaded performance of the band extension task.....	245A
Fig. 5.162 INB results for subject 1 during posture extension. ....	248A
Fig. 5.163 INB results for subject 1 during movement. ....	248A
Fig. 5.164 INB results for subject 2 during posture extension. ....	250A
Fig. 5.165 INB results for subject 2 during movement. ....	250A
Fig. 5.166 INB results for subject 3 during posture extension. ....	251A
Fig. 5.167 INB results for subject 3 during movement. ....	251A

# TABLE OF CONTENTS

<b>1</b>	<b>INTRODUCTION .....</b>	<b>1</b>
1.1	Physiology of Movement.....	1
1.2	Corticomuscular Rhythmicities.....	2
1.3	Movement Intention Detection.....	3
1.4	Aims and Objectives.....	4
1.5	Further Implications .....	6
1.6	Thesis Outline .....	6
<b>2</b>	<b>LITERATURE REVIEW .....</b>	<b>8</b>
2.1	Movement Related Components Of The Nervous System.....	8
2.2	The Brain and its relation to movement.....	8
2.2.1	Movement Related Components of the Brain.....	9
2.2.2	The cerebral hemispheres .....	9
2.2.2.1	The cerebral cortex and its involvement in motor control.....	9
2.2.2.1.1	Primary motor cortex .....	9
2.2.2.1.2	Premotor cortex.....	11
2.2.2.1.3	Supplementary motor area .....	12
2.2.2.1.4	Parietal lobe.....	13
2.2.2.2	Subcortical areas involved in movement control .....	13
2.2.2.2.1	Basal ganglia and voluntary movement .....	13
2.2.2.2.2	The Diencephalon & Thalamus .....	14
2.2.2.2.3	The Brainstem .....	15
2.2.3	Corticospinal tract.....	15
2.2.3.1	Cerebellum.....	17
2.3	Spinal cord .....	18
2.3.1	Spinal Reflexes .....	19
2.3.1.1	The stretch reflex .....	19



<b>2.4</b>	<b>Peripheral Nervous System and Movement Control .....</b>	<b>20</b>
2.4.1	Motor Neurons and Motor Units .....	20
2.4.2	Muscle Afferents.....	20
2.4.3	Plexuses of the ventral rami – Brachial Plexus.....	21
2.4.4	Muscular System.....	21
<b>2.5</b>	<b>Movement-Related Changes in Rhythmic Brain Activity.....</b>	<b>22</b>
2.5.1	Rhythmic nature of brain activity .....	22
2.5.2	Cortical imaging .....	22
2.5.2.1	Electroencephalographic activity .....	22
2.5.2.1.1	Origin of electrical brain activity .....	23
2.5.2.2	Magnetoencephalographic Activity.....	24
2.5.2.3	Electrocorticogram (ECoG).....	25
2.5.2.4	Positron Emission Tomography .....	25
2.5.2.5	FMRI .....	26
2.5.3	Organisation of the Nervous System at Cell Level.....	26
2.5.4	Cortical Rhythms - Frequency Bands.....	27
2.5.4.1	Idling Alpha activity.....	28
2.5.4.2	Non Idling Alpha Activity .....	30
2.5.4.3	Beta and Gamma band synchronisation/desynchronisation .....	31
2.5.4.4	Intracortical Synchronisation – Desynchronisation.....	34
<b>2.6</b>	<b>Neurogenic activity during motor tasks .....</b>	<b>36</b>
2.6.1	Tremor .....	36
2.6.2	Posture tremor.....	36
2.6.3	Movement tremor .....	38
2.6.4	Task Specificity .....	41
2.6.5	Motor Unit synchronisation.....	42
2.6.6	Corticomuscular Synchronisation.....	45
2.6.6.1	Spatial Localisation .....	47
2.6.6.2	Functional Specificity.....	48
2.6.6.3	Temporal characteristics of corticomuscular coherence .....	48
<b>2.7</b>	<b>Neural plasticity.....</b>	<b>512</b>
2.7.1	Cortical reorganisation and recovery .....	51
2.7.2	Cortical reorganisation following CNS injury.....	52
2.7.3	CNS plasticity.....	52
2.7.4	Cortical reorganisation following PNS disorder.....	55
2.7.5	Amputees .....	56
2.7.6	Activity Dependent Plasticity .....	57
2.7.7	Plasticity and learning.....	58
2.7.8	Plasticity and rehabilitation .....	59
<b>2.8</b>	<b>Attention .....</b>	<b>60</b>
2.8.1	Attention as a cognitive process .....	60
2.8.2	The single channel and flexible central resource capacity .....	60



2.8.3	Physiology of attention.....	61
2.8.3.1	Parietal and temporal lobe influences on attention.....	61
2.8.3.2	Frontal lobe.....	63
2.8.3.3	Cingulated cortex.....	64
2.8.3.4	Thalamic influences.....	64
2.8.3.5	Basal ganglia.....	65
2.8.3.6	Other subcortical structures.....	66
2.8.3.7	Cerebellum.....	66
2.8.4	Attention influenced motor control?.....	67
<b>2.9</b>	<b>Neuroprosthetic control.....</b>	<b>689</b>
2.9.1	EMG Based Control.....	69
2.9.1.1	Myoelectric Prostheses.....	69
2.9.1.2	Functional Electrical Stimulation (FES).....	70
2.9.2	EEG based control.....	71
2.9.2.1	Short review of EEG based control.....	72
2.9.2.2	The future of BCI.....	74
<b>2.10</b>	<b>Summary.....</b>	<b>76</b>
<b>3</b>	<b>METHODOLOGY.....</b>	<b>78</b>
<b>3.1</b>	<b>Introduction.....</b>	<b>78</b>
3.1.1	Groups of experiments.....	78
<b>3.2</b>	<b>GENERAL EXPERIMENTAL TECHNIQUES.....</b>	<b>79</b>
<b>3.3</b>	<b>EEG recording set up.....</b>	<b>79</b>
<b>3.4</b>	<b>Subject recruitment criteria.....</b>	<b>80</b>
<b>3.5</b>	<b>Subject preparation.....</b>	<b>80</b>
<b>3.6</b>	<b>EMG recording set-up.....</b>	<b>82</b>
<b>3.7</b>	<b>Other apparatus and recording techniques.....</b>	<b>83</b>
3.7.1	CED 1401.....	83
3.7.2	Gyroscope.....	83
3.7.3	Instrumented ring.....	84
3.7.4	Pneumatic Tourniquet.....	84
3.7.5	Bimanual motor task.....	85

Fig. 5.145 Pooled coherence map of all subject data, between right BBLH EMG and multiple bipolar EEG channels during flexion posture (Intermittent Posture Flexion (IPF), Maintained Posture Flexion (MPF)). .....233A

Fig. 5.146 EMG frequency characteristics during Intermittent Movement Extension (IME), Continuous Movement Extension (CME). .....234A

Fig. 5.147 Pooled coherence map of all subject data, between right wrist ECRL EMG and multiple bipolar EEG channels during extension movement (Intermittent Movement Extension (IME), Continuous Movement Extension (CME)).....234A

Fig. 5.148 Pooled coherence map of all subject data, between right wrist FCR EMG and multiple bipolar EEG channels during extension movement (Intermittent Movement Extension (IME), Continuous Movement Extension (CME)).....234A

Fig. 5.149 Pooled coherence map of all subject data, between right BBLH EMG and multiple bipolar EEG channels during extension movement (Intermittent Movement Extension (IME), Continuous Movement Extension (CME)).....234A

Fig. 5.150 EMG Frequency characteristics during Intermittent Posture Extension (IPE), Maintained Posture Extension (MPE).....235A

Fig. 5.151 Pooled coherence map of all subject data, between right wrist ECRL EMG and multiple bipolar EEG channels during extension posture (Intermittent Posture Extension (IPE), Maintained Posture Extension (MPE)). .....235A

Fig. 5.152 Pooled coherence map of all subject data, between right wrist FCR EMG and multiple bipolar EEG channels during extension posture (Intermittent Posture Extension (IPE), Maintained Posture Extension (MPE)). .....235A

Fig. 5.153 Pooled coherence map of all subject data, between right BBLH EMG and multiple bipolar EEG channels during extension posture (Intermittent Posture Extension (IPE), Maintained Posture Extension (MPE)). .....235A

Fig. 5.154 Pooled power spectra of right ECRL (a) and APB (b), intermuscular coherence (c) and intermuscular cumulant during low motor attention and high attention. ....240A

Fig. 5.155 Pooled corticomuscular coherence map for the right ECRL with bipolar EEG recordings during the precision task during low and high motor attention. ....241A



Fig. 5.156 Pooled corticomuscular coherence map for the right APB with bipolar EEG recordings during the precision task during low and high motor attention. .....	241A
Fig. 5.157 Pooled power (a, b), intermuscular coherences (c, d) and cumulant plots (e, f) of homologues ECRL and APB muscles during dedicated performance of the elastic band precision extension task and the same task during simultaneous performance of mental arithmetic task .	243A
Fig. 5.158 Pooled corticomuscular map of right ECRL coherences with bipolar EEG recordings during the dedicated and cognitively loaded performance of the band extension task.....	244A
Fig. 5.159 Pooled corticomuscular map of right APB coherences with bipolar EEG recordings during the dedicated and cognitively loaded performance of the band extension task.....	244A
Fig. 5.160 Pooled corticomuscular map of left ECRL coherences with bipolar EEG recordings during the dedicated and cognitively loaded performance of the band extension task.....	245A
Fig. 5.161 Pooled corticomuscular map of left APB coherences with bipolar EEG recordings during the dedicated and cognitively loaded performance of the band extension task.....	245A
Fig. 5.162 INB results for subject 1 during posture extension. ....	248A
Fig. 5.163 INB results for subject 1 during movement. ....	248A
Fig. 5.164 INB results for subject 2 during posture extension. ....	250A
Fig. 5.165 INB results for subject 2 during movement. ....	250A
Fig. 5.166 INB results for subject 3 during posture extension. ....	251A
Fig. 5.167 INB results for subject 3 during movement. ....	251A



# TABLE OF CONTENTS

<b>1</b>	<b>INTRODUCTION .....</b>	<b>1</b>
1.1	Physiology of Movement.....	1
1.2	Corticomuscular Rhythmicities.....	2
1.3	Movement Intention Detection.....	3
1.4	Aims and Objectives.....	4
1.5	Further Implications .....	6
1.6	Thesis Outline .....	6
<b>2</b>	<b>LITERATURE REVIEW .....</b>	<b>8</b>
2.1	Movement Related Components Of The Nervous System.....	8
2.2	The Brain and its relation to movement.....	8
2.2.1	Movement Related Components of the Brain.....	9
2.2.2	The cerebral hemispheres .....	9
2.2.2.1	The cerebral cortex and its involvement in motor control.....	9
2.2.2.1.1	Primary motor cortex .....	9
2.2.2.1.2	Premotor cortex.....	11
2.2.2.1.3	Supplementary motor area .....	12
2.2.2.1.4	Parietal lobe.....	13
2.2.2.2	Subcortical areas involved in movement control .....	13
2.2.2.2.1	Basal ganglia and voluntary movement.....	13
2.2.2.2.2	The Diencephalon & Thalamus .....	14
2.2.2.2.3	The Brainstem .....	15
2.2.3	Corticospinal tract.....	15
2.2.3.1	Cerebellum.....	17
2.3	Spinal cord .....	18
2.3.1	Spinal Reflexes .....	19
2.3.1.1	The stretch reflex .....	19

<b>2.4</b>	<b>Peripheral Nervous System and Movement Control</b> .....	<b>20</b>
2.4.1	Motor Neurons and Motor Units .....	20
2.4.2	Muscle Afferents.....	20
2.4.3	Plexuses of the ventral rami – Brachial Plexus.....	21
2.4.4	Muscular System.....	21
<b>2.5</b>	<b>Movement-Related Changes in Rhythmic Brain Activity</b> .....	<b>22</b>
2.5.1	Rhythmic nature of brain activity .....	22
2.5.2	Cortical imaging .....	22
2.5.2.1	Electroencephalographic activity .....	22
2.5.2.1.1	Origin of electrical brain activity .....	23
2.5.2.2	Magnetoencephalographic Activity.....	24
2.5.2.3	Electrocorticogram (ECoG).....	25
2.5.2.4	Positron Emission Tomography .....	25
2.5.2.5	FMRI .....	26
2.5.3	Organisation of the Nervous System at Cell Level.....	26
2.5.4	Cortical Rhythms - Frequency Bands.....	27
2.5.4.1	Idling Alpha activity.....	28
2.5.4.2	Non Idling Alpha Activity .....	30
2.5.4.3	Beta and Gamma band synchronisation/desynchronisation .....	31
2.5.4.4	Intracortical Synchronisation – Desynchronisation.....	34
<b>2.6</b>	<b>Neurogenic activity during motor tasks</b> .....	<b>36</b>
2.6.1	Tremor .....	36
2.6.2	Posture tremor.....	36
2.6.3	Movement tremor .....	38
2.6.4	Task Specificity .....	41
2.6.5	Motor Unit synchronisation.....	42
2.6.6	Corticomuscular Synchronisation.....	45
2.6.6.1	Spatial Localisation .....	47
2.6.6.2	Functional Specificity.....	48
2.6.6.3	Temporal characteristics of corticomuscular coherence .....	48
<b>2.7</b>	<b>Neural plasticity</b> .....	<b>512</b>
2.7.1	Cortical reorganisation and recovery.....	51
2.7.2	Cortical reorganisation following CNS injury.....	52
2.7.3	CNS plasticity .....	52
2.7.4	Cortical reorganisation following PNS disorder.....	55
2.7.5	Amputees .....	56
2.7.6	Activity Dependent Plasticity.....	57
2.7.7	Plasticity and learning.....	58
2.7.8	Plasticity and rehabilitation .....	59
<b>2.8</b>	<b>Attention</b> .....	<b>60</b>
2.8.1	Attention as a cognitive process .....	60
2.8.2	The single channel and flexible central resource capacity .....	60



2.8.3	Physiology of attention .....	61
2.8.3.1	Parietal and temporal lobe influences on attention.....	61
2.8.3.2	Frontal lobe.....	63
2.8.3.3	Cingulated cortex.....	64
2.8.3.4	Thalamic influences.....	64
2.8.3.5	Basal ganglia.....	65
2.8.3.6	Other subcortical structures .....	66
2.8.3.7	Cerebellum.....	66
2.8.4	Attention influenced motor control?.....	67
<b>2.9</b>	<b>Neuroprosthetic control.....</b>	<b>689</b>
2.9.1	EMG Based Control.....	69
2.9.1.1	Myoelectric Prostheses .....	69
2.9.1.2	Functional Electrical Stimulation (FES).....	70
2.9.2	EEG based control .....	71
2.9.2.1	Short review of EEG based control .....	72
2.9.2.2	The future of BCI .....	74
<b>2.10</b>	<b>Summary.....</b>	<b>76</b>
<b>3</b>	<b>METHODOLOGY .....</b>	<b>78</b>
<b>3.1</b>	<b>Introduction.....</b>	<b>78</b>
3.1.1	Groups of experiments.....	78
<b>3.2</b>	<b>GENERAL EXPERIMENTAL TECHNIQUES .....</b>	<b>79</b>
<b>3.3</b>	<b>EEG recording set up .....</b>	<b>79</b>
<b>3.4</b>	<b>Subject recruitment criteria.....</b>	<b>80</b>
<b>3.5</b>	<b>Subject preparation.....</b>	<b>80</b>
<b>3.6</b>	<b>EMG recording set-up.....</b>	<b>82</b>
<b>3.7</b>	<b>Other apparatus and recording techniques.....</b>	<b>83</b>
3.7.1	CED 1401 .....	83
3.7.2	Gyroscope. ....	83
3.7.3	Instrumented ring.....	84
3.7.4	Pneumatic Tourniquet.....	84
3.7.5	Bimanual motor task.....	85

<b>3.8</b>	<b>Experimental protocols.....</b>	<b>86</b>
3.8.1	Introduction.....	86
3.8.2	EEG and EMG frequency estimates during move-hold sequence, maintained posture and continuous movement.....	87
3.8.2.1	Task 1 - Move hold sequence .....	87
3.8.2.2	Task 2 – Postural Tasks- Maintained wrist extension-Maintained wrist flexion.....	88
3.8.2.3	Task 3 - Continuous slow wrist flexion-extension movement .	89
3.8.3	Influences of attention and cognitive loading in corticomuscular coherence. ....	90
3.8.3.1	Instrumented ring compression experiment. ....	90
3.8.3.2	Bimanual extension of an elastic band .....	91
3.8.4	Effects of deprivation of sensory feedback in corticomuscular coupling. ....	92
<b>4</b>	<b>ANALYTICAL METHODS.....</b>	<b>97</b>
<b>4.1</b>	<b>Introduction.....</b>	<b>97</b>
<b>4.2</b>	<b>The Discrete Fourier Transform.....</b>	<b>98</b>
4.2.1	Power spectrum estimate .....	99
4.2.2	Coherence estimate.....	101
4.2.3	Phase spectrum .....	103
4.2.4	Cumulant density .....	105
4.2.5	Pooled frequency estimates. ....	106
4.2.5.1	Interpretation of the pooled frequency estimates .....	107
<b>4.3</b>	<b>Frequency estimates in time.....</b>	<b>110</b>
4.3.1	Spectrogram .....	110
4.3.2	Other frequency estimates in time. ....	111
<b>4.4</b>	<b>Special topics.....</b>	<b>112</b>
4.4.1	Pooled estimates in time .....	112
4.4.2	Cumulant components .....	113
4.4.3	Phase estimate of out of phase synchronised signals.....	114
4.4.4	Simulation cell model .....	115
4.4.4.1	Leaky Integrate and fire neuron with refractory period.....	116
4.4.4.2	Poisson processes .....	116
4.4.4.3	Variable sinusoidal waveform. ....	117
4.4.5	Construction of bipolar EEG montages .....	117
4.4.6	Topographic maps of cortical and corticomuscular activity.....	118
<b>4.5</b>	<b>Analytical methods sources of error.....</b>	<b>119</b>



<b>5</b>	<b>RESULTS .....</b>	<b>122</b>
<b>5.1</b>	<b>Temporal and Spatial characteristics of EMG, EEG, EMG\EEG coupling .....</b>	<b>122</b>
5.1.1	Introduction.....	122
5.1.2	Data Pre-Processing and analysis .....	123
5.1.3	Temporal EMG frequency characteristics. ....	124
5.1.3.1	Movement flexion phase EMG coupling.....	125
5.1.3.2	Posture flexion phase EMG coupling.....	130
5.1.3.3	Movement extension phase EMG coupling.....	133
5.1.3.4	Posture extension phase EMG coupling.....	135
5.1.3.5	Summary.....	138
5.1.4	Cortical and Corticomuscular frequency characteristics. ....	140
5.1.4.1	EEG Power Spectral density task dependent features .....	142
5.1.4.1.1	EEG spectral changes between movement flexion and posture flexion.....	143
5.1.4.1.2	EEG spectral changes between posture flexion and movement extension.....	144
5.1.4.1.3	EEG spectral changes between movement extension and posture extension.....	145
5.1.4.1.4	EEG spectral changes between posture extension and movement flexion.....	146
5.1.4.2	Topographic maps of EEG spectral power.....	147
5.1.5	Summary of task dependent EEG power results. ....	152
5.1.6	Corticomuscular coupling task dependent features. ....	153
5.1.6.1	Flexion movement phase .....	154
5.1.6.1.1	ECRL coupling .....	154
5.1.6.1.2	FCR coupling .....	157
5.1.6.1.3	BBLH coupling .....	160
5.1.6.2	Flexion posture phase .....	163
5.1.6.2.1	ECRL coupling .....	163
5.1.6.2.2	FCR coupling .....	167
5.1.6.2.3	BBLH coupling .....	170
5.1.6.3	Extension movement .....	173
5.1.6.3.1	ECRL Coupling.....	173
5.1.6.3.2	FCR coupling .....	176
5.1.6.3.3	BBLH coupling .....	179
5.1.6.4	Extension posture .....	181
5.1.6.4.1	ECRL coupling .....	181
5.1.6.4.2	FCR coupling .....	185
5.1.6.4.3	BBLH coupling.....	189
5.1.6.5	Summary of corticomuscular coupling results .....	191
5.1.7	Topographic coherence and cumulant maps.....	193
5.1.7.1	Monopolar corticomuscular coherence topographic maps.....	193
5.1.7.2	Bipolar corticomuscular coherence topographic maps.....	195
5.1.7.3	Cumulant topographic maps.....	196

5.1.7.4	Summary of topographic coherence and cumulant map results. ..	199
5.1.8	Time dependent frequency characteristics.....	201
5.1.8.1	Summary of time dependent frequency characteristics results	221
5.1.9	Continuous movement and maintained posture.....	223
5.1.9.1	Intermittent and Continuous Movement Flexion.....	224
5.1.9.2	Intermittent and Maintained Posture Flexion.....	226
5.1.9.3	Intermittent and Continuous Movement Extension.....	228
5.1.9.4	Intermittent and Maintained Posture Extension .....	230
5.1.9.5	Summary of continuous movement and maintained posture results.....	233
<b>5.2</b>	<b>Attention and cognitive influences in corticomuscular coherence.</b>	<b>235</b>
5.2.1	Influence of attention in corticomuscular coherence.....	235
5.2.1.1	Summary of attentional influence results .....	238
5.2.2	Influence of cognitive loading in corticomuscular coherence .....	239
5.2.2.1	Summary of cognitive loading influence results .....	242
<b>5.3</b>	<b>Afferent sensory influences in corticomuscular coherence .....</b>	<b>243</b>
5.3.1	Results for Subject 1 .....	244
5.3.2	Results for Subject 2.....	246
5.3.3	Results for Subject 3.....	247
5.3.4	Summary.....	248
<b>6</b>	<b>DISCUSSION.....</b>	<b>249</b>
<b>6.1</b>	<b>Introduction.....</b>	<b>249</b>
6.1.1	Novel methodological and analytical features.....	250
6.1.2	Main findings.....	244
<b>6.2</b>	<b>Task dependent rhythmic EMG-EEG features.....</b>	<b>255</b>
6.2.1	Introduction.....	255
6.2.2	EMG task related features.....	255
6.2.3	EEG and corticomuscular characteristics .....	262
6.2.3.1	EEG Characteristics.....	262
6.2.3.2	Corticomuscular characteristics.....	265
6.2.3.3	Spatial organisation of corticomuscular features.....	267
<b>6.3</b>	<b>Comparison of intermittent movement and posture with continuous movement and maintained posture.....</b>	<b>270</b>
6.3.1	Differences between maintained posture – intermittent posture ..	270



6.3.2	Differences between intermittent movement – continuous movement .....	271
6.4	<b>Effects of attention in corticomuscular coupling.....</b>	<b>274</b>
6.5	<b>Effects of cognitive loading in corticomuscular coherence.....</b>	<b>276</b>
6.6	<b>Effects of deafferentation in corticomuscular coherence .....</b>	<b>279</b>
6.7	<b>Implications for neuroprosthetic control.....</b>	<b>283</b>
7	<b>CONCLUSION .....</b>	<b>286</b>
7.1	<b>Summary of thesis.....</b>	<b>286</b>
7.2	<b>Functional significance.....</b>	<b>288</b>
7.3	<b>Future work.....</b>	<b>289</b>
8	<b>BIBLIOGRAPHY .....</b>	<b>305</b>
9	<b>APPENDICES .....</b>	<b>317</b>
9.1	<b>Appendix 1 - Subject variability.....</b>	<b>317</b>
9.2	<b>Appendix 2 – EEG power.....</b>	<b>322</b>
9.3	<b>Appendix 3 - Interpretation of coherence phase and rhythmic cumulant results; a simulation study.....</b>	<b>325</b>
9.3.1	Introduction.....	325
9.3.2	Literature review.....	325
9.3.2.1	The concept of spike triggered average and parameter estimates of time domain point processes. ....	325
9.3.2.2	Simple neuronal networks .....	327
9.3.2.2.1	Paired neurones with a single common excitatory input.	327
9.3.2.2.2	Paired neurones with a single common inhibitory input..	327

9.3.2.2.3	Balanced excitation-inhibition in simple counting neurons 328	
9.3.2.2.4	Neurons with partially common excitatory and/or inhibitory input sources without correlation.....	329
9.3.3	Simulation study .....	330
9.3.3.1	Example 1 - Neurones receiving a common excitatory input	330
9.3.3.2	Example 2 - Neurones receiving a common inhibitory input.	331
9.3.3.3	Example 3- Non oscillatory inputs producing oscillatory output 332	
9.3.3.4	Example 4 - Common oscillatory inputs .....	333
9.4	<b>Appendix 4 - Information for volunteers.....</b>	<b>334</b>



# ***1 INTRODUCTION***

The Edwin Smith papyrus with the oldest reference to the brain describes the appearance of the cortical surface (similar to melting copper) and relates injuries to certain localised parts of the brain with deficiencies in walking or loss of speech in spite of the fact that legs and face were intact. It was written around 1700 BC but most of the information is based on texts written around 2640 BC (Breasted 1930).

## ***1.1 PHYSIOLOGY OF MOVEMENT***

The study of human motor control is a multidisciplinary field involving knowledge of biology, medicine and engineering. Movement is a highly sophisticated process, requiring the coordination of actions. It involves many areas of the cerebral cortex, subcortical structures, cerebellum and spinal cord working together with the peripheral nerves, muscles and sensory receptors. The activation of the nervous system must control a highly complex biomechanical apparatus comprising the skeleton and muscles (Cordo and Harnad 1994). Moreover, not all movements are the same. Some of our actions require high power some require fine control, while some of them require both power and fine control.

Movements can be classified into two main categories; voluntary movements and reflexive movements (Kandel et al. 2000). Voluntary movements are organised around the performance of a purposeful task. The goal oriented nature of the task defines the joints and body segments to be activated. Voluntary movements are initiated and generated internally and are not direct responses to environmental stimuli. Sensory and environmental information is processed and evaluated. It affects the initiation of a movement but the mechanisms of information processing and triggering a movement are different and the result not always predictable. In contrast, reflexes are often associated with a stereotyped motor response to a stimulus and the initiation and information dependency mechanisms are linked. Almost all movements have both voluntary and reflexive components while common physiological components are involved in both types of movement.

The complexity in studying the control mechanism underpinning motor behaviour explains the incomplete understanding of voluntary movement. This thesis

will address specific issues, based on observations on the influences of certain neuronal rhythms to voluntary movement with the goal of trying to improve our understanding of the processes that operate to generate and control movements. The work described in the thesis specifically examined the frequency content of electrophysiological signals acquired during normal voluntary movement. Implications for neuroprosthetic control are also examined as these electrophysiological signals could be used in the activation and control of assistive devices for the disabled.

## ***1.2 CORTICOMUSCULAR RHYTHMICITIES***

Many theories have been developed in the past 20 years that tried to explain the physiological processes involved in movement; from the decision to make a movement to the execution of the movement itself. However few have been systematically verified. Recently, a significant effort to address this issue has led researchers to look for statistical associations between representative signals from the cortex and the muscles activated during movement tasks. One promising area for research has been the frequency domain analysis of time varying processes such as electroencephalogram (EEG), magnetoencephalogram (MEG) and electromyogram (EMG) (Rosenberg et al. 1989; Halliday et al. 1995; Amjad et al. 1997; Halliday et al. 1998). Even though this effort has not yet resulted in a comprehensive theory and a complete model that relates cortical activity to movement, a substantial physiological background on the involvement of oscillatory neural circuits to motor output has been developed.

Despite the incomplete knowledge of how the brain controls human movement, it has been known from anatomical, physiological and clinical studies that the area of the cortex called the primary motor cortex exhibits significant degree of control over the muscles of the body. Modern imaging methods including positron emission topography (PET) and functional magnetic resonance imaging (fMRI) demonstrate increased activity in the primary motor cortex (Yousry et al. 1997) and other motor areas of the brain like premotor cortex (Picard and Strick 2001) supplementary motor cortex and somatosensory areas (Ruben et al. 2001)) during movement execution. The above studies highlight these areas as important structures



in the planning, execution and monitoring of voluntary movement. Lesions in these areas cause accordingly serious motor impairment or paralysis.

Experimental studies carried out on man (Conway et al. 1995; Salenius et al. 1997; Conway et al. 1999) and primates (Baker et al. 1997; Baker et al. 2001; Baker et al. 2003) have revealed a relationship between beta (15-30Hz) activity from areas of the motor cortex and the corresponding EMG activity of contralateral muscles during voluntary posture contractions. This feature of motor behaviour is observed in man as 15-30Hz coherence between cortex and muscle activity. Similar coupling also occurs between synergistic coactive muscles. The coherence observed appears to be highly correlated with the performance of postural motor task and is thought to occur from underlying coupling between the cortex and the motoneuronal pool via the corticospinal tract (Brown 2000). This feature appears to be task related since it is suppressed during active joint movements (Kilner et al. 1999). However, movements also show characteristic rhythmic features. It has been demonstrated from EMG and kinematic studies that with the suppression of the 15-30Hz coherence during movement an 8-12Hz modulation emerges in EMG recordings (Vallbo and Wessberg 1993). This 8-12Hz bursting feature of the EMG is believed to reflect a pulsatile descending motor command.

### ***1.3 MOVEMENT INTENTION DETECTION***

Both the 8-12Hz and 15-35Hz oscillatory activity seen in the EMG appears to be task dependent possibly due to specific patterns of rhythmic activity generated within the CNS. From an engineering perspective this raises the possibility to use these different rhythms in intention detection systems and devices for neuroprosthetic control. Although, amplitude modulation of EMG has been used as an actuating signal to control the function of artificial limbs and neuroprosthetic devices, its effectiveness as an intention detection system is limited. Part of this limitation relates to the need of the user/patient to activate muscle groups not always associated with the motor behaviour replicated by the prosthesis. Lengthy motor learning/training periods are needed and often not successfully completed by all subjects. In addition, the effects of muscle fatigue produce complex and difficult to predict changes in the EMG signals. Accordingly, over time an extremely high



percentage of amputees provided with myoelectric prostheses will abandon their use. Even relatively recent studies with modern myoelectric hands have shown drop off percentages as high as 50% (Wright et al. 1995; Routhier et al. 2001). Similarly, voluntarily generated changes in features of the electroencephalogram (EEG) can be used to drive devices (such as communication aids (McFarland et al. 1997; Vaughan et al. 1998)) but these systems also suffer from a poor initial relationship to the required behaviour, are hindered by lengthy training periods, are error prone, slow and tiring to use. These features make current neuroprosthetic systems unattractive for wide use in the regulation of active prosthetic limbs and most existing assistive devices.

The possible advantage of using the frequency characteristics of EMG-EEG signals that modulate with motor behaviour is that the task itself is easy to define and can be easily visualized by the patient. One consequence of this should be to reduce the need for training as the control of the device is linked by a close relationship with a simple cognitive or motor task. However, in choosing a signal for use as a control input it is crucial that it fulfils several requirements. The most important are robustness, simplicity to detect and ability to be successfully monitored over prolonged periods.

The stochastic and non stationary nature of EMG and EEG is a serious drawback for the use of EEG and EMG for the control of neuroprostheses. Therefore there is the need for more sophisticated and intelligent processing of those signals. The neuroprosthetic systems should be adaptive and flexible in order to cope with signal variations and neural function variations (plasticity) for recovering patients. The neuroprosthetic systems should also be highly customisable in order to adapt to different patients needs since great variations of the examined physiological signal have been identified in normal and patient populations.

## ***1.4 AIMS AND OBJECTIVES***

The growing interest in the development of robust methods of intention detection for use in the activation and regulation of prosthetic devices and communication aids for motor impairments led to the examination of the physiological signals that reflect the rhythmic activity in the nervous system, to the



investigation their functional significance and determine whether they may possibly be used as intention detectors or actuators within neuroprosthetic controllers. The main objectives of this study are given below.

1. Determine non invasive recording conditions of rhythmic activity from the motor cortex using multichannel EEG (electrode sites and recording configuration) in combination with EMG. Modern recording configurations involving multiple recordings from a large number of electrodes allow the examination of the topography of activity around a wide recording area rather than assuming the optimal recording site based on previous studies.
2. Develop a signal processing framework to monitor time dependant changes in frequency domain characteristics during different types of motor tasks and during the transition phases during posture and movement in order to identify distinctive task-specific modulations. The aim is to gain more insight into nervous system oscillations and their relation to movement. These oscillations are expressed as EEG activity, rhythmic muscular action and EMG activity, as well as corticomuscular coherence and muscle coupling. The identification of task specific frequency components in normal subjects that could be used as movement intention indicators is also an important issue for neuroprosthetic control.
3. Explore the relationship between corticomuscular coherence and changing levels of attention and cognitive loading. Corticomuscular coherence is very likely to express information flow from central to the peripheral nervous system. In a controlled experimental environment, with dedicated subjects, there is evidence of usability of coherence and other frequency features as intention detection indicators. Real life conditions present many distractions to a user and attention influences on the performed task will have to be examined to see if they affect the robustness of the examined signals.
4. Explore if sensory feedback influences corticomuscular coherence. In many potential uses of prosthetic devices sensory feedback will be abnormal. For example in amputation or spinal cord injury the normal pattern of feedback from the limb or spinal segments may be lost. It is therefore important to see to what extent the descending motor command is affected by the loss of the ascending sensory information.

## ***1.5 FURTHER IMPLICATIONS***

The aims and objectives of this study are very important topics in the area of motor control and neuronal rhythms. Satisfactory answers to the stated issues may also have implications for neuroprosthetic control and often new opportunities to develop assistive technologies that can improve the quality of life of the severely motor disabled.

The limitations of conventional neuroprosthetic interfaces have put boundaries to the functionality of these systems for the patient/user. These limits have driven the scientific community to pursue alternative solutions. This study attempts to extract more information from readily available signals and establish what features of movement are coded in the frequency content of signals or in the correlations between the frequency content of two physiological signals. At the same time issues like persistence and robustness of the signals under different conditions, repeatability of features for the same individual and variability of the signal features in the population will require to be evaluated.

## ***1.6 THESIS OUTLINE***

This thesis is divided into seven main chapters. The current chapter comprises chapter one – the introduction where some essential background information as well as the aims and the scopes of the project are presented.

The literature review (chapter 2) provides a theoretical background to the study and contains an introduction to the nervous system and its involvement in movement. Following a consideration of the components of the motor system, the rhythmic nature of activity in the nervous system is then presented and discussed in relation to movement control. At this point the functional significance of synchronisation in motor control is also considered. Influences of pathological or non-pathological changes in the form of plasticity are also discussed. One of the main issues of this thesis is also how attention affects motor control, and it is examined in detail. Finally some insights in the past, present and future of neuroprosthetic control, will be presented.

Chapter 3 presents the experimental methodology. The experimental set-up and protocol, experimental techniques and apparatus used for the experiments carried



out. In chapter 4 the basic analytical methods used for the processing and analysis of the data acquired during the experimental sessions are presented. Chapter 5 provides the experimental results with chapter 6 providing a discussion on the findings presented in chapter 5. The thesis concludes with chapter 7 which contains recommendations on future work.

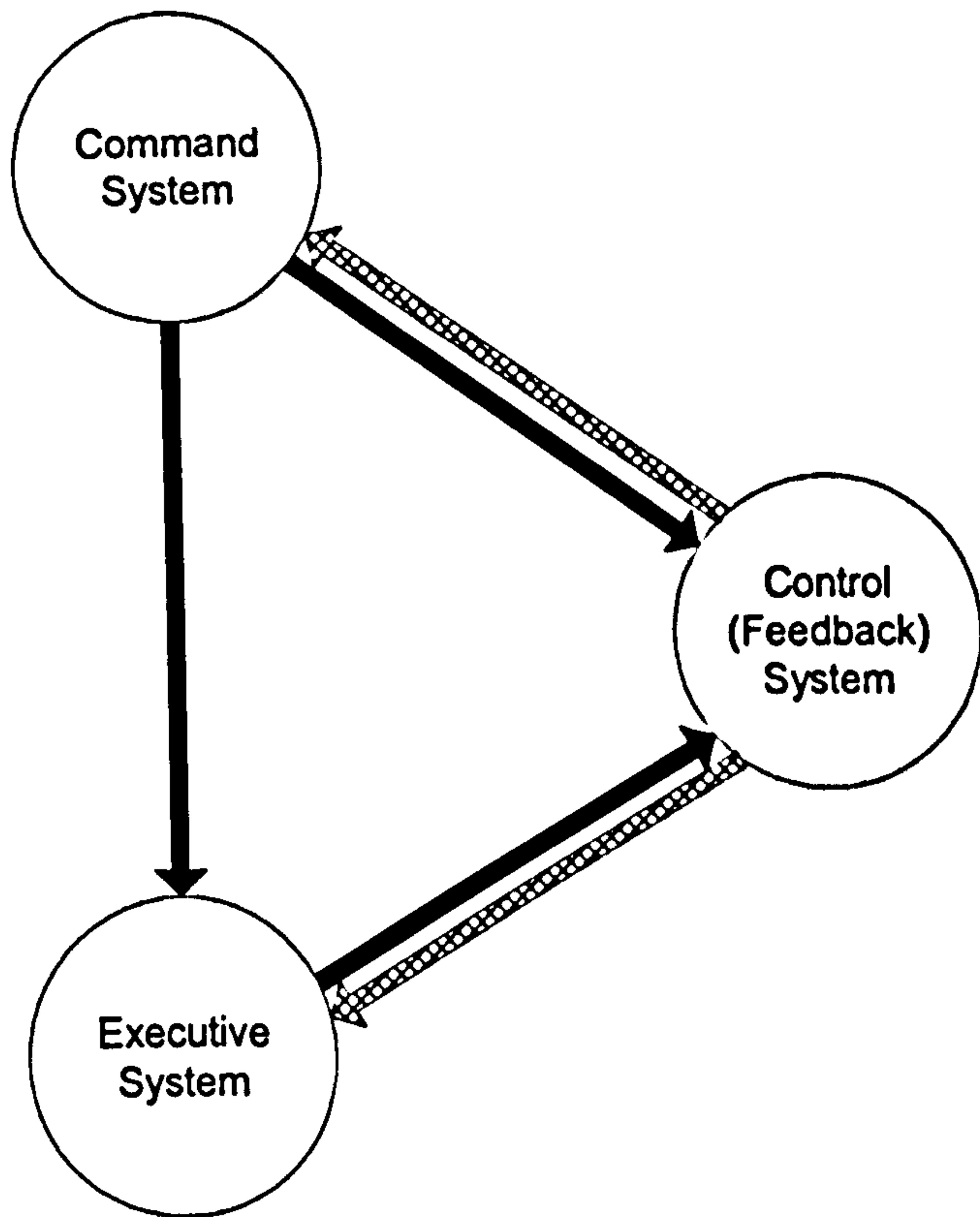


**Fig. 2.1** The three functional subsystems of motor control adapted from (Mandl 2000).



## ***2 LITERATURE REVIEW***

### ***2.1 MOVEMENT RELATED COMPONENTS OF THE NERVOUS SYSTEM***

The central nervous system provides the basis for conscious intelligence together with the awareness of one's sensations, actions, emotions, and environment as a subjective reality (Mandl 2000). To achieve purposeful actions the nervous system relies on the frequency and temporal patterns of electrical impulses (action potentials) to transmit and process sensory information and to distribute motor commands to the peripheral musculature. The interaction of the nervous system with the external world is based on a process of abstraction: When simultaneous activation of several sense organs occurs, the nervous system selects and abstracts only certain key features of the complex sensory input and evokes appropriate motor responses.

### ***2.2 THE BRAIN AND ITS RELATION TO MOVEMENT***

The human brain, probably the most complex organ in the body, hides many of its secrets largely due to its vast interconnected structure and organisation. To map the brain regions or modules and correlating activity with behaviour, has been an extensive and continuous pursuit for the scientific community. Relating brain maps to motor function has been accomplished up to a certain extent. These maps were taken under consideration for the placement of EMG and EEG electrodes on the appropriate sites studies performed in the framework of this thesis. However, the association of the anatomical components to function does not appear to be uniquely defined or 'hard wired'. The brain emerges as a dynamic system, differentially engaged according to ongoing situation and task, involving parallel function of more than one component.

In a simplified way that is sketched in Fig. 2.1, the brain's command system includes the motor cortex and association cortex in frontal and parietal lobes, portions of the basal ganglia, portions of the thalamus and portions of the cerebellum. The executive system largely comprises the motor cortex, the corticospinal pathways, a number of brainstem motor nuclei and the spinal segmental motor

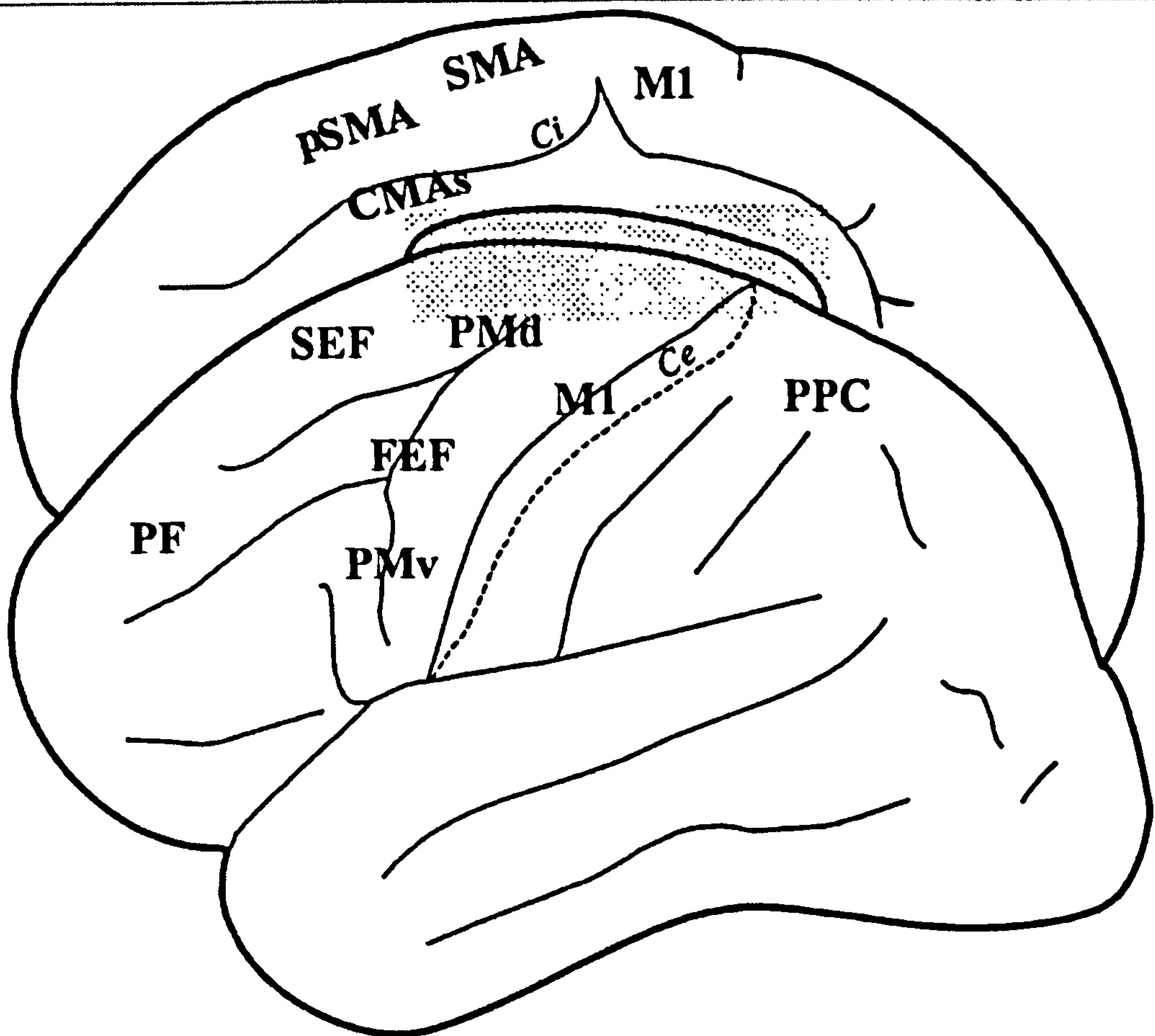


**Fig. 2.2** Motor areas of the human brain plotted onto a highly simplified sketch of the cerebral hemispheres. The lateral surface of the left hemisphere is shown below the medial surface of the right hemisphere. Rostral is to the left; dorsal is up. The dashed line indicates the fundus of the central sulcus, showing that the primary motor cortex is located mainly within the rostral (anterior) back of that sulcus. The stippled area on the medial surface represents the corpus callosum. Ce, central sulcus; CMA, cingulate motor areas; FEF, frontal eye field; M1, primary motor cortex; PF, prefrontal cortex; PMd, dorsal premotor cortex; PMv, ventral premotor cortex; PPC, posterior parietal cortex; SEF, supplementary eye field; pSMA, presupplementary motor area; SMA, supplementary motor area (Wise and Shadmehr 2002).



circuits. The control system includes neural proprioceptive pathways originating from skin and muscle receptors together with portions of the brainstem, thalamus and cerebellum (Mandl 2000).

### ***2.2.1 Movement Related Components of the Brain***

Three major divisions of the brain that are recognized to participate in the movement are:

- the paired cerebral hemispheres.
- the brain stem
- the cerebellum

### ***2.2.2 The cerebral hemispheres***

The cerebral hemispheres of the adult brain are composed of the cerebral cortex, the underlying white matter, and various subcortical neuronal nuclei. Each hemisphere relates to motor and sensory functions on the contralateral side of the body.

#### ***2.2.2.1 The cerebral cortex and its involvement in motor control***

The cerebral cortex plays a large role in executive/cognitive brain functions. The sensorimotor areas of the cerebral cortex integrate visual, proprioceptive and other sensory information during movement planning and execution of voluntary movement tasks. The motor cortex of the frontal lobe is largely associated with the control and planning of voluntary movement. It is subdivided on functional and anatomical basis as illustrated in Fig. 2.2, into three main areas; a primary motor area (M1), a premotor cortex (PM) and a supplementary motor area (SMA).

##### ***2.2.2.1.1 Primary motor cortex***

The primary motor cortex (M1) is the area of the brain which contains the majority of the neurones which make up the fast conducting corticospinal tract which in higher primates exerts a mono and polysynaptic excitation of contralateral spinal motoneurons (Porter and Lemon 1993). Because of this spinal projection direct electrical stimulation of the motor cortex exerts localised movements on the contralateral side of the body. Similarly, injury to parts of M1 causes motor weakness on the contralateral half of the body.

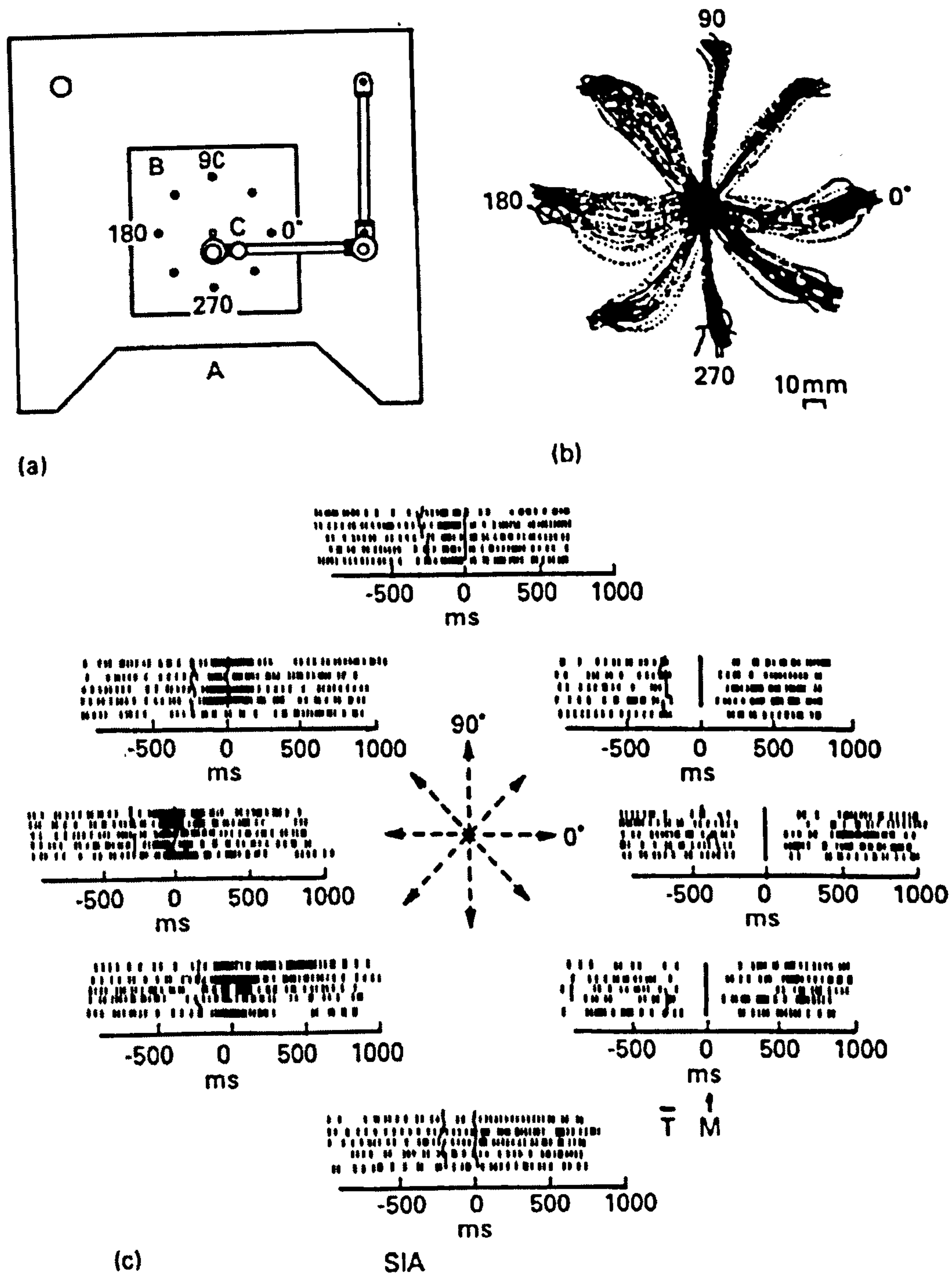


**Fig. 2.3** Direction of movement is encoded in the motor cortex by the pattern of activity in an entire population of cells (Georgopoulos et al. 1982). A monkey was trained to move a handle (a) to eight locations arranged radially in one plane around a central starting position (b). Each row of tics in each raster plot (c) represents activity in a single trial for a single neuron; 5 neurons are represented with each neuron's activity aligned at zero time (the onset of the movement). It was shown that individual cells located in the motor cortex fire preferentially in connection to the movement. The entirety of this activity resulted in a population vector that closely matched that of the direction of movement.



The primary motor cortex receives somatosensory inputs from the primary somatosensory cortex. In fact it receives proprioceptive information from the muscles to which it projects and tactile information via the somatosensory cortex through so called transcortical circuits. Additional sources of input arise from the posterior parietal area, which is involved in integrating multiple sensory modalities during motor planning.

During early 20<sup>th</sup> century neurosurgical procedures it was demonstrated that the human motor cortex is somatotopically organised (Penfield and Boldrey 1937; Penfield 1975). Thus different areas of the motor cortex when stimulated result in evoked twitches in different parts of the body. The amount of cortical surface dedicated to body region and therefore the number of cortical neurons (and hence corticospinal fibres) associated with movement of that body part is proportional to the level of precision exercised in performing movements and not the magnitude of the power required for the motor action. Direct microstimulation of the cortex during surgery rarely activates individual muscles but result in activity in groups of muscles. This is explained by anatomical and physiological findings in man and primates that show that the terminal distributions of individual corticospinal axons diverge to motor neurons innervating more than one muscle (Shinoda et al. 1981).

One of the most controversial issues in neurophysiology is whether muscles or movements are represented in the primary motor cortex. The activity of motor cortical neurons was related to variables such as movement or force at individual joints, more than forty years ago (Evarts 1968). A different perspective came from primate reaching studies, and relates the M1 activity to the movement of the limb rather than the individual joints (Fig. 2.3) (Georgopoulos et al. 1982; Georgopoulos et al. 1983). These studies showed that a population vector constructed from the firing rates of many cortical neurons tends to correlate with the direction of the hand movement. Subsequent work from various laboratories has given contradictory results as far as the relationships between hand motion and neural activity is concerned, at both the single-cell and population levels. Others have supported different relationships between hand motion and neural activity. An extrinsic connection, related to the direction of movement in space independent of the muscle activity (Takei et al. 1999), a muscle relationship, related to the activity of



individual or groups of muscles (Todorov 2000) and a joint relationship, related to the angle of the wrist joint (Hoffman and Strick 1999) have been suggested. Initially it was claimed that both “muscles” and “movements” are strongly represented in M1 (Kakei et al. 1999). However, this view was challenged, with the suggestion that many of the previously-described correlations between motor cortical activity and hand motion can be explained with a simple model in which the activity of cortical neurons encodes the activation of a group of muscles (Todorov 2000).

#### ***2.2.2.1.2 Premotor cortex***

Movements can also be produced by direct electrical stimulation of the premotor cortex or PreMotor Area (PMA). This often elicits more complex movements than M1 involving multiple joints and similar to naturally coordinated hand movements. Recent studies have shown that there are four main premotor areas in humans and primates. Motor maps of the face and extremities correspond to every single PMA as for M1. The premotor areas project to the primary motor area, and also directly contribute to the corticospinal tract. The areas of termination of the premotor areas and the M1 in the spinal cord overlap, suggesting that the PMA could control hand movements independent of the M1 and vice versa. This may be significant in relation to recovery of function following stroke. The premotor areas also receive inputs from areas of the parietal cortex and they are interconnected with dense connections themselves. The primary motor and premotor areas also receive input via different sets of nuclei in the ventrolateral thalamus, from the basal ganglia and cerebellum (Kandel et al. 2000).

Lesions in the premotor areas cause more complex deficits than those seen following primary motor cortex lesions. Premotor areas have been connected with movement planning and motor preparation. Internally triggered movements like the sequencing of finger movements or manipulating an object involve activity arising mainly from the supplementary motor areas. Movements initiated mainly by external stimuli involve primarily the lateral premotor areas (Kandel et al. 2000). Similar patterns of activity in premotor and posterior parietal areas appear during visual imagery of a movement. A study demonstrated that a population of neurons in the monkey ventral premotor cortex (mirror neurons) discharge both when the monkey performs a grasping action and when it observes the same action performed by other



individuals (Gallese et al. 1996; Rizzolatti et al. 1996). Several recent PET studies have shown that during motor imagery of grasping actions premotor and inferior parietal areas are strongly activated (Decety et al. 1994) indicating that a similar population of cells exist in man. Mental rehearsal of a movement has similar time course and simulates task performance. These observations may explain the value of mental rehearsal prior to performance of demanding motor activities. Also, activation during a specific task changes over time with training as the task becomes more automatic. In a study comparing cerebral blood flow it was found that complex movements and imagined complex movements activate the PMA and may require similar amount of planning. Simple or repetitive movements activate mainly the M1 (Rao et al. 1993).

### ***2.2.2.1.3 Supplementary motor area***

The importance of the supplementary motor area (SMA) for planning and internal representation has been examined in primate experiments ((Mushiake et al. 1991) in (Kandel et al. 2000)). The monkeys were instructed to touch three panels in a memorised sequence and in a visually guided sequence (the panels were lit in that sequence). The neurons in the primary motor cortex were active to the same degree before and during both tasks. In contrast the neurons of the supplementary motor area were active before and during the memorised task while neurons of the lateral premotor areas fire during the visually guided task only. In addition, the firing pattern of the SMA neurons was specific to particular combinations of tasks suggesting a involvement in motor planning (Kandel et al. 2000). Stimulation of the supplementary motor area can produce bilateral movements, probably because this area coordinates movements on the two sides of the body (i.e. bimanual tasks) (Kandel et al. 2000).

The presupplementary motor area (pSMA) is an area lying anterior to SMA having no clear somatotopy (Kandel et al. 2000). While the SMA is involved in the execution of memorised movements, the pSMA is thought to be involved in the process of memorising sequences of movements (Hikosaka et al. 1996) as well as being active during the preparatory period before the trigger of a signal for a reaching task (Matsuzaka et al. 1992).



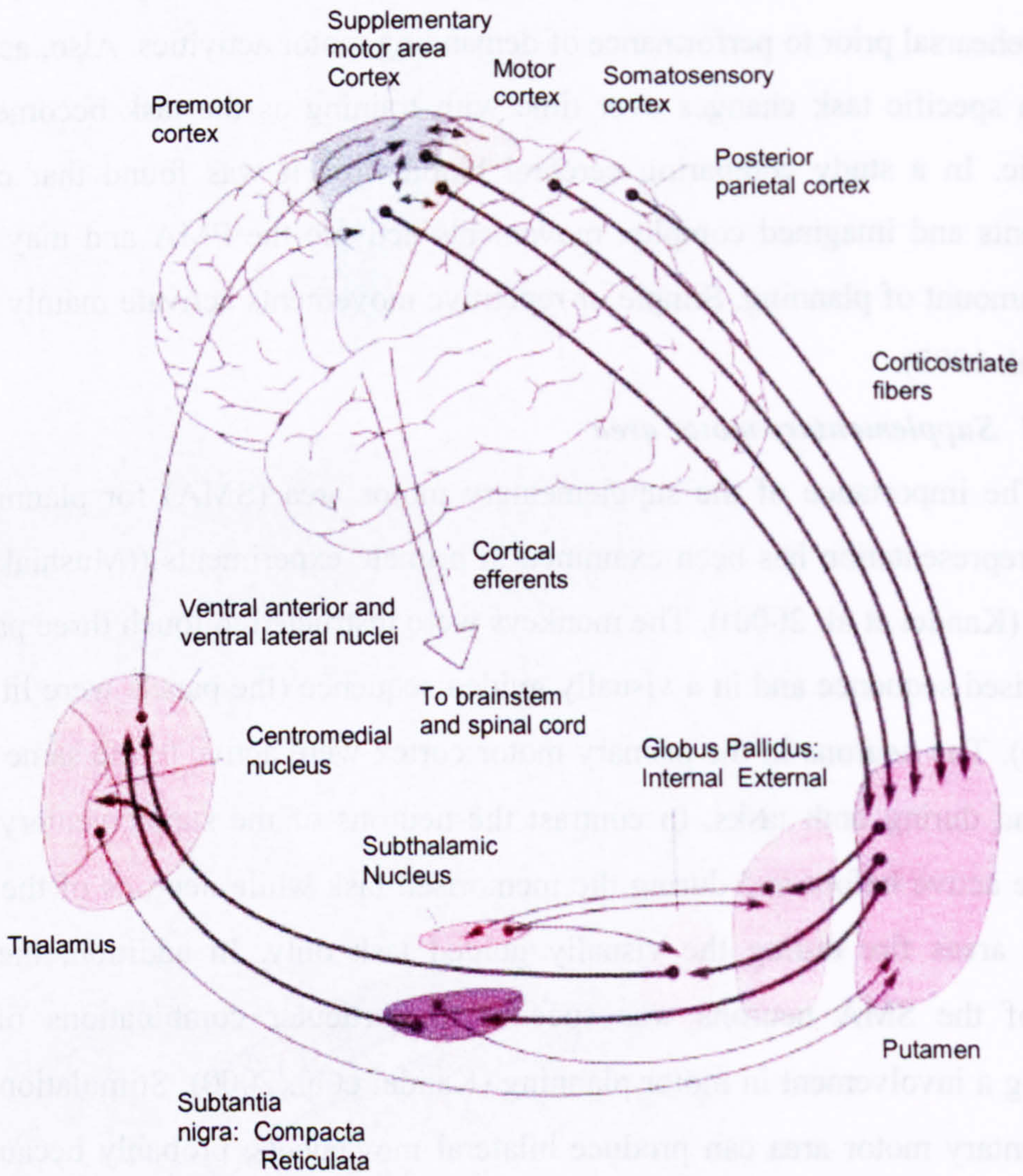


**Fig. 2.4** Motor circuit of the Basal Ganglia (Kandel et al. 1995)



#### ***2.2.2.1.4 Parietal lobe***

The parietal lobe is divided into three parts: a postcentral gyrus, a superior parietal lobule, and an inferior parietal lobule. The postcentral gyrus of each hemisphere is largely concerned with somatic sensation, forming a body image, and relating one's body image with extrapersonal space. It receives both superficial and deep sensory input, from the contralateral half of the body. The somatosensory cortex contains not one unique but several somatotopic maps. The primary somatosensory cortex (anterior parietal cortex) contains four complete representations of the body's surface. The superior parietal lobule is regarded as an association cortex, part of which may be concerned with motor function. The inferior parietal lobule is a cortical region concerned with the integration of multiple sensory signals. The motor regions receive input from the thalamus as well as the sensory areas of the cerebral cortex.

#### ***2.2.2.2 Subcortical areas involved in movement control***

Previously, it was described how motor related areas of the cortex affect human movement. However, an important number of subcortical structures are also involved in motor control. Scalp EEG can pick up cortical signals. However, it is not able to obtain adequate signal from subcortical structures. The presumed function of these structures in relation to movement is going to be described.

##### ***2.2.2.2.1 Basal ganglia and voluntary movement***

A detailed review of basal ganglia anatomy and physiology is out of the scope of this thesis and only a brief review of its function is given here. The cerebral cortex is massively interconnected with a large group of subcortical nuclei deep within the cerebral hemispheres known as the "basal ganglia" that play a major role in normal voluntary movement. The basal ganglia do not have any direct input or output connections to the spinal cord. Their nuclei receive direct input from the cerebral cortex and send their output to the brain stem and via the thalamus back to the cerebral cortex as seen in Fig. 2.4. The basal ganglia are very important for movement but are not exclusively motor in function. It has been proposed that the basal ganglia sub-serve functions associated with skeletomotor and oculomotor control, working memory, attention, and emotional behaviour (Alexander et al. 1986). It is also apparent that movement disorders resulting from basal ganglia



dysfunction (Parkinson's disease and Huntington's disease) result in motor, sensory, visual, emotional, behavioural and cognitive disturbances. The basal ganglia have also been implicated in forms of habit learning (Wilson and Keil 1999). Individuals with Parkinson's disease or Huntington's disease have been shown to be impaired in the performance of tasks that depend on habit learning (Knowlton et al. 1996). Portions have also shown to be active during the performance of tasks that require learning a sequence of movements (Jenkins et al. 1994; Kermadi and Joseph 1995; Mushiake and Strick 1995). These observations suggest that the basal ganglia may play a critical role in what has been termed procedural or motor-skill learning (Wilson and Keil 1999) and a consideration of this process may be important in determining control strategies and training protocols for the usage of neuroprosthetic control devices.

#### ***2.2.2.2 The Diencephalon & Thalamus***

The diencephalon consists of two main subdivisions: the thalamus and the hypothalamus. The thalamus is involved in the relay and distribution of most, but not all, sensory and motor signals (apart from olfactory) to specific regions of the cerebral cortex including a large projection to the primary sensory areas. More than 50 thalamic nuclei have been identified. Some of them project to the primary sensory cortex. Others contribute to motor function conveying information from the basal ganglia and cerebellum to motor areas of the frontal lobe. Importantly, a major output from the cerebellum projects to various thalamic relay nuclei in a pattern similar to that for somesthetic input. Through those connections the thalamus is thought to play a role in cognitive functions as memory and attention in addition to its role as a relay and integrating centre for motor and sensory signals (Kandel et al. 2000).

The outer covering of the thalamus is formed by a sheet like structure, the reticular nucleus. An implication of the existence of the reticular nucleus is that all functional components of the thalamus like behavioural, motor, sensory, emotional or attentional are interconnected and interrelated making thalamus not a simple relay station but an important integrating centre in its own right (Kandel et al. 2000).

#### ***2.2.2.3 The Brainstem***



Lying below the diencephalon are the midbrain and hindbrain (pons and medulla oblongata). These parts of the brain stem are characterized by the reticular formation and a massive basal collection of fibres descending from the cerebral cortex to the brain stem and spinal cord. The reticular formation contains a core collection of cells of various sizes that project to the thalamus, the cerebellum, and the spinal cord. Surrounding this core are long ascending and descending tracts in which various cranial nerve nuclei are embedded (Kandel et al. 2000).

The midbrain provides important linkages between components of the motor control system, the cerebellum, the basal ganglia, and the cerebral hemispheres. The pons' main function is to convey (relay) information about movement and sensation from the cerebral hemisphere to the cerebellum. Located in the periphery of the pons are long ascending and descending tracts that connect the brain to the spinal cord (Kandel et al. 2000).

Fibres derived from the cerebral cortex lie on or near the ventral surface of the midbrain, pons, and medulla. At the midbrain they gather into two bundles which descend into the pons, where most terminate upon cell nuclei that project into the cerebellum (corticopontine tract). The medullary pyramids forming the corticospinal tract can be found here (Kandel et al. 2000).

### ***2.2.3 Corticospinal tract***

Regarded as the most important tract concerned with skilled voluntary activity in humans, the corticospinal tract (or pyramidal tract) originates from cells in the premotor, primary motor, and primary sensory cortex, and synapse on the motoneuronal pools enabling communication between these distant elements of central and peripheral nervous system (Fig. 2.5). Anatomically it contains about one million fibres, 40% of which originate in the M1. It forms a significant part of the posterior limb of the internal capsule and is a major constituent of the crus cerebri in the midbrain. In the lower medulla about 90 percent of the fibres decussate and descend in the dorsal part of the lateral funiculus of the spinal cord with about 10% of the fibres descending ipsilaterally until they reach the level of the spinal cord at which they terminate. Of the fibres that do not cross in the medulla, approximately 8% cross in cervical spinal segments (Kandel et al. 2000).



The descending corticospinal tract crosses the opposite side of the spinal cord the same way that the ascending somatosensory system does. As the tract descends, fibres and collaterals are given off at all segmental levels, synapsing upon interneurons and directly with motor neurons. Approximately 50 percent of the corticospinal fibres terminate within cervical segments. Corticomotoneuronal cells not only branch to synapse on motoneurons innervating a particular muscle, but also exert their facilitatory influence over motoneurons lying in different muscles. The monosynaptic connections to motoneurons are considered important for producing independent finger movements in man given that this ability does not exist in lower mammals that have fused finger movements and a less developed corticospinal tract. The indirect connections through spinal interneurons are very important for tasks where coordination of large groups of muscles is required such as reaching (Kandel et al. 2000).

Each corticomotoneuronal axon is capable of delivering synapses to large numbers of motoneurons. It is the cooperative action of the large numbers of corticomotoneuronal cells that provides the structural basis for the refined motor performance of the human hand since individual corticomotoneuronal cells exert relatively weak contributions to the motoneurons they synapse on. This aids in the selection of particular motor-units, giving the capacity to fractionate the use of distally acting muscles. The presence of short-term synchronisation between motor-units in the same and in different synergistic muscles is believed to reflect activity in a common presynaptic input to the motoneurons innervating these muscles. It is believed that much of the short-term synchrony has a corticospinal origin, most likely in the primary motor cortex (Kandel et al. 2000).

The spinal neurons also receive inputs from other motor areas in the frontal lobes, including the SMA and the pre-motor areas as well as from the somatosensory cortex and the ipsilateral primary and association motor areas. The propriospinal neurones also receive inputs from corticobulbar pathways, which incidentally originate from the same motor areas of the frontal lobe. The higher mammals have evolved with increasing numbers of bilateral SMA and pre-motor projections to the ventromedial intermediate zone (Kandel et al. 2000).



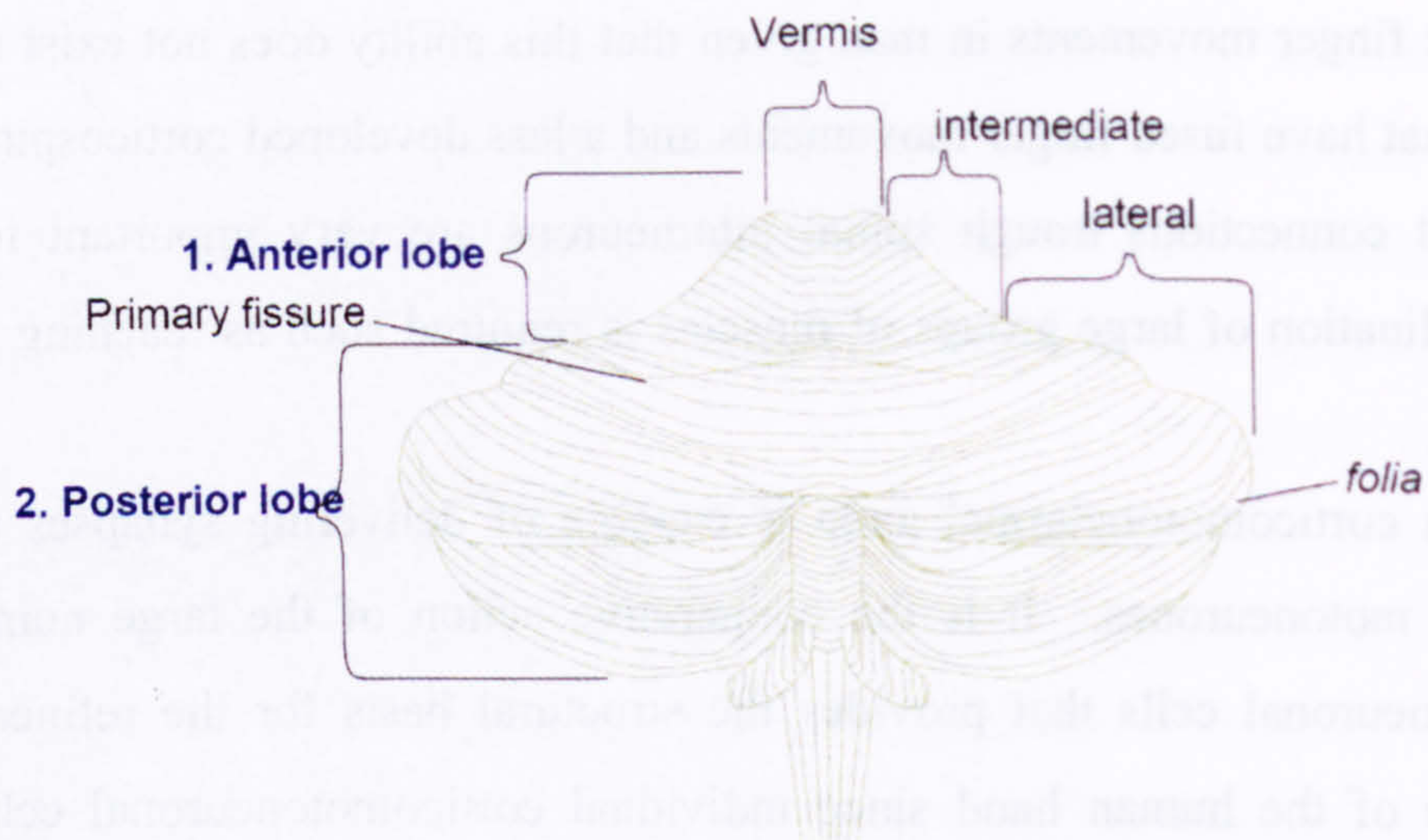


**Fig. 2.6** Anatomy of the cerebellum. From top to bottom it is divided into three lobes; anterior, superior posterior and inferior posterior lobe. From midline out the cerebellum is divided into the vermis, intermediate, and lateral parts. The folia or folds of the cerebellum run horizontally and are smaller than in the cerebral cortex (<http://www.med.uwo.ca> 2005).



A relatively small lesion to the internal capsule of the corticospinal tract may result in contralateral muscle weakness, spasticity, greatly increased deep tendon reflexes, and certain abnormal reflexes. Bilateral corticospinal tract infarction causes tetraparesis or tetraplegia.

### ***2.2.3.1 Cerebellum***

The cerebellum is a central structure extremely significant for motor control from which an EEG signal through the scalp can not be obtained (Fig. 2.6). The cerebellum constitutes only 10-15% of the entire brain weight, yet it contains more than half of all its neurons. It is divided into distinct regions, with each one receiving projections from different parts of the brain and spinal cord and projecting to different motor systems. The major function of the cerebellum is to enable the learning of performance of movements in an accurate and smooth way. Lesions of the cerebellum produce a constellation of disturbances, including intention tremor, ataxia, hypotonus, easy fatigability, and disturbances of speech. Spatial accuracy and temporal coordination of movement suffer, as well as balance, muscle tone, motor learning and certain purely cognitive functions (Kandel et al. 2000).

The cerebellum is provided with vast amounts of information about the goals, commands and feedback signals associated with the planning and performance of movement. The main recipients of the cerebellar output are the premotor and motor systems of the cerebral cortex and brain stem, systems controlling spinal neurons and motor neurons directly. Synaptic transmission in the circuit models is plastic. It was observed that motor disturbances in an animal caused by a partial lesion of the cerebellum were gradually compensated for due to the functional plasticity of cerebellar tissues (Wilson and Keil 1999) a feature that is very important for motor adaptation and learning.

The cerebellum traditionally has been viewed for more than a century as a neural device with a singular motor control function. It has been suggested that the lateralmost part of the cerebellar hemisphere is involved in cognitive as well as motor functions (Leiner et al. 1986; Leiner et al. 1993), including thought, sensory discrimination, attention, working memory, semantic association, verbal learning and memory, and complex problem solving (Allen et al. 1997).



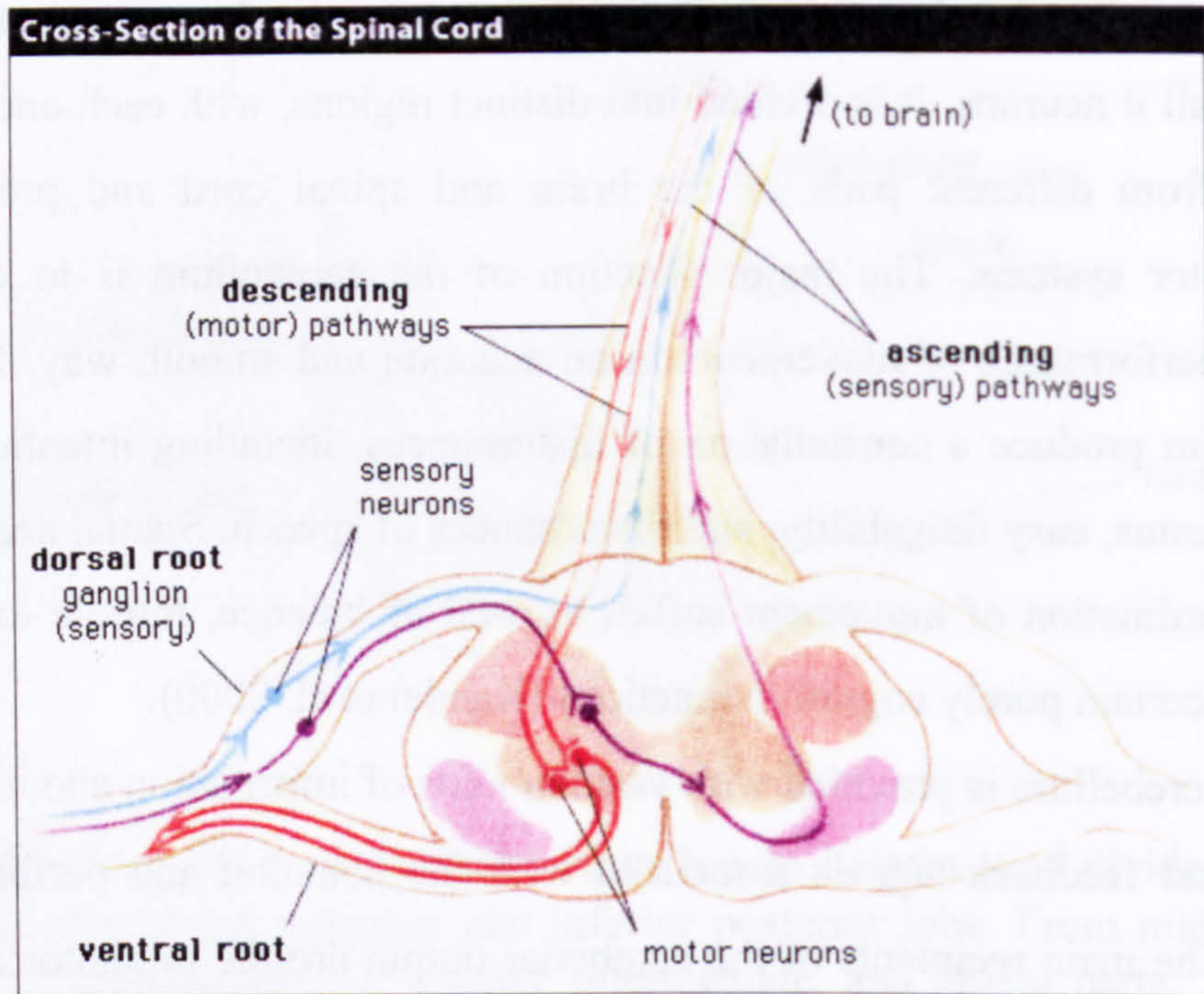


**Fig. 2.7** A cross-section of the spinal cord shows the different view of the organization of the ascending (blue - sensory) and descending (orange - motor) pathways (<http://science-education.nih.gov> 2005).



## **2.3 SPINAL CORD**

The conscious thoughts and intentions may originate in the brain, but the awareness of the limbs and the trunk and the control over posture and movement depend on continuous communication between the brain and the peripheral nervous system through the spinal cord. The spinal cord is structurally and functionally integrated with the brain. It extends from the medulla oblongata of the hindbrain to a level between the first and second lumbar vertebrae of the backbone (Kandel et al. 2000).

A cross section of the spinal cord (Fig. 2.7) reveals long tracts of myelinated nerve fibres, known as white matter, arranged around the periphery of a symmetrical, butterfly-shaped cellular matrix of gray matter. All parts of the spinal gray contain interneurons which distribute and process motor and sensory signals. Some interneurons may modulate or change the character of afferent signals, while others play key roles in generating patterned reflexes. Sensory tracts ascending in the white matter of the spinal cord arise either from cells of spinal ganglia or from intrinsic neurons within the gray matter that receive primary sensory input.

Many of the fibres, or collaterals, of the spinothalamic tracts end upon cell groups in the reticular formation, while the principal tracts convey sensory impulses to relay nuclei in the thalamus. Impulses from stretch receptors are carried by spinocerebellar tracts, transmitting to portions of the anterior lobe of the cerebellum and are involved in mechanisms that automatically regulate muscle tone without reaching consciousness.

Tracts descending to the spinal cord are concerned with voluntary motor function, regulation of muscle tone, reflexes and equilibrium, visceral innervation, and modulation of ascending sensory signals. The largest and most important tract for motor function in humans is the corticospinal tract which arises in the primary motor cortex (M1) and has been described before. Smaller descending tracts, which include the rubrospinal tract, the vestibulospinal tract, and the reticulospinal tract, originate in discrete and diffuse nuclei in the midbrain, pons, and medulla. Most of these brain-stem nuclei themselves receive input from the cerebral cortex, the cerebellar cortex, deep nuclei of the cerebellum, or some combination of these (Kandel et al. 2000).



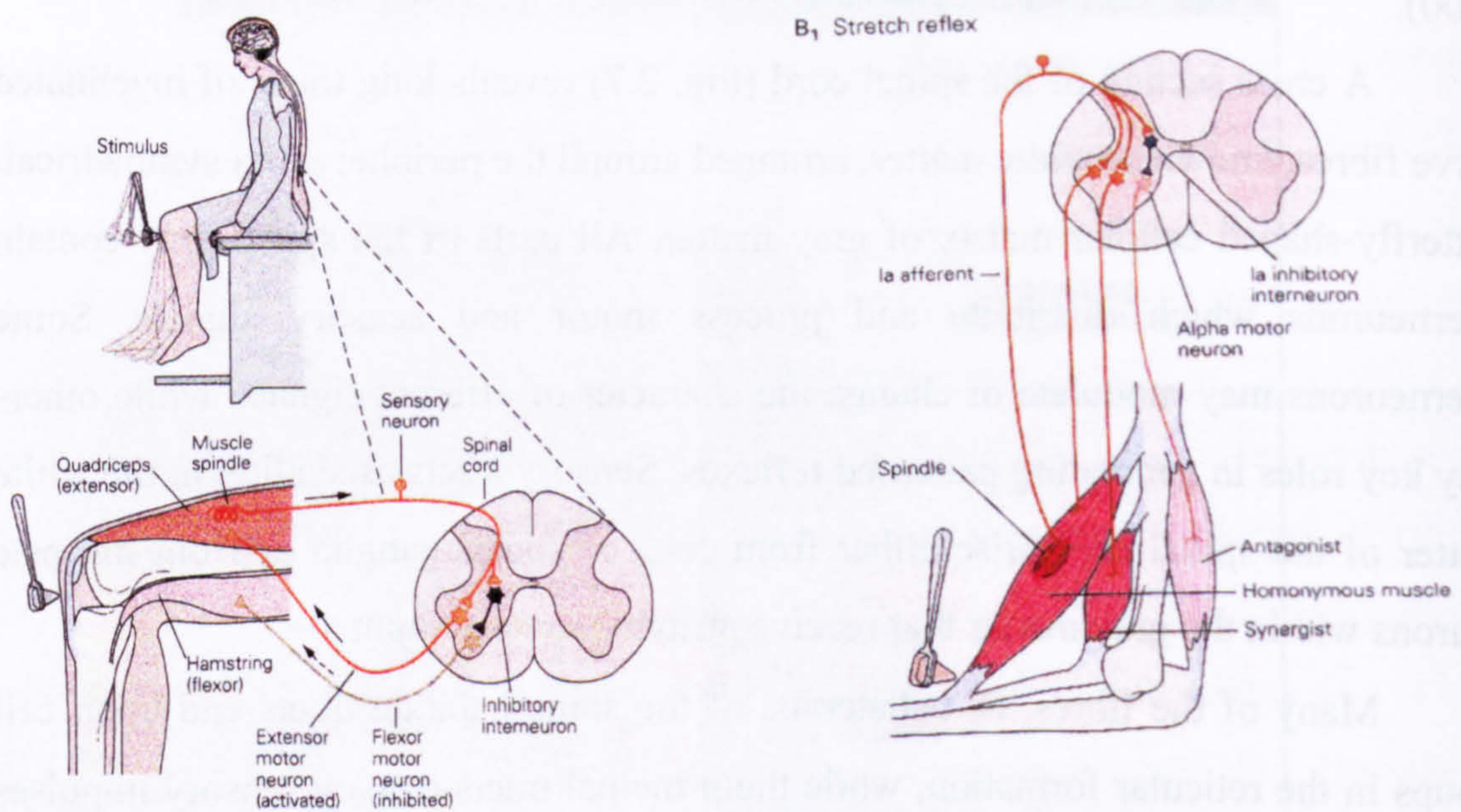


**Fig. 2.8** Stretch reflex. Stretch reflexes are mediated via monosynaptic pathways. Ia afferent fibres from muscle spindles make excitatory connections on two sets of motor neurons: alpha motor neurons that innervate the same (homonymous) muscle from which they arise and motor neurons that innervate synergistic muscles. They also act through inhibitory interneurons to inhibit the motor neurons that innervate antagonist muscles. When a muscle is quickly stretched the Ia afferents increase their firing rate. This leads to a contraction of the same muscle and its synergists and relaxation of the antagonist. The reflex therefore tends to counteract the stretch, enhancing the spring-like properties of the muscles (Kandel et al. 2000).



### ***2.3.1 Spinal Reflexes***

Spinal reflexes are often described as stereotyped motor reactions to an input signal. There are many different spinal reflexes; for example: the flexion (withdrawal) reflex, designed to move the limb away from the site of a harmful stimulus, the myotatic or stretch reflex that is associated with the control of muscle length; and the inverse stretch reflex controlling muscle tension. These short latency reflex responses are generated by the spinal segmental neural circuitry.

#### ***2.3.1.1 The stretch reflex***

The stretch reflex has been connected with control of posture and is associated with the production of physiological tremor (Hallett 1998). The monosynaptic stretch reflex can be easily demonstrated by one of the most well known clinical test the “tendon tap” (Fig. 2.8). The slight but fast muscle elongation caused by the indentation of the tendon by a hammer is sensed by the muscle spindles, receptors located within the muscle. Subsequently the receptors via fast conductive sensory neurons to the spinal cord cause a monosynaptic excitation of motoneurons of the same muscle and consequently a transient reflex contraction. Muscle spindles sense muscle length (static and dynamic) and also transmit these signals to the CNS via large myelinated afferents.

In addition to the short latency spinal reflex initiated by muscle stretch which cannot be voluntarily controlled, there is a later response which can be voluntarily controlled. This long-latency component is believed to have a cortical origin. In humans, particularly for the muscles of the arm, wrist and fingers, there is a second pathway through which a stretch can result in a compensating activity in the motoneurons. This pathway begins with the Ia afferents, goes up the spinal cord through the dorsal column-medial lemniscal pathway, reaches the thalamus, then the somatosensory and motor cortex, and then comes back down to the spinal cord through the cortico-spinal tract. The latency of this loop is about 70 ms. However, unlike the short-loop, its activity is programmable by the brain: voluntarily we can change the response to a stretch (if the stretch is expected, we can ignore it, or respond vigorously). This longer transcortical reflex component may be important in contributing in corticomuscular synchronisation.



## **2.4 PERIPHERAL NERVOUS SYSTEM AND MOVEMENT CONTROL**

The peripheral nervous system connects the CNS with the sensory and motor effectors of the entire body. It is composed of spinal nerves, cranial nerves, and certain parts of the autonomic nervous system. As in the central nervous system, peripheral nervous pathways are made up of neurons and synapses.

### **2.4.1 Motor Neurons and Motor Units**

In the ventral part of the spinal cord, motor neurons are organized into motor pools, which innervate particular muscles. Alpha motor neuron axons terminate on extrafusal muscle fibres. Gamma motor neuron axons terminate on intrafusal muscle fibres. Motor pools extend over two to four spinal segments, with medially situated motor pools innervating axial muscles and laterally situated motor pools project to limb muscles, with those contacting distal muscles located most laterally. A motor unit is a motor neuron and the muscle fibres it controls. Each motor neuron innervates many muscle fibres, which receive input from only one motor neuron. The number of fibres in a motor unit varies according to function and within each muscle. Motor units that contribute to fine movements, such as those of the fingers, usually have a small number of muscle fibres. Large diameter motor neurons typically innervate more muscle fibres (Wise and Shadmehr 2002).

### **2.4.2 Muscle Afferents**

Sensory neurons provide the CNS with information about muscle length force and other information. They have cell bodies in a dorsal root ganglion, with one axon projecting to sensory receptors in the periphery and another terminating in the CNS. The diameter of muscle-afferent axons determines the group they belong to; group I or group II. Group I (Ia and Ib) has the larger fibre diameter and therefore faster transmission rates. Group Ia and II fibres innervate the muscle spindles. Muscle spindles are fine intrafusal muscle fibres that taper at the end and contain a fluid-filled capsule at the centre. Muscle-afferent fibres wrap around muscular elements within the capsule. Group Ia fibres are the primary muscle spindle afferents; group II



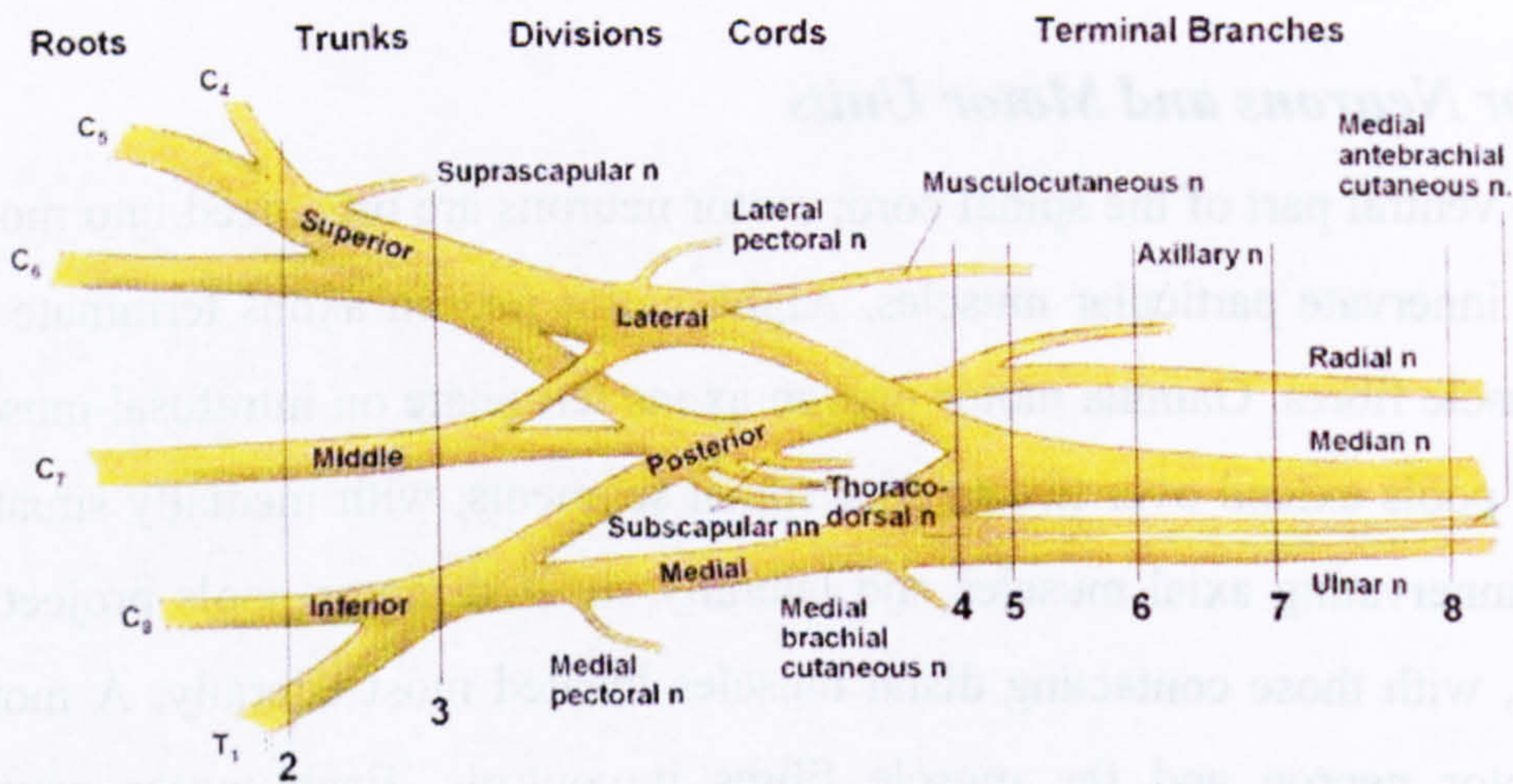


**Fig. 2.9** Schematic Diagram of the brachial plexus  
 ([http://www.asra.com/mbp\\_cd/Figure\\_pages/Figure1.html](http://www.asra.com/mbp_cd/Figure_pages/Figure1.html) 2005)



fibres are called secondary muscle spindle afferents. Group Ib fibres innervate Golgi tendon organs, which are located in the transitional region between extrafusal muscle fibres and tendons (Wise and Shadmehr 2002).

### ***2.4.3 Plexuses of the ventral rami – Brachial Plexus***

Since the experiments performed within the framework of this thesis involve upper extremities, an outline of the brachial plexus, the part of the PNS acting on the arm forearm and the hand is going to be presented (Fig. 2.9). The brachial plexus provides motor, sensory, and autonomic fibres to the shoulder and upper extremities. The three major nerves of the arm, forearm, and hand are the radial, median, and ulnar. The radial nerve innervates the triceps, anconeus, and brachioradialis muscles, eight extensors of the wrist and digits, and one abductor of the hand; it is also sensory to part of the hand. The median nerve branches in the forearm to serve the palmaris longus, two pronator muscles, four flexor muscles, thenar muscles, and lumbrical muscles; most of these serve the wrist and hand. The ulnar nerve serves two flexor muscles and a variety of small muscles of the wrist and hand (Fig. 2.10).

### ***2.4.4 Muscular System***

Muscles produce motion and maintain posture. The muscles which move the body are classified as striated muscles and often referred to as skeletal muscle. Striated muscle fibres are under the control of the axons of the individual motoneurons that innervate them but a single motoneuron can innervate a population of muscle fibres. A motor unit consists of a single motoneuron, its axon and the population of muscle fibres it innervates. It is considered to be a functional element in motor behaviour.

The main experiments in this thesis explored voluntary movement over the wrist joint. The wrist is a complex hinge joint, allowing two degrees of freedom. As well as flexion (controlled by flexor carpi radialis, flexor carpi ulnaris, palmaris longus) and extension (controlled by extensor carpi radialis longus, extensor carpi radialis brevis, extensor carpi ulnaris), it can exhibit adduction (flexor carpi ulnaris, extensor carpi ulnaris) or abduction (flexor carpi radialis, extensor carpi radialis longus, extensor carpi radialis brevis). The human wrist is acted on by muscles in antagonistic pairs, in which each agonist muscle group is paired with an antagonistic muscle group (Fig. 2.10).



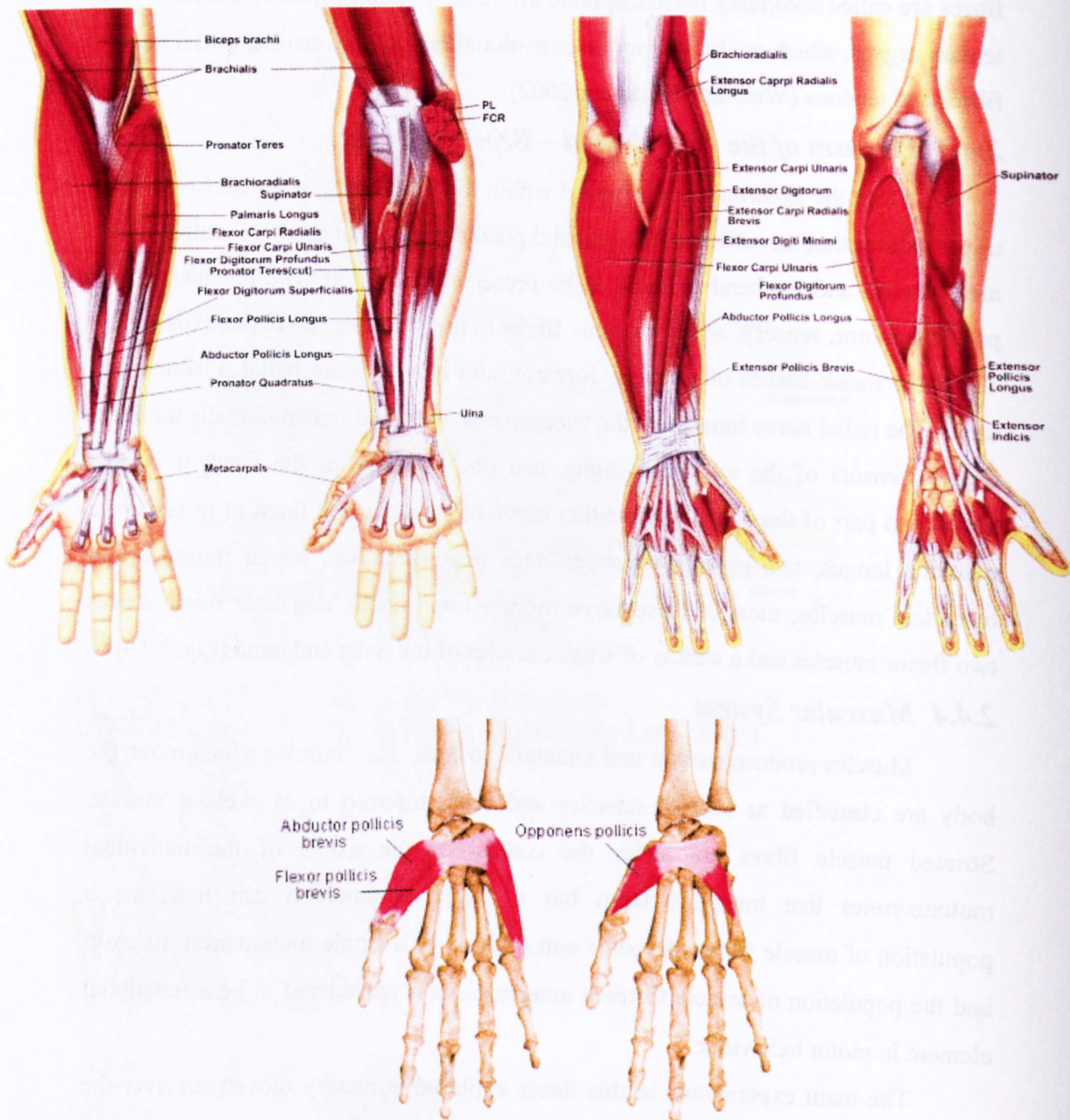


**Fig. 2.10** Anatomy of the forearm and hand muscles  
 (<http://www.paddleball.com/paddles/Accessories/wristbuilder/faqs.htm> 2005)



## ***2.5 MOVEMENT-RELATED CHANGES IN RHYTHMIC BRAIN ACTIVITY***

### ***2.5.1 Rhythmic nature of brain activity***

Rhythms exist throughout nature (Winfree 1980) and it should be no surprise that the brain can also produce and depends upon rhythmic activity. However, due to the lack of a comprehensive understanding of the brain there is no proven and accurate biophysiological model that can describe the brain's oscillatory behaviour. Ongoing research is continuously providing useful findings on rhythmic brain activity. Understanding the role of its rhythms may provide a key to understanding the neural code used by the CNS in transmitting motor information and commands.

### ***2.5.2 Cortical imaging***

Neuroimaging is the non-invasive technology used to explore the spatial and temporal organization of the brain's neural systems. fMRI, PET, EEG, MEG are the main types commonly employed today for the study of motor control. These techniques can be separated into two groups. The first group includes methods that can obtain electrical activity and frequency information, like EEG and MEG. The second group reveals centres of activity without retaining the frequency content of the activity like fMRI and PET. These modern neuroimaging techniques have made a significant contribution towards identifying and localising the brain activity and its relation to human behaviour.

#### ***2.5.2.1 Electroencephalographic activity***

EEG was the main method for obtaining movement related brain activity for the set of experiments performed in the framework of this thesis. The first electrical variations in animal brains were detected in 1875 (Caton 1875 in Goldman et al. 2000). The fact that these signals are the result of underlying brain activity and that they change with the mental state of human subjects, soon became clear. Today it is common knowledge that the sources for the observed electroencephalographic activity are ion currents generated by nerve cell membranes. In this way excitable brain cells collect excitatory and inhibitory inputs and communicate the result to other cells as excitatory or inhibitory input (Feige 1996).



### ***2.5.2.1.1 Origin of electrical brain activity***

The EEG is mainly generated by pyramidal cell postsynaptic potentials that form an extracellular cortical dipole layer. Pyramidal neurons are the major projection neurons in the cortex (Fig. 2.11) (Feige 1996). Today it is known that ion currents through nerve cell membranes are the primary cause of the EEG. Pyramidal cells constantly exchange potassium ions from outside the cell against sodium ions from their interior. The smaller potassium ions can flow through the membrane through specialised ion channels more easily than the sodium ions which results to a net outflow of positively charged potassium ions and a corresponding negative electrical potential between the cell interior and exterior. For a typical resting neuron, the potential is about 70 mV more negative inside the neuron. Excitable brain cells establish with the concentration gradient and electrical polarization a means of collecting excitatory and inhibitory inputs and communicating the result to other nerve cells (Spehlmann et al. 1999).

Excitatory and inhibitory postsynaptic potentials EPSP and IPSP correspond to depolarization or hyperpolarisation of the cell membrane respectively caused by transmission from synaptic terminals of other neurons on the dendrites or the soma of the neuron the transmission acts either through messenger chemicals changing membrane ion permeability or by direct electrical contact. At the basal part of the cell soma where the axon is formed, excitatory and inhibitory postsynaptic potentials sum within the cell to determine the firing frequency at which the action potentials occur. The action potentials are actively carried along the axon sometimes over large distances through the activity of additional voltage and time dependent ion channels in the axon membrane that cause a temporary strong depolarisation and even a polarity reversal in response to a small initial trigger depolarization. Arriving at the synaptic endings the action potentials influence the firing frequencies of other neurons by eliciting postsynaptic potential that summate in the cortex and flow through the surrounding conductive tissue to reach the scalp surface where they are recorded as the EEG. Several factors affect this and include the depth and orientation of the net primary current. In addition to postsynaptic potentials, the action potentials probably also contribute to the EEG, although their role has not clearly been



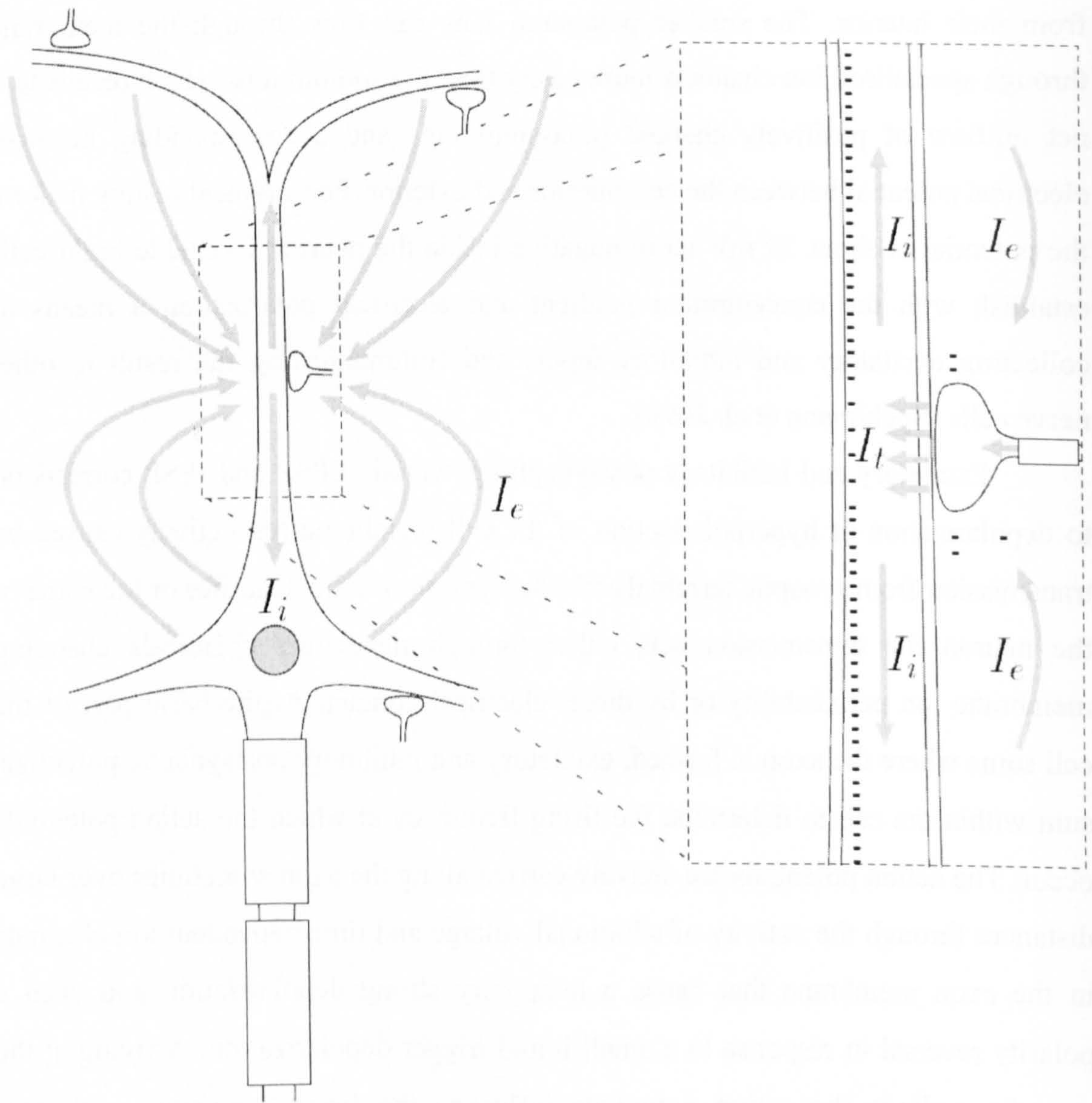


**Fig. 2.11** Schematic view of a pyramidal cell. Excitatory and inhibitory synapses connect to the neurons dendrites and ALTER the resting membrane potential. The summed changes influence the membrane potential at the axon myelinated axon at the base of the neuron where action potentials originate. The detail on the right shows an active excitatory synapse which causes a current  $I_t$  flow of positive charge into the dendrite, reducing the negative charge inside and increasing it outside. The charge densities are then compensated by the intracellular and extracellular currents  $I_i$  and  $I_e$  (Feige 1996).



established. They have a much smaller field distribution (less penetration into the extracellular scale) and are much shorter in duration than postsynaptic potentials (about 1ms compared to postsynaptic potentials of 15 to more than 200ms). Action potentials, therefore do not contribute significantly to scalp EEG recordings (Kandel et al. 2000).

A dipole point source occurs when a single positive and single negative charge are located close to each other at a single point which may be a simple useful dipole approximation of a more complex pattern of electrical sources in the brain. The dipole orientation is represented by a line connecting the negative and positive charges. A vertical or radial dipole point source is oriented from the centre of the brain to the brain surface while a horizontal or tangential dipole is oriented parallel to the brain surface (Murro 1999).

### ***2.5.2.2 Magnetoencephalographic Activity***

Another way of measuring brain activity in a non invasive manner is Magnetoencephalography (MEG) that measures the magnetic fields associated with electrical current flow. MEG is complementary to EEG and is often used in studies regarding movement related activity. The first attempts to record the magnetic activity of the brain involved the use of a magnetic coil (Cohen 1968) but this only became an effective way of measuring brain activity with the introduction of superconducting sensors (Cohen 1972). Their high sensitivity to small fields is very important since the strength of the magnetic field outside the head is only about 500fT, 8 orders of magnitude smaller than earth's magnetic field. In contrast with EEG, the sources of MEG are mainly intradentritic currents resulting from EPSP and IPSPs, as much of the magnetic fields produced by the diffuse volume current flow or by transmembrane currents cancel due to symmetry. Action potentials are also characterised by two current dipoles of opposite direction, whose magnetic fields mostly cancel (Feige 1996).

Both MEG and EEG have advantages and disadvantages over each other. For example while tissues are transparent to magnetic fields recorded by MEG, electric currents flowing through tissues and detected by EEG are affected by the different conductivities. This distorts the signal and requires a volume conductor model in order to accurately project the underlying activity that produces the EEG. In contrast



MEG can not record activity for radially oriented dipoles within a spherical head while EEG is most sensitive to these sources. However, because of the folded brain structure, a large part of the activity is located in sulci, this is not an important limitation for MEG. The advantages and disadvantages of each method are still under discussion and much of this relates to cost and availability of the different methods. MEG has been successful in source localisation as a result of the simple head model required in contrast to complicated volume conductor models of EEG. EEG on the other side has a very long record in clinical applications like epilepsy, sleep research and neuropharmacology. In recent years with the increase of spatial density of electrodes (10 electrode configurations have been replaced with 32-128 and in some cases 256 electrodes) and the progress in volume conductor models combined with sophisticated frequency domain analysis methods, have increased the quality of obtained data and have made source localisation for EEG more realistic and accurate. The increase of the number of recorded channels was a result of the decrease of the cost of amplifying hardware as well as the cheap processing power offered by modern personal computers. The high cost of modern MEG devices combined with more flexible EEG experimental setups give to the latter an advantage. The different and complementary nature of these methods also suggests that could be used together for obtaining the maximum of information (Feige 1996).

### ***2.5.2.3 Electrocorticogram (ECoG)***

ECoG is the technique of recording the electrical activity of the cerebral cortex by means of surgically inserted electrodes placed directly on it. The main advantage over the EEG is the more direct nature of the signal obtained avoiding the distortion of the signals that occur when currents go through skull and skin. Results obtained with electrocorticography are better than with EEG since ECoG can extend the range of frequencies seen during imaging and includes “high gamma” activity which is absent in EEG due to the low pass filtering characteristics of the skull and other interposed tissues (Brown 2000). Intraoperative ECoG is acquired during surgery usually with local anaesthesia with the patient awake.

### ***2.5.2.4 Positron Emission Tomography***

Positron emission tomography has also been used in motor control experiments. It is a nuclear medicine visualisation technique that produces an image



of the distribution of a previously administered radionuclide in any section in the body. The image interpretation is based on the fact that changes in the cellular activity of the brain are invariably accompanied by changes in the local blood flow and oxygen and glucose (radioactively labelled materials) accumulate in brain areas that are metabolically active. This type of method provides a functional view of the brain. The spatial resolution of PET, between 3-8mm is better than that of EEG and event related electric potentials (Kandel et al. 2000).

#### ***2.5.2.5 Functional Magnetic Resonance Imaging (fMRI)***

fMRI is a technique for determining which parts of the brain are activated by different types of physical sensation or activity, such as sight, sound or the movement of a subject's fingers. Of the two current ways of mapping alterations in neuronal activation non invasively, the most commonly used method relies on the weak magnetic interactions between the nuclear spins of water protons in tissue and blood, and the paramagnetic deoxyhemoglobin molecule, termed BOLD (blood oxygen level-dependent) contrast, (Ogawa and Lee 1990; Ogawa et al. 1990; Ogawa et al. 1990) and is similar to the effect described for blood alone (Thulborn et al. 1982).

fMRI is subject to a number of limitations which limit its use. It relies on secondary and tertiary responses, metabolic and hemodynamic, to increase neuronal activity with limiting temporal characteristics and spatial specificity. With respect to temporal resolution, the sluggish metabolic response and even more sluggish hemodynamic response to changes in neuronal activity suggest that better than approximately 0.5sec time resolution may not be achievable with current fMRI techniques (Wilson and Keil 1999).

#### ***2.5.3 Organisation of the Nervous System at Cell Level***

In order to understand the way the nervous system controls human movement it has been useful to examine the influences of different subcomponents on motor control. Equally important for the comprehension of neural functions and the correct interpretation of EEG signals is to understand the function of the nervous system at the cell level.



Neurons in the nervous system are organized into highly interconnected neural networks. A simple neural pathway is formed by a chain of nerve cells linked end-to-end to convey electrical messages from one part of the body to another (i.e. from a sense organ to a muscle, or from one part of the nervous system to another) (Mandl 2000). Most neurons in the CNS are “spontaneously” active even in the absence of any deliberate physical or mental activity, continuously generating sequences of action potentials even during sleep. The frequency of such action potentials (APs) may range from about 1 impulse/sec, to perhaps 100 - 200 impulses/sec. Such neurons may respond to an appropriate stimulus with either an increase, “excitation”, up to a maximum of some 1000 APs/sec, or a decrease, “inhibition”, down to zero APs/sec in the spontaneous discharge level, suggesting that information about the stimulus event is encoded either via excitation or via inhibition of the resting level of the spontaneous action potential frequency. This means that for the nervous system both excitation and inhibition have specific informational value (Mandl 2000).

The signal transmission from sense organ to muscle, in response to a sensory stimulus, is a complicated process: At the receptors, as well as at the synaptic junctions (either between consecutive neurons, or between neuron and muscle), non-propagating graded potentials (receptor potentials, synaptic potentials) are generated whose size is a function of stimulus intensity and duration. Along neuronal axons and muscle fibres, however, the relevant signals consist of all-or-none action potentials (action potentials, spike potentials), initiated by a given local receptor potential or synaptic potential, and propagating at finite speeds along the axonal membrane of the neuron to initiate another local graded potential in the next neuron. The frequency of these action potentials is related to the magnitude (amplitude and duration) of the local graded (receptor or synaptic) potentials, and by implication to the magnitude of the external stimulus (Mandl 2000).

The information about the outside world is therefore initially encoded by sensory receptors as an amplitude-modulated slowly varying local electrical potential (receptor potential), is transmitted via frequency-modulated (pulse-coded) signals along axons, and then replicated again as a local amplitude-modulated signal (synaptic potential) at each of the cell-to-cell (or cell-to-muscle) junctions.



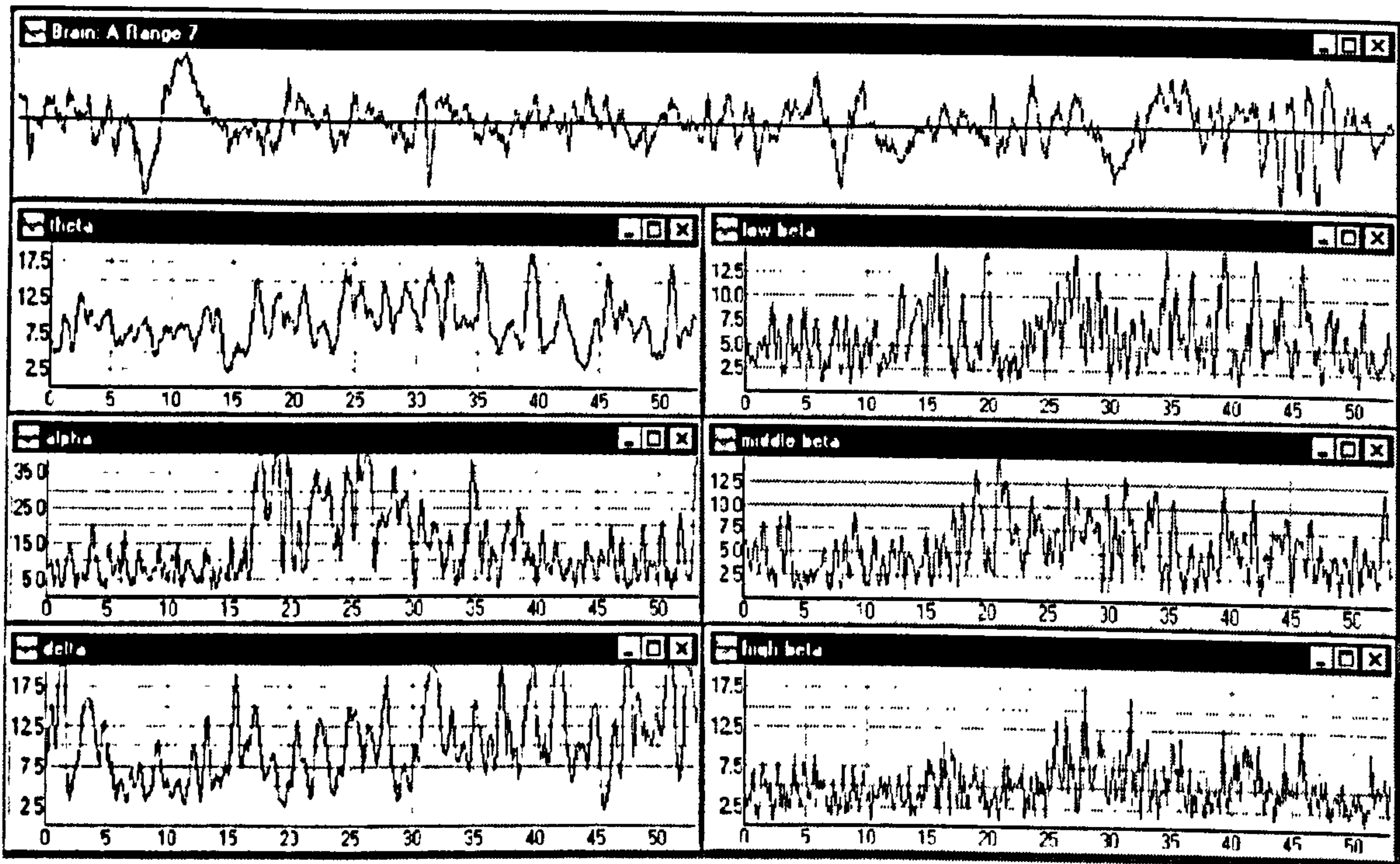


**Fig. 2.12** Raw signal and filtered components identified in the scalp EEG. The labels on the task-bars of individual windows indicate the individual band. The EEG signal is represented in  $\mu\text{V}$  (Allanson 2000).



Accordingly, all afferent sensory information about the external world, and all efferent motor commands, are encoded and transmitted by the nervous system in alternating patterns of amplitude modulated and pulse-code (frequency) modulated electrical energy - the universal “language” of the nervous system (Mandl 2000).

#### ***2.5.4 Cortical Rhythms - Frequency Bands***

The first frequency component of the human EEG to be detected was alpha activity, due to its high amplitude the similarities across different individuals. This was the first indication that frequency is an important feature of EEG activity. Historically the frequency bands that have been commonly used to characterise the components of the EEG are:

- 0.5-3 Hz delta
- 4-7 theta
- 8-13 alpha
- 14-30 beta
- >30 gamma

Some of the above mentioned frequency components can be seen in Fig. 2.12

##### ***2.5.4.1 Idling Alpha activity.***

The alpha rhythm is one of the most dominant frequency bands in the EEG spectrum and its variations suggest that it is functionally meaningful. However, the fact that strong alpha activity often appears when eyes are shut and disappears when they reopen would rather suggest that alpha activity is inversely correlated to the brain’s processing of information. In viewing the brain as an information system, the information content of a series of states is correlated to the system’s entropy. So when the predictability of a signal is high (strong alpha) which means low entropy the information content of this frequency is low. In contrast when information content is high, the neurons are differentially and independently active with the overall activation showing little or no regular time course. Therefore, the alpha rhythm does not appear to be the result of information processing. However, when it locally disappears it is likely that it indicates the activation of the corresponding cortical area (Feige 1996).



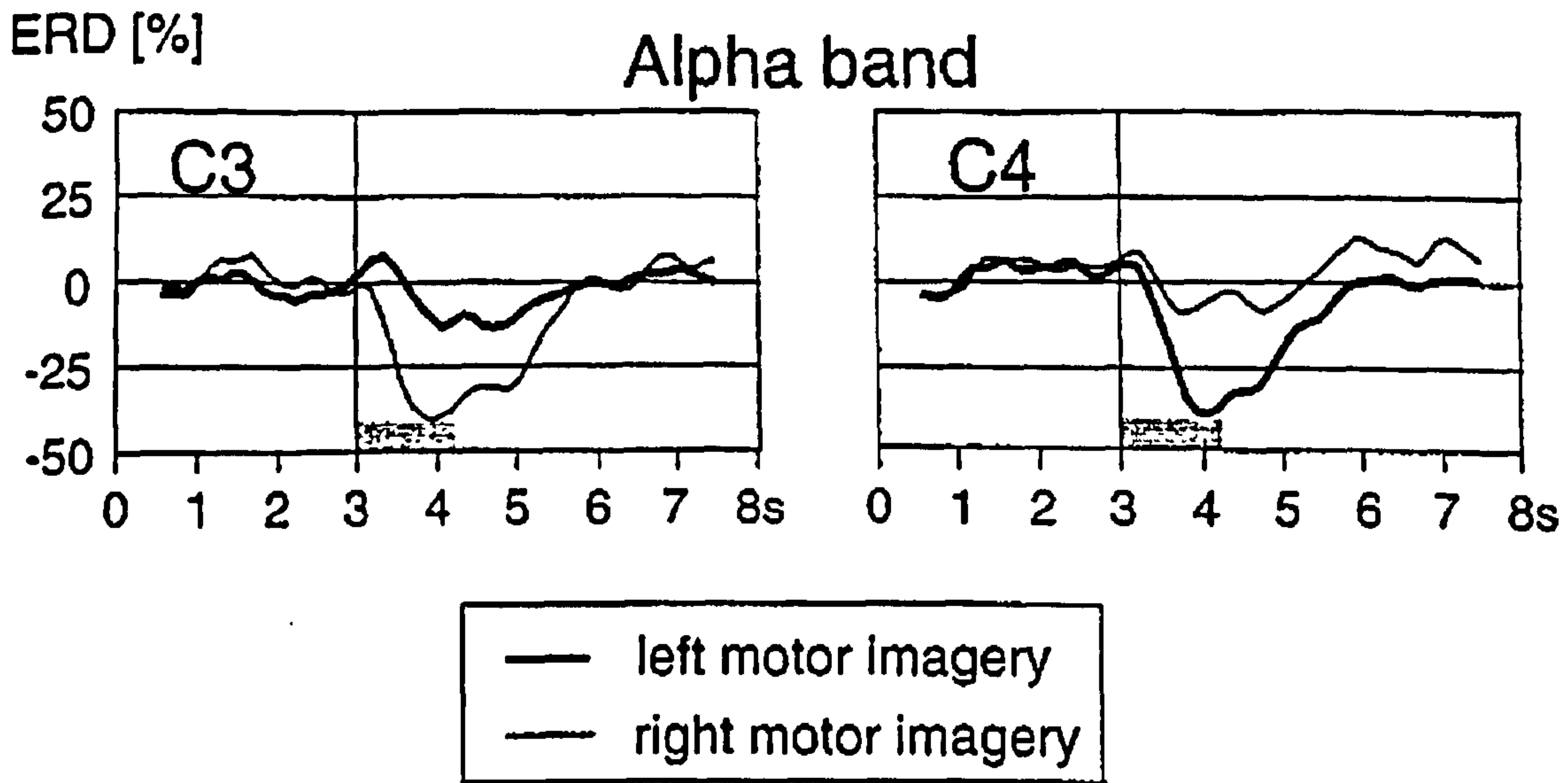


**Fig. 2.13** Grand average alpha band ERD curves recorded during motor imagery from the left (C3) and right sensorimotor cortex (C4) of 16 subjects. Positive and negative deflections, with respect to baseline (0.5s to 2.5s), represent a band power increase (ERS) and decrease (ERD), respectively. The gray bar indicates the time period of cue presentation (Neuper and Pfurtscheller 1996).



It is a paradox that desynchronisation (decrease of synchronous oscillatory activity) of EEG activity appears to facilitate the local high frequency synchronisation (increase of synchronous oscillatory activity) for sensory and motor processing. It has been long known to researchers that inactive cortex is characterised by low synchronous idling activity (at around 10 and 20 Hz) that are blocked by sensory stimuli or voluntary movements (Penfield and Boldrey 1937). The occipital alpha rhythm of the visual cortex, the “mu” rhythm of the sensorimotor cortex, and the “tau” rhythm of the auditory cortex are rhythms in the alpha frequency band connected with the selective idling of specific cortical areas. Furthermore, the desynchronisation seems to be localised to the cortical area involved. For example, for finger movement the mu rhythm seems to be suppressed over the sensory cortex that is related with finger muscle control. It is interesting that motor imagery suppresses the mu rhythm (Fig. 2.13, Fig. 2.14, Fig. 2.15) (Neuper and Pfurtscheller 1996; Pfurtscheller and Neuper 1997) as with motor planning and visual imagery suppress the occipital alpha rhythm (Salenius et al. 1995).

Event related synchronisation, (ERS) is the opposite of ERD and represents a localised increase in synchronous oscillatory activity timelocked to a specific event. It is interesting to note that the decrease in alpha rhythm in various cortical areas seems to enhance alpha activity in other areas and vice versa. ERD was found over the primary hand area during finger movement and over the primary foot area during toe movement. ERS, in the form of an enhanced 10Hz “mu” rhythm on electrodes overlying the primary hand area, was observed during visual processing but also during foot movement. In both cases, the hand area is not needed to perform a task and, therefore, can be considered to be in an idling state (Pfurtscheller et al. 1997). During visual stimulation, an ERD over the occipital cortex is accompanied by 10Hz ERS over the sensory cortex, while during movement or medial nerve stimulation the cortex displays the opposite behaviour. This inverse behaviour has been associated with attentional processes in which ERD is considered to represent increased selective attention to a task while ERS represents attentional decrease (Pfurtscheller 1989; Klimesch et al. 1996).

The ability of the CNS to display linked rhythmic behaviour of functionally discrete cortical components suggests the existence of a common oscillatory input. It



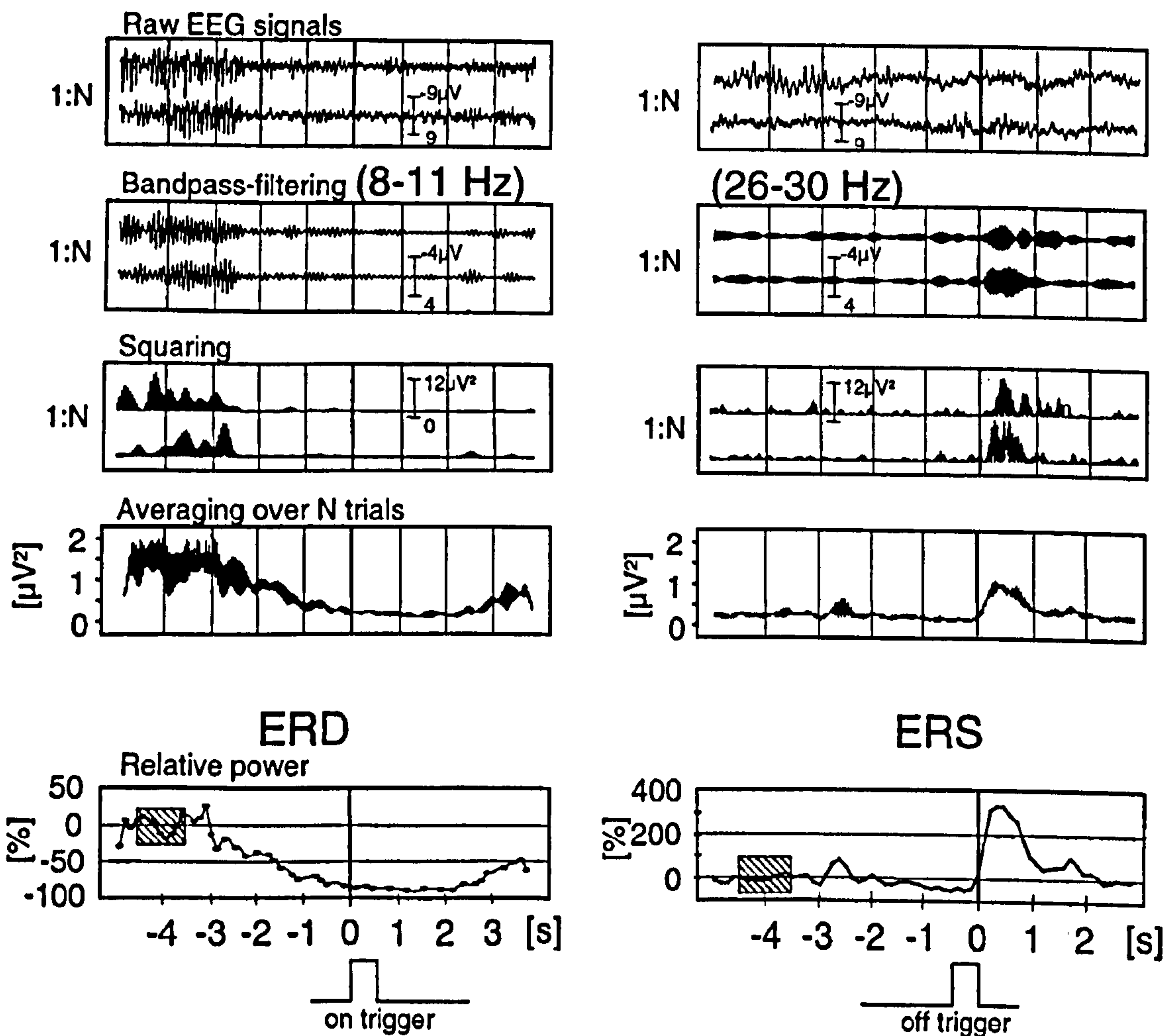


**Fig. 2.14** Principle of ERD (left panel) and ERS (right panel) processing. A decrease of band power indicates ERD and an increase of band power ERS. Note the different triggering with ERD and ERS processing (modified from (Pfurtscheller et al. 1999)).



is quite likely that subcortical structures participate in this process. In this respect the thalamus has been considered to be responsible for the idling rhythmic input since oscillatory generators have been identified within it (Kozelka and Pedley 1990; Steriade et al. 1990; Pfurtscheller 2003) (Feige 1996). The extensive connections between the thalamus with the sensory cortical areas, its involvement in attentional processes and its role as a relay and powerful processing centre underlines its potential role in gating processes that synchronise or desynchronise discrete cortical areas. Desynchronized alpha band activity has also been attributed to increased cellular excitability in thalamocortical systems, whereas synchronized alpha band activity occurring immediately after movement execution, or over remote cortical regions, reflects a cortical idling state (Steriade et al. 1993; Toro et al. 1994; Pfurtscheller and Lopes da Silva 1999; Deiber et al. 2001)

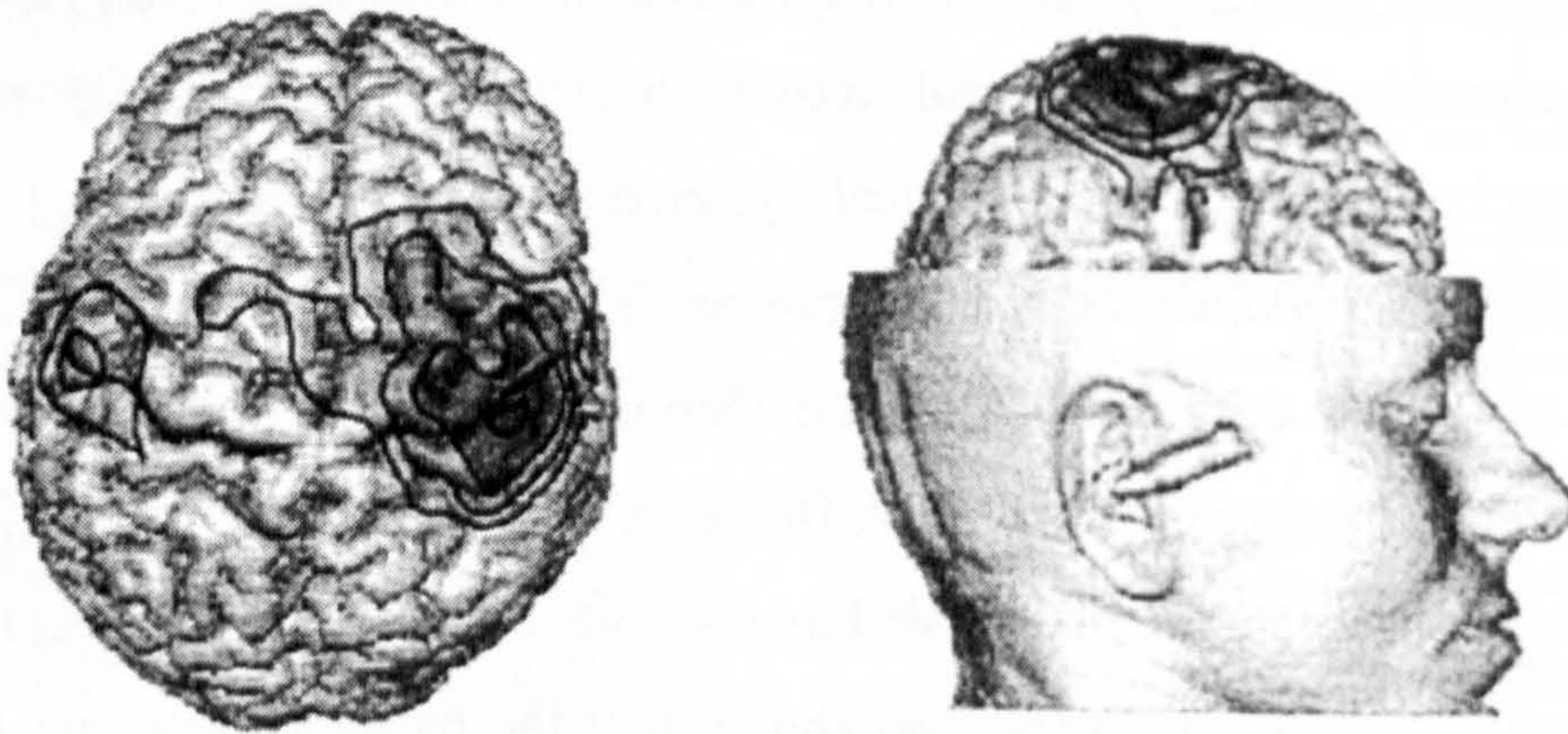
The basal ganglia may also have a role in cortical ERS/ERD. Work on patients with Parkinson's disease has shown that the basal ganglia can liberate the frontal cortex from alpha idling rhythms (desynchronisation), so that they may become coherent in the gamma range. (Brown and Marsden 1999; Wang et al. 1999). Basal ganglia ERS/ERD were also studied during the invasive exploration of an epileptic surgery candidate. During a simple self-paced motor task, a power decline (ERD) was observed in the putamen in both the alpha and beta frequency bands, and a rebound phenomenon (ERS) in the beta frequency band, concurrent with the movement of each hand (Sochurkova and Rektor 2003).

#### ***2.5.4.2 Non Idling Alpha Activity***

As stated already, spontaneous alpha rhythms has been often considered to reflect an idling state of the brains functional components. However, the alpha rhythm is more than just a spontaneous rhythm. It is also considered to be a prototype of a dynamic process which governs a large ensemble of integrative brain functions (Schurmann and Basar 2001). Alpha patterns can be induced or initiated by a stimulus without being time locked to it. Alpha patterns can also be evoked precisely time-locked to a stimulus (Basar et al., in: Basar and Bullock, 1992). Alpha patterns can be movement- and memory-related (Pfurtscheller and Klimesch, in: Basar and Bullock, 1992). Finally, alpha patterns can be emitted: well trained subjects emitted time-locked bursts of alpha band energy for up to 1s before an



## Left motor imagery



## Right motor imagery

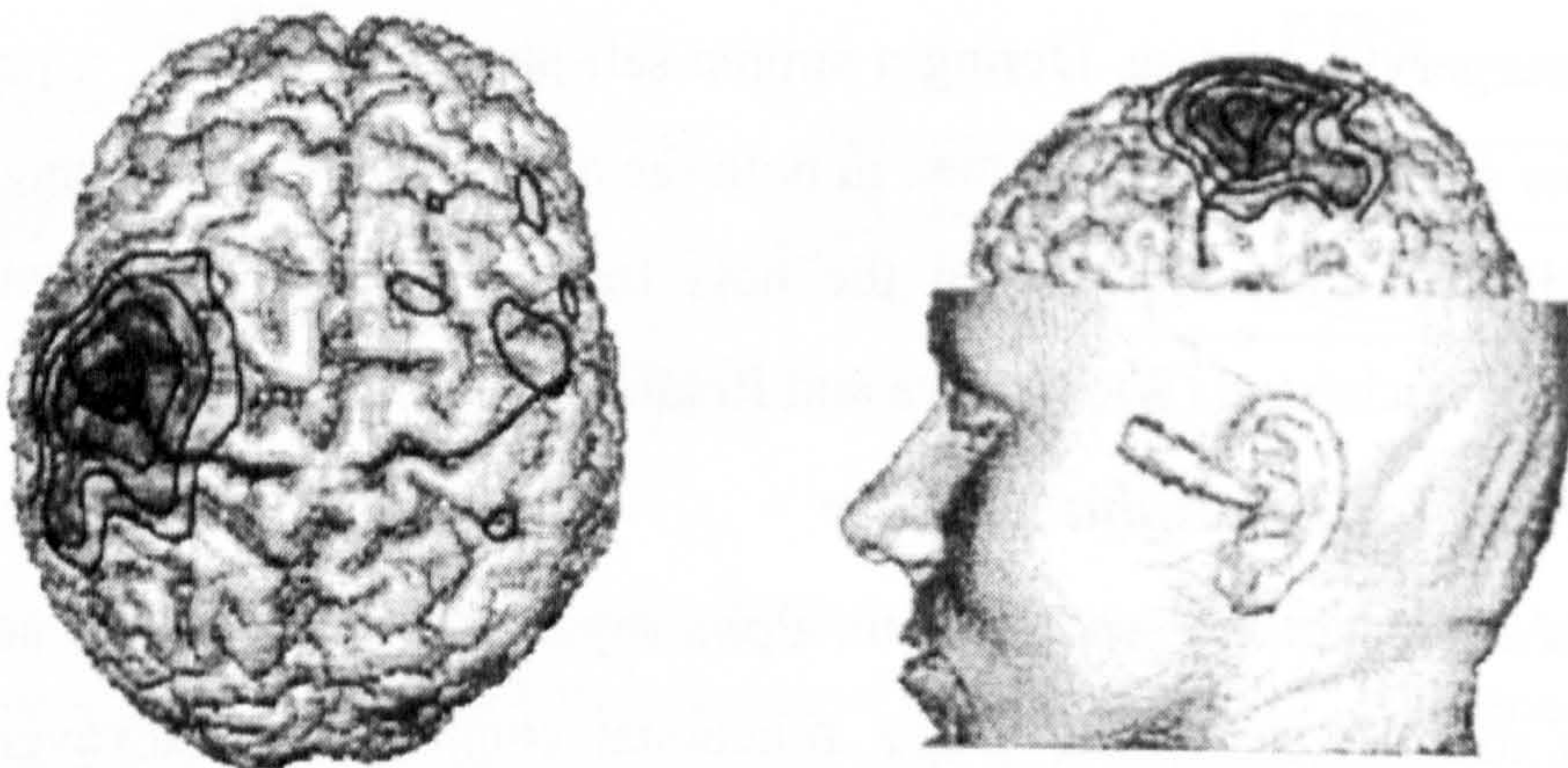


**Fig. 2.15** ERD maps for a single subject calculated for the cortical surface of a realistic head model. The spline surface Laplacian method was applied to the bandpass filtered (9–13 Hz) single-trial EEG data and the distribution of the alpha band ERD was calculated for left and right motor imagery. The spline Laplace maps are shown at  $t = 625$  ms after presentation of the cue (arrow in left or right direction) (Neuper and Pfurtscheller 1996).



expected target. The alpha locking to the future moment, when a target will be delivered, is robust and statistically significant. (Basar et al., in: Basar and Bullock, 1992).

The dynamics of alpha processes (spontaneous, evoked induced, emitted) in connection to interrelated, parallel or cognitive processes like memory movement and sensation give an illustrative picture of the complexity and multimodality of CNS. On the other side it creates a framework for the deeper understanding of the integrative functions of the CNS through a dynamic approach and combining different levels of analysis. Results from non-linear dynamics support the hypothesis that alpha activity is not simple “noise” but a deterministic signal rather than an idling process of the brain (Schurmann and Basar 2001).

An idling and non idling aspect of the alpha band could also coexist in the same frequency band. Furthermore considering the idling process not as a passive but as a significant functional component we could say that both theories do not contradict but complement each other. That partially explains the paradox that experiments measuring alpha band power report desynchronisation while those measuring evoked alpha may report synchronisation (Klimesch et al. 2000).

A study on non linearity of alpha rhythm involving recordings and a simulation model showed that the alpha rhythm is a dynamic heterogeneous entity with two types of alpha rhythm: 98.75% of the epochs recorded (type I alpha - idling) could not be distinguished from filtered noise during which the activity of the brain has such a high complexity that it cannot be distinguished from a random process. In 1.25% of the epochs recorded (type II alpha – non idling) non-linearity was found (Stam et al. 1999).

#### ***2.5.4.3 Beta and Gamma band synchronisation/desynchronisation***

Idling rhythms have been identified in beta and gamma bands. Considering the near 10, 20, 40 Hz frequencies and the high amplitude of alpha activity it has been suggested that the last two are harmonics of the alpha activity. Even though harmonics exist in a small percentage of the population beta band existence has been demonstrated even in the absence of alpha activity. The different spatial and temporal characteristics of observed ERS/ERD for the three bands also suggest the distinct nature and functional attributes of the discussed rhythms.



More specifically, beta-band ERD follows a distinct but similar pattern to alpha band ERD with power decreasing before the onset and during movement and recover after the movement has been established. The duration of the decrease of beta band ERD seems to be shorter than the one of the alpha band with quicker recovery and during maintained contractions beta band synchronisation goes over the rest state level for a short period of time soon after the task has been established, in contrast to the alpha band. The spatial distribution of the beta band ERD is less widespread than alpha band and is more anteriorly localised.

It has been suggested that the basal ganglia control the release of cortical elements from low-frequency alpha and beta rhythmic idling activity during voluntary movement (Brown and Marsden 1999). A study involving voluntary thumb, index finger and wrist movement showed a similar ERD was found for “mu” (10-12 Hz) and for two frequency bands in the range of beta (16-20 Hz and 20-24 Hz) during motor preparation, while significant differences concerning beta synchronization were observed after movement off-set. Pre-movement desynchronisation seems therefore relatively independent of the forthcoming type of movement, whereas the post-movement beta synchronization might depend on the activated muscle mass (Pfurtscheller et al. 1998). Since basal ganglia have been implicated in the initiation of motor responses (Hauber 1998) it is quite possible that the basal ganglia are responsible for the pre-movement desynchronisation while a different structure like the thalamus induces post movement desynchronisation. Also the post-movement beta ERS, that expresses the recovery of the primary motor area after movement, in patients with Parkinson’s disease (basal ganglia disorder) is significantly smaller than normal subjects (Pfurtscheller et al. 1998).

The behaviour of alpha and beta event related desynchronisation is different for movements around different joints. The spatial distribution of the alpha- and beta-ERD and of the post-movement beta-ERS for proximal (shoulder) and distal (finger) movements, shows topographic differences which may refer to the somatotopic organization of the primary sensorimotor cortex with shoulder representation medial to hand and fingers (Stancak et al. 2000). In addition, extension and flexion movements of a joint like a finger joint, induce unequal beta synchronization over



the contralateral primary motor area possibly due to different complexity of the neuronal networks controlling these movements (Stancak 2000).

Even though the view that EEG ERD in the alpha and beta bands express functional activation of the sensorimotor cortex, ECoG studies have revealed differences in studies concentrating on response and not preparation. Beta and alpha ERD seemed to correspond to the traditional somatotopy with the beta being more discrete and specific. However, beta ERD was often transient or absent. The alpha ERD was more widespread than previously thought with overlapping somatotopic representations of different body parts. It was suggested that alpha ERD may reflect activity within a broad synaptic network with distributed cortical representations (Crone et al. 1998).

Gamma band oscillations are not generally observed over a large proportion of the population. For subjects that display such behaviour, gamma band oscillations have been observed during fast and slow finger movements and strong isometric contractions. The 40-Hz oscillations (36-40 Hz) reveal a sharp power increase shortly before movement-onset and have been associated with attentional mechanisms of movement preparation (Mima et al. 1999). Cortical gamma band oscillations have been associated with focused attention and the efferent drive to the muscles during very strong contraction (partly correlated with the Piper rhythm in the electromyogram) (Brown et al. 1998; Mima et al. 1999). However, the 40 Hz EEG-EMG coherence is not specific to the muscle Piper rhythm which is seen only with strong contraction. (Mima et al. 2001)

Increase in the gamma range activity while decrease in the alpha range activity has been observed in forearm sensorimotor cortex and adjacent areas during the performance of visuomotor tasks like tracking a moving visual target with a joystick-controlled cursor, threading pieces of tubing, and pinching the fingers sequentially against the thumb (Aoki et al. 1999). These experiments further support the hypothesis that coherent gamma oscillations may play a role in sensorimotor integration of attention.

As has been already shown, widespread and large amplitude alpha oscillations do not necessarily reflect information process within the brain but more an idling or regulatory state. Higher entropy corresponding to more irregular neuron



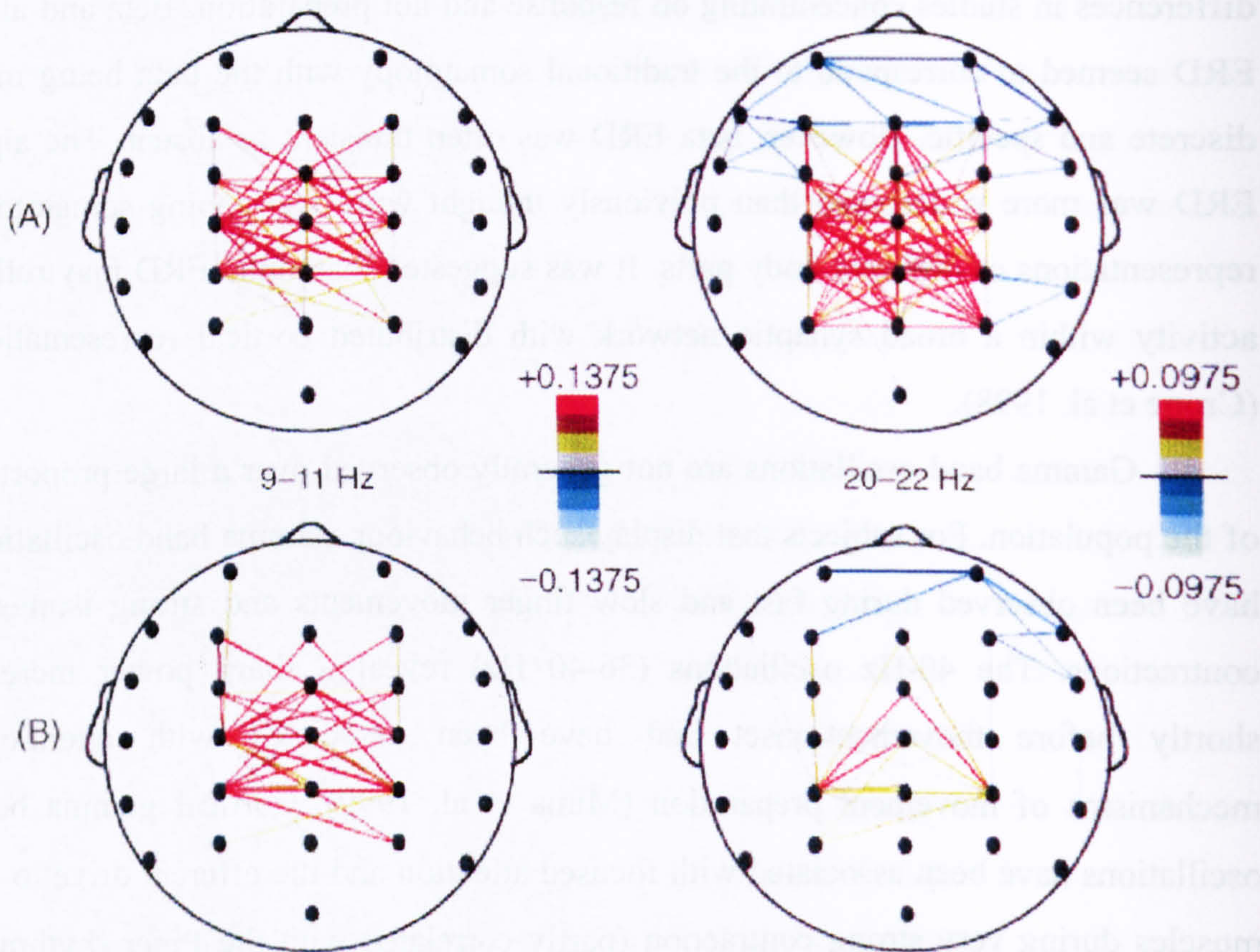


**Fig. 2.16** Grand average of topographic task-related coherence maps for 8 subjects. The dots indicate electrode positions. Task-related coherence changes are shown in colour-coded lines. Red lines indicate maximal task-related coherence increases (“functional coupling”) and light green indicates maximal task-related coherence decreases (“decoupling”). In all frequency bands and both types of movements [internally paced finger extensions (A); externally paced finger extensions (B)], task-related coherence increases were focused over the central region with a maximum of links converging on electrode C3, and to a smaller extent CP3 and CP4. With both internally paced and externally paced finger extensions, links were present between left and right lateral central electrodes and between left central and mesial frontocentral electrodes. The main difference between conditions was the increased amplitude and number of links between bilateral and mesial premotor and sensorimotor areas during internally paced finger extensions. This was most prominent in the 20–22 Hz band. In the 9–11 Hz frequency range, this difference between conditions was smaller but not significant (Gerloff et al. 1998). Electrode positions are given according to the international 10-20 system.



firing with lower predictability, reflecting higher information processing. However, if the activity of the neurons was completely irregular, the activity would be almost impossible to be measured. Furthermore, actions controlled by the brain, such as movements, cannot be controlled adequately by single neurons given the irregular firing nature of single cells. So it is more likely tasks to be controlled by cell assemblies of many broadly tuned neurons would make possible to achieve the level of accuracy required for movement tasks. The neurons are functionally linked through a network of excitatory and inhibitory postsynaptic connections. It is known that a neuron receives input from more than one EPSP's and IPSP's (Feige 1996). Temporal summation involves action potentials arriving at the terminus of one presynaptic axon at close intervals so that each succeeding postsynaptic EPSP builds on the previous ones. In this way, the postsynaptic depolarisations accumulate to form a grand EPSP that results in a new frequency of action potentials in the axon of the postsynaptic neuron. In spatial summation, the information input (action potential frequency) in a number of presynaptic neurons arrives sufficiently close together to release enough neurotransmitter chemical to accumulate and depolarize a sufficient area of the postsynaptic membrane to attain a grand EPSP and generate a new frequency of action potentials in the postsynaptic axon.

In this context, synchronisation of groups of neurons may reflect information processing; hypothesis that may seem to contradict what has been presented so far. However, the functional synchronisation would be quite localised compared with the widespread nature of idling rhythms and its amplitude would be significantly smaller, which also makes it difficult to identify within a dominant idling spectrum. The variable occurrence time, frequencies and locations depending on the performed task make things even more complicated as far as detecting and localising this kind of activity is concerned (Feige 1996).

#### ***2.5.4.4 Intracortical Synchronisation – Desynchronisation***

One very important issue is the intracortical synchronisation in the form of intracortical coherence between multichannel recordings of the EEG signal. Synchrony has long been regarded as a correlate of neuronal connections between involved cortical areas that reflects information flow within different functional components of the brain (Feige 1996) and can be revealed by studying task related



changes in neuronal activation. These task dependent coupling changes are referred to as task related coherence (TRCoh). Various studies have demonstrated task dependent functional coupling between different cortical sites along with regional activation (Fig. 2.16) (Gerloff et al. 1998; Andres et al. 1999). The performance of novel skilled tasks has been associated with coupling between premotor and sensorimotor areas. This coupling is reduced after a lengthy learning period (Andres et al. 1999). Externally paced movements have been reported to result in increased alpha and beta TRCoh in the central regions while internal pacing resulted to increased beta TRCoh of premotor and sensorimotor areas (Gerloff et al. 1998). TRCoh has also been reported between motor and sensory visual cortical areas during a visuomotor force tracking task (Classen et al. 1998). Functional coupling between motor and visual areas may also explain common 10 and 3 Hz oscillations that have been observed to modulate eye and finger movements during a visuomotor task like tracking a visual target (McAuley et al. 1999).

The interpretation of such results is not straightforward since in some cases coherence may be the result of volume conduction effects rather than neuronal connectivity. Microelectrode studies and partial coherence analysis methods and extensive research in this area have suggested that the majority of the observed coherence is due to connectivity rather than from volume conduction, passively carrying signals to multiple electrodes. The fact that in most of the referred studies, changes in interregional coherence were not related to regional power changes, and gave different topographies, supports the connectivity theory (Feige 1996). Coherence is not automatically high in bands and areas where spectral power is high. This doesn't explain completely the mechanism and the function of these intracortical connections while it may reflect direct intracortical connectivity or common input initiated from subcortical structures (Feige 1996).



## **2.6 NEUROGENIC ACTIVITY DURING MOTOR TASKS**

### **2.6.1 Tremor**

No human movement or posture task is completely smooth but it is always associated with tremor – involuntary rhythmic velocity modulation or rhythmic movements of small amplitude. Healthy tremor, contrasting to pathological tremor is a completely natural phenomenon occurring in perfectly healthy people. The mechanism behind the healthy generation of tremor is a combination of neurological and biomechanical factors.

### **2.6.2 Posture tremor**

Physiological tremor is postural tremor that occurs in healthy individuals during maintained postural tasks. Oscillatory mass spring characteristics of skeleton and muscle, as well as neurogenic features are responsible for this tremor. The natural resonant frequency in a mass spring system is dependent on the inertia of the mass and the stiffness of the spring. Therefore the frequency and amplitude of tremor at different joints operated by different muscles under different loads and of different size might be expected to vary greatly. Stretch reflexes with their long feedback delay also generate neurogenic frequency components that vary according to the distance of the joint from the spinal cord. Thus, seen across different limbs, a wide spectrum of oscillations of different amplitude and frequency can be observed.

Some components of tremor are independent of the joint, the joint biomechanics and the inertia loading. The joint independent nature of these components (independent from distance from CNS) suggests central origin. More specifically neural generators located in the central nervous system seem to be responsible for the two specific frequency bands, 8-12Hz and 15-35Hz being observed (Elble and Randall 1976; Conway et al. 1995; Conway et al. 1995). As mentioned before, tremor also contains mechanistic components (Elble and Randall 1978). The resonant frequency of some joints, for example the wrist joint, whose resonant frequency is in 8-12Hz area, can contribute to the corresponding component of physiological tremor. However, the main source of that component is believed to be the group firing characteristics of recruited motoneurons.



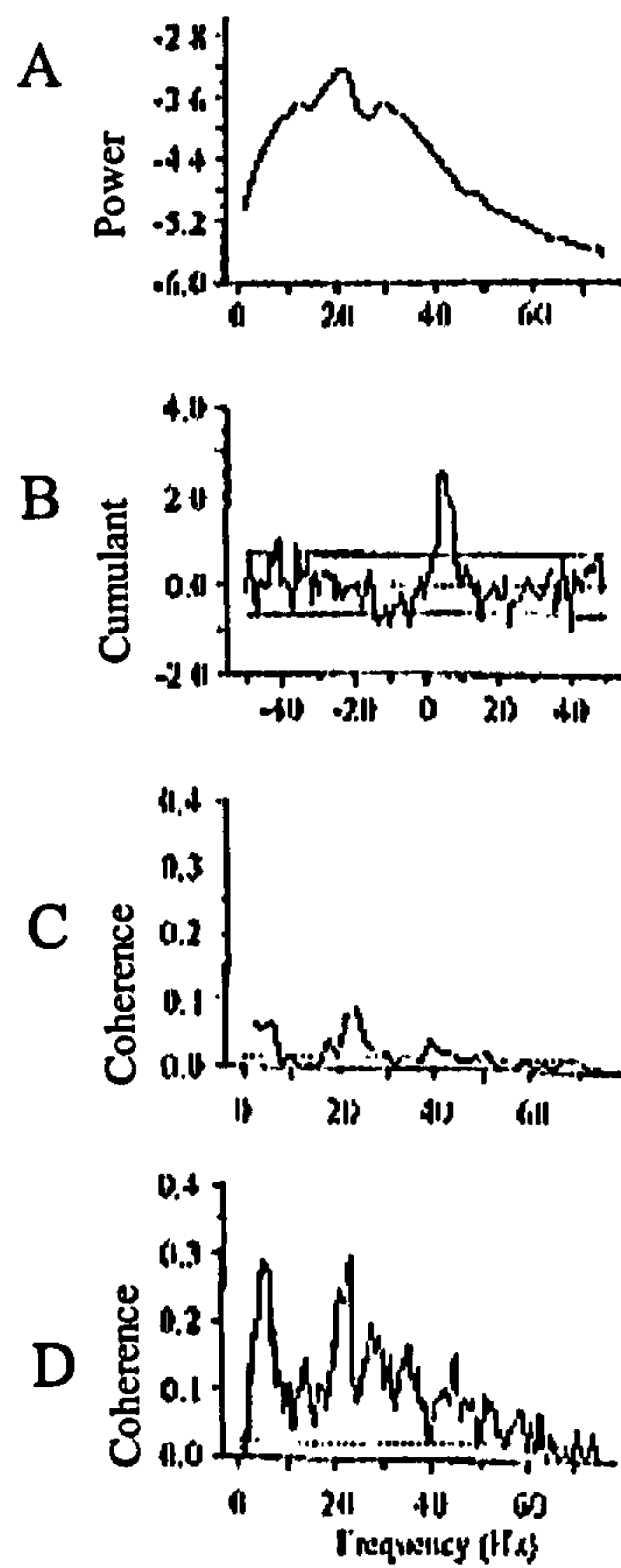


**Fig. 2.17** Relationship between motor-unit and physiological tremor. A is the auto-spectrum of finger tremor during a maintained finger extension task. B shows the cumulant density between two motor-unit spike trains recorded during the task are presented in B. C illustrates the coherence between the motor-unit spike trains while D shows the motor-unit/tremor coherence estimate (Conway et al. 1995).



Correlation between surface EMG, single motor-unit activity and motor-unit pairs with tremor records has been reported for the 8-12 Hz frequency band (Elble and Randall 1976). Thus, the individual recruited motoneuronal firing characteristics were considered responsible for the near 10Hz tremor component since the firing frequency of individual motoneurons usually occurs around 10Hz. However, it was later shown that even though the discharge frequency of individual motoneurons usually occurs in the same 8-12Hz area, there has been no evidence of association between an individual motoneuron firing rate and tremor frequency. As the level of the contraction increases we have an increase of the firing frequencies as with the number of recruited motoneurons. Therefore it is unlikely for the individual motoneuronal characteristics alone to be responsible for that component. Rather it is believed that the modulation of firing rates from a motor-unit pool is reflected in the rhythmic motor output.

What has been recently shown is that in coherence estimates (a frequency domain description of the coupling) between pairs of single motor-units discharges as well as between single motor-units and tremor during isometric contractions (Fig. 2.17), two main high correlation frequency bands in 8-12Hz and 15-30Hz ranges were present (Conway et al. 1995; Halliday et al. 1999). The fact that these bands are independent of the load suggests the central origin of the frequency components under discussion in the tremor records and the underlying rhythmic motoneuron discharges. As has been mentioned already, different loads did not affect the frequency bands of high correlation that remain the same. Experiments for a loaded and unloaded finger demonstrated that a significant increase of the magnitude of the coherence estimate between motor unit and tremor records seems to occur for the loaded case despite the fact that there was no change in the frequency peaks of the EMG tremor records (Halliday et al. 1999). Similar studies have also shown that 8-12, 20-25 Hz neural rhythms of physiological tremor have a stable frequency. The amplitude of the 20-25 Hz band was modulated by mechanical-reflex feedback since the EMG-tremor coherence decreased with finger loading (Vaillancourt and Newell 2000). However, the size and frequency of coherence can show considerable variability, both within different muscle pairs for each subject, and across subjects Fig. 2.18 (Kilner et al. 1999).



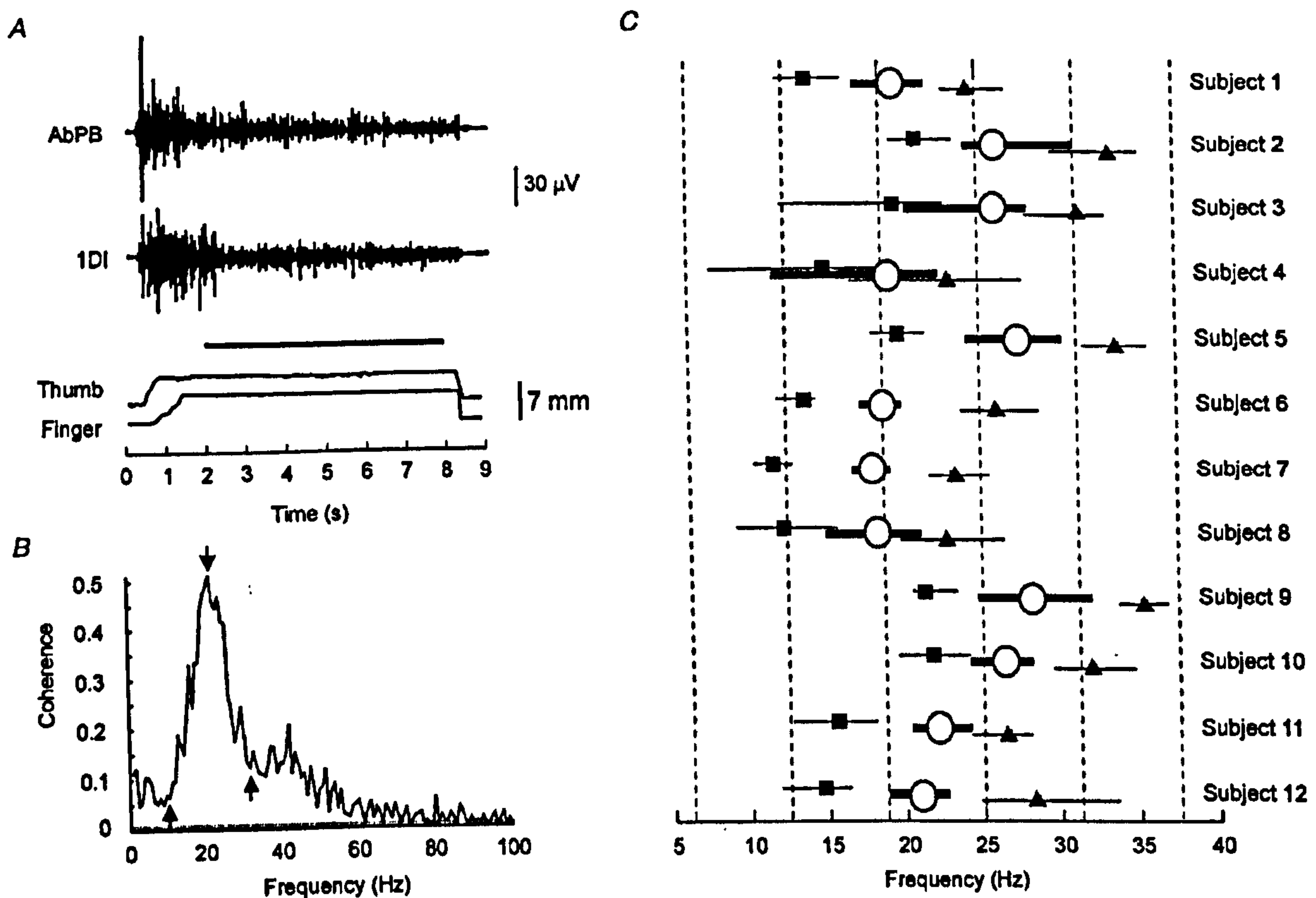


**Fig. 2.18** Variability in EMG Coherence during a hold task. (A) EMG activity from two hand muscles (1DI and APB) and index finger and thumb lever positions recorded from subject 12 during a single trial of the LF hold task. (B) the coherence spectrum calculated from the muscles shown in A for 50 trials. Coherence was calculated during the steady hold phase (horizontal bar in A). (C) frequency distribution of the coherence peak for the muscle pairs showing significant coherence in each subject. For each subject the range of frequencies for the minimum, maximum and peak frequencies for different muscle pairs are indicated by the horizontal bars and the average values are shown by filled squares, filled triangles and open circles, respectively. The minimum, maximum and peak frequencies were measured by eye. The arrows in B give examples of the points measured (Kilner et al. 1999).



Patients suffering from the syndrome of persistent mirror movements characterized by abnormal bilateral corticospinal projections and normal subjects have been used to study the origin of Enhanced Physiological Tremor (EPT) (Koster et al. 1998). The hypothesis was that if a supraspinal mechanism was involved in EPT, the activity of EPT should be coherent between both sides in subjects with this abnormality. EPT was evoked by intravenous salbutamol. No control subject showed a significant right-left- coherence of tremor activity while significant coherence was found in persistent mirror movements between 8 and 12 Hz. When the mechanical tremor frequency of one hand was reduced by loading, coherences and phase spectra of the EMGs remained unchanged. The 8-12 Hz component of EPT and possibly of normal physiological tremor is transmitted transcortically, most likely originating from two separate generators for both sides (Koster et al. 1998). Other studies involving mirror movements provide evidence to support the hypothesis that the neurogenic component of physiological tremor is supraspinal in origin (Mayston et al. 2001). According to the previous study, this neurogenic component ranges from 6 to 40 Hz.

Other frequency components have been observed during posture. A high frequency in the EMG caused by modulation of motor unit activity, known as the Piper rhythm occurs during strong isometric contractions and submaximal movement tasks. Rhythmic oscillations in the electromyogram (EMG) at about 50 Hz during voluntary contraction were first described back in 1907 (Piper 1907). The reason that motor unit population is modulated at this frequency seems to be the central nervous system and more specifically the contralateral motor cortex since MEG studies have shown high coherence between EMG and MEG in the region of the contralateral precentral and central sulcus, at 35-60 Hz during maximal isometric contractions (Brown et al. 1998).

### ***2.6.3 Movement tremor***

Voluntary movement tremor was first described in 1956 in a study where tremor of 7-12 Hz was reported at the wrist, elbow, shoulder ankle, knee, and hip joints during movement (Marshall and Walsh 1956). 8-10 Hz modulations of angular velocity of the forearm have been also demonstrated during visual tracking (Navas



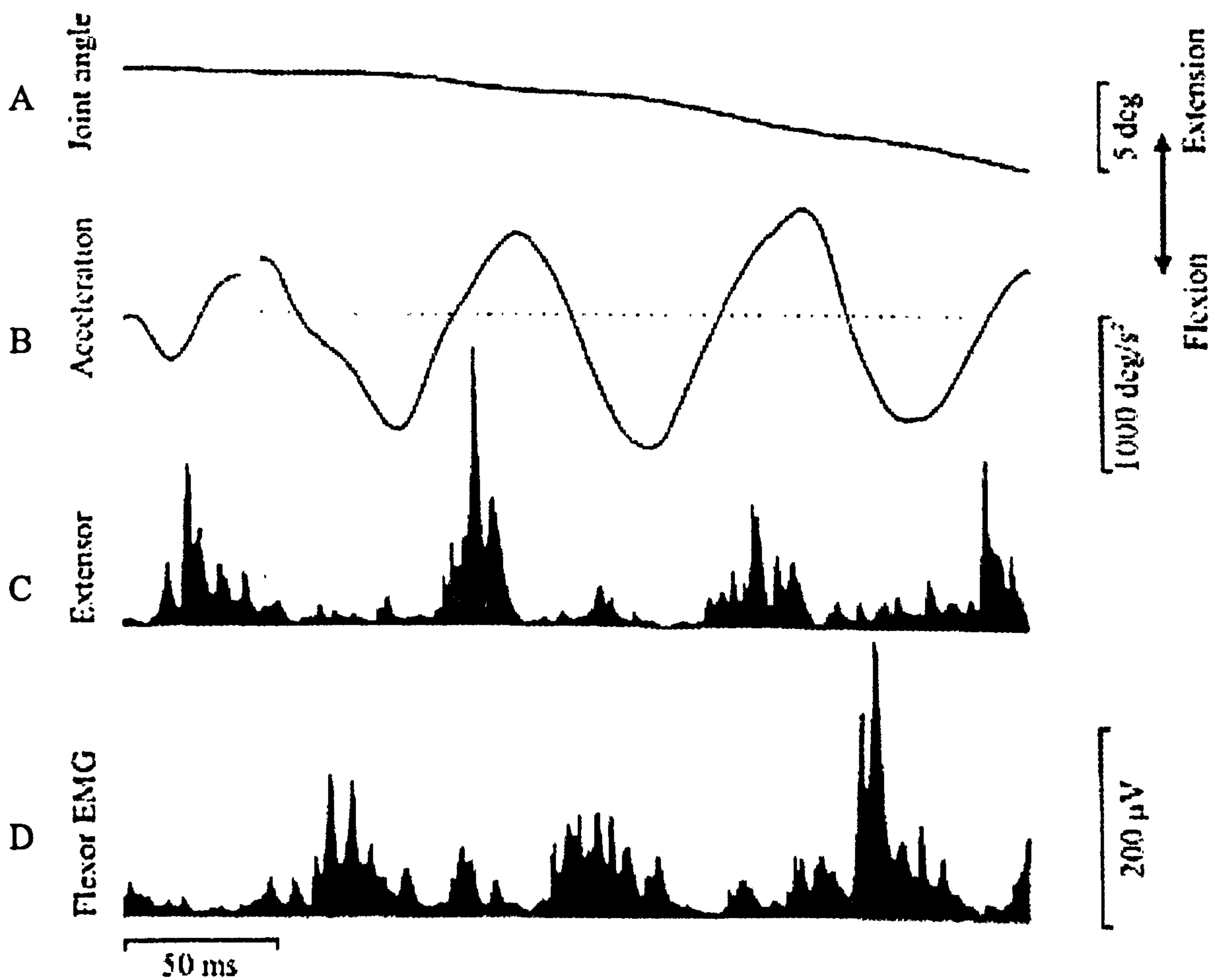


**Fig. 2.19** Biphasic agonist and antagonist EMG modulation during voluntary movements. (A) shows the joint angle of a slow voluntary finger extension movement. This movement is characterised by step discontinuities which appear as modulation in the velocity of the moving finger that are reflected in the tremor record that reveals repeated accelerations and decelerations during the movement (B). Rectified EMG of agonist (C) and antagonist (D) reveals biphasic bursts where activity in the extensor (agonist) EMG occurs just prior to the start of the acceleration phase while braking burst of activity in the flexor (antagonist) EMG occurred shortly after and prior to the deceleration phase (Vallbo and Wessberg 1993).



and Stark 1968). For finger movements of slow and moderate speed it was found that movement was not smooth but was composed of discontinuities in the 8-10Hz range. Importantly the frequency was relatively constant for the same subject even for tests separated by a few months time. The frequency was also present under a variety of loading conditions and over a large range of velocities of movement (Vallbo and Wessberg 1993).

The main component of voluntary movement tremor is contained in the same frequency range as normal physiological tremor at 8-12Hz. The biomechanical characteristics of the joints and the stretch reflex loops could account for this tremor. This characteristic wrist movement tremor could originate from the mechanical resonance of the wrist which is in the area of 10Hz. The same frequency however, emerges for finger movements despite that the finger system resonance is 20-25 Hz. Therefore, mechanical resonance cannot account for the specific oscillations. Furthermore, the common tremor frequencies observed at different joints suggests that this tremor is also of central origin since the different length of the reflex loop for different joints would alter the conduction times and produce different frequencies. More evidence that these discontinuities were of neural origin was produced by the observation that the underlying EMG activity was modulated in phase with the speed variations (Vallbo and Wessberg 1993). Similar conclusions have been drawn for the elbow joint. Oscillations within the band of 8-12Hz were observed in EMG and acceleration records. The bicep's activity was found to be responsible for that frequency (Conway et al. 1997).

Another interesting result of this group of studies was that when the antagonist muscle is active, its activity is modulated in the same with agonist 8-12 Hz range producing double pulses (Fig. 2.19). The agonist producing a driving pulse while the antagonist produces a braking pulse a few tens of ms later throughout the duration of the movement (Vallbo and Wessberg 1993). In this respect it is important to determine if the stretch reflex contributes to the generation of these EMG bursts. The finger physiological tremor has a component due to the stretch reflex loop. This component occurs in the same frequency range as the movement tremor. The same stretch reflex loop could be causing the movement tremor. This would suggest a model, in which the 8-10 Hz stretch reflex discontinuities are added to a smoothly



changing central motor command. In experiments designed to test this, it was shown that human muscle spindles are sensitive enough to detect minute speed variations and their afferent discharge clearly showed modulation related to these discontinuities (Wessberg and Vallbo 1995). However, several suggestions indicate that the spinal stretch reflex loop is not the origin of the discussed oscillations. Firstly the mechanics of the finger and the kinematics structure of the movement are too complex for a monosynaptic feedback loop, as stretch reflex is, to control. Another important argument ruling out the stretch reflex is that it lacks adequate power to cause the observed discontinuities. Only small reflex responses could be demonstrated, when large external perturbations, like muscle stretching, were added during voluntary movements (Wessberg and Vallbo 1996). Another study also has shown that the response of the individual spindle afferents to perturbation was uniform in repeated tests regardless of the size of the reflex, e.g. whether it was large or lacking altogether (Al-Falahe et al. 1990; Al-Falahe et al. 1991). Furthermore experiments involving suppression of the stretch reflex with intramuscular injections of local anaesthetic and experiments on a patient with severe peripheral deafferentation, showed persistence of the 8-12Hz rhythm and motor unit coupling (Farmer et al. 1993). The discontinuities observed during movement cannot therefore be generated by the stretch reflex.

It has therefore been suggested that, during movement, the 8-10Hz discontinuities arise from central neural structures. Accordingly, the 8-10Hz signal may be the reflection of a pulsatile motor command from the brain (Vallbo and Wessberg 1993). In this model of voluntary motor control, a central oscillator generates the 8-10Hz pulses even though there has been no conclusive evidence as far as the specific origin of this activity. These pulses then activate the motor patterns of agonist-antagonist double pulse as observed at the segmental level in the EMG (Fig. 2.19). With a fixed frequency, the overall speed of movement could be defined, modulated by the amplitude of the pulses. The maximum frequency of rhythmic movement cannot exceed the pulse frequency. In this respect it is very difficult to generate voluntary rhythmic repetitive movements at 8Hz or higher.

An interesting observation that also suggests the central origin of the tremors under discussion involves parkinsonian patients treated with ventrolateral



thalamotomy. After the surgical procedure both the parkinsonian (4-7Hz) and physiological tremor (8-12Hz) components were reduced which suggests that ventrolateral thalamotomy interrupts a common circuit involved in the supraspinal component of both physiological and pathological tremors. Thus the thalamus may be involved in circuits generating physiological tremor in humans. (Duval et al. 2000)

#### ***2.6.4 Task Specificity***

The similarities and the differences of the frequency profiles between movement and posture and their implications have engaged the interest of the scientific community. During movement and posture, an 8-10Hz component exist in the motor output while a 15-30Hz component additionally occurs only during posture. It is not clear whether a common mechanism is generating the near 10Hz and its origin for movement and posture. The distinct characteristics of the posture load dependent 15-35 frequency component suggest that it is generated from different neural processes than the posture load independent 8-12Hz EMG-tremor coherence (Vaillancourt and Newell 2000).

A 30-35 Hz peak coexisting with the 8-10Hz component in the motoneuron-acceleration coherence during slow finger movements has been reported (Wessberg and Kakuda 1999). This may suggest that the behaviour of motor-units during posture and movement may have common attributes and derive from an integrated underlying mechanism. If that is the case the 15-35Hz modulation may be enhanced during voluntary contractions and suppressed during movement (Halliday et al. 1999).

The majority of the studies targeting the 8-10Hz band have suggested that the frequency occurrences during posture and movement are related phenomena (Wessberg and Kakuda 1999). However, this may not be the case. Both movement and posture tremor demonstrate finger EMG\acceleration coherence in the area of 8-10Hz. High motoneuron-acceleration coherence in the area of 8-10Hz may be observed for movement tremor, but for postural tremor this is not the case. That suggests that the two phenomena are observed as activity in the same frequency range rather than being directly related. Movement tremor seems to be a direct



monosynaptic, cortex to motoneuron connection while posture involves extra neuronal circuitry (probably at CNS level) that modulates the firing rates of the active motoneuronal pools in a way that such tremor is produced.

Studies on patients with defects on the central and peripheral nervous systems have given evidence that both targeted frequency bands are of central origin (Farmer et al. 1993). A patient with severe peripheral deafferentation displayed normal coherence for both frequency components while still displaying motoneuronal synchronisation. Considering that deafferentation deprives the CNS of afferent information this indicates that the under discussion frequencies are not the result of any feedback mechanism but may originate from higher structures. In addition, further evidence on that provide the behaviour of the affected side of stroke patients that appears to be different from the unaffected side as well as normal subjects. Patients with corticospinal tract lesions lacked the high component of motor unit synchronisation. This strongly suggests the involvement of this structure in the production of this rhythm (Farmer et al. 1993).

### ***2.6.5 Motor Unit synchronisation***

Traditionally, it was believed that motor units in man fire independently of one another, and synchronization of motor unit discharges only occurs during powerful contractions, during fatigue following training, or in disease. The application of analysis techniques like cross-correlation of EMG recordings showed that motor-unit synchronization may occur in healthy subjects during gentle isometric contraction (Dietz et al. 1976; Sears and Stagg 1976; Dengler et al. 1984), while the previous studies were primarily based on visual inspection of the EMG (Farmer et al. 1997).

During voluntary movement and especially during gentle isometric contractions, recruited motor-units display a high occurrence of synchronous firing which is described as short term motor unit synchronisation, detected by central peaks in the cross correlation histogram. It was suggested that last order common (branching) presynaptic fibres would momentarily increase the probability of firing of both neurones by evoking simultaneously occurring synaptic potentials (Sears and Stagg 1976). Short term synchronisation between motor units has been detected in a



variety of muscles. Motor unit synchronization was later studied within different muscles (Kirkwood et al. 1982). Short-term synchronization has been detected in motor-neuron activity recorded from different segments of the thoracic spinal cord in cat that suggested common presynaptic inputs to motoneurons of breathing muscles acting as agonists. Short term synchronization and its distribution on different co-contracting human hand muscles has also been studied (Bremner et al. 1991). That revealed that motor unit synchronization falls as recordings are made from more distant muscles and that synchronization favoured certain muscle synergies. Motor-unit recordings taken from muscle fibres of the first and second dorsal interosseous muscles (1DI:2DI) have been examined using cross correlation demonstrated short term synchronisation between spike trains. Coherence between the motor-units of the different muscles in 1-7Hz and 18-29Hz was also present. The fact that the results were very similar to the ones obtained from motor units in the same muscle (1DI:1DI) further suggested a common drive to different but functionally homogeneous motor-neuron pools (Farmer et al. 1993).

Studies examining the distribution of motor-unit synchronisation over muscles found evidence for a common drive between pairs of muscles that share a common joint or joint complex (such as the metacarpophalangeal joints), while no evidence was found for a common drive to co-contracting muscles that did not share a common joint (Gibbs et al. 1995). In analogous hand and foot muscle pairs, the degree of synchrony was significantly greater for lower limb pairs. Furthermore the common drive that was detected with lower limb muscle pairs was significantly larger during balancing tasks than during either lying or standing. It can be concluded that activity in both last-order branched presynaptic fibres and presynaptic synchronization is involved. These findings suggested that synchrony is a functional rather than an anatomical feature, expressing movement patterns rather than fixed circuitry controlling isolated muscles or pairs of muscles.

The discussed synchronization could either arise from central or reflex mechanisms with more consistent evidence suggesting the latter. Patients with central lesions show a loss and a change in the time course of motor unit synchronization comparing the affected with the unaffected hand and healthy subjects. Cross correlation analysis of recordings from the affected arm revealed a



lack of a central peak. Coherence analysis also revealed a decrease in the incidence and size of the coherence peaks for recordings from the affected arm especially for the 16-32Hz frequency range (but not in the 1-7Hz band). The improvement of some stroke patients also parallel changes in the level of motor unit synchronization (Farmer et al. 1993). Furthermore motor unit synchronization was still observed in patients with severe peripheral deafferentation (Farmer et al. 1993).

Studies examining the distribution of muscular coupling, examining distribution of motor unit synchronisation over the forearm and hand muscles (Conway et al. 1998; Bray 1999; Mulcahy 2001) showed results comparable to the previous study (Gibbs et al. 1995). EMG recorded from a variety of muscles acting about the fingers and the wrist during the performance of a variety of different postural tasks requiring differing patterns of muscle coactivation revealed the presence of distinctive coupling in the beta band range between the active muscles during the maintained postures in the form of frequency domain coherence. This coupling was present between muscles acting about the same joint as well as between muscles acting about the different joints, indicating that synchrony is generated by functional rather than anatomical presynaptic organisation.

Thus, it has already been proposed that muscle synergy requires the presence of a common synaptic drive, in the form of presynaptic inputs, to the motoneuron pools of the contracting and co-contracting synergistic muscles. More evidence that the common synaptic drive shared between two groups of motor neurones synchronizes the timing of discharges between the motor-neurone groups came from recordings of motor-unit discharges during co-contraction of ipsilateral pairs of thumb muscles in cerebral palsy patients and healthy subjects, and in pairs of lower-limb muscles in subjects with cerebral palsy and control subjects. Common synaptic drive, likely to be partially derived from activity in branched corticospinal-tract neurones, produced motor-unit synchronization between pairs of thumb muscles in control subjects but was absent in all subjects with cerebral palsy. Motor unit synchronization was not found between lower-limb antagonist muscles that co-contracted abnormally in cerebral palsy, nor was synchronization present in more widely separated muscle pairs (Gibbs et al. 1995).



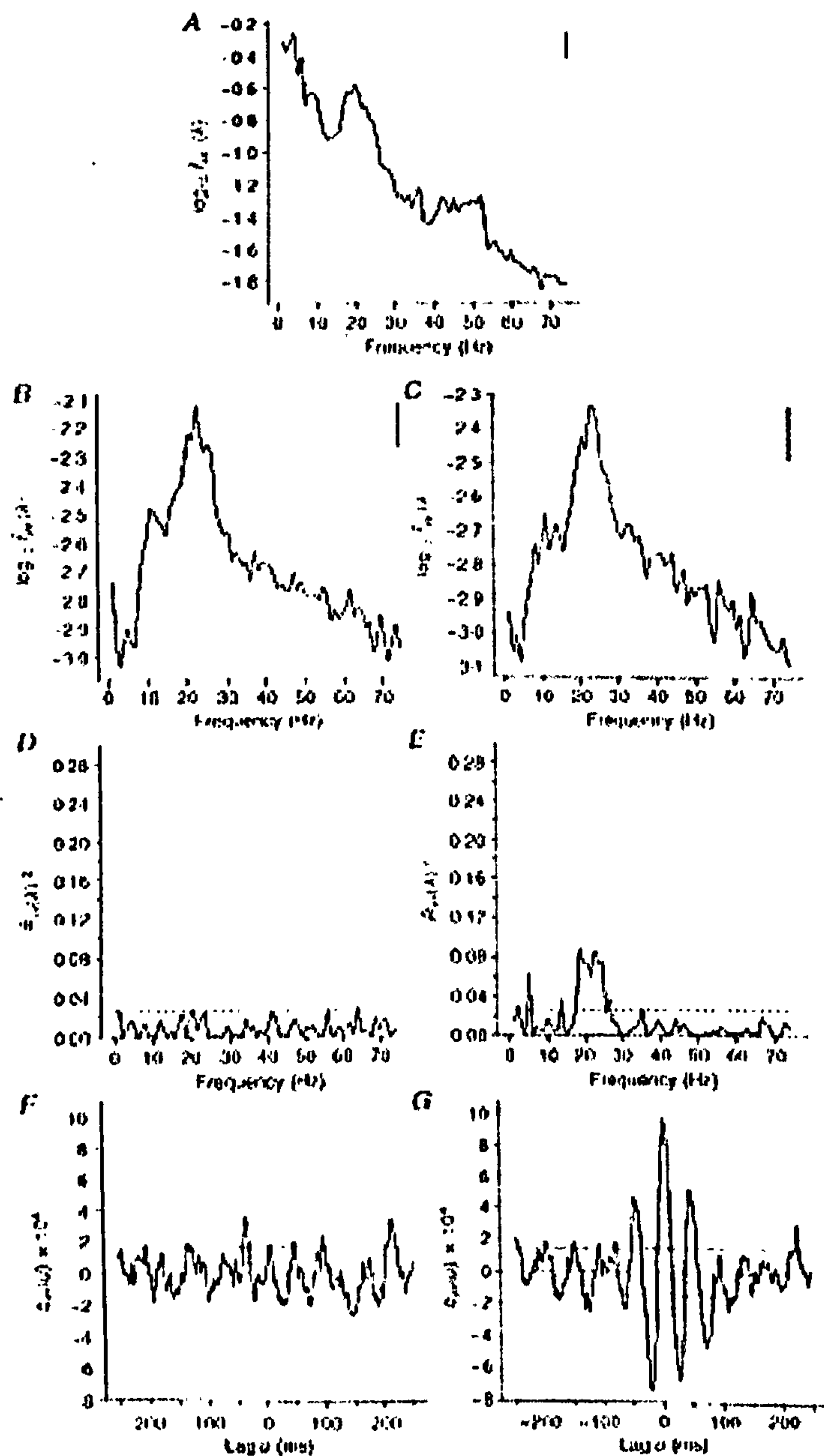


**Fig. 2.20** Relationship between MEG and EMG during simultaneous contraction of left and right 1DI muscles. The MEG, ipsilateral 1DI EMG and contralateral 1DI EMG are illustrated in A, B, and C respectively. The coherence between the MEG and ipsilateral (D) and contralateral (E) are also illustrated. In F and G the estimated cumulant densities between MEG and ipsilateral (F) and contralateral (G) EMG are plotted (Conway et al. 1995).



In a different study performed on children with hemiplegic cerebral palsy and marked mirror movements showed that the motoneuron pools of homologous left and right hand muscles received common synaptic input from abnormally branched presynaptic axons. This suggested involvement of the abnormally branched corticospinal tract fibres whose common inputs are provided by origin is the undamaged motor cortex (Farmer et al. 1991). In healthy adults, cross correlation analysis does not detect any shared synaptic input to motoneuronal pools innervating left and right hand muscles coming to a conclusion that this kind of activity is produced by simultaneous activation of crossed corticospinal pathways originated from the corresponding left and right cortices (Mayston et al. 1997; Mayston et al. 1999; Mayston et al. 2001).

### ***2.6.6 Corticomuscular Synchronisation***

The association between cortical and muscular rhythmicities has long been considered. However, most of the research was based on visual comparison of EMG and cortical activity showing similarities between the cortical motor rhythms and the modulation of motor-unit discharges during hand tremor. Thanks to the use of advanced time and frequency domain techniques, direct evidence of synchronisation between cortical and muscular activity has arisen. Motor-unit firing is thus believed to be driven by direct descending cortical activity. The cortical command is transmitted via descending spinal tracts and ends up to the motoneurons of co-contracting muscles, which surface is covered by presynaptic synapses. It is interesting to mention that synchronisation is present not only between motor-units in the same contracting muscle. It can also occur in different co-contracting muscles but only when the muscles are involved in the same postural task (Bremner et al. 1991).

It was thus long known that the motor cortex has a significant contribution in the production of human movement but the presence of a considerable content of cortical signal in the EMG activity, resulting in an increased spatially localised coherence (known as corticomuscular coherence) was recently discovered. The first actual demonstration of corticomuscular coherence came from a study that involved simultaneous MEG recordings of cortical activity over the primary motor cortex and needle single motor unit EMG of the ipsilateral and contralateral first dorsal



interosseous muscles (1DI) during maintained voluntary contractions (Fig. 2.20) (Conway et al. 1995). During maintained contraction there was significant coherence between the two signals for a band of frequencies with the peak coherence confined largely within the beta range of cortical activity (13-35 Hz). The results were also related to the previously observed synchronization of hand muscle motor units at frequencies of 16-32 Hz (Farmer et al. 1993) and suggested involvement of cortical neurons in the generation of motor unit synchronization.

Ongoing research in primates and humans has provided further evidence of movement related cortical oscillations using MEG and EEG as well as direct cortical recordings (Conway et al. 1995; Salenius et al. 1997), EEG (Halliday et al. 1998; Mima et al. 2000) and ECoG (Toro et al. 1994; Marsden et al. 2000). The objective is to associate the knowledge that we have for the oscillatory activity of the brain and the tremor activity providing the functional link between them. The first observations of corticomuscular coherence showed significant correlation in the beta band (15-35Hz) that coincided with the autospectrum EMG peak in the same frequency area for weak isometric contractions and was largely suppressed during movement and strong contractions (Conway et al. 1995). Other frequency peaks in alpha and gamma band EMG autospectra did not result to an analogous peak in the same frequency area for coherence. However, corticomuscular coherence in the gamma band has been reported during maximal contractions (Brown et al. 1998; Brown 2000).

EMG can contain rhythmic oscillations in the gamma band producing a muscle sound known as Piper rhythm (Piper 1907) that also present during movements as it was recently shown (Brown et al. 1998). Occasionally, MEG-EMG coherence in the 40 Hz range seems to occur during preparation and execution of slow movements, like slow finger movements (Salenius et al. 1996) or very strong contractions and has been associated with attention processes in the brain (Mima et al. 1999; Brown 2000). Nevertheless these phenomena are not consistent since they are observed in some subjects prominent to gamma frequencies. Corticomuscular coherence in the 30-60 Hz area has also been reported. Coherence between cortex and muscle in the Piper band is most evident during strong isometric contractions or during movement. It has been suggested that synchronisation in the gamma band may provide a means of binding together the cortical elements involved in movement



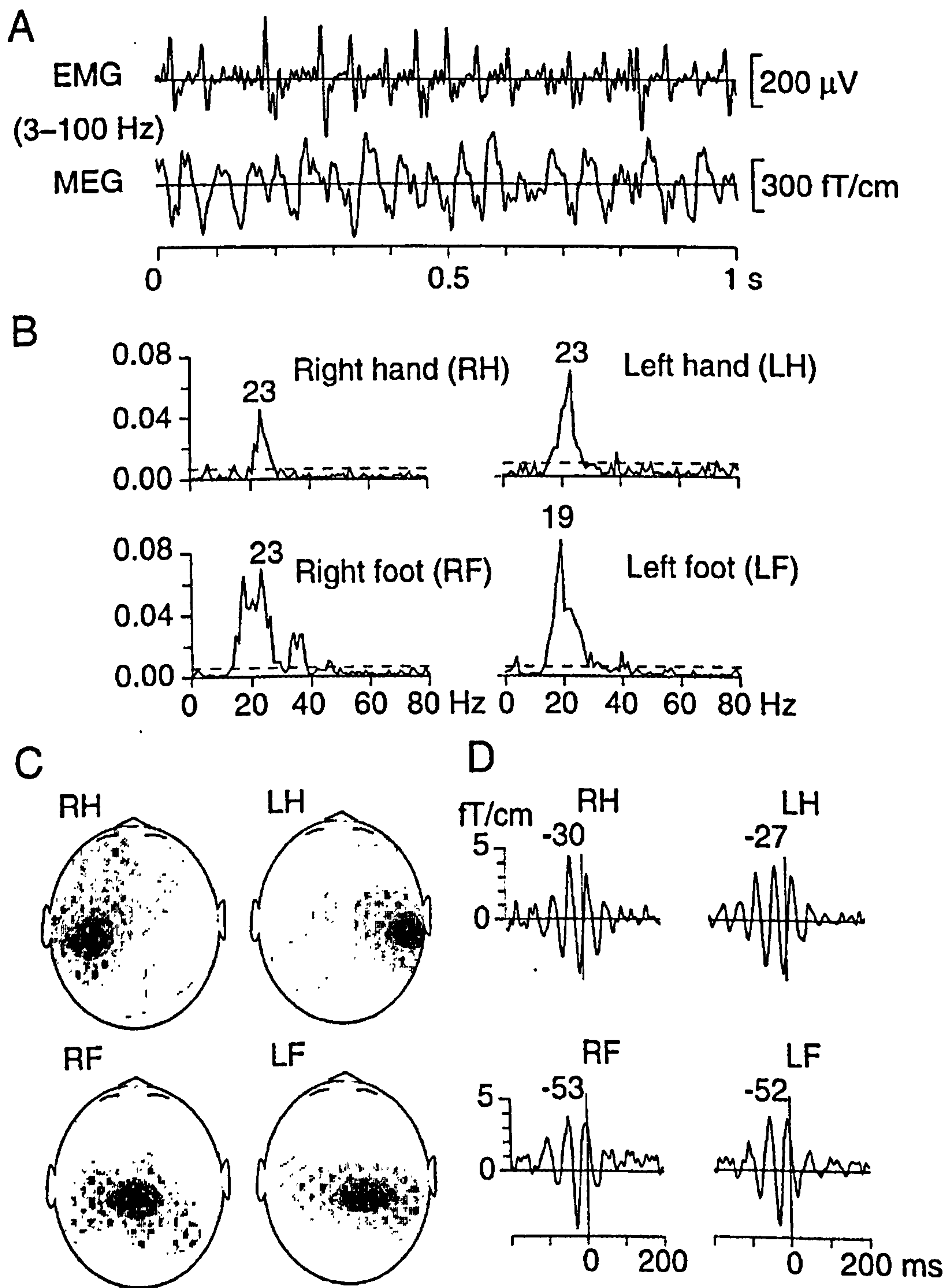


**Fig. 2.21** A: Raw EMG from contracting left flexor hallucis brevis muscle and coincident raw MEG signal over right foot area. B: coherence spectra between MEG and EMG for isometric contraction of left and right interosseus (hand) and flexor hallucis brevis (foot) muscles. Dashed lines: 1% significance level. C: spatial distributions of strongest peaks of coherence spectra. Head is viewed from above. D: time domain MEG signals, averaged with respect to onset of motor unit potentials in EMG (Salenius et al. 1997).



execution under conditions that vary from moment to moment and require some attention (Brown 2000). There are no reports of coherence above gamma frequencies. The low pass filter characteristics of the skull and other interposed tissues may be responsible.

As shown already, 8-10Hz rhythm is a strong component of tremor, EMG, EEG and MEG autospectra. There is also strong indication for the central origin and the descending motor command nature of the rhythm. However, there hasn't been wide and consistent observation of corticomuscular coherence in this band neither in EEG nor in MEG. However, 10Hz coherence has been demonstrated for some subjects during maintained contractions (Mima et al. 2000).

#### ***2.6.6.1 Spatial Localisation***

The first reports of corticomuscular coherence involved single channel MEG recordings (Conway et al. 1995). Single channel EEG recordings confirmed the corticomuscular coupling (Halliday et al. 1998). The site of the recording was the 1DI area above the motor cortex area corresponding to the forearm muscles which activity was recorded. Multi-channel methods with higher spatial resolution confirmed that coherence topology corresponds to somatotopic maps of the projected muscles. As suspected, the primary motor cortex seems to be the main source of descending rhythmic cortical activity activating the muscles and coherence was strong (maximum) in the area of the contralateral motor cortex that corresponds to the projected coupled muscle (Fig. 2.21) (Salenius et al. 1997; Mima et al. 2000). However, with increasing spatial resolution (more EEG or MEG recording channels) and more in depth investigation researchers suggested that these corticomuscular coupling representations of different muscles largely overlap. For example, there seems to be high overlapping between arm muscles and hand muscles activity maps. These suggestions are in line with the hypothesis that not only muscles but actions are represented in the motor cortex and reports of synchronisation between motor units in different muscles only during synergistic activity for related task and absence of synchronisation for unrelated tasks (Gibbs et al. 1995; Mima et al. 2000).

Cortical sources related to posture have been also located from the MEG signal which was averaged timelocked to the onset of motor unit potentials by Gross (2000). A spatial filtering algorithm was used to estimate the source activity. Sources



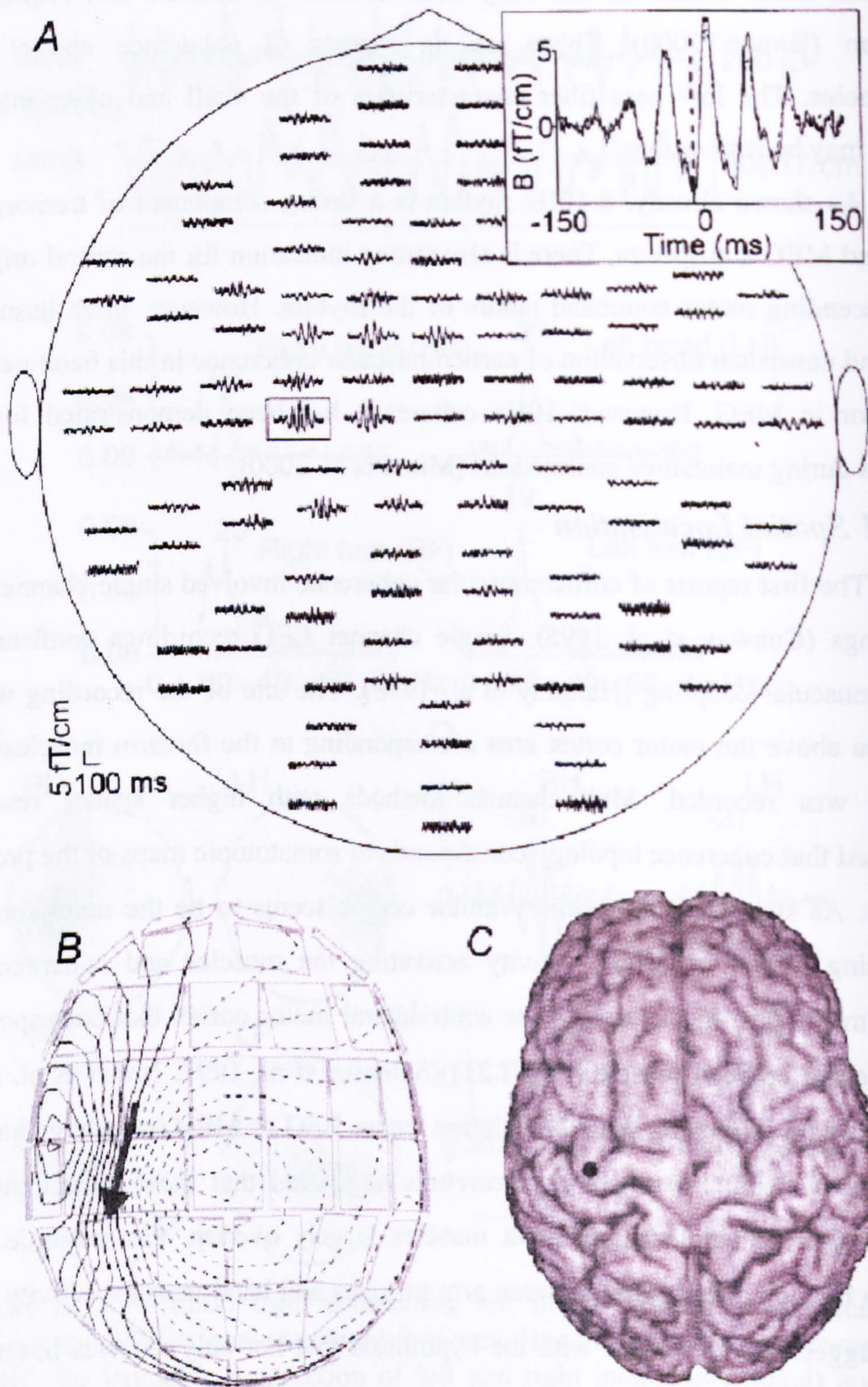


Fig. 2.22 *A* shows the unfiltered averaged MEG signal timelocked to the motor units of the right extensor indicis muscle (phase triggered average). Clearly damped oscillations are evident in the channels above the hand area of the left hemisphere. *B* shows the spatial distribution of the magnetic field at the time of the first negative peak preceding the EMG onset which reveals a dipolar field pattern that can be modelled by a single dipole in the hand area of the left primary motor cortex seen in *C* (Gross et al. 2000).



were found in the primary motor cortex (M1) contralateral to the contracted muscle (Fig. 2.22). Significant 20Hz range coherence between rectified EMG and M1 EEG activity was seen for all examined subjects (Gross et al. 2000).

### ***2.6.6.2 Functional Specificity***

As with the frequency content of the EMG signals, and motoneuronal coupling, corticomuscular coherence appears to be task specific. That means that depending on the task, variations in coherence between muscular and cortical activity occur in certain frequency bands. This feature suggests that corticomuscular coherence could also be used as action intention detection. Movement and posture are the two main action tasks we wish to identify by using corticomuscular coherence. The significance of research in this area is obvious. All frequency information containing brain mapping techniques like MEG, ECoG and EEG in conjunction with EMG have been used by a number of researchers and useful results have been derived. Corticomuscular coherence in the beta band during postural tasks has been reported and well documented by a number of researchers as well as its suppression during movement tasks. During movement there is no significant evidence of corticomuscular synchrony.

### ***2.6.6.3 Temporal characteristics of corticomuscular coherence***

Despite of the attention that the corticomuscular coherence has attracted, there is still some controversy around the temporal relationship between cortical and muscular activity when they appear to be coherent. A zero phase shift, meaning a zero phase lag has been found between MEG and EMG oscillations (Conway et al. 1995), based on the 0ms peak in the second order cumulant as well as studies involving EEG instead of MEG (Halliday et al. 1998) . This contradicts with the hypothesis that corticomuscular coherence expresses direct cortical drive to the muscles. Other studies showed a more rational result, that cortical oscillations leads muscular (Brown et al. 1998; (Salenius et al. 1997, Hari and Salenius, 1999 ; Mima and Hallett 1999; Mima and Hallett 1999). The latencies reported however, (3-8ms for first dorsal interosseous, 17-25ms for tibialis anterior) were much shorter than would be expected from corticomuscular conduction times through fast pyramidal pathways. The delay difference between muscles was consistent with conduction times via fast pyramidal pathways. The 15-20ms longer latency for lower than upper



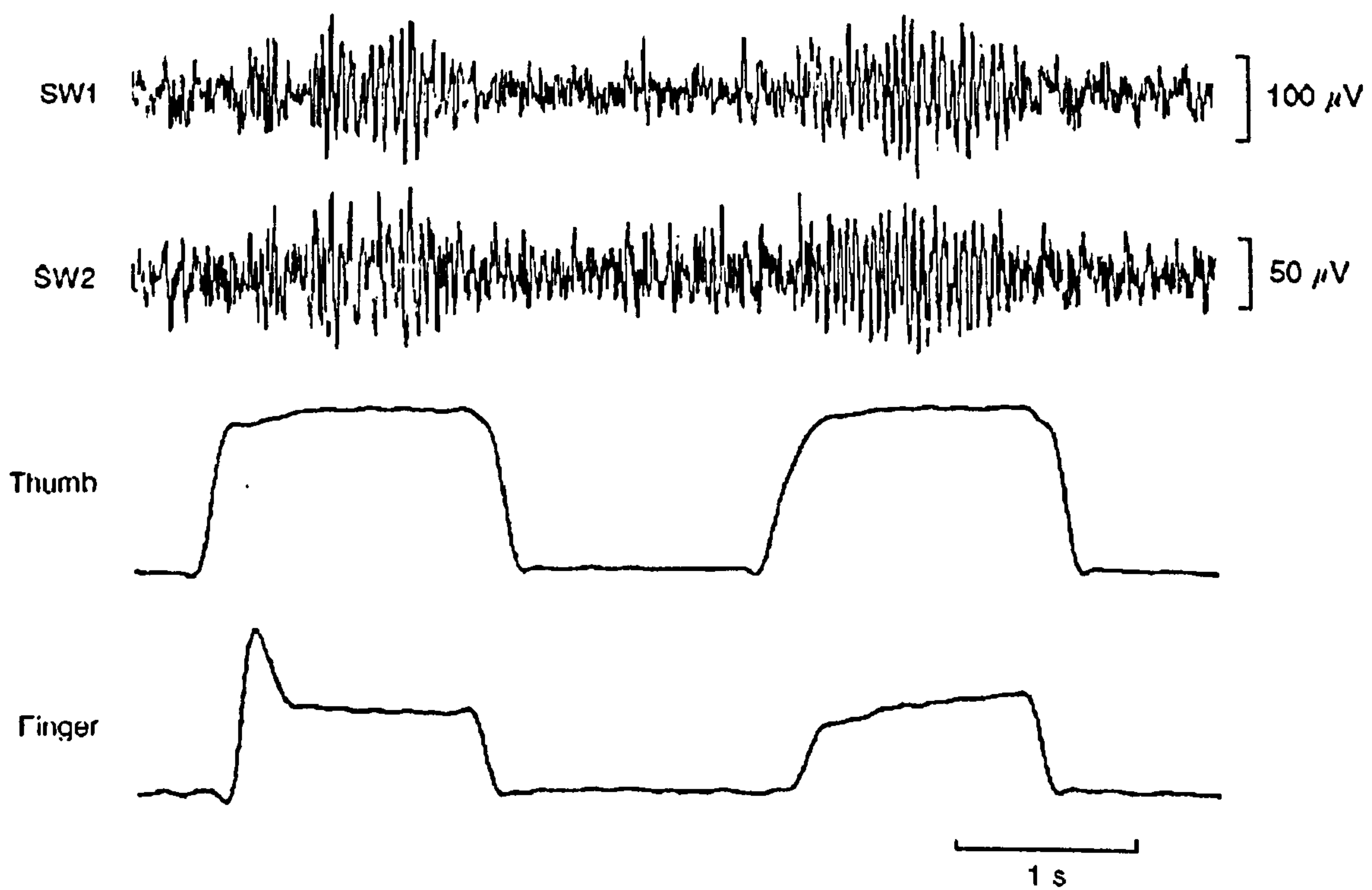


**Fig. 2.23** Primate synchronous slow wave oscillations during precision grip task. Example of a section of recording showing slow waves from two cortical sites (SW1 and SW2), together with the position of finger and thumb levers. Oscillations appear during the hold period of the task, which appear synchronous between the two sites. (Baker et al. 1997)



limb muscles, corresponds with measurable differences in conduction times between these anatomical compartments (Hari and Salenius 1999).

The rhythm generator could also lie in the subcortical structures of the brain and not the cortex. Therefore the cortical and EMG activities observed are the projection of the subcortical activity. The corticomuscular lag is the cortex-muscle conduction time, as revealed from Transcranial Magnetic Stimulation (TMS) studies, minus the subcortical-cortex conduction time. The human reticulospinal tract however, and other descending motor pathways arising from the subcortical structures are relatively sparse and divergent in diameter with slow conduction velocities, which would result in even longer time delays to the muscles. This inconsistency may result from inappropriate way for calculating the latency from second order cumulant graphs, since time lags are in agreement with realistic conduction times, comparable to those seen after transcranial magnetic stimulation (TMS), if measured from the main down-going peak instead of the strongest upgoing peak, in order to extract physiologically meaningful information concerning the time lag between activity in the cortex and muscle (Brown et al. 1998). There is evidence from monkey data (Murthy and Fetz 1996; Murthy and Fetz 1996; Baker et al. 1997) (Fig. 2.23, Fig. 2.24) and EEG and MEG recordings in patients with cortical myoclonus (Kugelberg and Widen 1954; Mima et al. 1998; Mima et al. 1998) that cortical motor output discharge occurs at the time of the peak of the negative wave of the oscillatory field potentials in the deep lamina V cells of the cortex (Murthy and Fetz 1992; Baker et al. 1997). This deep negative field potential is associated with a surface positivity.

Several other points may contribute to the inconsistent findings regarding phase lags between MEG and EMG signals. All studies used Fast Fourier Transform (FFT) based analysis techniques that require stationarity of the signals which is not the case for MEG, EEG and EMG. Moreover, to assume a broad region with a linear dependence of phase difference on frequency is not always valid. Furthermore the width of the frequency band chosen for the linear dependence and the degree of linearity in that band can affect the results. To overcome these problems instantaneous phases from the Hilbert transform were used to calculate delays between MEG and EMG during weak isometric muscle contractions (Gross et al.



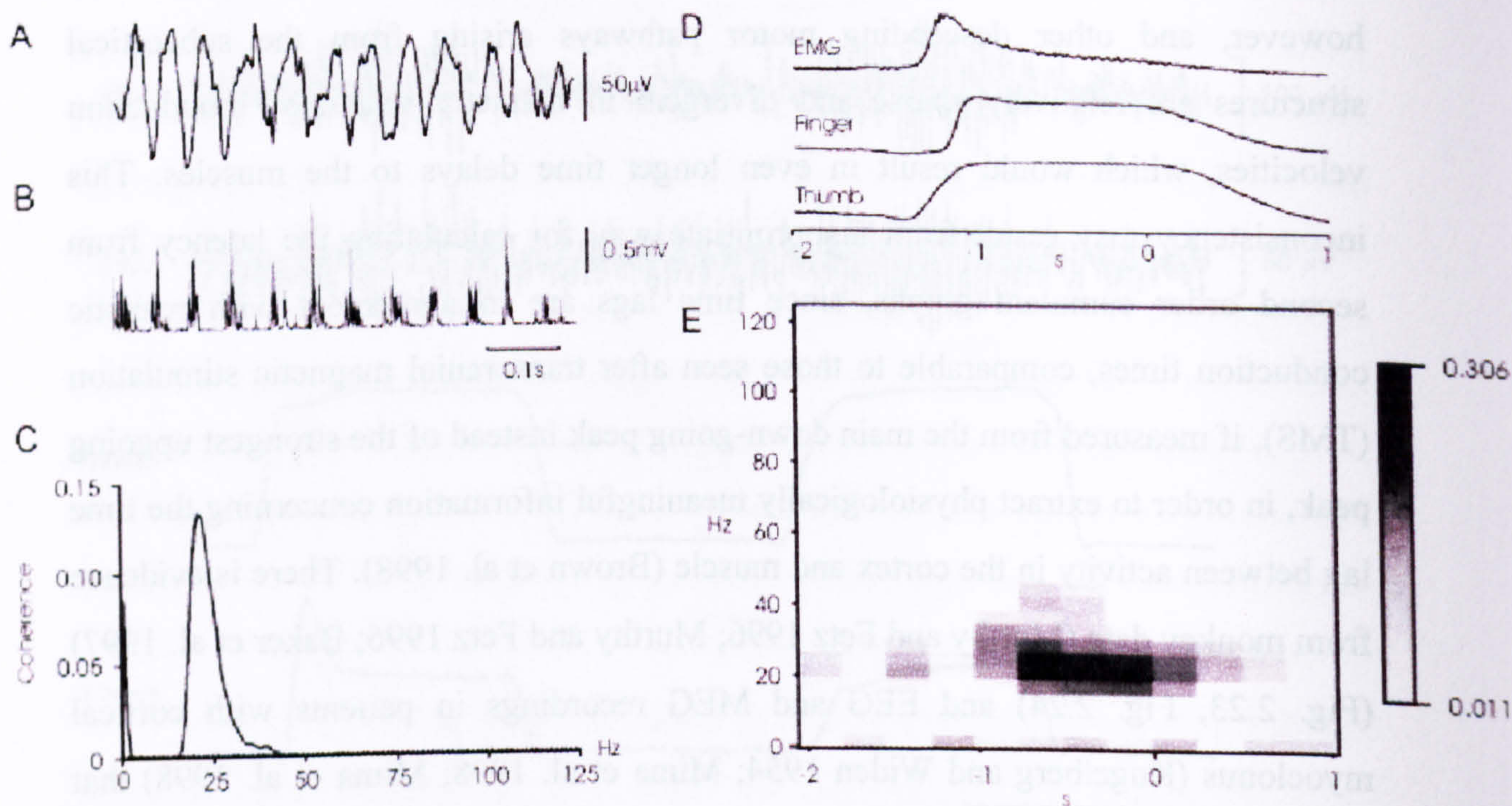


**Fig. 2.24** A. Cortical slow-wave recording from primary motor cortex of a macaque monkey performing a precision grip task.

B. Simultaneously recorded rectified electromyogram (EMG) from the adductor pollicis muscle. Clear oscillations can be seen in the cortical recording, which are phase-locked to bursts in the EMG.

C. The coherence calculated between slow-wave and rectified EMG, using all data available from one recording session. The peak around 25 Hz indicates consistent phase locking between the two signals in this frequency band.

D. Variation during the task of the rectified adductor pollicis EMG and the finger and thumb lever-position signals. Analysis has been time-locked to the end of a successful hold period of the precision grip task (0 s).

E. Variation in coherence with task performance. The abscissa shows time during task performance. The ordinate shows coherence frequency. The grey scale indicates how the coherence between cortical signal and EMG varies with time, using the scale on the right. D and E averaged from 274 successful trials of the task (Baker et al. 1999).



2000). The delays determined both from phase differences between MEG and EMG and from signals averaged with respect to zero phase of the EMG nicely agreed with absolute corticomuscular conduction times to arm and leg muscles. Functionally, this implies a hierarchical organization of the beta band corticomuscular interaction supporting the perception that motor cortex drives the spinal motoneuron pool (Hari and Salenius 1999).

The model that is suggested by the above findings is based on the concept of a centrally located oscillator transferring synchronous motor command to the muscles, being the cause of corticomuscular coherence. However, the cortex receives sensory activity as well. The spatial resolution of recording methodologies usually doesn't differentiate between motor or sensory cortices due to the fact that they are very close together. There is the possibility that the observed corticomuscular coherence is not merely descending or ascending information but a combination of both. That may lead the second order cumulant to wrong results and to a peak showing dominance of the descending character of the phenomenon with the ascending component altering the results giving an incorrect lag time.



2000). The delay determined both from phase differences between EEG and EMG and from signals averaged with respect to zero phase of the EMG. In fact, with absolute corticomuscular conduction times in arm and leg muscles. Functionally, this implies a hierarchical organization of the brain that corticospinal projections supporting the perception that motor cortex drives the spinal motoneuron pool (Hess and Salinas 1997).

The model that is suggested by the above findings is based on the concept of a centrally located generator transferring signals to motor output and sensory input.

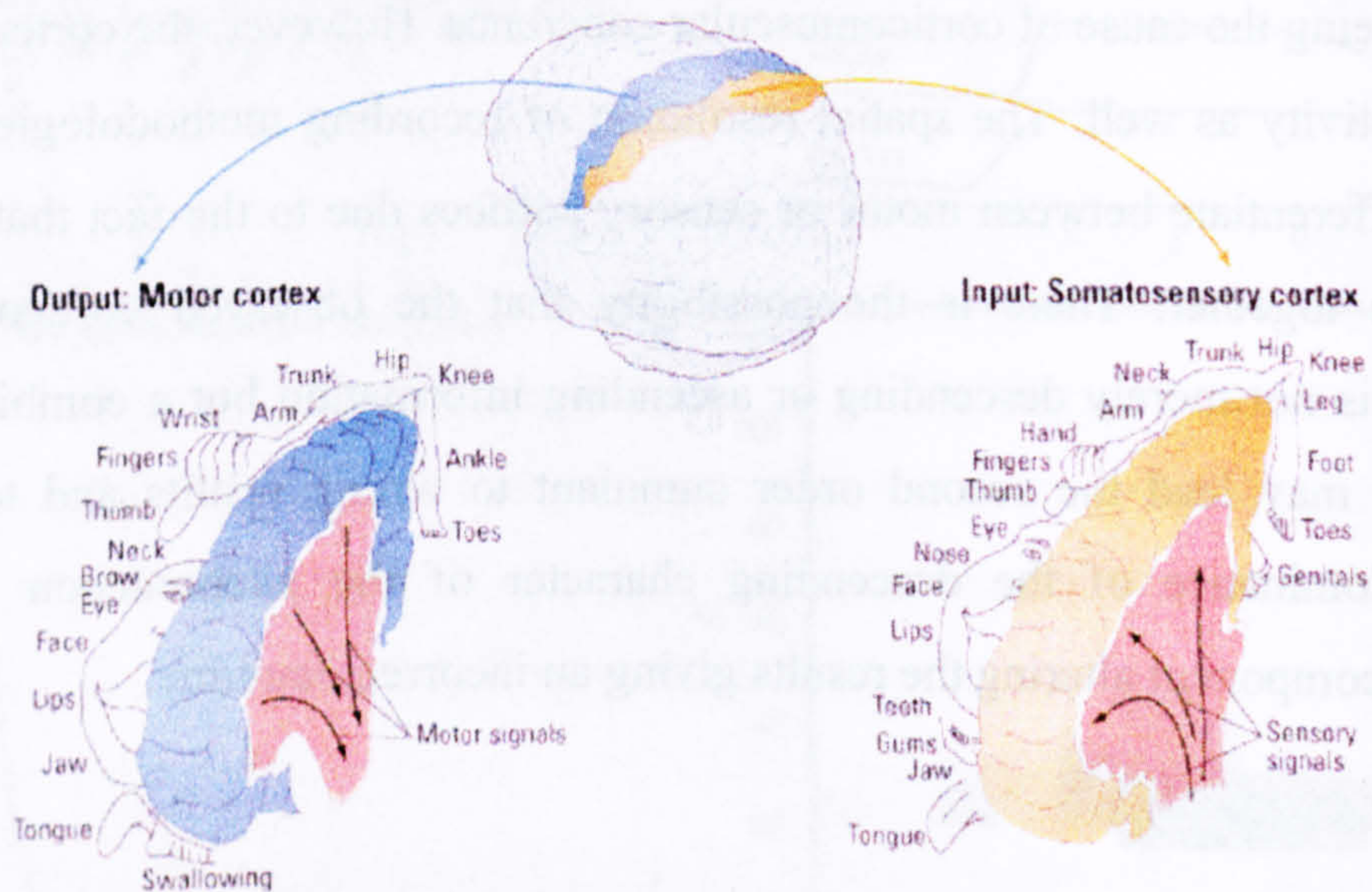


**Fig. 2.25** Motor and sensory homunculus. The motor and sensory homunculus show the areas of the cortex concerned with the body's motor and sensory function respectively (<http://piclib.nhm.ac.uk> 2005).



## **2.7 NEURAL PLASTICITY**

The concept of plasticity originated in the medical sciences. It refers to the ability of an organism to be modifiable. This variability and flexibility enables humans to adapt to a great range of changing environmental conditions. This chapter will demonstrate the implication of neural plasticity in neuroprosthetic control.

### **2.7.1 Cortical reorganisation and recovery**

During the past few years, the development of precise models that simulate map formation in the primary sensory cortex has been attempted. As early as 1937, it was revealed that the surface of the cerebral cortex contained a map of the body surface called the homunculus as illustrated in Fig. 2.25 (Penfield and Boldrey 1937; Metman et al. 1993). The term “map” refers to the fact that sensory stimuli are projected onto the cortex so that close cortical elements within a primary sensory region are excited by stimuli from close areas of the body surface. The body is pictured on both sides of the central sulcus in a distorted form; for example, the fingers, the lips and the tongue take up more of the brain’s surface area than the back or the lower legs, and the area representing the thumb is equal to the area representing an entire arm.

However, the brain is constantly changing. At birth the brain is only partially myelinated and diffusely interconnected. The adult brain develops into a complex system. It is finely tuned in order to deal with the demands of the environment and fulfil its evolutionary objective, through many precise sensory cognitive and motor pathways. Through learning and memory and the effects of context and attention the mature brain adapts to changes (external or internal like trauma or injury) in order to respond in an optimised way (Ward 2001).

The potential for reorganization in the adult brain has been underestimated in the past. Just recently the scientific community began to understand the organisational fundamentals involved in functional recovery (Rossini and Pauri 2000). Within the last ten years it was discovered that cortical maps are highly plastic in adult animals and humans after various neurogenic disorders. This means that the representation will change immediately, or in the long term after the occurrence of a



disorder. The mature brain appears to be a dynamic system adapting to new conditions.

### ***2.7.2 Cortical reorganisation following CNS injury***

Stroke or cerebrovascular accident is the most common form of CNS injury. It is also the number one cause of disability and the third leading cause of death in the UK. It is the result of temporary or permanent ischemia to part of the brain because of thrombosis or embolism or the result of haemorrhage following aneurism. Parts of the brain that are directly associated with movement can be affected. The recovery and the reorganisation of the central nervous system after a stroke are extremely interesting.

Another common form of CNS injury is caused by head trauma. That could be penetrating head injuries, compressive head injuries and closed head injuries that present the major problem in civilian life and cause of disability. Tumours and surgical procedures for removing them is one more cause of brain damage as well as any other surgical procedure in the brain (removing of epileptic focus) is a potential danger of CNS injury.

### ***2.7.3 Central nervous system plasticity***

Immediate and long term changes in the functional organisation of the brain changes have been shown after minor or serious CNS injury. When a functional system is partially damaged, recovery within the system is possible. Experimental and clinical studies have shown that approximately 1/5 of the pyramidal fibres are sufficient to ensure recovery of fractionated hand finger movement. Hence, a within-pyramidal system reorganization, when possible, is a major candidate for functional recovery of motor control of upper limb and hand. (Rossini and Pauri 2000)

Recently, experimental evidence further support the hypothesis that neuronal aggregates adjacent to a lesion in the sensorimotor brain areas can progressively aid and substitute to the function of the damaged neurones (Rossini and Pauri 2000). Such a reorganisation in the affected hemisphere of a patient with a monohemispheric lesion, would significantly modify the rough interhemispheric symmetry of somatotopic organisation of the sensorimotor cortices, both in terms of



absolute surfaces and number of 'recruited' neurons, as well as of spatial coordinates that has been observed in healthy humans by different methods of functional brain imaging, including PET, fMRI, TMS and MEG (Rossini and Pauri 2000). Neuronal failure in the affected area would induce remote modulatory effects on cortical excitability of unaffected areas of the same hemisphere, via cortico-cortical connections, and of the contralateral unaffected hemisphere via transcallosal fibres (Rossini and Pauri 2000). These changes would also induce changes to the non affected hemisphere maintaining balance or integration between corresponding cortical fields (Calford and Tweedale 1990).

Spinal cord injury is also a major cause of disability. Direct or indirect trauma can cause complete spinal cord injury where no sensory or voluntary motor function is present below the level of the injury and incomplete SCI where there is no total disruption below the level of the lesion with the intact ascending and descending fibres continue to function. Paraplegia and tetraplegia are two common disabilities where because of SCI the patient doesn't have any sensory or motor function below the level of legs or arms respectively.

It has been repeatedly shown that the primary sensorimotor cortex of the adult brain possesses the ability to reorganise itself after a SCI (Green et al. 1998), (Cohen et al. 1991), (Cohen et al. 1991), (Bruehlmeier et al. 1998). More specifically spinal cord injury resulted in enlargement of the map of outputs targeting muscles proximal to the lesion level (Bruehlmeier et al. 1998). Other studies have also repeatedly shown how the primary sensorimotor cortex of the adult brain possesses the ability to reorganise itself after peripheral sensory deprivation, by allowing neighbouring cortical regions to expand into territories normally occupied by the input from the deprived sense organs. Studies also inferred a reorganization of the cortical motor system (Green et al. 1998). Their aim was to determine if cortical motor representation and generators change after partial or complete paralysis after Spinal Cord Injury (SCI) using EEG. They confirmed previous studies reporting evidence for a change in cortical motor function after SCI, derived from transcranial magnetic stimulation (Levy et al. 1990).

An other interesting study also used PET to compare resting cerebral glucose metabolism in patients with complete paraplegia or tetraplegia after spinal cord



injury and healthy subjects (Roelcke et al. 1997). It came to a conclusion that a transverse spinal cord lesion has an effect on cerebral energy metabolism in view of sensorimotor reorganisation. More specifically it revealed that global absolute glucose metabolism was lower in spinal cord injury than in normals. However, there were areas with relatively increased glucose metabolism particularly in the supplementary motor area, anterior cingulate, and putamen, regions involved in attention and initiation of movement probably because of secondary disinhibition of these areas. Relatively reduced glucose metabolism in patients with spinal cord injury was found in the midbrain, cerebellar hemispheres, and temporal cortex (Roelcke et al. 1997).

Significant reorganization of motor and sensory topographic maps occurs because of the deafferentation (and deafferentation) resulting from the SCI. However, it has been suggested that the changes in brain activation following spinal cord injury may reflect an adaptation of hand movement to a new body reference scheme secondary to sensory deprivation like reduced and altered spinothalamic and spino-cerebellar inputs (Bruehlmeier et al. 1998). PET revealed not only an expansion of the cortical 'hand area' towards the cortical 'leg area', but also an enhanced bilateral activation of the thalamus and cerebellum. The areas of the brain which were activated were qualitatively the same in both paraplegic and tetraplegic patient groups, but differed quantitatively as a function of the level of their spinal cord injury. This showed that patients with spinal cord injury exhibit extensive changes in the activation of cortical and subcortical brain areas during hand movements, irrespective of normal (paraplegic) or impaired (tetraplegic patients) hand function (Bruehlmeier et al. 1998).

Another interesting fact is that CNS lesions like cortical or SCI induce plasticity to the spinal cord itself (Wolpaw and Tennissen 2001). Despite of the fact that significant gait recovery has been considered unachievable following a clinically complete or severe incomplete spinal cord injury, the locomotion of spinal animals can be improved by training that provides complex temporal patterns of sensory information related to stepping that is interpreted by the spinal cord. This suggests human spinal networks can integrate and interpret complex sensory signals to produce functional efferent output and adapt to repetitive training that is considered



as a new rehabilitative approach (Harkema 2001). This implies that the spinal cord is more than a simple relay station to the commands from the brain but plays an active role in motor control (Rauch and Rittweger 2001). It is likely that it computes a limb representation from the peripheral input, which is compared to the internal model of the limb's physical properties in order to compute the motor output signal necessary for a certain movement (Kawato and Wolpert 1998; Kawato 1999). The internal model is updated continuously, which is partly due to an adaptive process within the spinal cord, but also influenced by the brain (Carrier et al. 1997). This suggests that motor learning also takes place in the spinal cord and not exclusively in the cerebellum.

#### ***2.7.4 Cortical reorganisation following PNS disorder***

Degenerative PNS like deafferentation or motoneuronal disease could also affect the CNS. Deafferentation is a loss of the sensory input from a portion or the whole of the body is usually caused by degeneration of the peripheral sensory fibres or organs, nerve injury, ventral root injury, nerve compression like tunnel carpal syndrome or surgical procedures to tackle pain disorders. The loss of afferent pathways results to lack of any afferent information to the brain while in some cases the efferent mechanism is still functioning. Deafferentation on the other side is the loss of motor output to a portion or the whole of the body because of motoneuronal disease that causes degeneration of motor neurons. Other causes of deafferentation are nerve injury, ventral root injury, nerve compression (e.g. carpal tunnel syndrome). Amputation of a limb, because of various reasons such as accidents or pathogenesis obviously results to a significant disruption of the peripheral nervous system and is another form of peripheral deafferentation/deafferentation, since a large number of efferent and afferent fibres and sensors are lost with the lost limb.

The effects of deafferentation/deafferentation can be emulated in an experimental environment using various techniques, in order to gain understanding of the pathological conditions. The experiments may involve both humans and animals. For humans reversible procedures like Ischemic Nerve Block (INB) where deafferentation comes as a result of hypoxia of afferent fibres after prolonged block of blood circulation in the forearm or injection of the nerve with anaesthetic agents



A



B

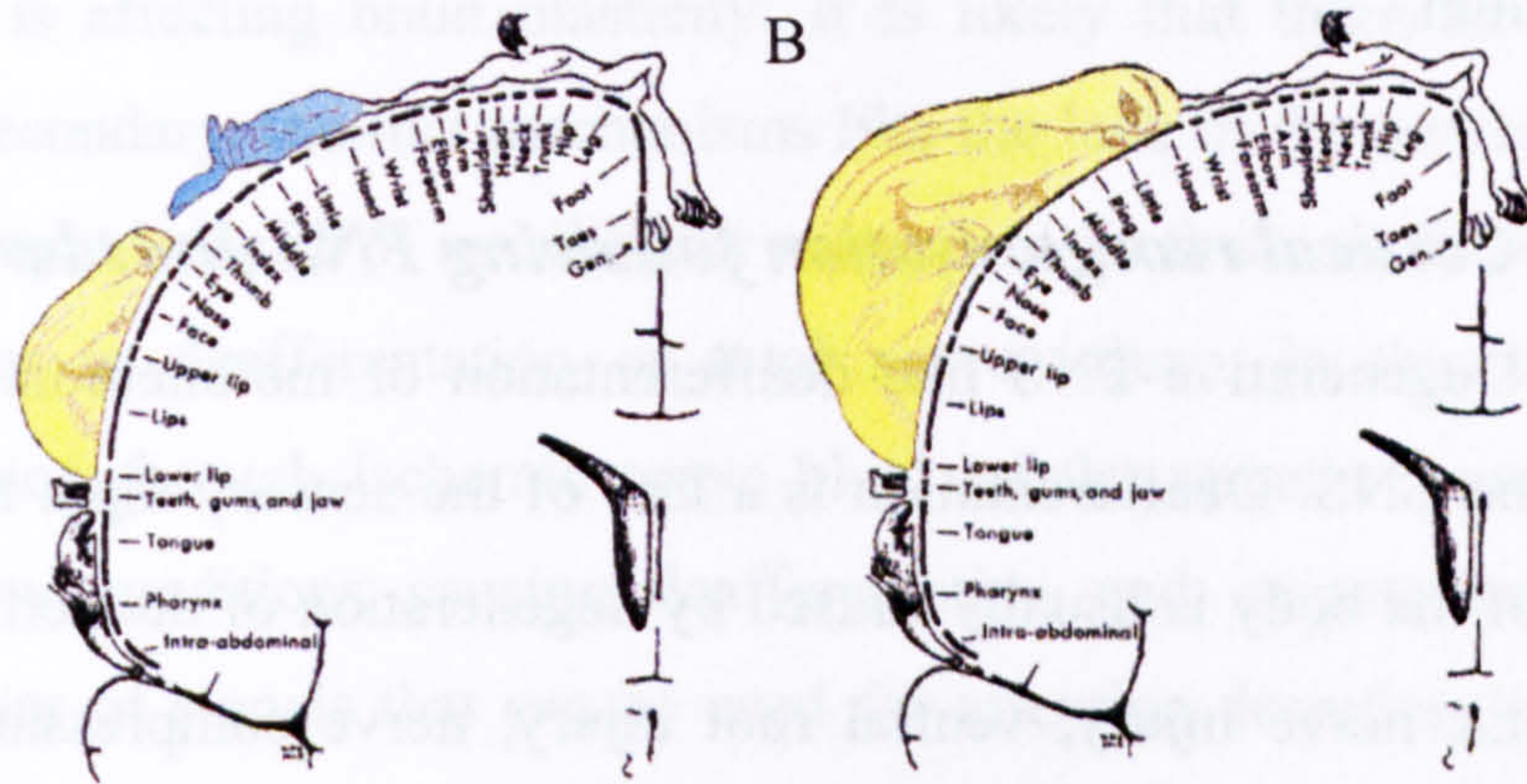


**Fig. 2.26 A.** Example of phantom limb sensations caused by stimulating arm. In this case there are two distinct spatial maps, one close to the line of amputation, the second higher up on the arm.

**B.** In the patient, touching an area on the face or the upper arm produces a tactile sensation associated with the lost hand. The hand area in the cortex is in between the arm and the face area. When the hand is lost, the corresponding cortical cells come under the control of these neighbouring areas that innervate the face and/or the upper arm. Thus, the referred sensations are to be expected if the sensory inputs from the face (and/or upper arm) invade the cortical territory formerly occupied by inputs from the amputated hand. The second picture shows the case where the face area has invaded the former hand region (Ramachandran and Hirstein 1998).



like lidocaine have been widely used. For animals both reversible procedures similar to the one used in humans as well as irreversible procedures involving nerve lesions and limb amputation have been used. In all the cases of peripheral nervous injury the common factor is lack of afferent input to the CNS to which the brain seems to be very sensitive. Since for peripheral nervous injury the brain is physically intact it is feasible to map the brain using the usual mapping techniques and to detect the cortical reorganisation.

There hasn't been enough evidence in the literature of how deafferentation alone (with the sensory fibres intact) because of motoneuronal disease, or ventral root injury is affecting brain plasticity. It is likely that there are plastic changes caused of secondary, indirect mechanisms like the lack of the movement component of sensory input because of inability for movement. In that case the effects should be quite similar to deafferentation or total nerve injury. In this thesis temporary deafferentation through ischemic nerve block of the upper extremity was used to emulate how conditions causing deafferentation and amputation can affect the characteristics of signals that can be used for intention detection in neuroprosthetic devices.

### ***2.7.5 Amputees***

Upper limb amputation in man was followed by severe reorganisation of the functional map of the sensory cortex. Tactile stimulation of the lip evoked responses not only in the normal face area but also within the cortical region associated to the amputated hand Fig. 2.26 (Ramachandran and Hirstein 1998). This shift of cortical areas was also accompanied by a significant increase in the area of representation of the intact hand because of increased sensory significance and increased use of the intact hand (Rossini and Pauri 2000). Unfortunately reorganization is not always a positive phenomenon. Phantom limb pain in amputees is associated with reorganization changes in the somatosensory system. There seems to be a high correlation between the magnitude of the shift (reflecting enhanced plasticity) of the cortical representation of the mouth into the hand area in motor and somatosensory cortex and phantom limb pain (Karl et al. 2001).



A study on pre and post operative amputee patients showed that in one patient, reorganization of the mouth area into the hand area took place immediately after the amputation while in another patient reorganization had occurred prior to the amputation possibly related to non-use of the arm several years prior to the amputation (Grusser et al. 2001). Despite of the fact that sensory deprivation is considered responsible for the plastic changes in the cortex after amputation little is known about the actual mechanisms that induce these significant large scale shifts in the cortical representation. There is a fairly good chance that subcortical structures and in particular the thalamus contribute to those changes. It was shown that thalamic changes produced by limb amputation appear to be an important substrate of cortical reorganization with cortical mechanisms of plasticity to contribute as well (Florence et al. 2000).

### ***2.7.6 Activity Dependent Plasticity***

Plasticity doesn't always occur only under pathological conditions and brain disorders. Another type of plasticity that we have to take under consideration is the use dependent plasticity. The sustained performance of simple or more complicated motor tasks are associated with neural plasticity. This reorganisation occurs in the long term with complex task acquisition but can also occur in a short term as rapid plasticity that could be the first step of skill acquisition and long term plasticity (Classen et al. 1998). These types of long and short term use dependent plasticity can be considered as a part of the adaptive behaviour and motor learning mechanism.

It has been shown that a short-lasting training of synchronous movements of the thumb and the foot induced a transient and mean shift of 7 mm of the centre of gravity of the hand muscle medially toward the foot area which vanished after about 1h (Classen et al. 1998). This modulation of the motor output has been ascribed to interactions between hand and foot representation areas in the motor cortex (Rossini and Pauri 2000). While rapid plasticity is probably the first step of skill acquisition, long-term, experience-dependent reorganisation may underlie the acquisition and retention of motor skills. Functional magnetic resonance imaging showed the enlargement of activated cortex by the practiced sequence compared with the



unpractised sequence, after 4 weeks of training with the changes persisting for several months (Karni et al. 1995; Rossini and Pauri 2000).

The mechanisms of plasticity are not completely clear but seem to include modifications in cortical properties like strength of internal connections representations patterns or neuronal modifications, morphological or functional. (Cohen et al. 1998). It has also been shown the plasticity of the sensory cortex for blind Braille readers. Enlargement of the cortical representation zones that occurs after enhanced stimulation of a body part (the fingers in this case) (Sterr et al. 1998). Blind people are also better in localising sounds than are the sighted, presumably aided by additional auditory processing in the occipital lobe (Lessard et al. 1998). As mentioned earlier plasticity doesn't always have positive effect (phantom limb pain in amputees and tinnitus, ringing in the ears). Overuse of fingers causes dystonia, the inability to control precise finger movements, in musicians.

### ***2.7.7 Plasticity and learning***

It has been already mentioned that plasticity of the spinal cord after a SCI can help the rehabilitation of the patient. In fact, activity dependent plasticity occurs in the spinal cord throughout life. Driven by the peripheral nervous system and the brain, this plasticity plays an important role in the acquisition and maintenance of motor skills in the healthy population and in the effects of spinal cord injury and other central nervous system disorders (Wolpaw and Tennissen 2001). The adaptive behaviour and motor mechanism appears to be based on the non hierarchical flow of information between the cerebral cortex, the basal ganglia/thalamus, the cerebellum and (as recently was suggested) the spinal cord. The cerebral cortex appears to be characterised by a process of unsupervised learning that affects its basic computational modules. The function of these computations is the representation of non-linear manifolds, such as a body schema in the posterior parietal cortex, and field computing (Morasso and Sanguineti 1997). The cerebellum is plausibly specialized in the kind of supervised learning exemplified by the feedback error learning model. Moreover, the cerebellar circuitry is well designed for the representation of time series, according to a sequence-in sequence-out type of operation (Braitenberg et al. 1997). The Basal ganglia are known to be involved in



events of reinforcement learning that are required for the representation of goal-directed sequential behaviour (Sutton and Barto 1998).

### ***2.7.8 Plasticity and rehabilitation***

The understanding of neural plasticity brought new potentials for therapy and neurorehabilitation (Ward 2001). One therapeutic approach is to force motivated patients with conditions like hemiplegia and aphasia to overuse the impaired system when some residual function still exists. (Taub et al. 1993). The early rehabilitation of stroke patients may be crucial for optimal results. The change of corticomuscular coherence after stroke or trauma and during the rehabilitation period may also be an expression of reorganisation and plasticity. It has been shown that the increased strength of corticomuscular coherence could be a measure of improvement of the patient's condition (Bray 1999). Other therapeutic approaches tackle the negative effects of plasticity, like constraint-induced therapies for focal hand dystonia in musicians (Candia et al. 1999) and efforts to fill the gap of sensory information for amputees for relief from phantom limb pain.

Either short term or long term plasticity may have a negative impact on rehabilitation with the use of neuroprosthetic devices. Changes related to the progress of a condition, the patients recovery as well as activity dependent plasticity occurring from the use of the neuroprosthetic device itself may affect the robustness and the basic parameters of automatic intention detection.



## **2.8 ATTENTION**

“Everyone knows what attention is. It is the taking possession by the mind, in clear and vivid form, of one out of what seemed several simultaneously possible objects or trains of thought. Focalisation, concentration of consciousness are of its essence. It implies withdrawal from some things in order to deal effectively with others.” (James 1890 in Wang et al. 2002)

### **2.8.1 Attention as a cognitive process**

Attention is a concept with which everybody is familiar. However, because of its subjectively evident nature, it is difficult to define what this cognitive experience really is. In the literature there is no widely accepted definition of attention since psychologists have been particularly reluctant to define. Therefore, attention can not be considered a unitary entity since it describes a diverse set of behavioural and cognitive processes.

This thesis will deal with the term attention in a more applied and simplified way related to human action and motor control. In simple terms, the human brain doesn't have the capacity to comprehend all the sensory information at once or perform unlimited simultaneous tasks. One can only consciously attend to, or think about, so much at a time. Several activities can be carried out at the same time in an effective way, only if what one is doing is within the capacity limits of their information processing system. For example driving requires little attention on the open road so one can converse relatively easily at the same time. However, when traffic becomes heavy, the conversation suffers because driving requires all the attention.

### **2.8.2 The single channel and flexible central resource capacity**

The single channel theory was the first formal theory and suggested that the human performer or operator constitutes a single limited processing capacity channel (Welford 1952; Broadbent 1958). This time based theory on attention assumed that the individual had difficulty doing several things at the same time because the information system took time to perform its functions and perform them only one at a time.



"Everyone knows what attention is. It is the taking possession by the mind, in clear and vivid form, of one out of what seemed several simultaneously possible objects or trains of thought. Focalisation, concentration of consciousness are of its essence. It implies withdrawal from some things in order to deal effectively with others" (James 1890 in Wang et al. 2002)

### 2.8.1 Attention as a cognitive process

Attention is a concept with which everybody is familiar. However, because of

its subjectively evident nature it is difficult to define what this cognitive experience really is. In the literature a widely accepted definition of attention since

psychologists have been particularly reluctant to define it precisely, attention can not

be considered a solitary cognitive process. This thesis will be developed in a way related to human activities that

do not have the capacity to perform unlimited simultaneous

activities. Several activities can be carried out at the same time in an

effective way if one is doing it within the capacity limits of their

attention. Several activities can be carried out at the same time in an

effective way if one is doing it within the capacity limits of their

attention. Several activities can be carried out at the same time in an

effective way if one is doing it within the capacity limits of their

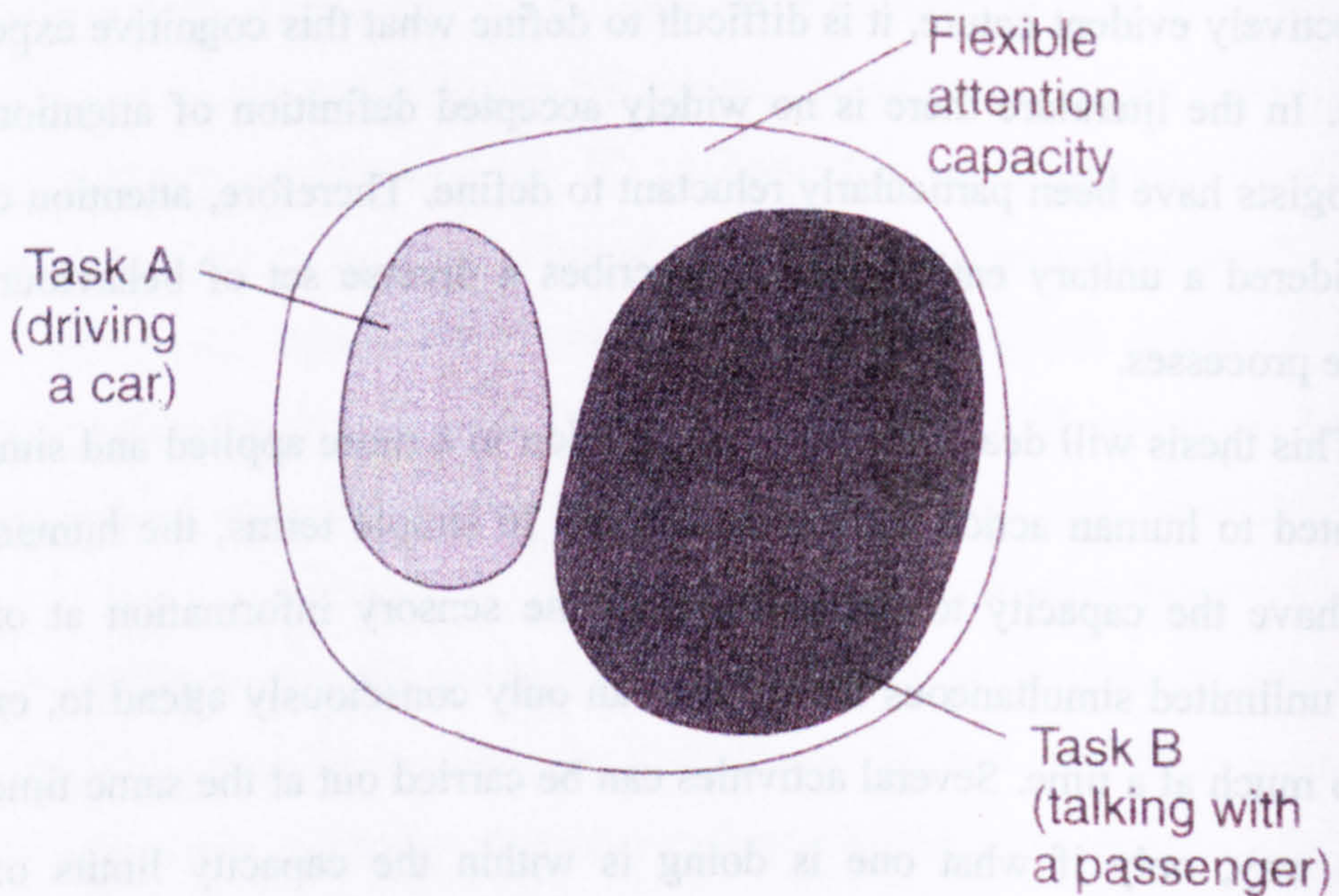


**Fig. 2.27** Example of the flexible attention capacity. (Magill 2004) Illustration of how two tasks can be performed simultaneously if the attention demanded by the two tasks does not exceed the available attention capacity. As long as the driving and conversing tasks represented by small circles can fit into the large circle, one can effectively carry out the tasks. Problems arise when the simultaneous tasks don't fit into the large circle.

### 2.8.2 The single channel and flexible central resource capacity

The single channel theory was the first formal theory and suggested that the

human performer or operator constitutes a single limited processing capacity channel

(Welford 1952; Broadbent 1958). This time based theory on which we are based but

the individual had difficulty doing several things at the same time because the

information system took time to perform its functions and perform them only one at

a time.



The flexible central resource capacity theory (Kahneman 1973) was developed after it became apparent from related investigation that it is often possible to respond appropriately to more than one stimulus at the same time so the single channel theory had to be revised. In this model the capacity limits of the central pool of resources are flexible. This means that the amount of available attention can change depending on conditions related to:

- the individual - arousal level varies within and between individuals
- the tasks - attentional demands differ across tasks
- the situation
- involuntary attention to novelty, meaningfulness
- selective attention to specific aspects of situation

These conditions govern both the available amount of attention and the allocation of attention to different tasks as is illustrated in Fig. 2.27. More sophisticated and up-to-date models have also been developed but the presented models are adequate for the objectives of the current study since they are simple, general and schematic enough to comprehend.

### ***2.8.3 Physiology of attention***

As with the definition of attention there is no widely accepted physiological model for attention. What is commonly accepted is that neurophysiological loci underlying attentional phenomena are numerous and are spread out over many parts of the brain. In this chapter we are going to demonstrate how some of these parts are directly or indirectly involved in the voluntary movement mechanism. This inevitably suggests that there is a high chance of one system influencing the other. As it will be demonstrated later in this thesis, attention is a highly significant function in normal movement and consequently in the operation of neuroprosthetic devices.

#### ***2.8.3.1 Parietal and temporal lobe influences on attention***

The parietal and temporal lobes are considered as sensory association areas providing a concise environmental representation. They provide a secondary analysis mechanism of sensory information integrating multiple types of information. This is



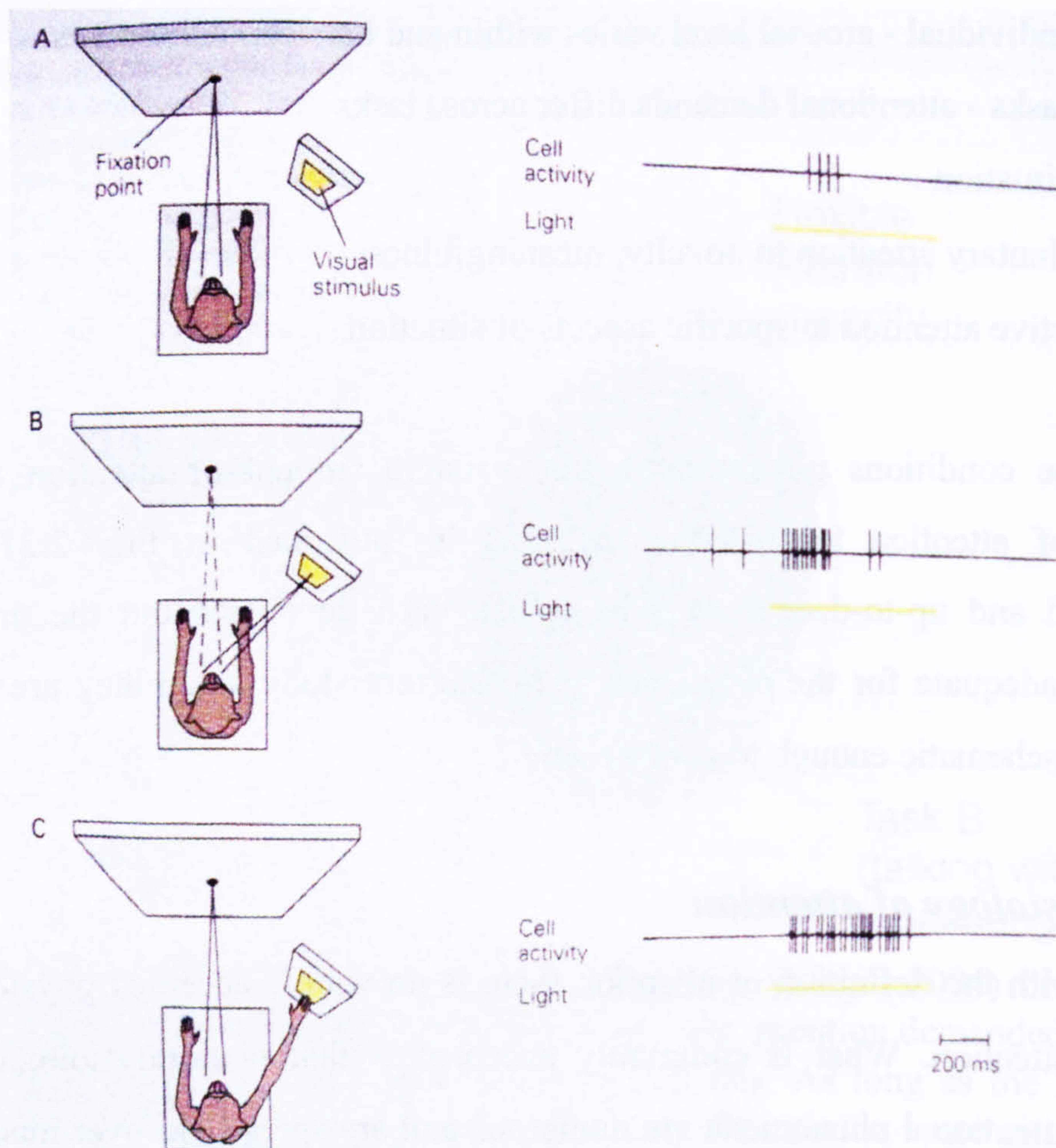


**Fig. 2.28** Neurons in the posterior parietal cortex of a monkey respond more effectively to a stimulus when the animal is attentive to the stimulus. A - A spot of light elicits only a few action potentials in a cell when the animal's gaze is fixed away from the stimulus. B - The same cell's activity is enhanced when the animal takes visual notice of the stimulus through saccadic eye movement. C - The cell's activity is further enhanced when the monkey touches the spot but without moving its eyes (from Wurtz and Goldberg 1989 in (Kandel et al. 1995)).



suggested by the fact that damage in these areas impairs complex cognitive functions that require mixing of multiple sources of information like reading. Attentional deficits may also occur with most striking examples being neglect syndromes since attention requires the integration of a plethora of visual, spatial, somatic and other information.

The inferior parietal lobe has been shown to be critical in sensory selective attention. It contains cells that show enhanced response when motivationally directed attention occurs (Cohen et al. 1993) . It has been also demonstrated that that for subjects performing a simple motor movement and showing activation of the inferior parietal lobe together with other higher-order motor areas (intermediate supplementary motor area, anterior Cingulate Motor Area (CMA)) these areas became active before the executive motor areas primary motor area and posterior supplementary motor area (Ball et al. 1999). This suggests that the early activation of the inferior parietal lobe and the anterior CMA may be related to attentional functions of these areas. The right posterior parietal cortex may have a pre-eminent role in visuospatial and orienting attention, and the existence of a distinct anterior parietal mechanism of motor attention have also been demonstrated used repetitive transcranial magnetic stimulation (Rushworth et al. 2001).

Posterior parietal lobe is important for spatial attention. Lesions of the posterior parietal cortex often result in attentional deficits, or contralateral neglect. Scientists have observed neurons in the parietal cortex of rhesus monkey that fire only if the animal put attention to a particular information (Fig. 2.28). Low alpha mesoparietal activation (task related power decrease) that was observed for transitions between motor sequences, likely reflects a posterior parietal motor command that initiates transitions between motor programs (Deiber et al. 2001). Task related power decrease for left and bimanual movements (more difficult tasks) shows the possible attentional activation of Posterior parietal cortex. The left posterior parietal cortex is related with motor attention since patients with left hemisphere lesions show ideomotor apraxia (a disturbance of voluntary movement in which a person cannot translate an idea into movement) and have problems performing sequences of movements. It has been suggested that these disorders are



consequence of a difficulty in shifting the focus of motor attention from one movement in a sequence to the next (Rushworth et al. 1997).

### ***2.8.3.2 Frontal lobe***

An important attention area in the frontal lobe is the anterior attentional network, located along the midline and sides of the frontal lobes and in parts of the basal ganglia. This network is concerned with bringing into our conscious awareness whatever is important. When one touches something very hot, one's hand is withdrawn before one realizes what has happened or has even felt the burn. The anterior attention system is activated when several conflicting decisions are available, but only one can be selected. Attentional deficits seem to be common in most forms of frontal lobe disorders. Lesions of the prefrontal cortex disrupt a number of attentional control functions like task learning performance involving discrimination and delayed response, motility, visual search, and social emotional functioning (Trehub 1991).

Experimental studies confirm a disorder of visual directed attention: unilateral lesions may produce a neglect to be differentiated from the spatial neglect of posterior lesions. Patients with bilateral lesions are impaired in describing complex pictures. Studies have also shown the role of the frontal lobes in the selective control of attention. There is also a clear-cut deficit in sustained attention. Despite the vast literature on the involvement of the parietal cortex in attention very few studies have examined its role in sustaining attention over time. Although one might expect that the same cortical regions involved in directing attention would also be required to maintain that attention over time, most studies of sustained attention have implicated the frontal lobes. Numerous studies using normal subjects have shown an increase in blood flow in the right prefrontal cortex during performance of many different types of tasks requiring sustained attention (Pardo et al. 1991; Vendrell et al. 1995; Eslinger and Biddle 2000). Thus there seems to be a widely accepted that the frontal lobes and particularly the right prefrontal cortex are important when attention must be sustained over time (Rueckert and Grafman 1998).

Frontal cortex has also a critical role of in the attentional control of movements. More specifically it has been shown to impair attentional control of unpractised movements during motor learning in man. (Richer et al. 1999)



### ***2.8.3.3 Cingulate cortex***

The anterior cingulate cortex a paralimbic brain region is richly interconnected with limbic structures and cortical areas, particularly the frontal cortex. It appears to exert significant influence over attention and especially intensive aspects of attention. It seems to play a role in modulating and creating a temporal continuity for affective - motivational impulses relative to ongoing stimuli that arouse attention (Cotterill 2001). Recent neuroimaging data further suggests that the cingulate gyrus appears to be a multimodal area involved in several types of cognitive activity, including attentional processes associated or not with motor tasks (Turak et al. 2002). Studies involving stroop tasks showed activation of the anterior cingulate in the incongruent condition (e.g., the noun blue displayed in red colour) when compared with the congruent condition (e.g., the noun blue displayed in blue colour) or neutral (noncolour word) (Posner and DiGirolamo. 1998). This demonstrated that an aspect of voluntary control is the suppression of automatic actions.

PET fMRI and EEG studies have also demonstrated the involvement of (prefrontal and) anterior cingulate cortex to attention to action (Jueptner et al. 1997) (Ball et al. 1999), where they were activated when subjects paid attention to the performance of the pre-learned sequence compared with automatic performance of the same task, result that is in line with a previous study (Passingham 1996). It has been already stated that that for subjects performing a simple motor movement and showing activation of the anterior cingulate it became active before the main motor areas. This further suggests that the early activation of the anterior CMA may be related to attentional functions.

### ***2.8.3.4 Thalamic influences***

The classic view of the thalamus is a passive relay station or a direct integrating system of sensory information which is critical for coordination of motor and sensory functions (Kandel et al. 1995). Unilateral thalamic lesions have been shown to cause attention disorders like hemispatial neglect (Karnath et al. 2002) (Rafal and Posner 1987; Manabe et al. 1999; Peru et al. 2000)). The thalamus seems to have an indirect role in the attentional disturbances since it fails to connect the cortical areas that control spatial allocation of attention and subcortical structures that



generate the arousal necessary to catalyse attention. A more direct role of the thalamus is also possible. Rather than being just a relay, it probably acts as an integration system, which influences the associative value of information managing the focus of attention. Ultimately the direct and indirect mechanisms interact in the control of attention. (Cohen et al. 1993; Portas et al. 1998) have also given evidence that the thalamus is involved in interaction of selective attention and arousal by observing that activity evoked in the ventrolateral thalamus by an attentional task changed as a function of arousal (LaBerge 1997)

### ***2.8.3.5 Basal ganglia***

The classical notion that the basal ganglia are dedicated exclusively to motor control has been challenged by the accumulation of evidence revealing their involvement in cognitive functions such as attention. (Doya 2000; Briand et al. 2001). Abnormally low volumes of basal ganglia nuclei has been demonstrated to lead to Attention Deficit Hyperactivity Disorder (ADHD) (Aylward et al. 1996).

Damage to the basal ganglia usually leads to motor akinesia and a kind of psychic akinesia termed abulia. A disconnection of input from output commonly characterise these phenomena, so that neither thought nor sensory information can be linked to mental or physical action. Since, as it has been proposed, a form of focused attention is necessary for the automatic binding of input to output, only with such attention to an object or situation will voluntary effort lead to the calling up and operation of a motor programme or sequence of thoughts. This attention should normally operate at an automatic level and not intrude into consciousness, except during largely demanding tasks when it may be perceived as a feeling of focused concentration or superattention. (Brown and Marsden 1998)

“That some defect of attention is important in diseases of the basal ganglia is revealed by the observation of paradoxical kinesis, in which patients with Parkinson’s disease so akinetic that they can barely move, may deftly sidestep an oncoming car or flee from a fire. The form of attention described here, however, has nothing to do with arousal, vigilance, or alertness. Similar paradoxical phenomena can occur during sleep, resulting in normal speech and gait, in patients who talk or walk in their sleep”. (Brown and Marsden 1998)



### ***2.8.3.6 Other subcortical structures***

The limbic system, the hypothalamus and the reticular formation are three subcortical systems that interact creating a network for the control of normal attention. Each system exercises a relatively specific influence on attention, though these influences are integrated to create an attentional tone. Reticular system lesions usually disrupt normal arousal and abnormalities of consciousness and patients often fail to react effectively to stimulation. Despite of the fact that the relationship of the activation of the reticular activation to attention appears to be non specific, the generalised activation produced by this region leads to changes in sensory sensitivity and the thresholds for response production (Trehub 1991).

### ***2.8.3.7 Cerebellum***

Until recently, models of the neural systems involved in attention did not include a role for the cerebellum. However, based on anatomical connections and recent physiological data, it has been proposed that neocerebellum, the evolutionarily newest region of the cerebellum, may play a significant role in cognitive processes. (Akshoomoff and Courchesne 1992; Brown et al. 1997; Middleton and Strick 1998; Doya 2000; Middleton and Strick 2000; Barrios Cerrejon and Guardia Olmos 2001) Cerebellar involvement in cognition has been assessed in further studies with healthy and neurologically impaired humans with focal cerebellar lesions, patients with autism a disorder involving Purkinje neuron loss restricted to the neocerebellum (Courchesne et al. 1994; Townsend et al. 1999), ADHD (Prats-Vinas 2000) and the cerebellar cognitive affective syndrome (Schmahmann and Sherman 1998). The results have led to new hypotheses that are providing suggestions about the role of the cerebellum in perception, attention, and other cognitive functions. Functional magnetic resonance imaging was used to demonstrate that attention and motor performance independently activate distinct cerebellar regions (Akshoomoff et al. 1997; Allen et al. 1997) discuss the idea of the cerebellum being a master computational system that anticipates and adjusts responsiveness in a variety of brain systems like sensory, attention, memory, language, affect, to efficiently achieve goals determined by cerebral and other subcortical systems. However, methodological shortcomings and the lack of confirmed theoretical models on the nature of the



cerebellar contribution to cognition limit some of the interpretation of the empirical studies available (Daum and Ackermann 1995).

#### ***2.8.4 Attention influenced motor control?***

It is quite obvious that the physiology of attention is a complicated mechanism involving a plethora of functional brain components, a heterogeneous collection of processes, each of which may be underpinned by different neuronal networks. These networks may interact, such that engaging one type of attentional process could influence the efficiency of another (Coull et al. 1998). This cognitive function is not isolated but closely related to movement since a number of the involved in attention modules are directly or indirectly involved in movement making it difficult to differentiate them. A study picturing that involved visual attention task, finger movement task and simultaneous visual attention and finger tasks (Indovina and Sanes 2001). The finger movement task alone yielded brain activation in structures normally involved in movement like the primary cortex supplementary motor area and cerebellum. Visual attention produced significant bilateral cerebellar and sparse cerebral cortical activation. During simultaneous performance of both tasks, the movement- related plus attention-related activation extended beyond the movement- alone or attention-alone activation sites, suggesting a novel activation pattern related to the combined performance of attention and movement. Additionally, the combined effects of visual attention and movement upon brain activation were probably not simple gain effects, since activation-related interactions were found in the left superior parietal lobule, the right fusiform gyrus, and left insula, indicating a potent combinatory role for visual attention and movement for activation patterns in the human brain. These results strongly suggest that movement mechanism and the neurogenic signals acquired could easily be influenced by simultaneous attention demanding processes. This however is a two way relationship since according to the premotor theory of attention (Rizzolatti et al. 1987) movement itself induces an attentional shift, which adds up considering that movement itself is an attention demanding task. The extent that these interactions occur and whether movement intention detection signals like corticomuscular and intermuscular coherences are affected by attention has been examined within the framework of this thesis.



## **2.9 NEUROPROSTHETIC CONTROL**

Impairment of motor function can have consequences on the independence and quality of life of the affected individual. The development of new neural prostheses aims to improve function and mobility, helping the patients to lead more productive, socially integrated and independent lives and also to reduce the health care (Creasey et al. 2000) and support services load (Neuralpro 2002). The scope of this thesis is to contribute towards that direction by developing the physiological and methodological background for effective intention detection type of control in neuroprosthetic devices.

The purpose of a neural prosthesis is to restore lost or impaired body functions. In case of damage of the CNS, peripheral stimulation can bridge the gap created by the loss of communication between the central nervous system and the working parts of the human body (Neuralpro 2002). When a whole part of the body is missing a neural prosthesis will link to the patients command centre and act mechanically as the missing limb.

Damage to the central nervous system through stroke or injury often results in loss of motor functions, and in most cases mobility is affected. Injuries at a low level of the spinal cord result in paralysed legs, but with normal control of trunk and upper extremities. The benefit from even limited mobility would be significant. Such a capability would be useful in transfers and reaching objects, reducing dependence on carers, and also would effect long-term improvements in cardiovascular tone. The psychological benefits would be also important (Neuralpro 2002). Amputation is also another major cause of movement disability affecting many patients. Amputation is often the result of an accident, tumour removal surgical procedures, diabetes, landmines etc. Neural prosthesis can benefit patients, by replacing their impaired function. The restored functionality or mobility as well as aesthetic improvements would also contribute to self esteem and confidence.

This thesis deals with certain aspects of the use of physiological signals for use in neuroprosthetic control. Currently most methods are based on the neural coding in the human sensorymotor system together with processing and classification of conducted electrical signals from muscle and nerve tissue. The information is captured from the natural sensorymotor system and should be able to predict



Impairment of motor function can have consequences on the independence and quality of life of the affected individual. The development of new neural prostheses aims to improve function and mobility, helping the patient to lead more productive, socially integrated and independent lives and also to reduce the need for care (Creasey et al. 2000) and support services (and therefore costs). The scope of this thesis is to contribute towards that direction by developing the physiological and methodological background for effective training of a novel type of control in neuroprosthetic devices.

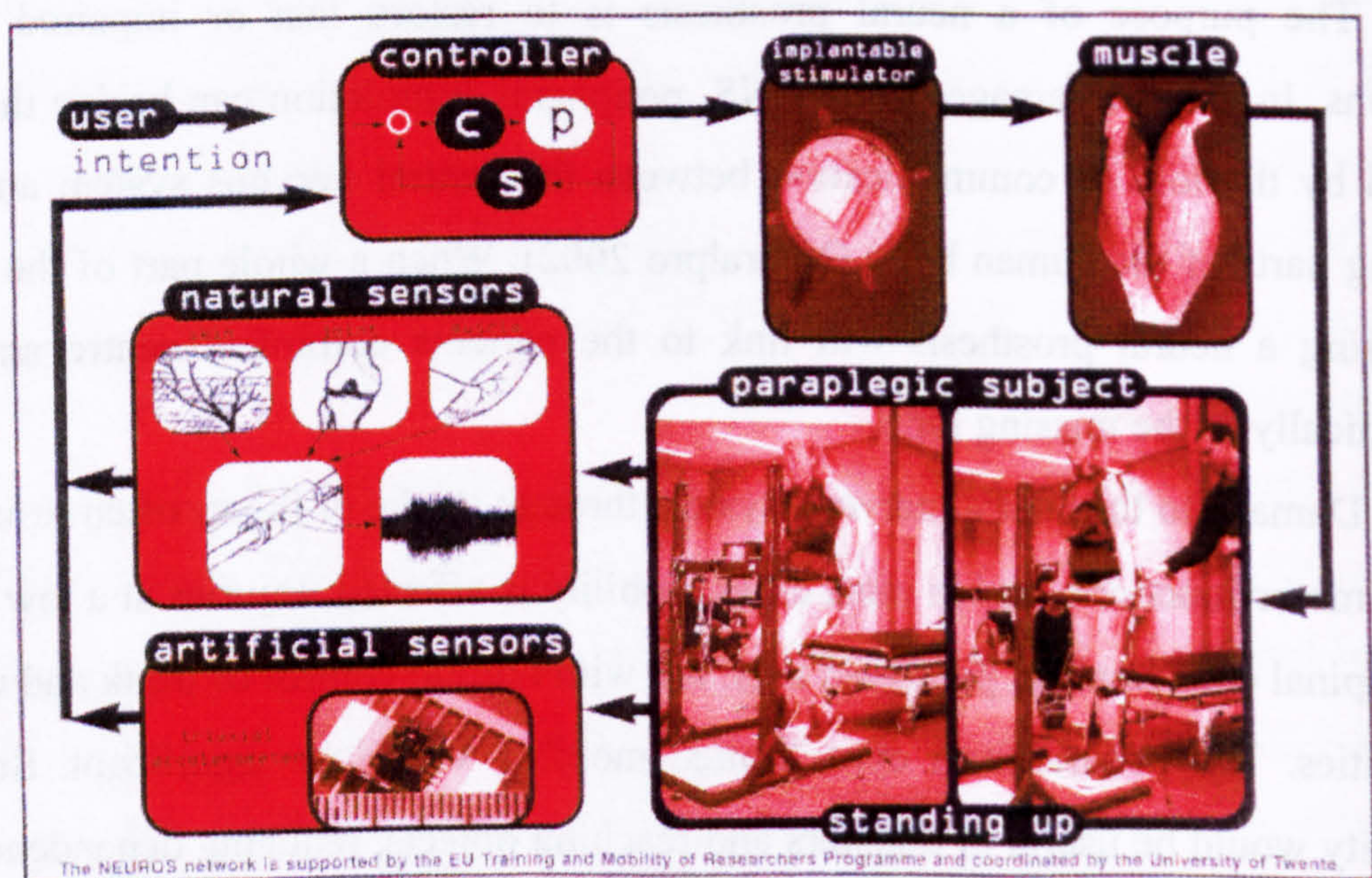


**Fig. 2.29** Intention detection model for FES neuroprosthesis for standing up of paraplegic patient. Adapted from “Neuros Network” website. <http://www.utwente.nl/bmti/neuros/> 1999



intention and voluntarily actuate self powered prosthetic devices or stimulate paralysed muscles Fig. 2.29. The recently discovered corticomuscular coherence, combined with other advances in the area, has potential for more effective clinical neuroprosthetic applications. Since the primary aim of neural prostheses is to improve function and independence of the user who is disabled, such a device should do exactly that, regardless of the degree of sophistication. In order for neural prosthetics to be useful, they need to function in their everyday environment, outside of the laboratory, controlled by the users themselves without the supervision and the aid of a researcher (Scott and Haugland 2001). Specific criteria for successful user command control interfaces have been reviewed (Crago et al. 1986; Hefftner et al. 1988; Johnson and Peckham 1990; Johnson et al. 1999; Lauer et al. 2000).

### ***2.9.1 Electromyogram Based Control***

In the early 1960s, after electromyography proved successful, researchers used EMG signals for controlling prostheses. The epidermal electrical activity, caused by underlying motor units can provide means of controlling neuroprosthetic devices. EMG carries a distinct signature of the voluntary intent of the central nervous system. It is usually recorded from active, unimpaired muscles of patient that have either lost a limb or are too weak to move because of injuries or neurological conditions. EMG control systems have also been used for communication devices (Lusted and Knapp 1996). However, the most common applications are myoelectric control for the control of external prostheses for the upper limb amputee and control of neuromuscular stimulation.

#### ***2.9.1.1 Myoelectric Prostheses***

Myoelectric prostheses have been used for over 30 years during which time these systems have become reliable and durable in most situations. (Uellendahl 2000). A typical myoelectric prosthesis is illustrated in Fig. 2.30. They are more often used on the upper extremities rather than lower extremities. Wearers of upper extremity prosthetic limbs learn to develop their own myoelectric patterns and program the system to recognise specific muscle contractions. In this way amputees can control the prosthetic limb using the activity of the muscles of the stump, their shoulder or even muscles of the contralateral side of the body. It has also been shown



that the extended use of such devices can reduce cortical reorganisation as well as phantom limb pain, a treatment resistant disorder.

Despite the sophistication of the solutions available, the dropout rates among patients are extremely high. In one study the rejection rate among children was 53% (Routhier et al. 2001). The dropout rates for above elbow and non dominant hand adult amputees can be even higher (Greatting 1991; Wright et al. 1995). Many factors like age, rehabilitation, training, early fitting can affect the long term use. Considering the fact that mechanical reliability of most systems today is excellent (despite the weight that is still quite high), the main limiting factor appears to be the nature of the man-prosthesis interface. The patient has to attend to the activation of muscle groups often not associated with the motor function replicated by the prosthesis. The process feels unnatural and requires high levels of attention and concentration and is highly dependent on visual feedback. Associated with this, there is a lengthy motor learning/training period that may not be successfully completed by all subjects. The effects of muscle fatigue on EMG signals are also a disadvantage since because the muscles of the stump or other muscle groups are easy to tire out.

### ***2.9.1.2 Functional Electrical Stimulation (FES)***

Neuromuscular stimulation for motion can be applied for therapeutic or functional purposes. Therapeutic applications include mainly methods for muscle conditioning through motor relearning. The functional applications aim to replace or augment the function of affected neuromuscular system (Munih and Ichie 2001) . The correction of the drop foot was the first (Liberson et al. 1961) and still most common FES system. The peroneal nerve of the affected side of a patient with hemiplegia is stimulated in order to assist the weak or non existing dorsiflexion. FES has since then extensively tested for other applications as lower extremity neuroprosthesis standing and walking of SCI patients.

Lower extremity applications of FES for restoring or improve standing and walking abilities in adults with complete or partial thoracic spinal cord injury, head trauma or stroke, have attracted the attention of many researchers in the last decades. FES in complete SCI, aims to provide limited functions of standing-up, standing, sitting, simple walking or cycling. FES is also useful as a form of exercise.





**Fig. 2.30** Typical below elbow myoelectric prosthesis. Small electrodes that fit intimately against the skin detect the minute residual muscle electrical activity as it contracts. When one is detected, circuitry tells the motor to open or close. The inner workings of the myoelectric arm reveal the circuit board, electrical connections, and electric motor. Adapted from Northwestern University Prosthetics and Orthotics Centre Website <http://www.nupoc.northwestern.edu> 2004.



FES for the restoration of motor function of the paralyzed upper extremities in motor disorders has significantly progressed in the last decade. Upper extremities are particularly difficult due to the fact that residual voluntary function for controlling the FES stimulator is usually low for patients with tetraplegia. Today there are several FES systems available in the world for clinical use. Such a commercial system is illustrated in Fig. 2.31. There are also several other projects in the world, which are aiming at development of FES systems for upper extremity function after spinal cord injury or stroke (Munih and Ichie 2001).

### ***2.9.2 Electroencephalography based control***

The use of brain activity for neuroprosthetic control has attracted the attention of the scientific community many years ago. As far back as 1967, subjects wired to an electroencephalograph (EEG) recording and graphing the electrical activity of the brain, were able with practice to reduce the amplitude of their brains' alpha rhythms, to transmit Morse code to a teleprinter (Dewan 1967 in Wolpaw et al. 2002). Since then many attempts had partial success or have been unsuccessful. Over the last decade, great advances have been made. The ultimate goal is the development of a Brain Computer Interface (BCI) that recognizes voluntary activity within the brain. Such a system should be able to control assistive device without requiring any physical movement. An example of such an experimental setup is given in Fig. 2.32. The main scope is to help patients suffering from conditions such as cerebral palsy, or spinal injuries, which inhibit physical control, but leave some intellectual faculties intact. Such an interface will allow patients with severe disabilities to have effective control of devices such as computers, and neural prostheses in their natural environments. This could increase an individual's independence, leading to a dramatically improved quality of life and reduce costs for the healthcare system. It mainly targets the group of patients that are totally paralysed and EMG based systems are not an option because of the lack of muscle activity.

Getting information into the brain is relatively easy through the natural sensory channels, such as sight or hearing. Interpreting output from the brain however by studying its electrical activity is a much harder problem. In theory the brain's intentions should be discernible in the spontaneous EEG (Wolpaw et al.



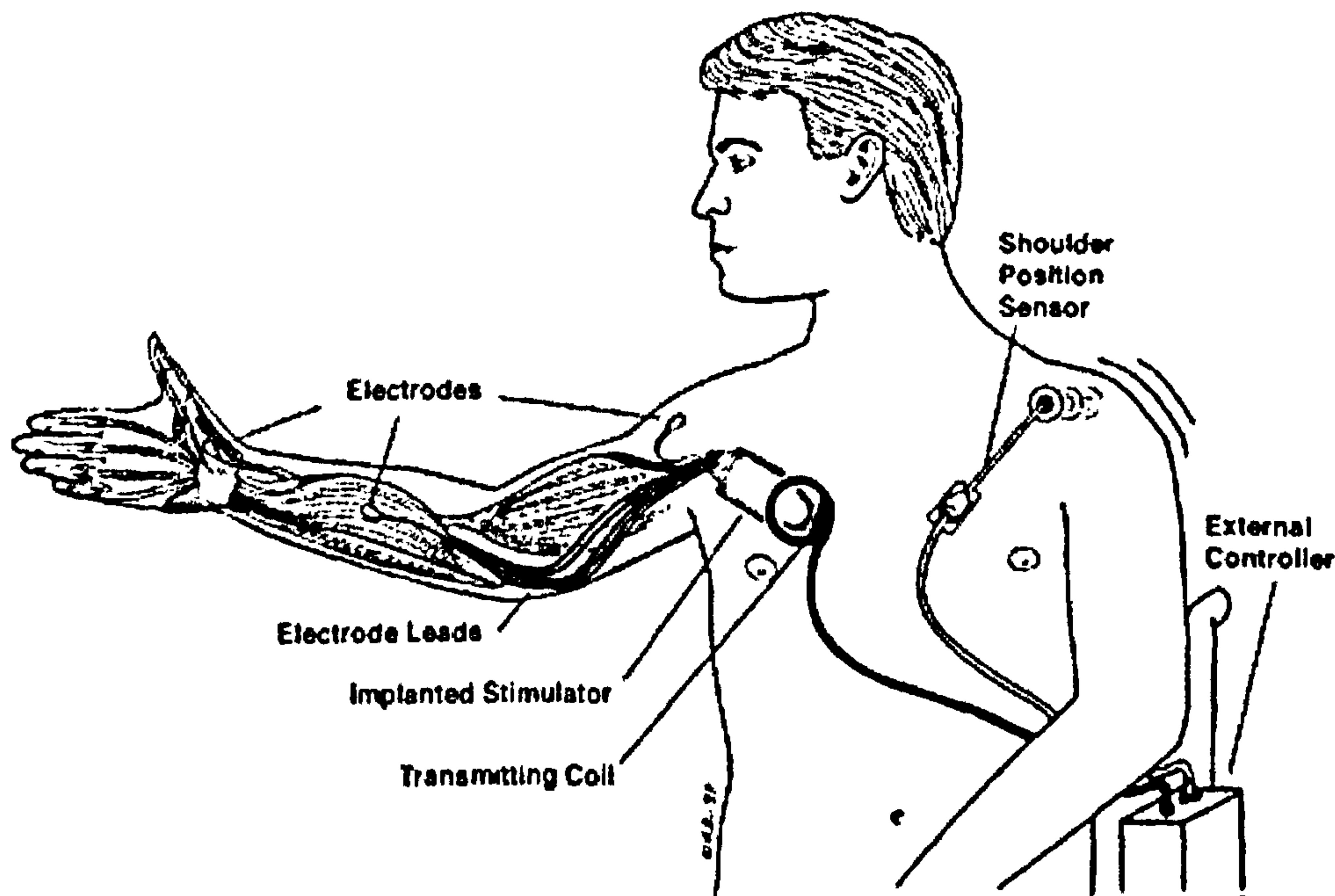


**Fig. 2.31** The Freehand System consists of surgically implanted components and an externally worn microprocessor. Eight electrodes attached to hand and forearm muscles are connected by internal electrode leads to a stimulator implanted in the chest. The implanted stimulator sends electrical stimuli to the electrodes, causing the muscles to flex and extend, creating grasp and release movements. A transmitting coil is worn externally over the location of the implanted stimulator. A shoulder position sensor, worn on the opposite shoulder, translates small learned shoulder movements into control signals. The microprocessor unit located on the wheelchair receives these signals and processes the information into radio waves which power the implanted stimulator via the transmitting coil. Adapted from <http://www.neurocontrol.com> 2005.



1991). However, the sheer complexity of the brain's structure and measurable activity produces EEG activity that is difficult to interpret. Only by focusing on very specific areas of brain activity, such as motor function, it has been possible to effectively analyse EEG data. The methodology involves the use of advanced signal processing, filters, Fourier transforms, and neural networks, in order to extract some useful information. Efforts have focused on training people to produce desired EEGs by modulating their brain activity through biofeedback mechanisms.

Voluntarily generated changes in features of the electroencephalogram (EEG) have been used to drive devices such as communication aids. However, these systems suffer from a poor initial relationship to the required behaviour, are hindered by lengthy training periods, are prone to error, and are slow and tiring to use. The equipment used is usually complex, and requires substantial calibration and tuning to work with specific individuals. These features make current EEG systems unattractive for clinical use in communication and the regulation of neuroprosthetic devices at the present moment.

### ***2.9.2.1 Short review of EEG based control***

***P300 detection.*** This technique (Farwell and Donchin 1988) for detecting the P300 component of a subject's event-related brain potential (ERP) was used to select from an array of 36 screen positions. The P300 component is a positive-going ERP in the EEG with a latency of about 300ms. A number of stimuli were presented to the subject paying attention to a particular, rarely occurring stimulus and respond to it in some non-motor way, such as by counting occurrences. With averaging the EEG response the P300 response can be detected. Results indicated that a character chosen from among 36 items could be detected with 95% accuracy within 26 seconds. The main drawback of P300-based BCIs is their slowness.

***EEG mu-rhythm conditioning.*** Several groups (Wolpaw et al. 1991; Wolpaw and McFarland 1994; Pfurtscheller et al. 1995) have experimented with subjects' abilities to move a cursor up or down on a screen toward a target placed randomly at the top or bottom by manipulating their mu-rhythm, a detectable pattern in a great majority of individuals in the EEG 8-12Hz frequency range, centred about 9.1Hz (Kuhlman 1978). Mu-rhythm amplitudes lower than a threshold level left the cursor in place or moved it downwards while higher amplitudes moved it upwards in



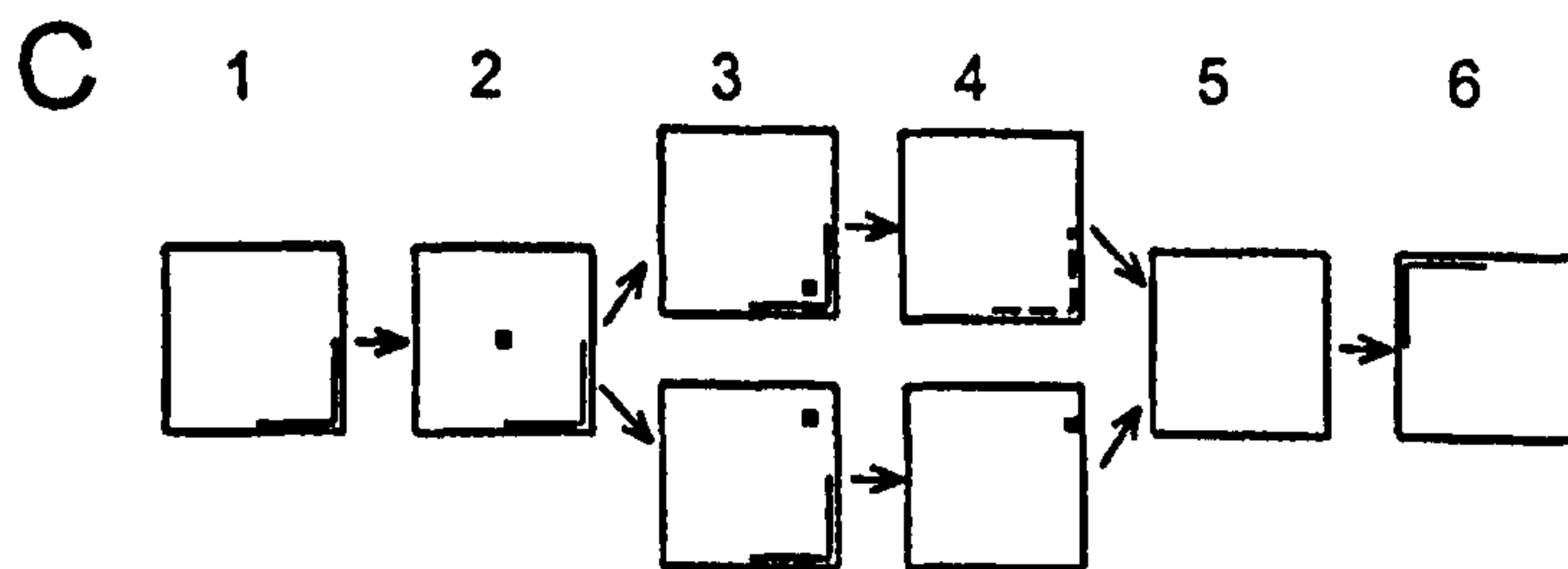
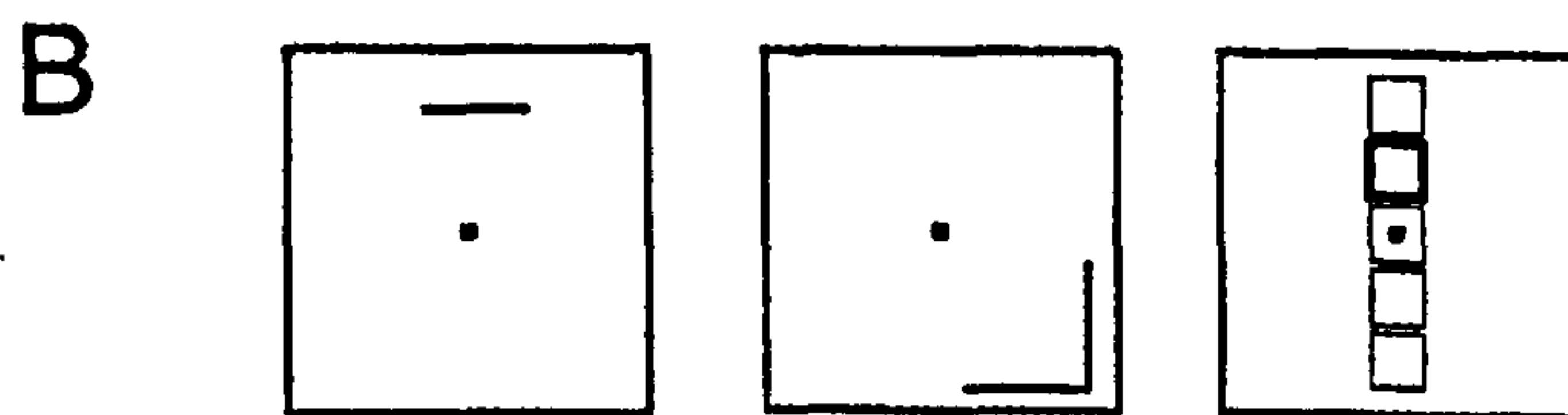
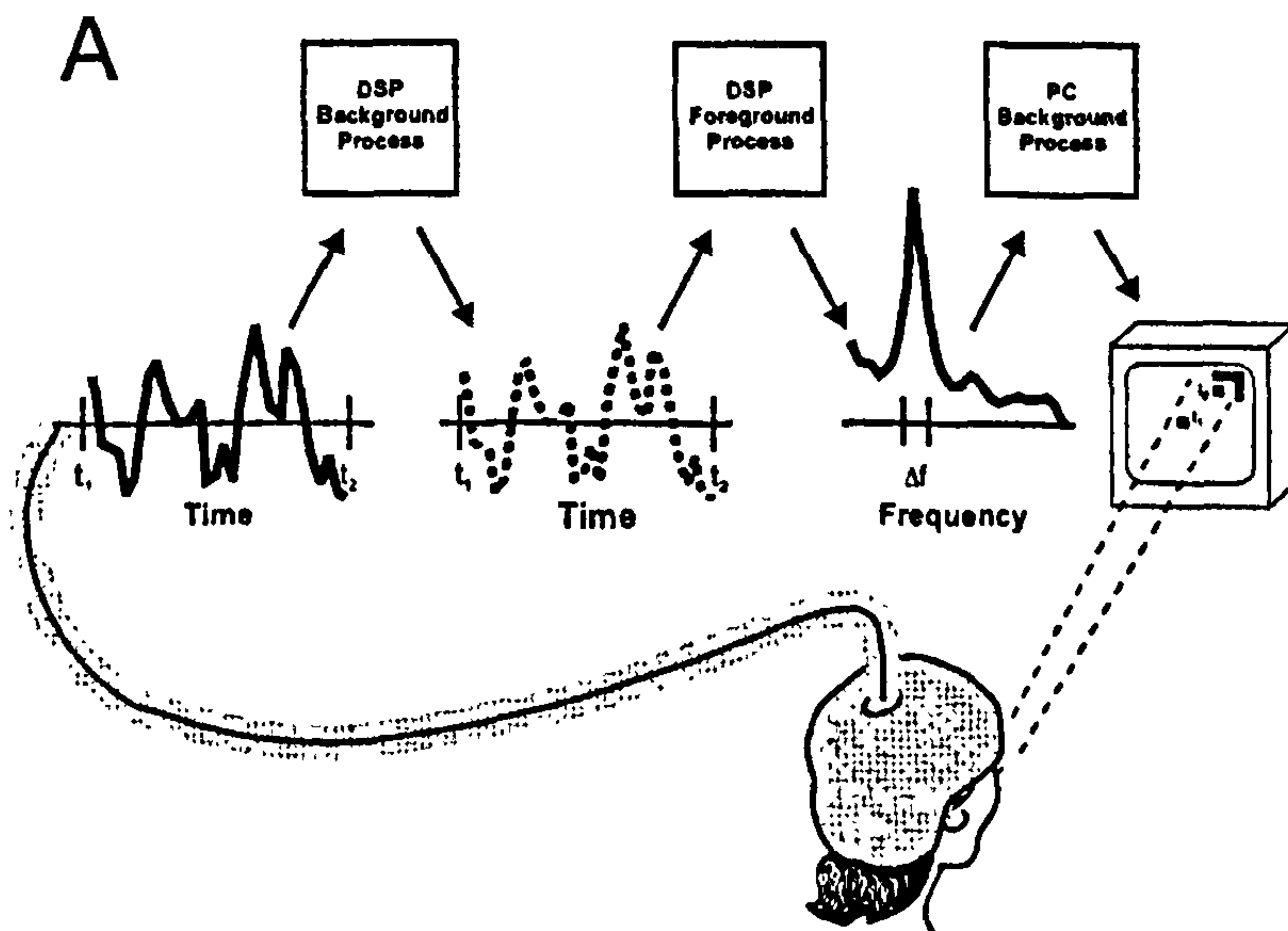


**Fig. 2.32** (A) Example of BCI operation. Scalp voltage is amplified, digitized, spatially filtered, and frequency analyzed 10 times/s. Amplitude in a specific frequency band is translated into cursor movements. (B) Three different control modes are used; an one-dimensional mode in which the target is on the top or the bottom edge and the cursor; the two-dimensional mode, in which the target is at one of four or more positions on the periphery of the screen and the cursor moves both vertically and horizontally controlled by the EEG; finally an one-dimensional mode, in which the target is in the highlighted box of a series of boxes arranged vertically on the screen and the cursor begins in the middle and moves vertically controlled by the EEG until it stays in one box for a defined period and thereby selects it. (C) Sequence of events during a trial. (1) The trial begins when a target appears in one corner. (2) After a brief period (e.g., 1 s) that allows the subject to see the location of the target and initiate the proper EEG, the cursor appears in the centre. (3) The cursor moves controlled by the EEG until it reaches the periphery. (4) If it reaches the part occupied by the target, a hit is registered, the cursor disappears, and the target flashes for 1s as a reward. If it reaches another part, a miss is registered, the target disappears, and the cursor remains fixed on the screen for 1 s. (5) The screen is blank for 1 s. (6) The next target appears. (Wolpaw et al. 2000)



increasing jumps (Wolpaw et al. 1991; Wolpaw et al. 2000). Contralateral suppression of the mu-rhythm during the 1-second period prior to a motor activity (e.g. pressing a microswitch using either the right or the left index finger) has been used to predict which response was to follow (Pfurtscheller et al. 1994). Event-related desynchronisation is characteristic for the contralateral, and an event-related synchronisation for the ipsilateral hemisphere.

***Visual Evoked Potential Detection.*** A 64-position block was presented on a computer screen and detected which block the subject looked at (Sutter and Tran 1992). Scalp electrodes placed over the visual cortex detect changes in the visual evoked potentials at that location while several simultaneously presented stimuli are made to change rapidly in some controlled way (switch 64 screen positions between red and green, or reverse a checkerboard pattern). The 64 positions represent the letters of the alphabet and commonly used words in the English language. Whenever the subject fixated on a letter, the commonly used words changed to words beginning with that letter, for quick selection of an entire word. Response times ranged from 1 to 3 seconds after an initial tuning process lasting 10-60 minutes have been reported.

***EEG Pattern Mapping.*** BCIs can be realised by classifying, detecting and mapping EEG patterns. A neural network featuring learning-vector quantization was used to map EEG patterns during the 1-second interval before a signal the experimental subject was instructed to wait for (Pfurtscheller et al. 1992). A back-propagation artificial neural network was used to study readiness potentials patterns in the EEG immediately prior to the subject's uttering one of five different Japanese syllables or moving a joystick in one of four different directions (Hiraiwa et al. 1990). EEG data was recorded during performance of 5 different tasks during which subjects had their eyes open or closed, for 10 alternative responses (Keirn and Aunon 1990). Feature vectors were constructed from the EEG patterns based on the Wiener-Khinchine method and classified using a Bayes quadratic classifier.

***Detecting lateral hemisphere differences.*** Induced lateral differences in relative brain hemisphere activation were examined after subjects heard arguments through left, right or both earphones which they either strongly agreed with or strongly disagreed with, as determined by prior interviews (Drake 1991). Subjects



exhibited greater discounting of arguments they disagreed with during left hemisphere activation as measured by ratings of truth.

*Activity of cortical neurons.* An implant that can monitor extremely small-scale activity in the brain's motor area has been developed (Kennedy and Bakay 1998; Kennedy et al. 2000). The implant is called "neurotrophic electrode" and is a hollow glass cone the size of a ballpoint pen's tip with a microscopically-thin gold wire, surrounded by nerve tissue extracted from the patient's leg, which stimulates neurons from the surrounding cortex to grow into the cell. The electrical activity recorded by the implant controls the sound of a buzzer, and the patient gradually learned which thoughts make the buzzer sound louder and faster. Later, the buzzer is replaced by a cursor on a computer screen, and the patient learned to "think" the cursor from side to side.

Researchers at the Max Planck Institute for Biochemistry in Munich have created a "silicon to neuron junction", which can directly stimulate/monitor a nerve cell without damaging it. Used in conjunction with existing "neuron transistors" which sense the ionic potential of a nerve cell, this technology paves the way for two-way communication. Dangers, mainly infection, of inserting electrodes into the brains exist (Fromherz 2002; Prinz and Fromherz 2003; Kaul et al. 2004).

### ***2.9.2.2 The future of Brain Computer Interfaces***

Brain Computer interface (BCI) research is regarded as a "red-hot" topic according to the "MIT Technology Review" issue that lists brain-machine interfaces as one of the 10 emerging technologies that will change the world, that will soon have a profound impact on the economy and on how we live and work (Regalado 2001). Complete human-brain computer interaction may be decades away and may never move beyond science fiction. In the next decade however, limited but practical systems for helping severely handicapped people communicate or operate appliances are seen as feasible.

EEG represents a good possibility for direct command input. However, at present, the relationship between EEG and intentional motion or communication has not been clear and great variability between patients has been demonstrated. When locked-in patients were trained to control one-dimensional cursor movement on a computer screen by using self-regulation of slow cortical potentials of the brain,



some patients learned to self-regulate their slow cortical potential amplitude very quickly, some needed a longer period of time while some did not learn it at all. (Wolpaw et al. 2000; Wolpaw et al. 2002)

Further progress in areas of neuroscience, knowledge of brain function as well as signal processing of the EEG is necessary. While EEG control may be a long-term goal, a short-term goal of man-machine interface would be an improvement of the conventional interfaces utilising residual voluntary EMG function or systems utilising functional associations between EEG and EMG (such as corticomuscular synchronisation).



## ***2.10 SUMMARY***

The literature review presented background information on some of the most important fundamental elements of the field. As the study of motor control and neuroprosthetic control are multidisciplinary fields, the introduction included a large number of topics, often quite diverse.

The movement related components of the nervous system were first presented. Elements of the relation of brain to motor control and the involvement cortical structures, subcortical structures, the cerebellum, spinal cord and the peripheral nervous system were illustrated. This information was useful for the design of the experimental protocols as well as the interpretation of the results. EEG and EMG electrodes had to be placed on anatomically correct areas, and results had to be interpreted according to their anatomical spatial specificity.

Known movement related changes in rhythmic brain activity were also presented. The origin of electrical brain activity, cortical rhythms in different frequency bands, idling and non idling brain activity, cortical synchronization/desynchronisation and neuroimaging techniques like EEG and EMG were then presented. Neurogenic activity during motor tasks was an important part of the literature review. It presented useful background information on movement and posture tremors and their task specificity. It also presented underlying mechanisms of tremor generation in the periphery and its relation with CNS activity in the form of corticomuscular synchronisation. The experimental protocols and results that will be presented later mainly examine tremor in relation to simultaneous CNS rhythmic activity, their synchronisation and their task specificity.

Neural plasticity is a key concept for the understanding of the function of the nervous system and the successful implementation of neuroprosthetic devices. Cortical reorganisation is a process always following CNS and PNS injuries and disorders and has implications in therapy and rehabilitation. Neural plasticity may be an important factor in the variability of the examined signals and the robustness of potential intention detection indicators. The INB experiment aimed to examine short term plasticity induced by deafferentation and its influences in corticomuscular synchronisation.



The influence of attention in the motor control mechanism was also examined. The fundamentals of attention as a cognitive process, the single channel and flexible central resource capacity theories were examined. The physiology of attention and the common CNS components involved in the attentional process and motor control as well as potential interactions were presented. Attention may also be a factor affecting the robustness of intention detection signals, and underlie the observed variability. The experiments that will be presented later in the thesis examine attention and its influences in motor control.

Elements of the neuroprosthetic control systems were also illustrated. EMG based control (e.g. myoelectric prostheses), EEG based control (e.g. brain computer interfaces), existing technologies, limitations and future challenges were presented. The advantages of using the proposed signals in relation to conventional approaches were highlighted.



## **3 METHODOLOGY**

### **3.1 INTRODUCTION**

The present study focused on identifying task dependency within EMG and EEG frequency domain estimates during voluntary movements. The view was to improve our understanding of physiological mechanisms involved in motor control and to explore potential strategies for intention detection in neuroprosthetic control. The experimental programme involved normal volunteer subjects who performed a set of simple and more complicated motor tasks while simultaneous recordings of EEG and EMG were acquired.

All experiments received ethical approval from the relevant committee of the University of Strathclyde and all procedures were reviewed by a departmental safety committee. All subjects provided informed and written consent.

#### **3.1.1 Groups of experiments**

3 main groups of experiments were performed:

Movement experiment (including wrist move-hold sequence, maintained posture, continuous movement)

Influence of attention on corticomuscular coherence

Effects of sensory deafferentation in corticomuscular and intermuscular couplings using Ischemic Nerve Block (INB).

The experiments were carried out in the Neurophysiology Laboratory of the Department of Bioengineering at the University of Strathclyde. The duration of the experiments varied depending on the instrumentation used and the time to complete the setup.



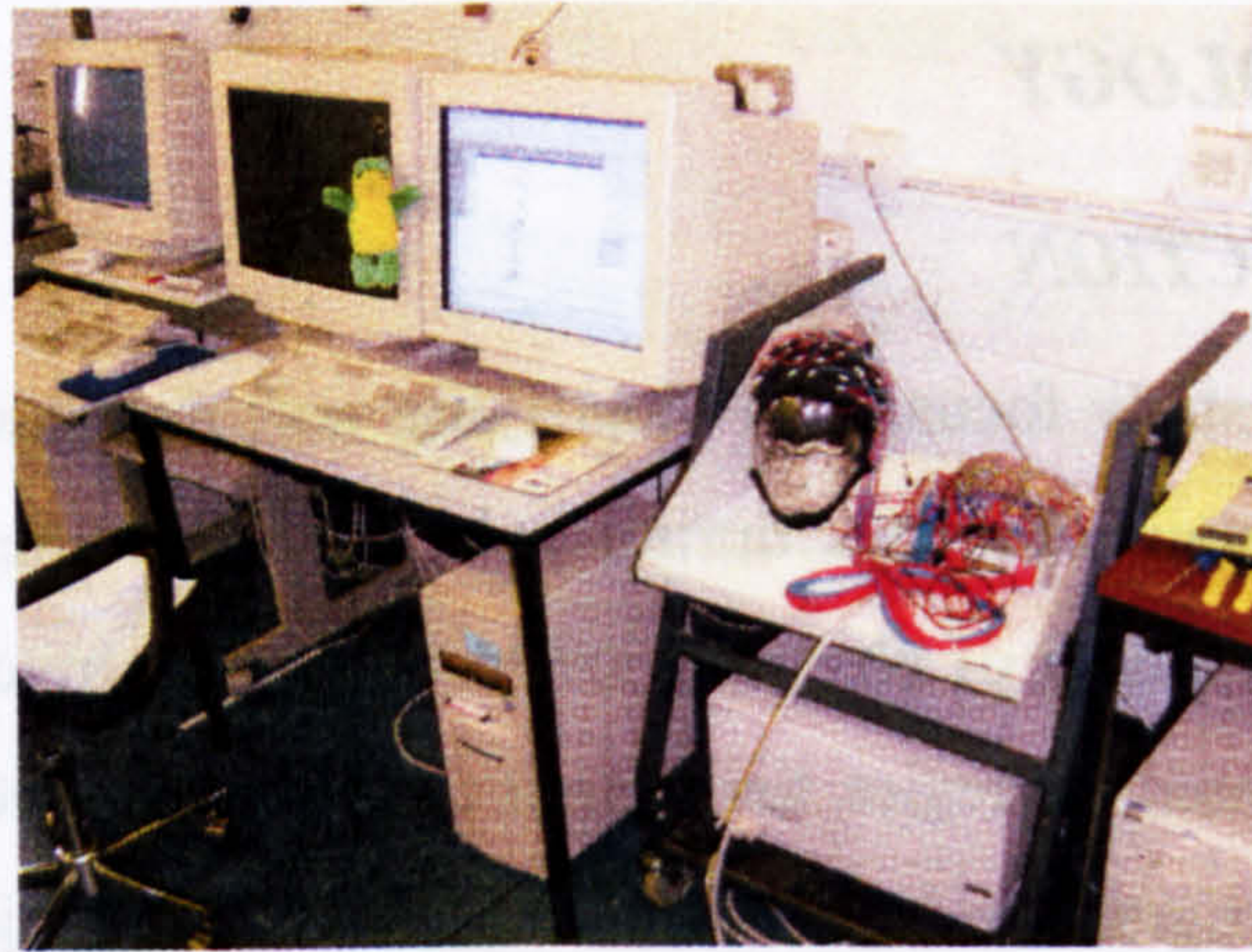


**Fig. 3.1** NeuroScan EEG and EMG recording system. The signal from electrodes on the QuickCap were channelled through the set-top box (pre-amplifier) to the main SynAmps amplifier. The amplified filtered and digitised signals were then stored on the hard drive of the computer and viewed on the monitor.

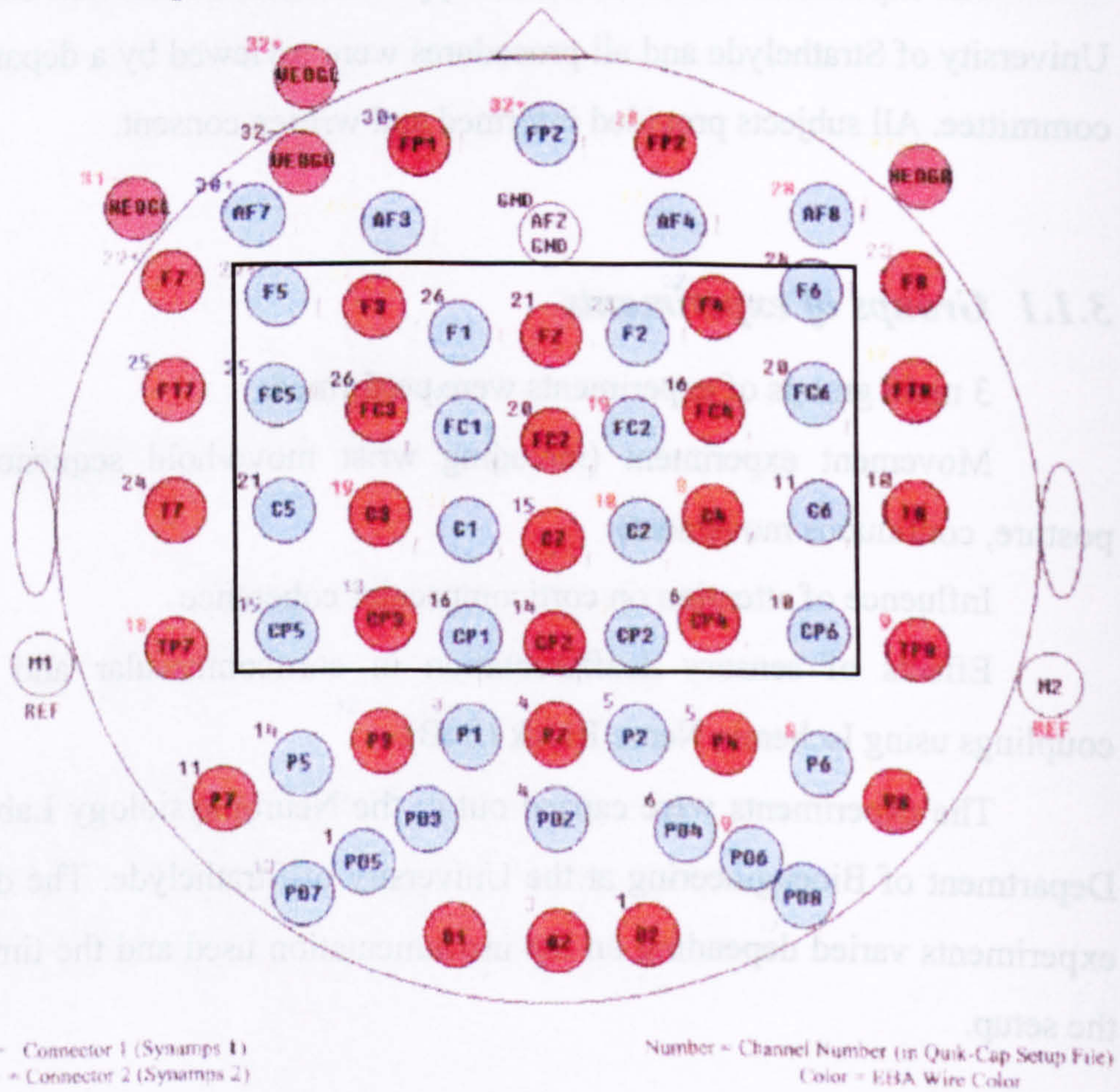


**Fig. 3.2** Electrode arrangement of the 64 electrode Quick-Cap. The 64 channel cap allowed configurations with denser positioning of the available 32 recording SynAmps channels, around areas of interest like motor and sensory cortices, compared with the fixed 32 channel Quick-Cap. The arrangement of the 32 electrode cap is indicated by the red electrodes while for the used 64 electrode one by both red and blue electrodes. The montage of the 28 electrodes used for the multiple electrode recordings used is also indicated.



### **3.2 GENERAL EXPERIMENTAL TECHNIQUES**

The two main experimental techniques used in the current set of experiments included surface EMG and EEG. In addition, other recording techniques used to record or influence movement were goniometry (measurement of wrist angular velocity), grip force measurement associated with compression of an instrumented ring dynamometer.

### **3.3 EEG RECORDING SET UP**

A typical multichannel EEG system consists of a low noise amplifier with an integrated data acquisition system and an electrode cap. In this study a 32 channel NeuroScan SynAmps system was used in conjunction with a 64 electrode NeuroScan electrode hat which allowed greater flexibility over the recording sites (Fig. 3.1).

The NeuroScan SynAmps is a 32 channel AC/DC amplifier and high speed digital acquisition system designed to record a wide variety of multichannel physiological signals. A SynAmps contains the analog components needed to amplify low amplitude physiological signals and the digital components needed to digitize, DC correct, digitally filter, log external events, and transfer data to a host computer through a SCSI interface, displaying, and storing the acquired data using proprietary software (SCAN 4.3).

The Quick-Cap electrode positioning system is a cap made from elastic fabric to provide a uniform fit over a wide range of head shapes and sizes. A medium size cap fitted with Ag/AgCl (silver/silver-chloride) electrodes attached to an external wiring harness was used. The wiring harness includes all EEG, as well as “reference” and “ground” connections to the NeuroScan preamplifier. The QuickCap electrode hat contained 64 electrodes arranged according to the international 10-20 system Fig. 3.2. The used recording protocol was based on a monopolar setup with a common linked ear reference for all recordings. The greater number of electrodes on the electrode cap (64) than the available number of recording channels (32) gave flexibility to achieve a higher spatial resolution over desired cortical areas than would be possible with a standard 32 channel cap. The targeted cortical areas were parts of the frontal and parietal lobe corresponding to primary motor and sensory areas, as well as motor association areas.



### ***3.4 SUBJECT RECRUITMENT CRITERIA***

The subjects for all the experiments were all healthy volunteers who consented to participate in the study. Some information regarding subjects can be seen in Table 3.1 and Table 3.2. There were no age restrictions or selection criteria based on handedness. No left handed subjects volunteered to participate. For the ischemic nerve block experiment female subjects could not be recruited for the danger of thrombosis in case of use of contraception.

Inclusion in the study required that:

The subjects should be in good general health.

The subjects should be free from any previous or existing neurological condition.

The subjects should have no muscle or skeletal injury at the time of the experiment.

### ***3.5 SUBJECT PREPARATION***

Before fitting the electrode cap to the subject, the amplifier configuration had to be set up by the data acquisition software running on the computer that controls the SynAmps system. This involved defining and labelling the group of recording electrodes to be recorded and specifying what signal conditioning was required. Sampling frequency was set at a 1000 Hz. A band-pass filter was used with high pass component set to the lowest possible frequency that would ensure that no movement artefacts would contaminate the recording. The typical low pass limit was 200Hz, acting as an antialiasing filter (for 1000Hz sampling frequency) and the high pass setting ranges from 0.3-1Hz.

The appropriate electrode plugs corresponding to the required electrodes were then connected to the pre-amplifier sockets corresponding to the physical channels assigned in the configuration. The hat was then loosely applied to the subject's head according to the manufacturer's guidelines (QuickCap\_manual 1998) and the ear linked reference electrodes were attached to the subject's ear lobes using conductive gel and micropore tape. Following this the cap was pulled down firmly over the head in a way that the midline frontal pole electrode location (FPz) was approximately 4cm above the nasion and aligned on an imaginary line running from the nasion to



theinion. In this way it was ensured that all electrodes are aligned correctly within the proportional 10:20 system, and achieve inter-subject and intra-subject repeatability and standardisation. A velcro chin strap also secured the position of the hat. AFz was used as the ground electrode. The wiring harness was then attached and secured in order to ensuring that there was adequate slack to allow head movement without pulling the cable and causing movement artefacts.

Following the positioning of the electrode hat each one of the hollow electrodes had to be filled with the recommended conductive gel (Quick-Gel). A blunted syringe was inserted through the hole in each electrode, through the hair down to the scalp surface. The syringe was lightly rocked while moved in a circular fashion to gently abrade the skin and a small amount of EEG electrolyte was injected. While injecting the electrolyte the syringe was lifted to guarantee that there is an unbroken path of electrolyte through the hair to the electrode disk.

The conductive electrode gel used comes in a liquid form and works as a conductive electrolyte filling the gap between the skin and the electrode, making the path conductive. It has also light abrasive properties breaking down the oils of the skin making it more conductive. The impedance of the electrodes was automatically measured on-line by the SynAmps system software which used a colour map to identify electrode impedances on the PC monitor. All impedances were kept to below 5K $\Omega$ . High impedance results in high environmental noise in the signal and contamination with mains (50Hz) interference noise in the signal and difficulty to decrease the impedance were highly dependent on the subject. The subjects were asked to wash their hair the morning of the experiment and to avoid applying any hair cosmetic products. This appeared to help improve skin conductivity possibly by reducing the natural skin oils present in the scalp and making it easier for the gel to diffuse into the upper layers of the skin.

The procedure of applying the electrodes with gel proved to be a time consuming procedure especially for subjects with long hair, since the tip had to penetrate the hair layer and bridge the skin electrode path with gel and difficulty was often experienced in reducing the impedance to the desired level. Despite of the fact that the quick cap allows rapid placement of multiple electrodes on the scalp it did not always justified its name. The average time of preparing a typical 28 electrode



the trial. In this way it was ensured that all electrodes are aligned correctly within the proportional 10:20 system, and achieve inter-subject and intra-subject repeatability and standardisation. A velvet chin strap also secured the position of the bar. A/z was used as the ground electrode. The wiring harness was then attached and secured in order to ensuring that there was adequate slack to allow head movement without pulling the cable and causing movement artefacts.

Each one of the hollow  
the gel (Out-Go). A  
electrode through the hair  
removed in a circular  
of EEG electrode was  
to prevent the electrode



Following  
electrode had  
planted average  
down to the scalp  
fashion to gain  
injected. While  
is an ambrosian

**Fig. 3.3** AgAcCl EMG electrodes, Electrode preparation pads and skin abrasive.

The conductive electrode  
conductive electrolyte filling the gap between the hair and the electrode, making the  
path conductive. It has also light abrasive properties helping down the side of the  
skin making it more conductive. The impedance of the electrodes was automatically  
measured on-line by the SynAmp system software which used a colour map to  
identify electrode impedance in real-time. The electrodes were kept to below  
5k $\Omega$ . High impedance  
contamination with  
decrease the impedance  
asked to wash their  
hair cosmetic products  
reducing the natural  
diffuse into the upper

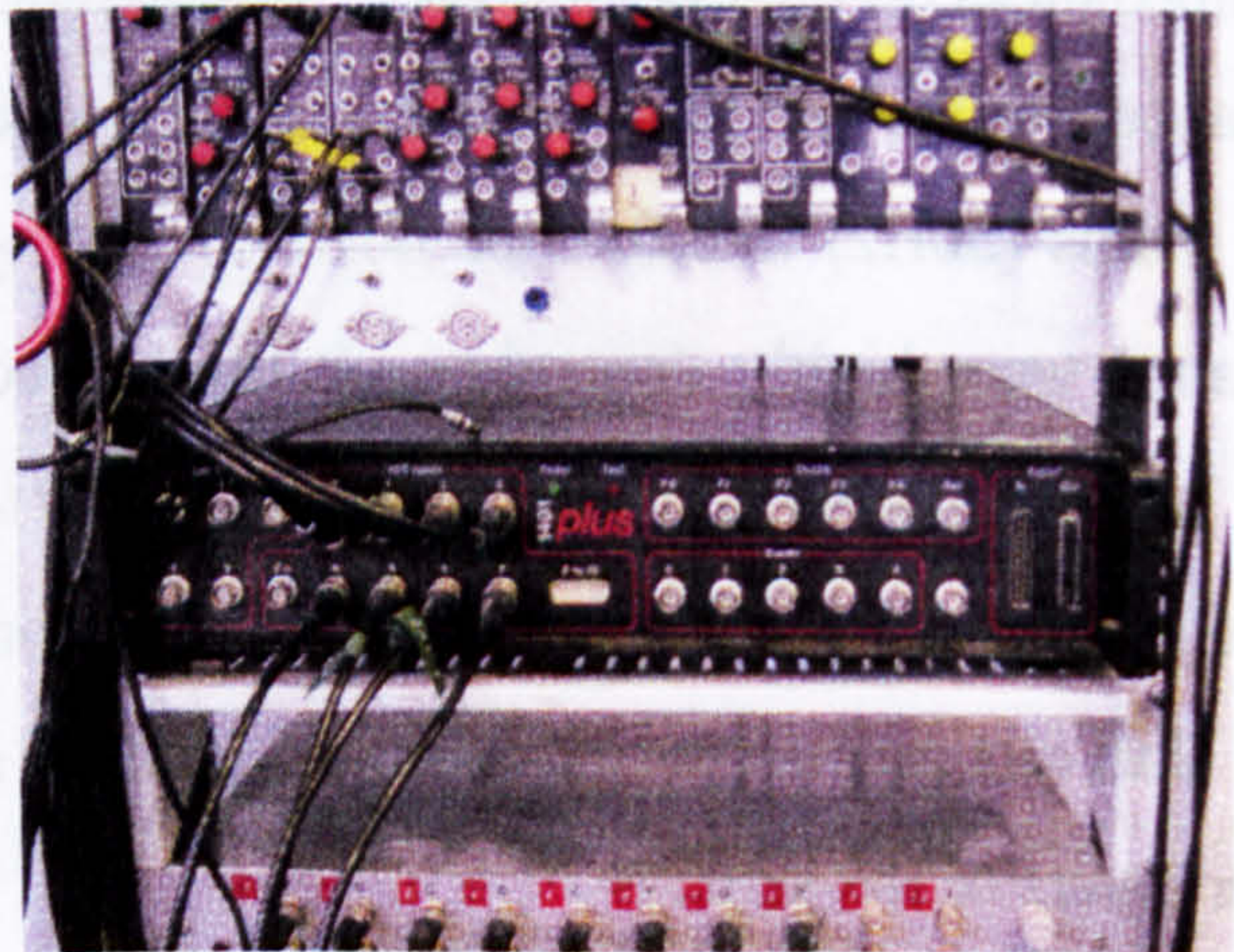


**Fig. 3.4** CED 1401plus data acquisition system

The procedure of applying  
concerning procedure especially for subjects with long hair since the pad to  
penetrate the hair layer and bridge the skin-electrode path with gel and difficulty was  
often experienced in reducing the impedance to the desired level. Despite of the fact  
that the quick cap allows rapid placement of multiple electrodes on the scalp, it did  
not always justify its name. The average time of preparing a typical 12 electrode



setup was 50min. This contributed to long experimental sessions and some discomfort to the subjects. In the few cases that the impedance was extremely difficult to be reduced, the experiment was carried out nevertheless. It has been reported that even with very high impedances in the order of 50kOhm, significant signal can be obtained without even abrasion of the skin in order to reduce infection risks (Ferree et al. 2001).

### **3.6 EMG RECORDING SET-UP**

In addition to recording EEG all experiments involved EMG recordings from arm and hand muscles (extensor carpi radialis longus, flexor carpi radialis, biceps brachii long head, abductor pollicis brevis) using the same instrumentation as with EEG (NeuroScan SynAmps). The preparation of the subject for the EMG recording started with the identifying the desired muscles to be recorded from by palpation whilst the subject actively contracted the wrist or the arm in a way that activated the target muscle. The identification of the muscle by this method is not always straight forward as muscular bulk and subcutaneous fat levels can vary considerably, especially in the female population. Once a recording site was determined the skin was carefully cleaned and slightly abraded using skin abrasive and Medicotest electrode preparation pads. A pair of Blue Sensor pre-gelled Ag/AgCl disposable electrodes (Fig. 3.3) was then placed side by side on the skin with an interelectrode distance of 1cm. For experiments requiring simultaneous EEG EMG recordings the Quick-Cap ground electrode was used.

The EMG signals were recorded using the 4 bipolar channels of the NeuroScan SynAmp. The sampling rate and filter properties were be the same as for the EEG. Usually the signals were amplified by a factor of a 100 with a sampling rate of 1000Hz and band-pass filter characteristics 0.3Hz to 200Hz or 1Hz to 200Hz.





**Fig. 3.5** The Gyration Microgyro 100 Gyroscope.

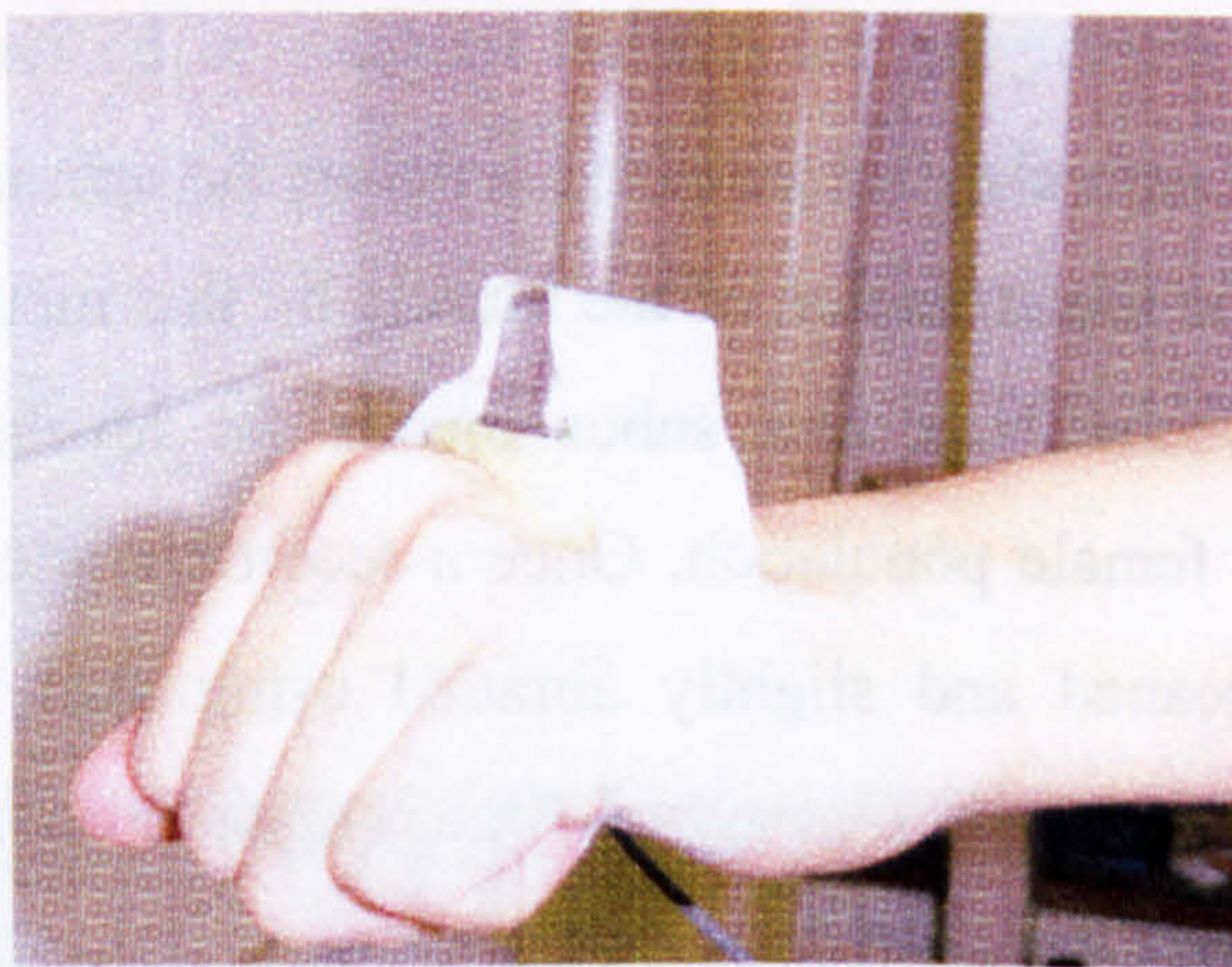


**Fig. 3.6** Gyroscope applied on a subject. It is secured with micropore tape. Foam padding is used between the upper palm and the gyroscope.

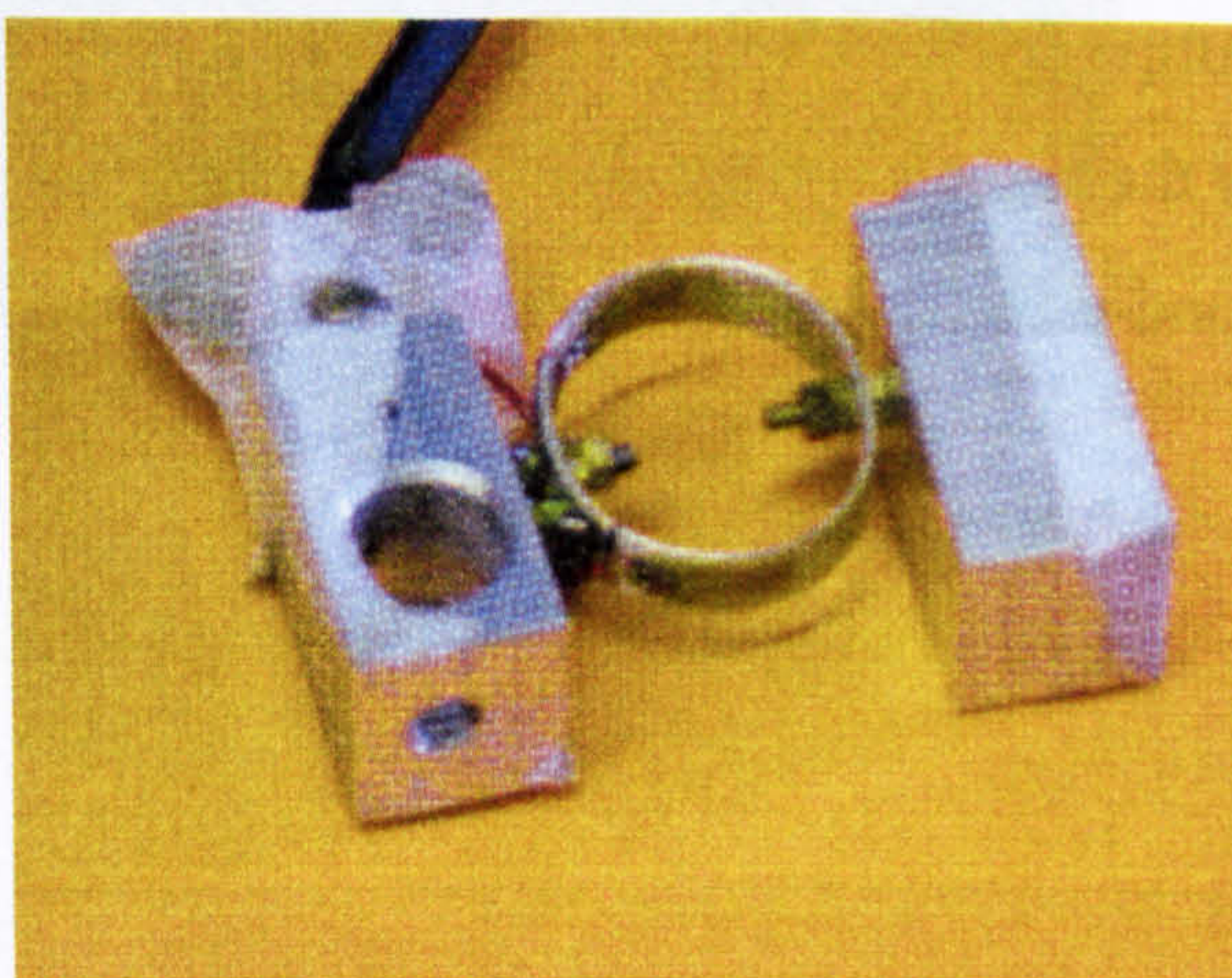


**Fig. 3.7** Close view of the instrumented ring used in attention experiments.



## **3.7 OTHER APPARATUS AND RECORDING TECHNIQUES**

### **3.7.1 CED 1401**

The SynAmps does not accept inputs from external amplifiers therefore when there is a need to record signals such as wrist angular velocity coming from a different amplifier amplifying gyroscope signal, an additional A/D (Analog to Digital) system had to be used. In these instances a CED 1401 data acquisition system (Fig. 3.4) that connects to a personal computer was used to record the signals derived from a miniature gyroscope. The software package used for the capturing and storing of data during these experiments was Spike2 (version 3.16, Cambridge Electronics Design), and the data was stored as a continuous time series. Spike2 was also used for producing output pulses and audio cues during the course of the experiments where the NeuroScan SynAmps was used. Audio cues were used to instruct subjects to begin or end a wrist movement. To generate the cues a sequencer program written in the Spike2 script language was written. It produced a sinusoidal waveform which was amplified by an audio amplifier (Neurolog system NL 304-Digitimer Ltd.). The signal was in turn connected to a speaker, so that each time a signal was created a high or low pitch audio cue was produced, instructing the subject to switch between tasks. The timing of the pulses was transmitted to the NeuroScan via a serial connection and logged as an events channel within files containing EEG and EMG data.

### **3.7.2 Gyroscope.**

A gyroscope was used in some experiments for recording the angular velocity of the wrist rotation. The Gyration Microgyro 100 used (Fig. 3.5) is a low cost dual axis rate gyroscope that generates a signal indicating rate of change in the angle of inclination (angular velocity) in degrees per second. The module was directly mounted on to a small printed epoxy board and connected to a bridge amplifier via a long flexible cable that provided the necessary input voltage and amplified the output signals. The amplifier output was connected to the CED 1401 data acquisition system and stored on the computer. The CED 1401 recording was synchronized with the



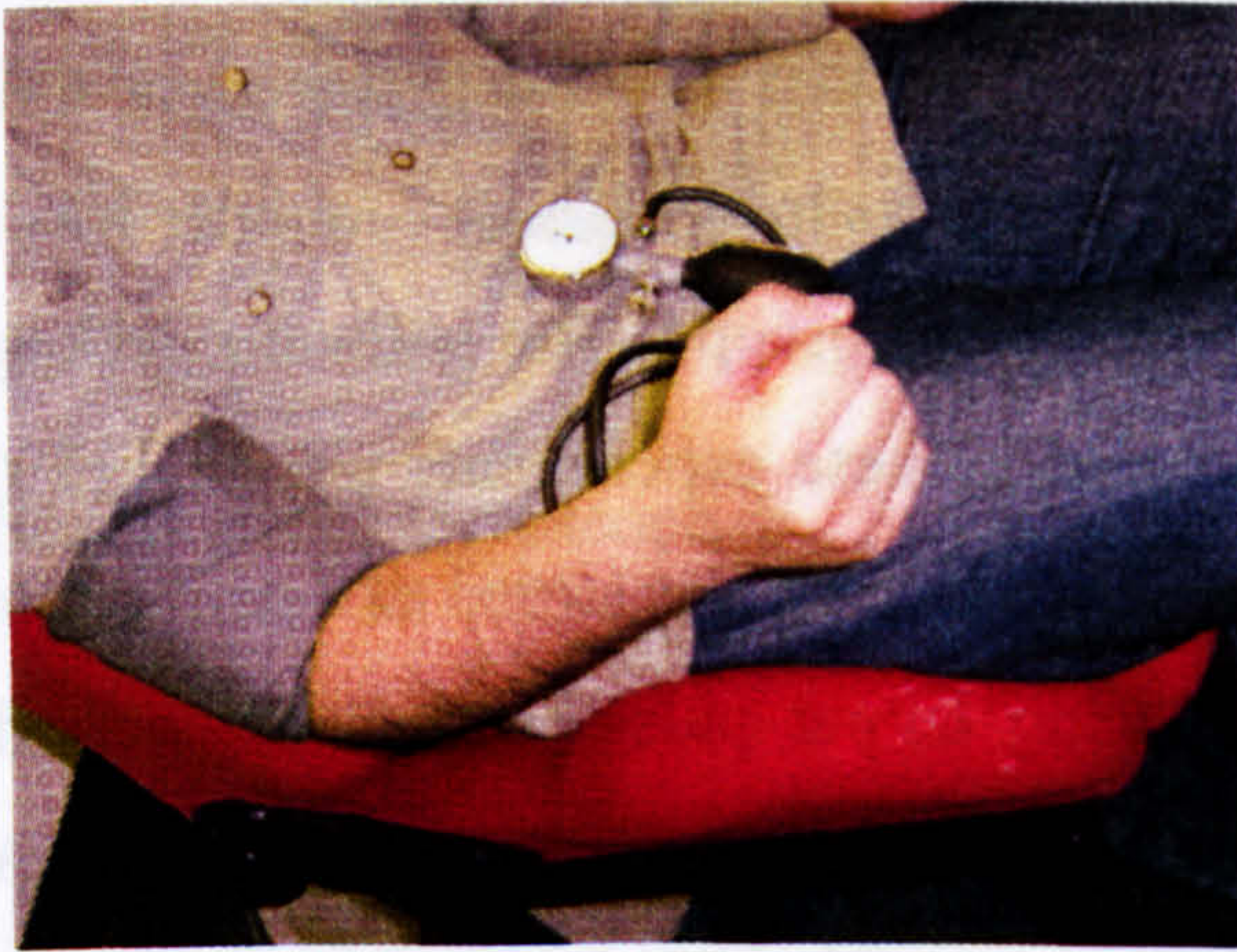


**Fig. 3.8** Sphygmomanometer applied on a subject just above the elbow.



**Fig. 3.9** Elastic band device used in attention experiments.



NeuroScan recording using digital pulses (events) recorded by both 1401 that produced them as well as the NeuroScan.

When used in experiments the gyroscope was carefully secured on the subjects' skin using self adhesive double sided tape. The site of placement was the metacarpophalangeal area (Fig. 3.6). This area lacks significant underlying muscle mass and activity, so there is limited low frequency noise from muscles or tendons. The cable was fixed on the forearm with micropore tape in a way that the weight of the cable would not obstruct the wrist movement. A small piece of foam padding was used between the gyroscope and the skin, offering comfort to the subject and necessary padding to reduce the effect of any underlying tendon activity. Micropore tape was also used to ensure that the sensor and cable were well secured on the hand.

### ***3.7.3 Instrumented ring***

A small ring transducer (Fig. 3.7) was also used for our experiments when measuring precision grip force. The sensor consisted of an instrumented ring constructed in such a way that the subject could apply pressure on two parallel metal bars attached to the ring. These transferred force directly to the ring. The deformation of the ring was transformed by strain gauges into current, which was in turn displayed on the oscilloscope, through a strain gauge amplifier. The ring used a common four strain gauge configuration and was designed and manufactured in house.

### ***3.7.4 Pneumatic Tourniquet***

The application and inflation of a pneumatic tourniquet (sphygmomanometer cuff as in Fig. 3.8) over the upper arm just above the elbow was used in some tests to induce ischemia and selectively block large diameter forearm and hand afferent fibres. Once in place, the cuff was inflated above the systolic blood pressure. The physiology of the smaller diameter efferent fibres makes them less susceptible to hypoxia than the large afferent fibres. This results to hypoxia which induces temporary sensory deafferentation before temporary motor deafferentation. This creates a time window where there is efferent input to the muscles but little or no afferent feedback.



### ***3.7.5 Bimanual motor task***

A simple device based on an elastic band was used (Fig. 3.9). Subjects were instructed to extend it to a set length and using both hands attempt to maintain the length constant. A ruler was attached on it giving the length before and after extension. Sticky tape attached the centre of the ruler on the elastic band. In that way the band can be extended to equal length in left and right directions. Narrow pieces of tape were also attached on the ruler and the band, indicating to the subject the target length that the band should be extended to.



## **3.8 EXPERIMENTAL PROTOCOLS**

### **3.8.1 Introduction**

The experimental protocols are going to be described. The subjects were seated comfortably in a reclining chair and performed a number of tasks. The movements performed were unobstructed. Specific instructions were given to the subjects regarding posture positions and speed of movement. However no casts were used to support or restrict movement leaving the subjects the freedom to perform the tasks in a comfortable manner within the set guidelines.

### **3.8.2 EEG and EMG frequency estimates during move-hold sequence, maintained posture and continuous movement.**

9 normal subjects participated in this experiment. The aim was to examine and compare the frequency characteristics in EMG and EEG signals during different phases and types of movement task. This included examination of the frequency characteristics existing between synergistic muscles in addition to relationships evident between EEG and EMG activities.

The movement sequence involved the performance of four individual movement tasks performed at the wrist:

- move-hold sequence
- maintained posture flexion
- maintained posture extension
- continuous movement (flexion-extension)

All wrist movement tasks were unconstrained and performed in the horizontal plane with no support for the forearm.



3.8.1 Introduction

The experimental protocols are going to be described. The subjects were seated comfortably in a reclining chair and performed a series of tasks. The movements performed were unobstructed. Specific instructions were given to the subjects regarding posture position and speed of movement. However, no cues were used to support or restrict movement leaving the subjects the freedom to perform the tasks in a comfortable manner within the set guidelines.

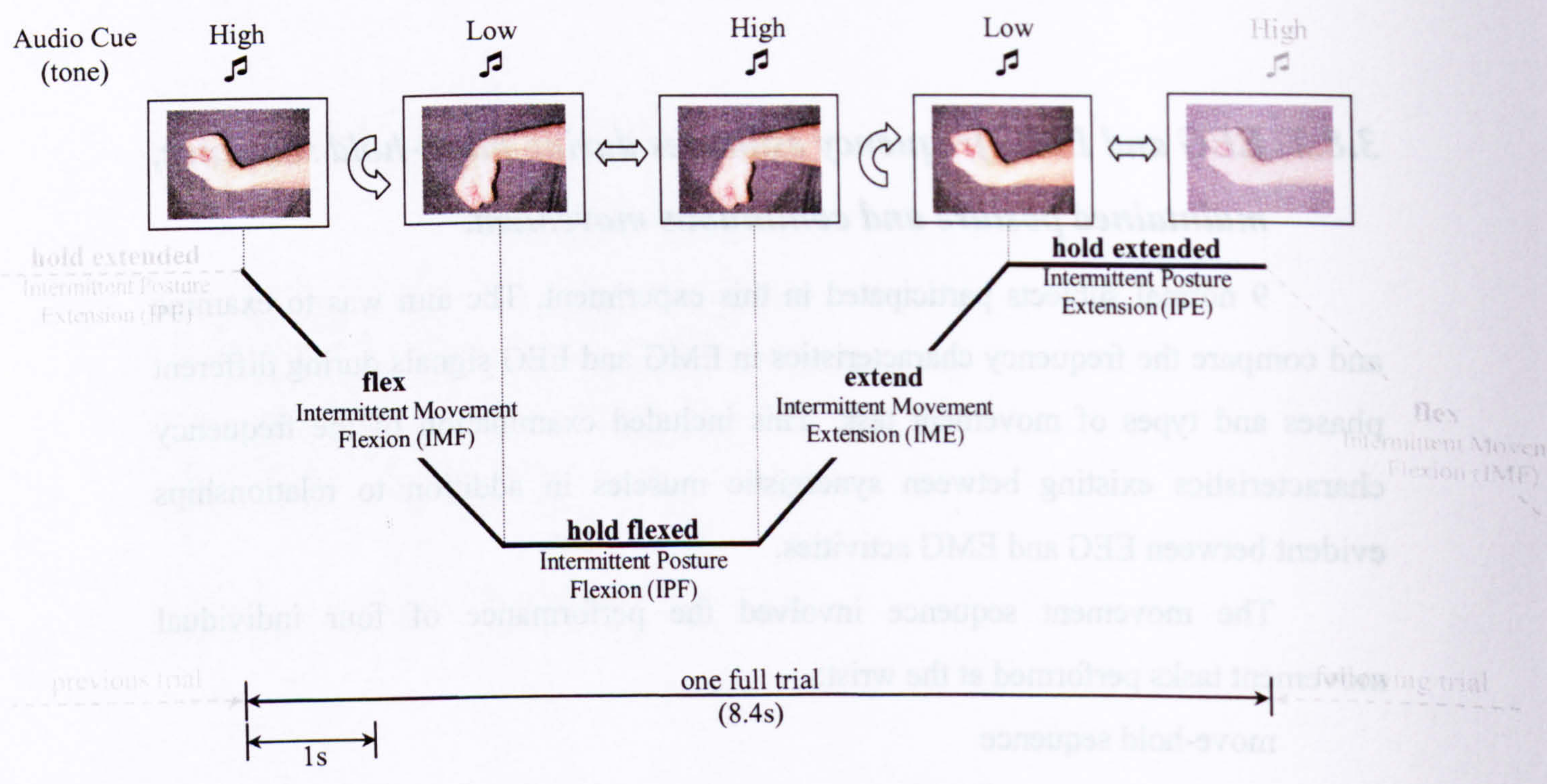


**Fig. 3.10** Experimental protocol for the move-hold sequence tasks.

One complete trial, consisting of four phases:

- Intermittent Movement Flexion (IMF)
- Intermittent Posture Flexion (IPF),
- Intermittent Movement Extension (IME)
- Intermittent Posture Extension (IPE)

A complete move-hold sequence task involves the continuous repetition of this trial over a set time period.



Subject	Sex	Age	Dominant side
1	M	30	R
2	M	26	R
3	M	28	R
4	M	25	R
5	F	25	R
6	F	27	R
7	M	27	R
8	M	24	R
9	F	28	R

**Table 3.1** Table containing the sex the age and the dominant side of the subjects

### **3.8.2.1** *Task 1 - Move hold sequence*

The move-hold sequence required the subject to perform repetitions of a sequence of wrist movements interspersed with periods of static position holding guided by audio cues (Fig. 3.10).

Each trial consisted of four phases:

Intermittent Movement Flexion (IMF)

Intermittent Posture Flexion (IPF)

Intermittent Movement Extension (IME)

Intermittent Posture Extension (IPE)

All movements were performed in the horizontal plane with forearm parallel to the ground and the hand held in a fist position. High and low pitched tonal cues separated by fixed time intervals of 2.1s indicated the start-end of each movement or posture phase. The duration of the tones was 50ms. The high pitched tone indicated the end of a posture phase and the start of a movement. The low pitched one indicated the end of a movement phase and the start of posture phase. Each trial was repeated 21 times until the end of the experimental session which resulted to total duration for each recording of 176.8s (2.1s each phase, 4 phases, 21 trials). Records containing the segmented individual phases were later created. Each record had a duration of 44.2s (2.1s for each phase, 21 trials). The subject started the experiment



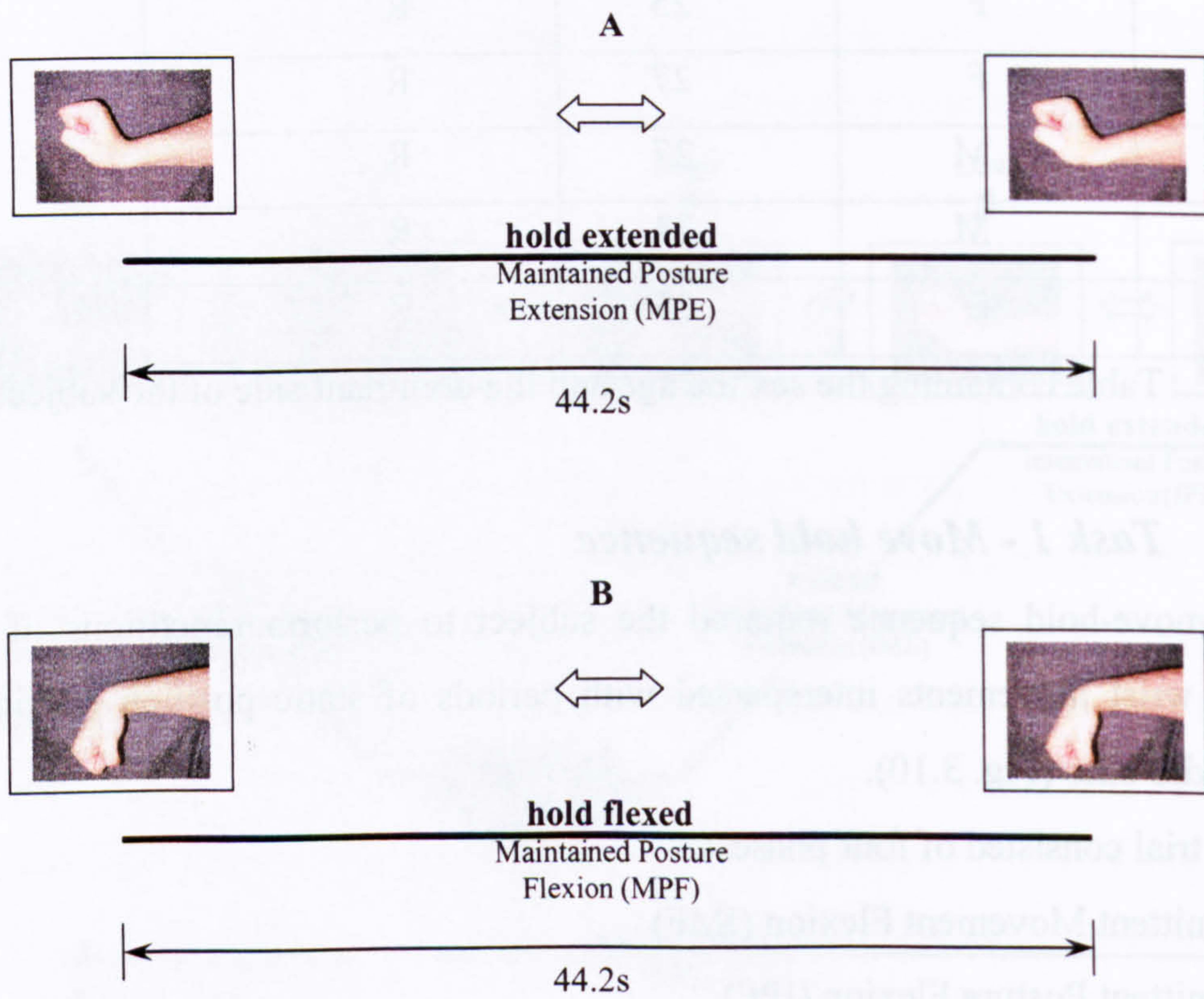


**Fig. 3.11** Experimental Protocol for the maintained posture tasks.

- A** Maintained Posture Extension
- B** Maintained Posture Flexion



with the wrist held in an extended posture. On the first cue, the subject slowly flexed the wrist from the fully extended position to a flexed position in a time interval of 2.1s. At the next cue, (low pitched tone), the subject maintained a fully flexed posture for a further 2.1 s. The next high pitched audio cue indicated when the movement from the flexed position to an extended position should commence. Finally the last low pitched audio cue instructed the subject to hold the extended posture. Subjects were instructed to move their wrist in a controlled manner in order to reach the fully extended or flexed postures precisely by the hold cue. EMG was recorded from the following wrist and elbow muscles which are required to be activated in this task:

*Wrist extensor:* Extensor Carpi Radialis Longus (ECRL)

*Wrist flexor:* Flexor Carpi Radialis (FCR),

*Elbow Flexor:* Biceps Brachii, Long Head (BBLH). Acts to stabilise elbow joint during this task.

EEG was recorded by a set of 28 cortical sites (Fig. 3.2).

Wrist angular velocity was also obtained using the gyroscope configuration.

### ***3.8.2.2 Task 2 – Postural Tasks- Maintained wrist extension- Maintained wrist flexion***

In this task (Fig. 3.11) the wrist was maintained in a fully extended or flexed position. The trial consisted of two separate phases:

Maintained Posture Extension (MPE)

Maintained Posture Flexion (MPF)

The posture took place with the wrist axis aligned to the horizontal plane with no support for the forearm and the palm held in a fist position. BBLH acted to support the forearm and hand in the parallel plane.

The duration for each trial was around 44.2s for each task in order to match the duration of the appended records containing the segmented individual phase data.

EMG was recorded from the following muscles:

*Wrist extensor:* Extensor Carpi Radialis Longus (ECRL)

*Wrist flexor:* Flexor Carpi Radialis (FCR)

*Biceps:* Biceps Brachii, Long Head (BBLH)

EEG was recorded by a set of 28 cortical sites (Fig. 3.2) with angular velocity.



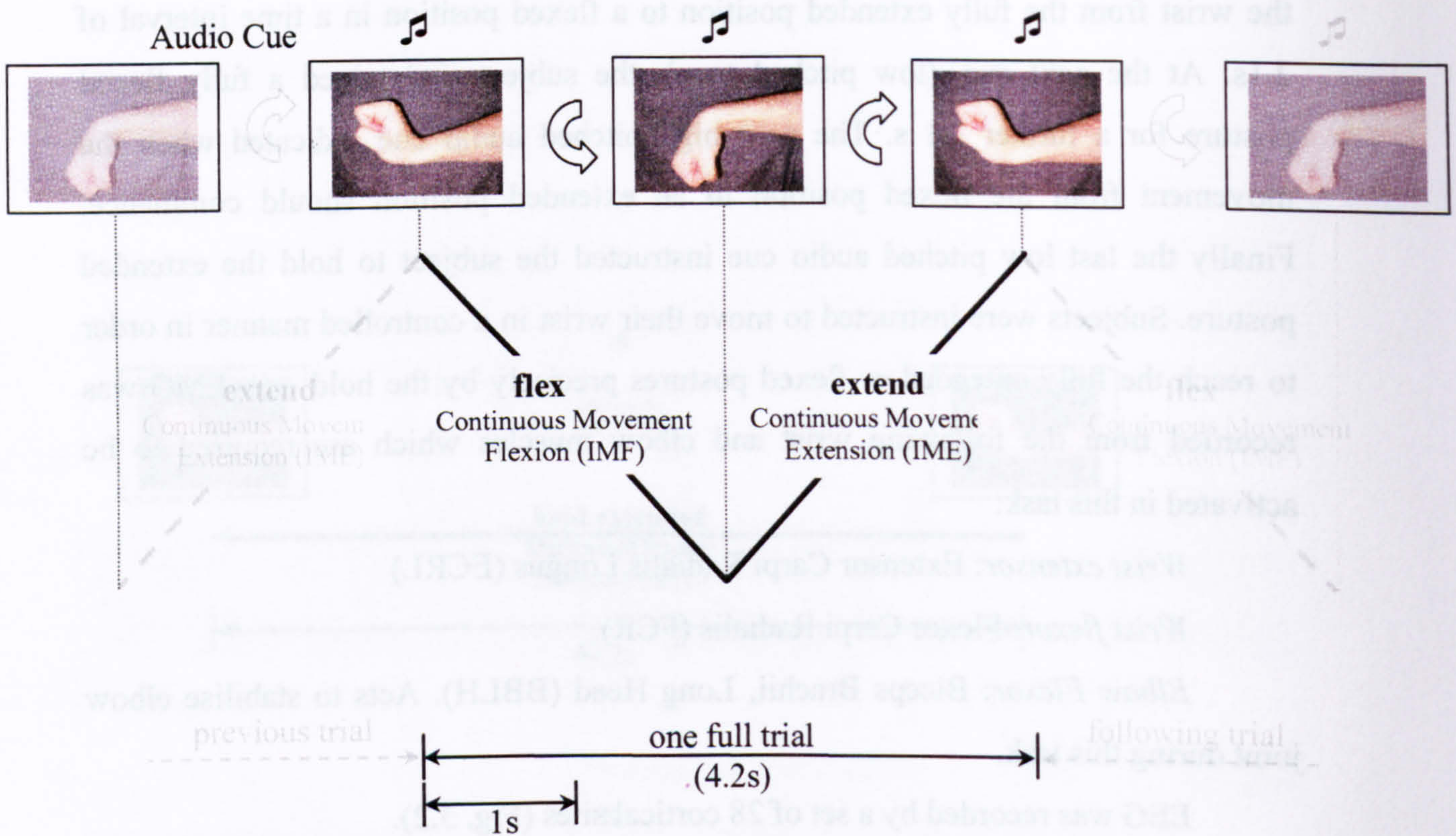


**Fig. 3.12** Experimental protocol for the continuous movement task. One complete trial, made up of two phases (flexion, extension) is illustrated. A complete continuous movement sequence task involves the continuous repetition of this trial over a set time period.



### ***Task 3 - Continuous slow wrist flexion-extension movement***

In this task (Fig. 3.12) the subject was instructed to perform a series of trials consisting of continuous motion of the wrist from fully flexed position to fully extended and vice versa. Each trial consisted of two phases:

Continuous Movement Flexion (CMF)

Continuous Movement Extension (CME)

All movements were performed in the horizontal plane with forearm parallel to the ground and the hand held in a fist position. 50ms audio cues separated by fixed time intervals of 2.1s indicated the start-end of each movement phase. Each trial was repeated 21 times until the end of the experimental session which resulted to total duration for each recording of 88.4s (2.1s each phase, 2 phases, 21 trials). Records containing the segmented individual phases were later created. Each record had duration of 44.2s (2.1s for each phase, 21 trials). The subject started the experiment with the wrist held in an extended posture. On the first cue, the subject slowly flexed the wrist from the fully extended position to a flexed position in the time interval of 2.1s. At the next cue, the subject moved from the flexed position to an extended position in 2.1s. Subjects were instructed to move their wrist in a controlled manner in order to reach the fully extended or flexed position precisely by the audio cue. EMG was recorded from the following wrist and elbow muscles which are required to be activated in this task:

*Wrist extensor:* Extensor Carpi Radialis Longus,

*Wrist flexor:* Flexor Carpi radialis,.

*Biceps:* Biceps Brachii, Long Head

EEG was recorded by a set of 28 cortical sites (Fig. 3.2).

Wrist angular velocity was also obtained using the gyroscope configuration.



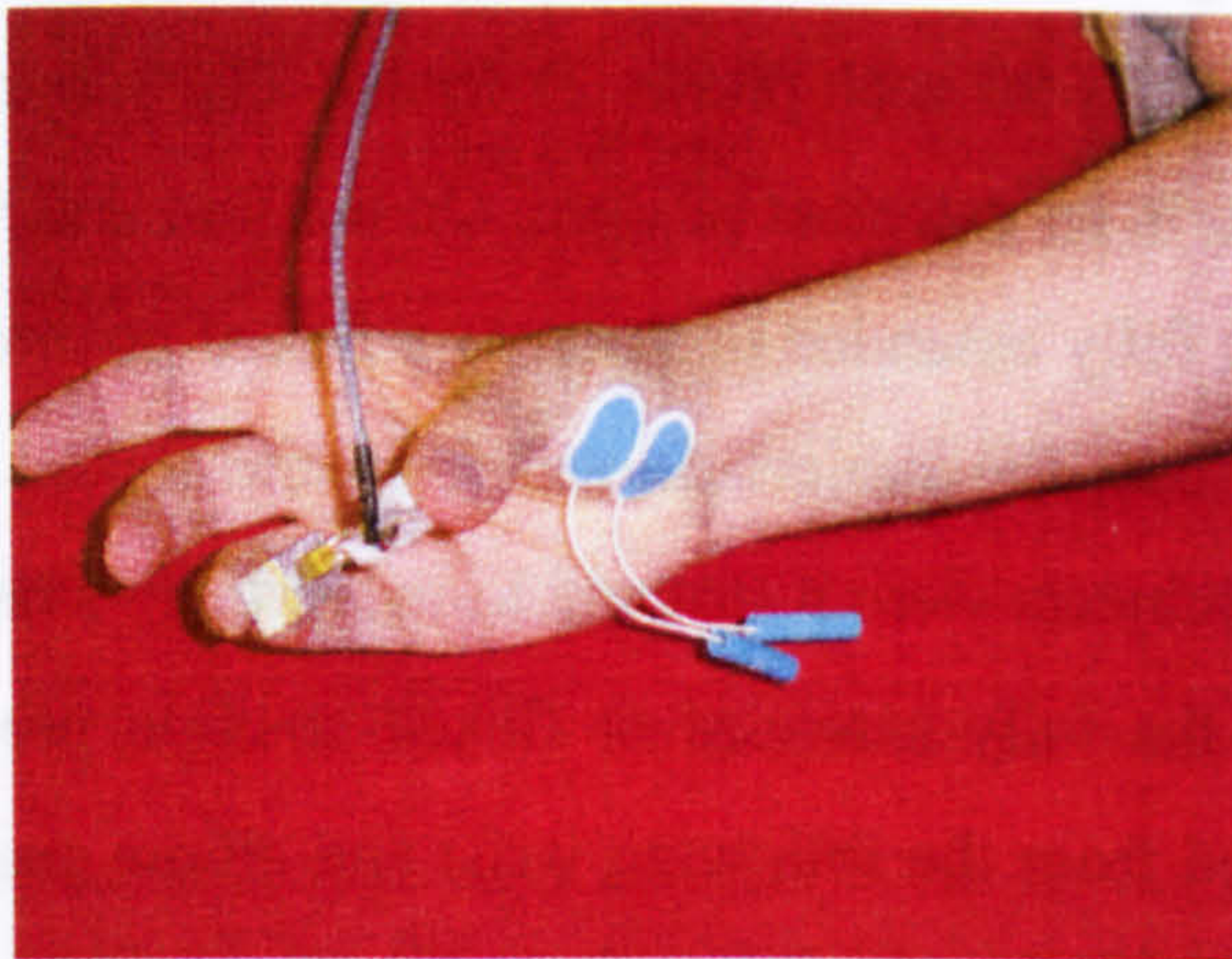


**Fig. 3.13** Electrode placement and grip used during the instrumented ring compression experiment.



### ***3.8.3 Influences of attention and cognitive loading in corticomuscular coherence.***

#### ***3.8.3.1 Instrumented ring compression experiment.***

Nine subjects participated in this experiment. The aim was to identify the way motor attention affects corticomuscular and intermuscular frequency domain estimates domain during a precision task. More specifically the aim was to identify distinct changes in the couplings (a) between a forearm and a hand muscle (b) between the two muscles and the cortex, during a task performance when compliance required high or low states of attention. The precision task involved the compression of an instrumented ring between right hand thumb and ring-little finger (Fig. 3.13) employing a small force of 3N. The wrist was in a slightly extended position, and the forearm was supported at a horizontal position. The output instrumented ring voltage from the strain gauge amplifier, representing the applied force was displayed on an oscilloscope. The subject was instructed to keep the line representing the pressure, aligned to a predetermined level marked on the screen of the oscilloscope.

The level of attention required to perform this task was determined by using a low and a high gain setting on the screen of the oscilloscope. At high gain the amplitude control of the feedback signal requires more attention as small variations in the force are exaggerated creating larger deviations from the target force than observed under the low gain condition. In the low gain condition it is easier for the subject to keep the force signal and the target level aligned. The target level represented the same force for both oscilloscope gain levels. It is obvious that both states required attention to the performed task. However by convention the relatively moderate attention demanding task is going to be called Low Attention (LA), and the relatively higher demanding task, High Attention (HA).

**Low Attention (LA):** During this task the subject was instructed to compress the instrumented ring between the thumb and the little finger while watching the force level on an oscilloscope (display speed 200ms/div) and match it to a constant level indicated on the screen by a straight line. The display gain of the oscilloscope was set to 0.01V/div.



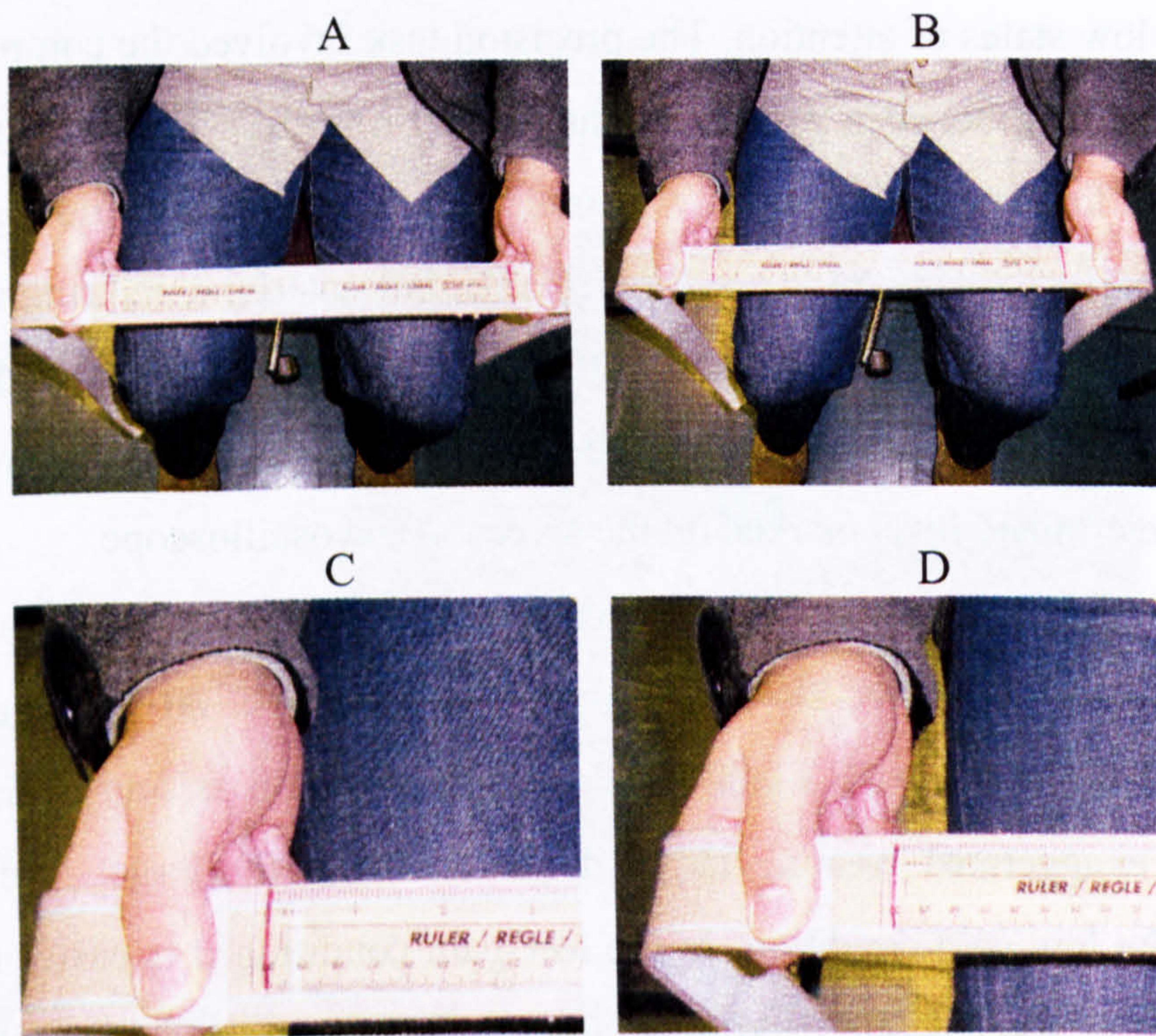


**Fig. 3.14** View (A, B) and close view (C, D) of bilateral extension of the elastic band. (A, C) Before the extension (B, D) during the extension. The ruler and the band are attached at the centre, allowing the two halves of the elastic band to be equally stretched. The target extension is indicated on the ruler with a red line and on the elastic band with a white line on each side. The white and red line were spaced 1 cm apart when the band was relaxed. During the extension the two lines should be aligned, resulting to an applied force of 975gr. Micropore tape was also affixed on the band indicating the site the subject should grasp.



High Attention (HA): The task was identical to the LA that was just described with the difference that the display gain of the oscilloscope was set to 0.1V/div, ten times higher than for LA. At this gain the deviations of force from the target appear larger to the subject, making it more difficult to attain the target.

EMG signals were recorded by:

Extensor Carpi Radialis Longus (ECRL)

Abductor Pollicis Brevis (APB).

EEG was recorded by a set of 28 cortical sites (Fig. 3.2). The order of the LA and HA tasks was interchanged in order to reduce the effects of fatigue. Four 1min trials were performed for each subject with around 1min rest intervals.

Because of technical difficulties the force level was not recorded. This was not essential for the aims of this experiment.

### ***3.8.3.2 Bimanual extension of an elastic band***

9 subjects participated in this experiment. The aim of this experiment was to study how corticomuscular and intramuscular frequency domain estimates are affected by attention and cognitive influences when engaged in a bimanual task. Dedicated performance of even simple tasks is difficult to be achieved even under experimental conditions. In the lab and in real life simultaneous cognitive tasks, not related with the performed movement may occur that may affect physiological signals that could be used for neuroprosthetic control.

The experiment involved the bilateral extension of an elastic band. Subjects were instructed to stretch the band at a constant length indicated by a ruler. They were also instructed to keep the wrists aligned with the arm so that wrist extensor muscles would be active. The extension task was performed under two conditions; the dedicated performance of the task and the cognitive loaded which involved the performance of the task with the subject carrying out a complicated mental arithmetic task.

The subject was comfortably seated in the reclining chair. They were instructed to take a firm grip using thumb and index fingers of both hands on the



extended elastic band. The subject extended the 50cm long band by 2cm corresponding to a force of 975gr and was instructed to keep the length of the band as close as possible to the given target for 1min (Fig. 3.14). The forearms were on the horizontal plane and were not supported.

The same task was also performed while the subject was instructed to count backwards subtracting seven sequentially starting from 100, 200, 300 or 400. Attention was divided between the arithmetic task and the motor task.

The order of performing the task with and without mental arithmetic was interchanged in order to reduce the influence of fatigue over the first or second condition. The total number of trials was 8; 4 with and 4 without the performance of the mental arithmetic. Each trial lasted around 1 min with 1 minute of rest time between tasks.

EMG was recorded from the following muscles:

Right extensor Carpi Radialis Longus (rECRL)

Right abductor Pollicis Brevis (rAPB)

Left extensor Carpi Radialis Longus (lECRL)

Left abductor Pollicis Brevis (lAPB)

#### ***3.8.4 Effects of deprivation of sensory feedback in corticomuscular coupling.***

3 subjects participated in this study. The aim of this experiment was to examine whether, factors resembling perturbations of the peripheral and central nervous system, can affect the corticomuscular and intramuscular coherence. More specifically, the aim was to examine how temporary sensory deafferentation will affect the neuronal mechanisms associated with observed EEG and EMG power as well as intermuscular and corticomuscular coherences. Temporary sensory deafferentation of the arm was induced by an ischemic nerve block consisting of tourniquet induced ischemia over the upper arm. The use of the ischemic nerve block is a common method examining peripheral nervous system changes and the subsequent nervous system plasticity, caused by the lack of afferent or efferent input (Glencross and Oldfield 1975; Ziemann et al. 1998; Ziemann et al. 1998; Ziemann et al. 2001).



A pneumatic tourniquet (sphygmomanometer cuff) placed over the upper arm just above the elbow level was inflated to at least 20 mmHg over the systolic blood pressure (~200 mmHg). Efferent fibres are less susceptible to hypoxia than the larger afferent fibres. This results in reduced or blocked afferent feedback from skin, joint and muscles for a short time window (~5min) where there was efferent output to the muscles.

Subjects were seated in a comfortable reclining chair. Surface EMG and EEG signals were recorded before, during and after the inflation of the sphygmomanometer cuff. Movement trials consisted of instructing the subject to maintain a wrist posture extension (70s) and perform continuous self paced continuous wrist movement (70s). The forearm was supported while both tasks were performed on the perpendicular plane, with the palm in a relaxed fist position facing down. One set of recordings was completed before ischemia, a second just after cuff inflation, a third 10 minutes after cuff inflation, a fourth 15 minutes after cuff inflation and a fifth just after the deflation of the cuff. The cuff was released around 20 min after the inflation.

EEG was recorded from FC1-C1 bipolar electrode pair. EMG was recorded from the following muscles:

Right Extensor Carpi Radialis Longus (ECRL)

Right Flexor Carpi Radialis (FCR),

Subject	Sex	Age	Dominant side
1	M	41	R
2	M	26	R
3	M	28	R

**Table 3.2** Table containing the sex, age and dominant side of the subjects that participated in the INB experiment.



### **3.9 METHODOLOGICAL SOURCES OF ERROR**

***Compliance with the experimental setup.*** The poor compliance with the experimental setup is a source of error. During the move-hold experiment subjects were instructed to move or hold following an audio cue at regular intervals. The compliance of the subjects with the protocol could not be quantitatively verified. Therefore 200ms before and after each audio cue instructing the subject to move or hold was discarded in order not to affect the quality of the data. In the time dependent estimates however that was not possible and the estimates during the transitions from movement to posture and vice versa may contain error.

Lapses of attention and fatigue could also affect the compliance with the experimental protocols and introduce error in the results.

***EMG electrode placement.*** The targeted muscles were the same in all examined subjects. However anatomical differences did not allow a standardisation of placement. Small differences in the electrode placement may reduce the quality of the data and increase the subject variability. Care was taken the electrodes to be placed over the right muscle and the EMG signal to be of sufficient quality.

***EEG electrode placement.*** The electrodes used were attached on the quickcap, arranged according to the standardised 10-20 international system. Care was taken at Fz electrode to be located 4cm from the nasion. However anatomical differences in the shape and size of the heads of subjects introduce a spatial error in the localisation of EEG spectral features.

***EMG Crosstalk.*** EMG crosstalk from muscles near the recording sites or from the recorded muscles of interest can contaminate the recorded signals. The small electrode size and interelectrode distance and location of recordings over the muscle as well as the adequate distance between recording sites was carefully planned to avoid crosstalk contamination. No recordings were performed from adjacent muscles which would have caused increased crosstalk.



***High impedance - 50Hz environmental noise.*** Adequate grounding on the subject eliminates this type of artefact from power lines. The problem arises when the impedance of one of the active electrodes becomes significantly large between the electrodes and the ground of the amplifier. In this situation, the ground becomes an active electrode that, depending on its location, produces the 50-Hz artefact. This artefact is often filtered by notch filters, but for lower frequency line noise and harmonics this is often undesirable. If the line noise or harmonics occur in frequency bands of interest they interfere with EEG that occurs in the same band.

***Movement artefacts.*** Head movements can mechanically affect the impedance of one or more electrodes, causing low frequency artefacts in the EEG and EMG signals. The subjects were advised to hold their head still during the experiments. Recording sessions that were affected were discarded and repeated.

***Muscle activity.*** Myogenic potentials are the most common artefacts caused by activity in different muscle groups including neck, jaw, facial muscles and the tongue. These signals have a wide frequency range and can be distributed across different sets of electrodes depending on the location of the source muscles. Generally, the potentials generated in the muscles are identified easily on the basis of duration, morphology, and rate of firing. Recording sessions with increased muscle activity were discarded and repeated. Subjects were also instructed to stay relaxed during the experiments.

***Visual induced artefacts - Eye Blink.*** The eye blink artefact is very common in EEG data. It produces a high amplitude signal that can be many times greater than the EEG signals of interest. Because of its high amplitude an eye blink can corrupt data on all electrodes, even those at the back of the head. Eye artefacts are often measured more directly in the electrooculogram (EOG), pairs of electrodes placed above and around the eyes. Eye movement artifacts are caused by the reorientation of the retinocorneal dipole. This artifact's diffusion across the scalp is stronger than that of the eye blink artifact. Eye blinks and movements often occur at close intervals producing an more complex effect.



***Pulse.*** The pulse, or heart beat, artefact occurs when an electrode is placed on or near a blood vessel. The expansion and contraction of the vessel introduce voltage changes into the recordings. The artefact signal has a frequency near 1.2Hz, but can vary with the state of the patient. This artefact can appear as a sharp spike or smooth wave.

***Link mastoid reference.*** The use of the link mastoid reference there is the possible contribution of slight impedance differences the possible contribution of slight impedance differences between the mastoids affecting the effective spatial location of the reference when they are physically linked (Kalin et al. 1998). Different choices of reference electrodes result in small but systematic changes in the distribution of EEG frequency power (Yao et al. 2005).

***Volume conduction effects.*** In some cases coherence may be the result of volume conduction effects rather than neuronal connectivity. Microelectrode studies, partial coherence analysis methods and the fact that coherence is not automatically high in bands and areas where spectral power is high have suggested that the majority of the observed coherence is due to connectivity rather than from volume conduction, passively carrying signals to multiple electrodes (Feige 1996).



## **4 ANALYTICAL METHODS**

### **4.1 INTRODUCTION**

The studies carried out within the framework of this thesis required the simultaneous observation of several physiological processes, mainly continuously varying waveforms, like recordings of surface EMG and multiple EEG recordings. The need to identify and characterise the interactions between those processes led to frequency, time-frequency and time domain analysis with elements of spatial domain as the choice of analytical methods used in this thesis. The experiments resulted in simultaneous observations of several signals like multiple EEG and EMG recordings. The methods used in this thesis are a set of frequency domain measures for characterising linear interactions between these signals. The approach adopted is that of spectral estimation procedures based on the finite Fourier transform.

Time and frequency domain parameters have been shown to have complementary natures and can be used to characterise different aspects of the same data despite that all linear time domain parameters are estimated by the frequency domain. Therefore it is necessary to use both domain representations to obtain maximum insight into the behaviour of complex neurophysiological systems.

The assumption of stationarity (signals have constant frequency content over time) of the finite Fourier transform also lead to the use of time frequency analysis in the form of short Fourier transform. EEG and EMG signals are non-stationary which means that their frequency content changes over time. Using time-frequency techniques the signal is divided into small enough segments where the signal contained in these segments can be assumed to be stationary. In this way temporal features of the frequency domain modulation can also be examined.

The multiple EEG recordings can also give a spatial information since the positions of the EEG electrodes are known, allowing the construction of activity maps.

These techniques have a long record of use which allows the comparison of the current experimental results with established studies. They are also well documented in both the statistical and functional aspects which means that theoretical parameters can be estimated while gaining insight and inference from the



experimental data and at the same time dealing with error and uncertainty facilitating the testing of hypotheses.

This chapter defines the finite Fourier transform of regularly sampled waveform data (time series). The construction of estimates of second order spectra based on complex products of the finite Fourier transforms of time series is also outlined. Estimates that can characterise the dependence between two time series and assess the coupling between simultaneously recorded signals have also been defined. Techniques to obtain a single estimate from different and independent pairs of signals across different trials from even different subjects have been described as well as the construction of time dependent estimates that will reveal the temporal signal dependencies across single and recurring trials. Most of the methods described have already been used by other researchers for physiological signal processing, but novel analytical features have also been introduced.

MATLAB ver 6.5 was used for the processing of the signals. Custom made routines coded in MATLAB as well as routines kindly provided by David Halliday were used as they are or modified as needed. The code provided by David Halliday is freely available in <http://www.neurospec.org>. SIMULINK ver 5.0 was used for the simulation models.

## ***THE DISCRETE FOURIER TRANSFORM***

The Discrete Fourier Transform (DFT) is a primary and very important tool for digital signal processing. The Fourier transform of a segment of length T from a time series,  $x$ , is written as (Brilinger 1972, 1974)

$$d_x^T(\lambda) = \int_0^T e^{-i\lambda t} x(t) dt \quad \text{Eq. 4.1}$$

$x(t)$  is a regularly sampled waveform, so the sampled values can be readily evaluated by an FFT algorithm of length T approximating the integral in the above equation by a discrete summation. So the Fourier transform of a segment of length T from a time series,  $x$ , is written as:

$$d_x^T(\lambda_j) \approx \sum_{t=0}^{T-1} e^{-i\lambda_j t} x_t \quad \text{Eq. 4.2}$$



where  $x_t$  are the sample values of  $x(t)$  at time  $t$ . The Fourier frequencies are given by  $\lambda_j = 2\pi j/T$ , for  $j = 0, \dots, T/2$ . This defines a range for  $\lambda_j$  of  $(0, \pi)$ , where  $\pi$  corresponds to the Nyquist frequency. In that way a Fourier decomposition of the segment of  $x(t)$  into constituent frequency components is performed, that highlights distinct periodic components in the data (Brillinger 1983).

#### Definition and estimation of second order spectra

The construction of estimates of second order spectra are based on complex products of the finite Fourier transforms of time series presented above.

The cross-spectrum estimate of a time series  $x$  and  $y$  of length  $T$  is defined as:

$$I_{xy}^T(\lambda_j) = \frac{1}{2\pi T} d_x^T(\lambda_j) \overline{d_y^T(\lambda_j)} \quad \text{Eq. 4.3}$$

Auto-spectrum is defined if  $x$  and  $y$  are identical

$$I_{xx}^T(\lambda_j) = \frac{1}{2\pi T} d_x^T(\lambda_j) \overline{d_x^T(\lambda_j)} = \frac{1}{2\pi T} |d_x^T(\lambda_j)|^2 \quad \text{Eq. 4.4}$$

This quantity is often referred to as the periodogram.

### 4.2.1 Power spectrum estimate

The power spectral density is one of the main tools used giving the distribution over frequency of the power contained in a physiological signal, based on a finite set of data. Non parametric methods will be used in which the estimate of the Power Spectral Density (PSD) is made directly from the signal itself. The simplest way of doing so is the periodogram as described above.

Practically the estimation of the periodogram translates to the simple calculation of the DFT of the samples of the process and take the magnitude squared as an result.

Therefore the periodogram estimate of the PSD of a length  $T$  signal  $x$  is:

$$\hat{f}_{xx}(\lambda_j) = \frac{1}{2\pi T} |d_x^T(\lambda_j)|^2 \quad \text{Eq. 4.5}$$

The Fourier frequencies  $\lambda_j$  can be expressed in Hz as  $\lambda_j = j/T\Delta t$ , where  $T$  is the number of points in the finite Fourier transform, and  $\Delta t$  is the sampling interval



in seconds. The sampling rate  $f_s = 1/\Delta t$ . In that way the above expression takes the form

$$\hat{f}_{xx}(\lambda_j) = \frac{1}{f_s T} |d_x^T(\lambda_j)|^2 \quad \text{Eq. 4.6}$$

where

$$d_x^T(\lambda_j) = \sum_{t=0}^{T-1} e^{-2\pi i j t / f_s} x_t \quad \text{Eq. 4.7}$$

The actual computation of  $d_x^T(\lambda_j)$  is performed only at a finite number of frequency points,  $N$ , using the FFT. In practice most implementations of the periodogram method compute the  $N$ -point PSD estimate

$$\hat{f}_{xx}(\lambda_k) = \frac{1}{f_s T} |d_x^T(\lambda_k)|^2, \quad \text{Eq. 4.8}$$

$$\lambda_k = \frac{k f_s}{N}, \quad k=0,1,\dots,N-1$$

where

$$d_x^T(\lambda_k) = \sum_{t=0}^{T-1} e^{-2\pi i k t / f_s} x_t \quad \text{Eq. 4.9}$$

It is wise to choose  $N > T$  so that  $N$  is the next power of two larger than  $T$  by simply padding  $x$  with zeros to the length  $N$ .

In statistical terms the periodogram is not a consistent estimator of the PSD and requires further smoothing.

The 95% confidence limits are used as a measure of significance of the power spectral estimates. Given an estimate  $\hat{z}$ , under the assumption of asymptotic normality, estimates of the upper and lower 95% confidence limits are obtained by estimating  $\pm 1.96(\text{var}\{\hat{z}\})^{1/2}$  about the mean or asymptotic value (Brillinger, 1974 and Halliday *et al.*, 1995).

For estimates of the power spectrum,  $\hat{f}_{xx}(\lambda)$ , the variance can be approximated by (Bloomfield, 1976) :

$$\text{var}\{\hat{f}_{xx}(\lambda)\} \approx L^{-1} (f_{xx}(\lambda))^2, \quad \text{Eq. 4.10}$$

and



$$\text{var} \left\{ \ln \left( \hat{f}_{xx}(\lambda) \right) \right\} \approx L^{-1}, \quad \text{Eq. 4.11}$$

where  $L$  is the degrees of freedom, in this case the number of disjoint section.

Therefore variance of the estimate  $\log_{10} \left( \hat{f}_{xx}(\lambda) \right)$ ,

$$\text{var} \left\{ \log_{10} \left( \hat{f}_{xx}(\lambda) \right) \right\} = L^{-1} (\log_{10} \ell)^2 \quad \text{Eq. 4.12}$$

When a smoothing window is applied to the spectral estimate, the degrees of freedom change to  $\nu = \frac{2 \times L}{\sum_{j=-m}^m W_j^2}$ , where  $m$  represents the size of the smoothing

window and  $W_j$  indicates the smoothing that has been applied to the estimate.

### 4.2.2 Coherence estimate

The coherence estimate is a normalised measure of linear association between two signals as a function of frequency. It is a quantitative measurement that reflects the extent to which two time series are synchronous or are phase locked at a given frequency. Coherence, is independent of the amplitude of the signals. It takes values from 0 to 1 where 0 would mean independent processes and 1 would indicate a linear correlation.

The magnitude squared coherence between two signals  $x$  and  $y$  is given by:

$$\left| \hat{R}_{xy}(\lambda) \right|^2 = \frac{\left| \hat{f}_{xy}(\lambda) \right|^2}{\hat{f}_{xx}(\lambda) \hat{f}_{yy}(\lambda)} \quad \text{Eq. 4.13}$$

This quotient is a real number between 0 and 1 that measures the correlation between  $x(n)$  and  $y(n)$  at the frequency  $w$ . The function is actually the squared magnitude of the cross spectral densities of the two processes divided by their autospectra. The estimates of the necessary second order spectra can be constructed using the Welch's method described above.



A confidence interval at the 100% point is given by  $1 - (1 - \alpha)^{1/(L-1)}$ , where L is the number of disjoint sections used to estimate the cross-spectra and auto-spectra. Therefore the 95% confidence limit for an estimate of coherence can be approximated by  $1 - 0.05^{1/(L-1)}$ . This result is valid for non-overlapping and non windowed sections. In other cases, using windowed and overlapping segments, the computation of the exact confidence limit is complicated. Spectral coherence can be calculated from either monopolar or bipolar pairs of EEG recordings. However using common reference data in coherence calculation (Fein et al. 1988) may bias coherence estimates toward inflated values because of possible contaminating activity at the common reference electrode.



### 4.2.3 Phase spectrum

Coherence assesses the magnitude of correlation between two signals in the frequency domain. The phase difference between two signals can give us information relating to timing. For time series  $x$  and  $y$  the phase spectrum,  $\Phi_{xy}(\lambda)$ , is defined as the argument of the cross spectrum estimate

$$\hat{\Phi}_{xy}(\lambda) = \arg\{\hat{f}_{xy}(\lambda)\} \quad \text{Eq. 4.14}$$

Phase estimates are only valid when there is significant coherence between the two signals. Where there is significant correlation over a wide range of frequencies and a delay between two signals, it is reasonable to extend the phase estimate outside the range  $[-\pi, \pi]$  radians, which avoids discontinuities in phase estimates. Such a phase estimate is often referred to as an unconstrained phase estimate.

However the interpretation is not straight forward since the phase estimate can be interpreted differently according to theoretical models. A useful model is the phase curve for two signals which are correlated with a fixed time delay, where the theoretical phase curve is a straight line, passing through the origin (0 radians at 0 frequency) with slope equal to the delay, and a positive slope for a phase lead, and negative slope for a phase lag (see Jenkins and Watts, 1968). In situations where the correlation structure between two signals is dominated by a delay it is possible to estimate this delay from the phase curve, such an approach, based on weighted least squares regression (Rosenberg et al. 1989). This method has the advantage of providing an estimate of the standard error for the estimated delay. An adaptation from the above publication is following.

According to the above technique the relation between input and output is given as  $\Phi(\lambda) = -\tau\lambda$  where  $\tau$  the time delay between these processes, which may be calculated by the slope of the least squares line fitted to the estimated phase curve. A weighted estimation method is used to calculate the lag and the standard error, because coherence between input and output processes is not constant.

Letting  $\Phi^T(\lambda_i) \equiv \Phi_i$  represent the estimated phase defined at  $\lambda_i = \frac{2\pi i}{T}$ ,  $i=1,2,\dots,n$ , then a regression model through the origin of the following form may be



set down  $\Phi_i = \beta\lambda_i + \varepsilon_i$ , where  $\beta = -\tau$ , and the  $\varepsilon_i$  are approximately normally distributed with mean zero and variance  $\sigma_i^2$ , and covariance  $\text{cov}\{\varepsilon_i, \varepsilon_j\} \cong 0$  for  $i \neq j$ .

$$\sigma_i^2 = \frac{1}{2L} \left[ \frac{1}{|R_1(\lambda_i)|^2} - 1 \right], \text{ where } L \text{ is the number of disjoint periodogram}$$

sessions from records of duration  $T$  used in estimating the spectra required to estimate  $\Phi(\lambda)$ .

The non constant variance suggests a weighted least squares estimate of  $\beta$ , that may be obtained by minimizing  $\sum \frac{1}{\sigma_i^2} (\Phi_i - \beta\lambda_i)^2$ . Setting  $\sigma_i^2 = \frac{\sigma^2}{w_i^2}$  where  $w_i$  is

the weight for the  $i^{\text{th}}$  value of the variance, then the weighted least squares estimate

of  $\beta$  is given by  $\hat{\beta} = \frac{\sum w_i \Phi_i \lambda_i}{\sum w_i \lambda_i^2}$ , which is an unbiased estimate of  $\beta$ , and it is

approximately normally distributed with variance  $\text{Var}(\hat{\beta}) = \frac{\sigma^2}{\sum w_i \lambda_i^2}$ . For  $\sigma^2$  an

obvious estimate is given by  $\hat{\sigma}^2 = \frac{\sum w_i (\Phi_i - \hat{\beta} \lambda_i)^2}{n-1}$ . The weights  $w_i$  can be taken as

inversely proportional to the estimated variance given by  $w_i \propto \frac{1}{\hat{\sigma}_i^2}$ . An approximate

95% confidence interval for the delay is  $-\hat{\beta} \pm t_{(n-1, 0.975)} \frac{\hat{\sigma}}{\sqrt{\sum w_i \lambda_i^2}}$ .



#### 4.2.4 Cumulant density

Cumulant density is a time domain parameter estimated from an inverse Fourier transform of a cross spectrum. It gives the correlation between two signals but this time as a function of time instead of frequency.

The second order cumulant density function between processes  $x$  and  $y$  is defined as:

$$q_{xy}(u) = \int_{-\pi}^{\pi} f_{xy}(\lambda) e^{i\lambda u} d\lambda \quad \text{Eq. 4.15}$$

which can be estimated by the following expression

$$\hat{q}_{xy}(u) = \frac{2\pi}{T} \sum_{|j| \leq T/2b} \hat{f}_{xy}(\lambda_j) e^{i\lambda_j u} \quad \text{Eq. 4.16}$$

where  $\lambda_j = 2\pi j/T$  are the Fourier frequencies, and  $b$  is the desired time domain bin width ( $b \geq 1.0$ ), a value of  $b=1.0$  results in a time domain estimate with the same temporal resolution as the sampling rate of the two signals. The cumulant density can be practically calculated using a real valued inverse FFT algorithm.

Cumulant density function can be considered as statistical parameters providing a measure of linear dependence between two signals. For two independent signals cumulant density should be zero but can also assume positive and negative values.

The variance of the hybrid cumulant density can be estimated as

$$\text{var}\{\hat{q}_{xy}(u)\} \approx \left(\frac{2\pi}{R}\right) \left(\frac{2\pi}{T}\right)^{(T/2-1)/b} \sum_{j=1}^{T/2-1} 2\hat{f}_{xx}(\lambda_j) \hat{f}_{yy}(\lambda_j) \quad \text{Eq. 4.17}$$

where  $\lambda_j = 2\pi j/T$ ,  $R$  is the record length,  $b$  the bin width, and  $T$  is the segment length used in the estimation of finite Fourier transforms. The 95% confidence limits are given by

$$0 \pm 1.96 \left[ \left(\frac{2\pi}{R}\right) \left(\frac{2\pi}{T}\right)^{(T/2-1)/b} \sum_{j=1}^{T/2-1} 2\hat{f}_{xx}(\lambda_j) \hat{f}_{yy}(\lambda_j) \right]^{1/2} \quad \text{Eq. 4.18}$$

Only values outside of the upper and lower 95% confidence limits can be taken as evidence of linear correlation between time series  $x$  and  $y$ .



### 4.2.5 Pooled frequency estimates.

Features of the data that are representative of a larger population can be highlighted by the pooled frequency estimates. Several pairs of records of simultaneously recorded physiological signals coming from different subjects and different recording sessions may be combined in order to derive a single frequency domain estimate. The estimates are constructed using the cross spectral densities and autospectra pooled from individual subjects.

The pooled auto-spectra can be defined as:

$$\frac{\sum_{i=1}^k \hat{f}_{a_i, a_i}(\lambda) L_i}{\left( \sum_{i=1}^k L_i \right)} \quad \text{Eq. 4.19}$$

which is real valued and the pooled cross-spectra as

$$\frac{\sum_{i=1}^k \hat{f}_{a_i, b_i}(\lambda) L_i}{\left( \sum_{i=1}^k L_i \right)} \quad \text{Eq. 4.20}$$

which is complex valued.

where  $k$  independent pairs of processes are considered,  $(a_i, b_i : i = 1, \dots, k)$  with  $L_i$  the number of disjoint sections used to estimate the second order spectra for the  $i^{\text{th}}$  pair of processes.

Using the pooled second order spectra just defined pooled coherence estimates can be obtained:

$$\frac{\left| \sum_{i=1}^k \hat{f}_{a_i, b_i}(\lambda) L_i \right|^2}{\left( \sum_{i=1}^k \hat{f}_{a_i, a_i}(\lambda) L_i \right) \left( \sum_{i=1}^k \hat{f}_{b_i, b_i}(\lambda) L_i \right)} \quad \text{Eq. 4.21}$$

The pooled coherence estimate is obtained by a weighted average of the individual second order spectra and is essentially a coherence estimate where all the processes from the individual subjects have been joined to form a long recording. The size of the individual subject recordings need not be the same but a long recording will have more effect on the final result than a short one. Like ordinary



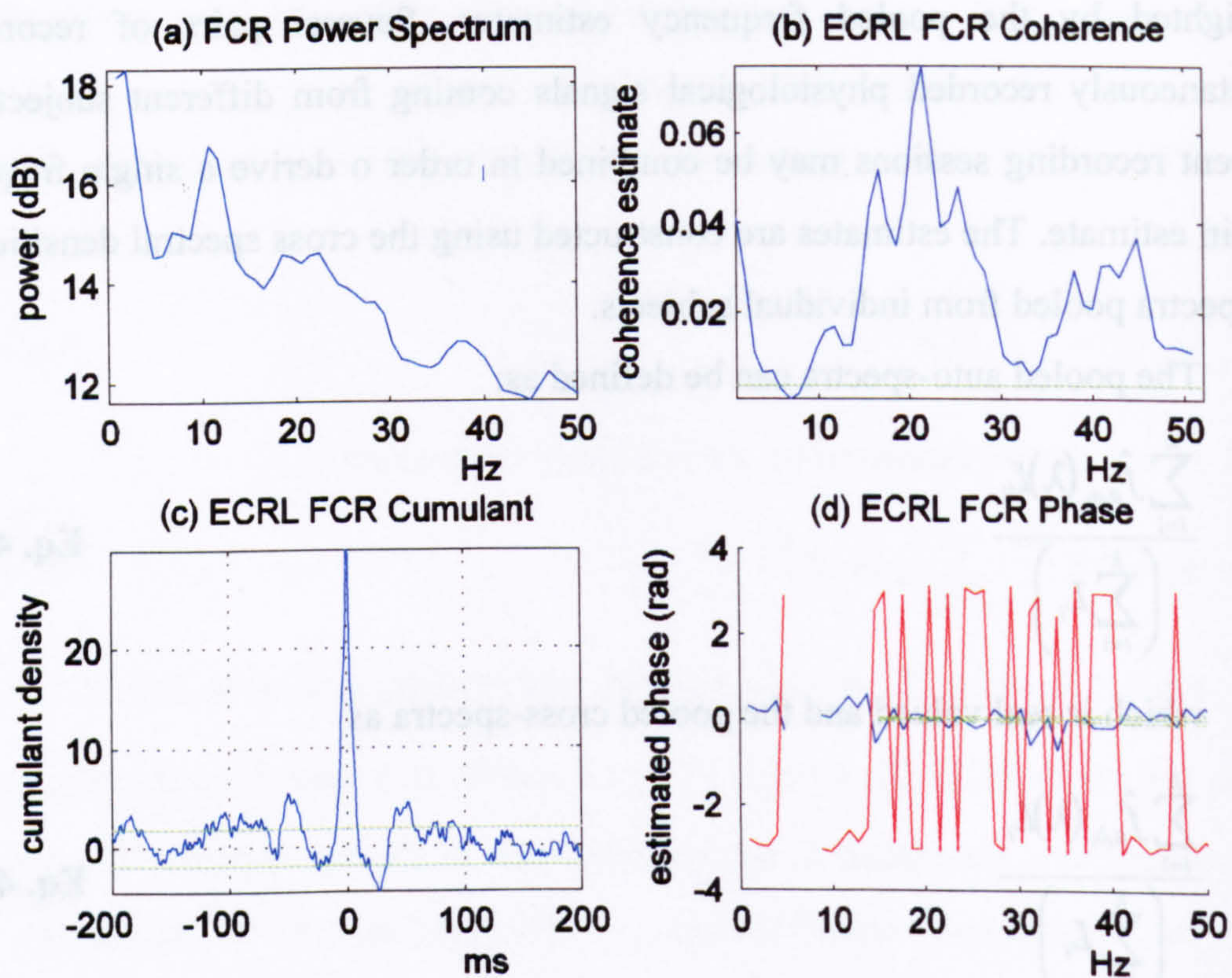


**Fig. 4.1** Example of frequency and time domain parameters estimation plotted with the associated 95% confidence limits and error estimates.



coherence estimates, pooled coherence estimates take values between 1 and 0. The 95% confidence limit is calculated as before

$$1 - (0.05)^{1/(\sum L_i - 1)} \quad \text{Eq. 4.22}$$

Considering the high variability of the results for different subjects, great care has to be taken into careful interpretation of pooled across subjects results. According to reports, pooled coherence can overestimate the significance of coupling (Baker 2000).

Based on the pooled cross-spectrum definition, pooled phase and cumulant density estimates can also be defined.

#### ***4.2.5.1 Interpretation of the Pooled frequency estimates.***

The methods used have a strong dual theoretical and physical existence, which means that problems can be approached by the statisticians perspective as theoretical parameters, whereas the experimentalist attempts to gain insight and inference from the data. The combination of these approaches as it emerges from the used analytical methods uses statistics to analyse experimental data to deal with error and uncertainty and in the setting up of procedures for testing hypotheses.

Once a parameter of interest has been defined, an estimation procedure can be developed, which for a finite amount of data will have some associated error. An important part of the present analysis is the use of confidence limits for all parameter estimates. Confidence limits are an essential part of the present statistical analysis, since they provide a guide to interpretation of estimates and allow the significance of any interesting features in parameter estimates to be assessed.

In the example that is presented in Fig. 4.1 three frequency domain estimates were calculated involving ECRL and FCR EMGs during interment posture extension (see 3.8.2.1): spectral estimate, coherence estimate, phase estimate while the cumulant estimate while a time domain estimate was also calculated by the frequency domain.

All the parameters in this section have been estimated using a segment length of  $T=1024$  points in the finite Fourier transforms. This defines the minimum frequency which can be resolved (and thus the spectral resolution) according to the



relationship  $f=1/(T dt)$  Hz where  $dt$  is the sampling interval for the data set. For  $dt=1ms$  the spectral resolution is  $f=0.976Hz$ . the data set is 44s resulting to a number of 43 complete segments.

### *Spectral estimates*

Fig. 4.1a shows the spectral estimates of the FCR EMG time series. The 95% confidence interval for the estimate is indicated by the solid vertical line in the top right of each graph. It is used as a measure of significance of the power spectral estimates therefore this line provides a scale against which to assess the significance of distinct features in each estimate. Comparison with this scale shows that the spectrum contains a number of frequency features. 0-5Hz frequencies are quite high while a very distinct frequency band is centred around 10Hz. Some more features are also present e.g. 20-25Hz and 35-42Hz.

### *Coherence estimates*

The linear pairwise interactions between the ECRL and FCR EMG signals are characterized in the frequency domain by coherence estimates shown in Fig. 4.1b. It is necessary to include the line on a coherence plot as an estimate of the upper 95% confidence limit. Estimated values of coherence lying below this line can be taken evidence for the lack of a linear association between the two processes, i.e. that zero coherence is plausible at that frequency. Therefore the coupling is statistically significant for the frequency bands at the coherence estimate is higher than the confidence interval. The coherence estimates between ECRL and FCR suggest that coupling occurs in two broad frequency bands of 15-30Hz and 35-47Hz.

### *Phase*

Information relating to timing can be obtained by examining the phase difference between the two EMGs. It derives the delay of the linear coupling also derives the degree of 95% confidence error. Phase estimates are only valid when there is significant correlation between the two signals. In Fig. 4.1c phase is valid 10-50Hz and derives a delay of  $0.1\pm 0.3ms$  using the application of the weighted least



squares regression analysis (Rosenberg et al. 1989) to estimate the slope of the phase curve and the confidence error.

### *Cumulant*

Second order cumulant density functions provide a time domain measure of association between two processes which complements the frequency domain representation provided by coherence functions.

The ECRL\FCR second order cumulant density estimate is shown in Fig. 4.1*d*. The cumulant density estimate plotted for lag values of  $\pm 200$ ms. It illustrates short-term synchrony between the EMGs, with a central peak of around 15ms in width. The latency of the peak occurs at about 0ms, in agreement with the delay estimated from the phase that gave  $0.1 \pm 0.3$ ms. Small sidebands are present, these are taken to represent the periodic structure present in the common inputs responsible for the short-term synchrony. In this case the interval from the peak at 0ms to each is around 50ms, this represents a periodicity of 220Hz, which is consistent with the central feature in the coherence estimate in Fig. 4.1*b*.



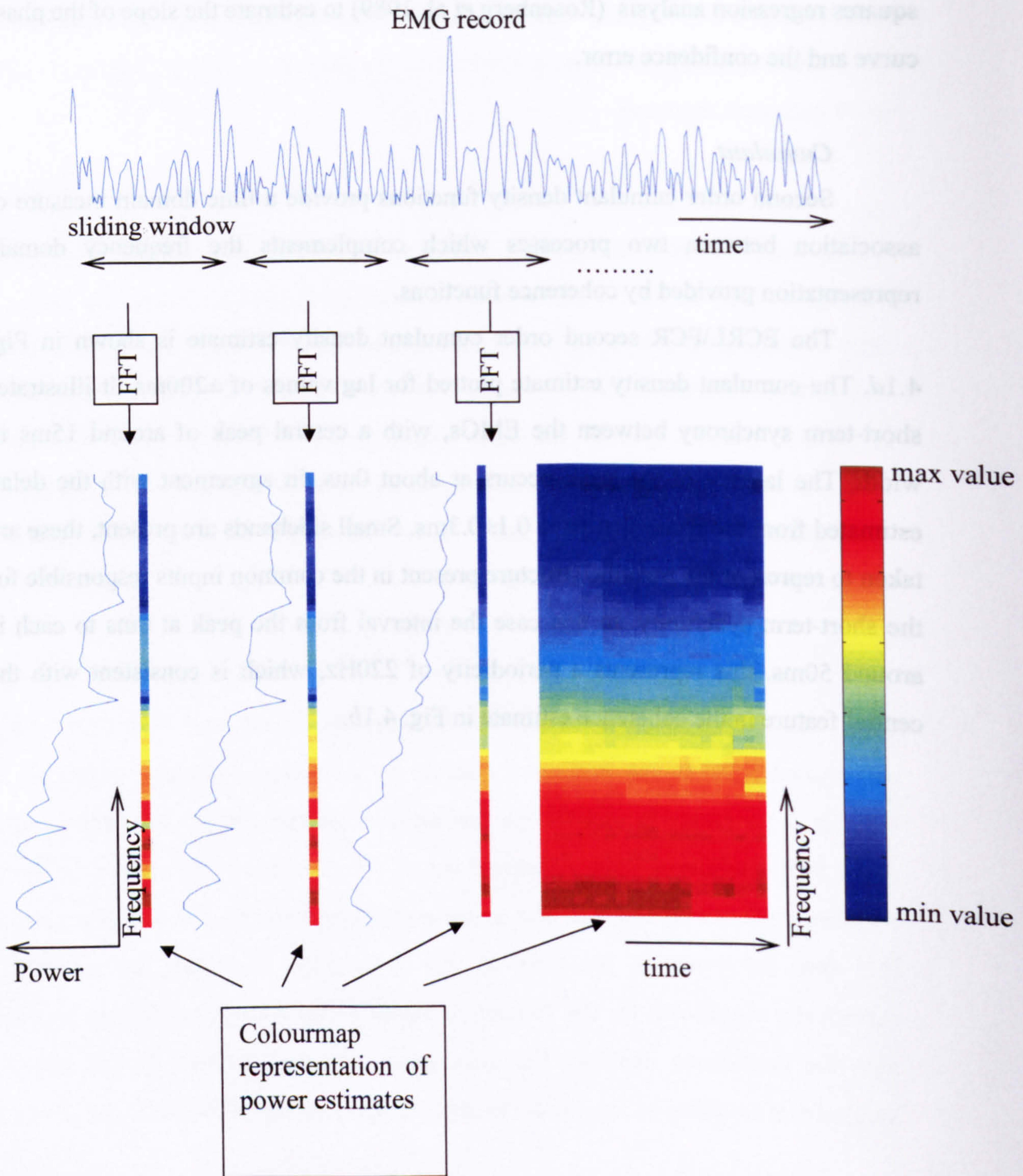


**Fig. 4.2** The figure illustrates the procedure for producing a spectrogram from time series data. A sample of an EMG recording is represented. The data is first divided into equal length overlapping or non-overlapping sections. The periodogram for each of these sections is constructed, and represented as a one dimensional image. A series of individual periodogram estimate images is used to produce the spectral representation of power in time. The final spectrogram is displayed as an image where the colourmap is optimised to take values from the highest to the lowest contained value.



## ***4.3 FREQUENCY ESTIMATES IN TIME***

### ***4.3.1 Spectrogram***

The spectrogram gives the time-dependent power spectrum for a signal and displays the information in the form of an image, showing the magnitude of the time dependent Fourier transform versus time. In this way time dependent power spectral variations over the examined frequency range can be observed in physiological signal records.

The time-dependent Fourier transform is the discrete time Fourier transform for a sequence that is computed using a sliding window technique which is called short-time Fourier transform. It is a standard technique which has numerous applications in signal processing and mainly in frequency tracking where it can show how the frequency content of a signal changes with time. For the analysis individual frequency features will be displayed and their behaviour tracked throughout the task enabling the identification of task-specific features. The data is divided into equal length overlapping (or disjoint) sections while the periodogram for each of these sections is constructed, and represented as a one dimensional image. A series of individual periodogram estimate images is used to produce the spectral representation of power in time. The final spectrogram is displayed as an image where the colourmap is optimised to take values from the highest to the lowest contained value. A schematic representation of the process for constructing a spectrogram can be seen in Fig. 4.2

The important parameters of the spectrogram are the segment length (sliding window), the overlapping between segments and the FFT window length. Their values are a compromise between frequency resolution, variance, time resolution and computational resources. Longer segments can decrease the variance, but the time resolution will also be decreased. Experimentation showed that a segment length of around 2sec (2048 samples) FFT length 256 and time overlap of 64 ms gives a relatively good representation of the changes in the frequency content.



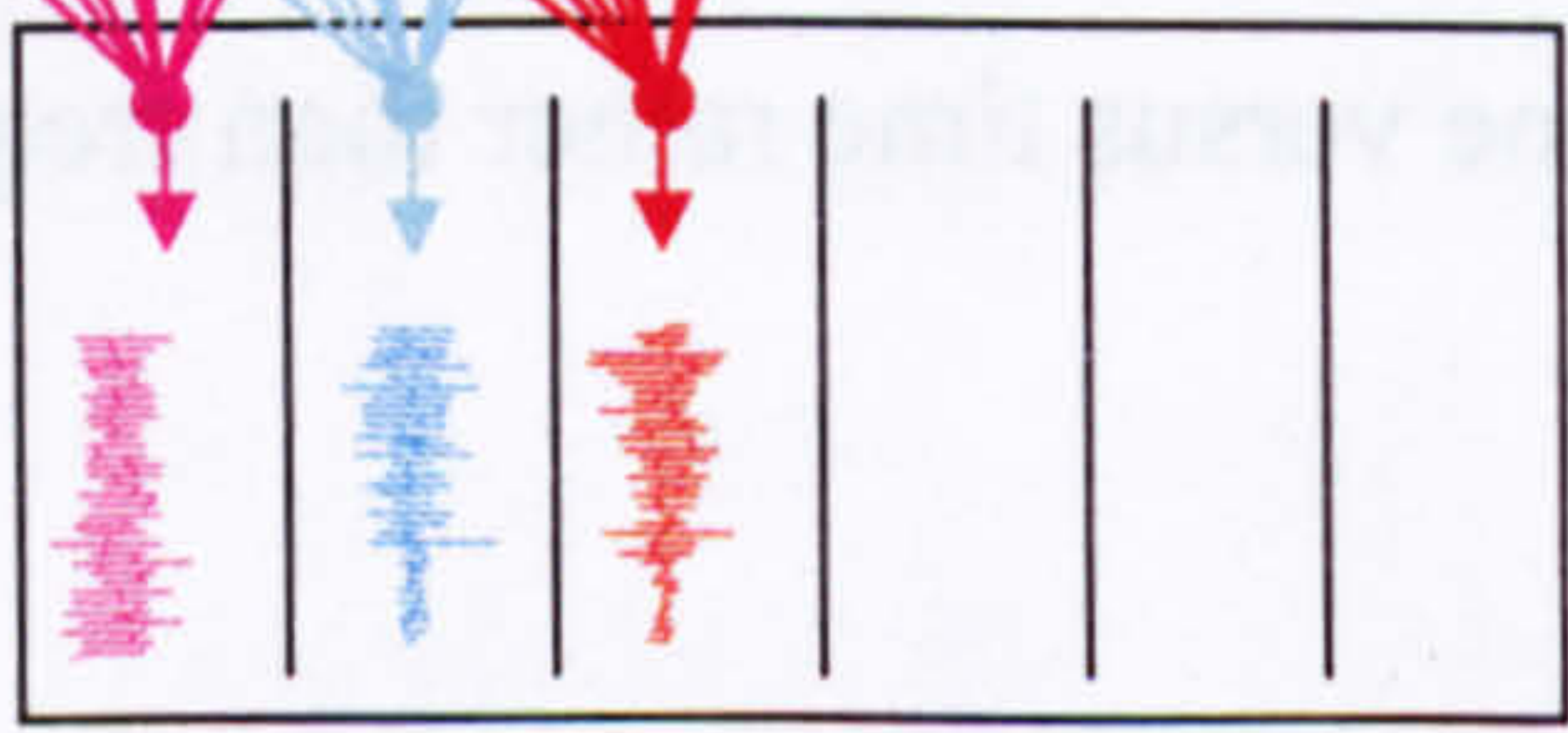
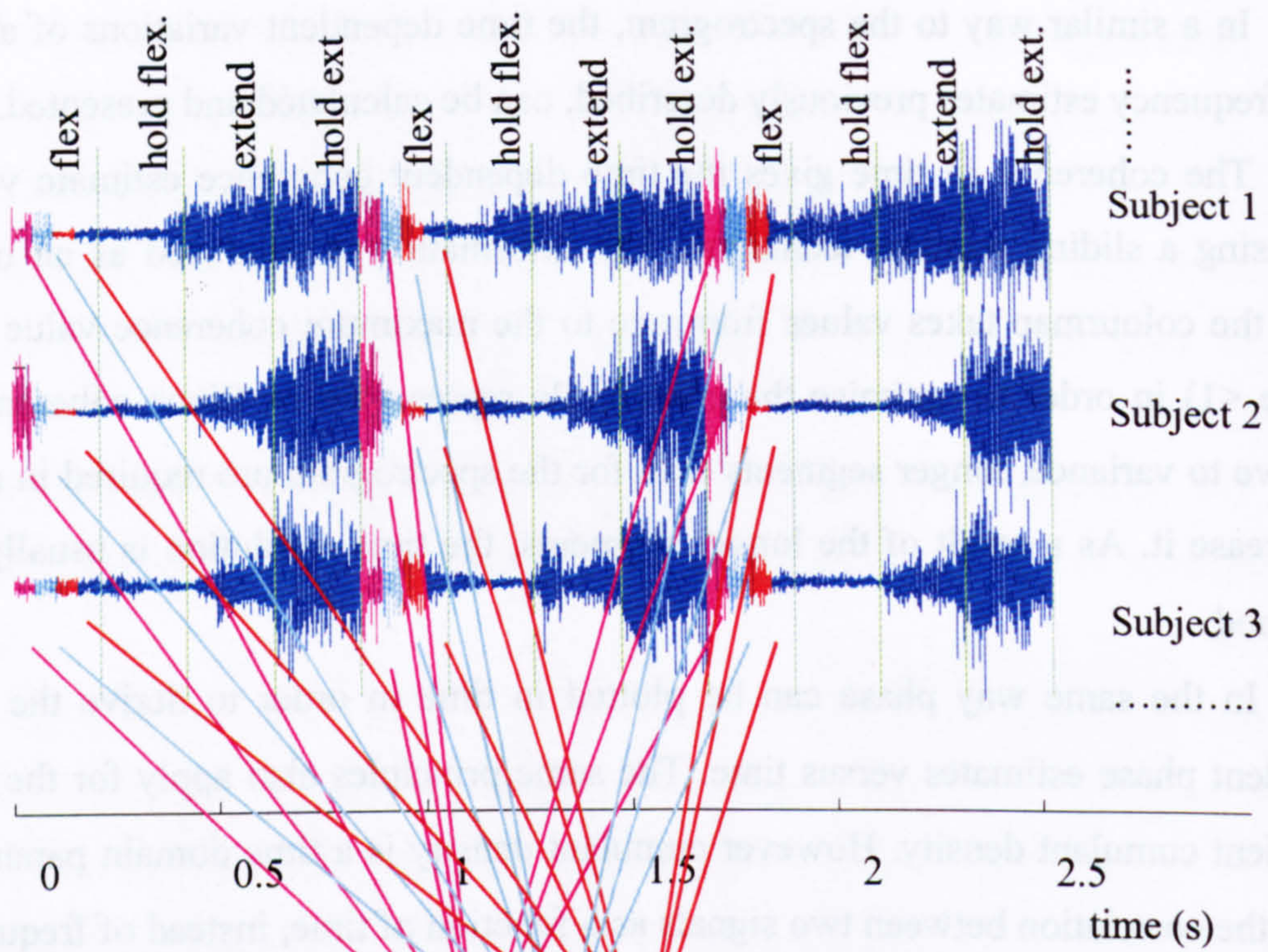
### ***4.3.2 Other frequency estimates in time.***

In a similar way to the spectrogram, the time dependent variations of all the other frequency estimates previously described, can be calculated and presented.

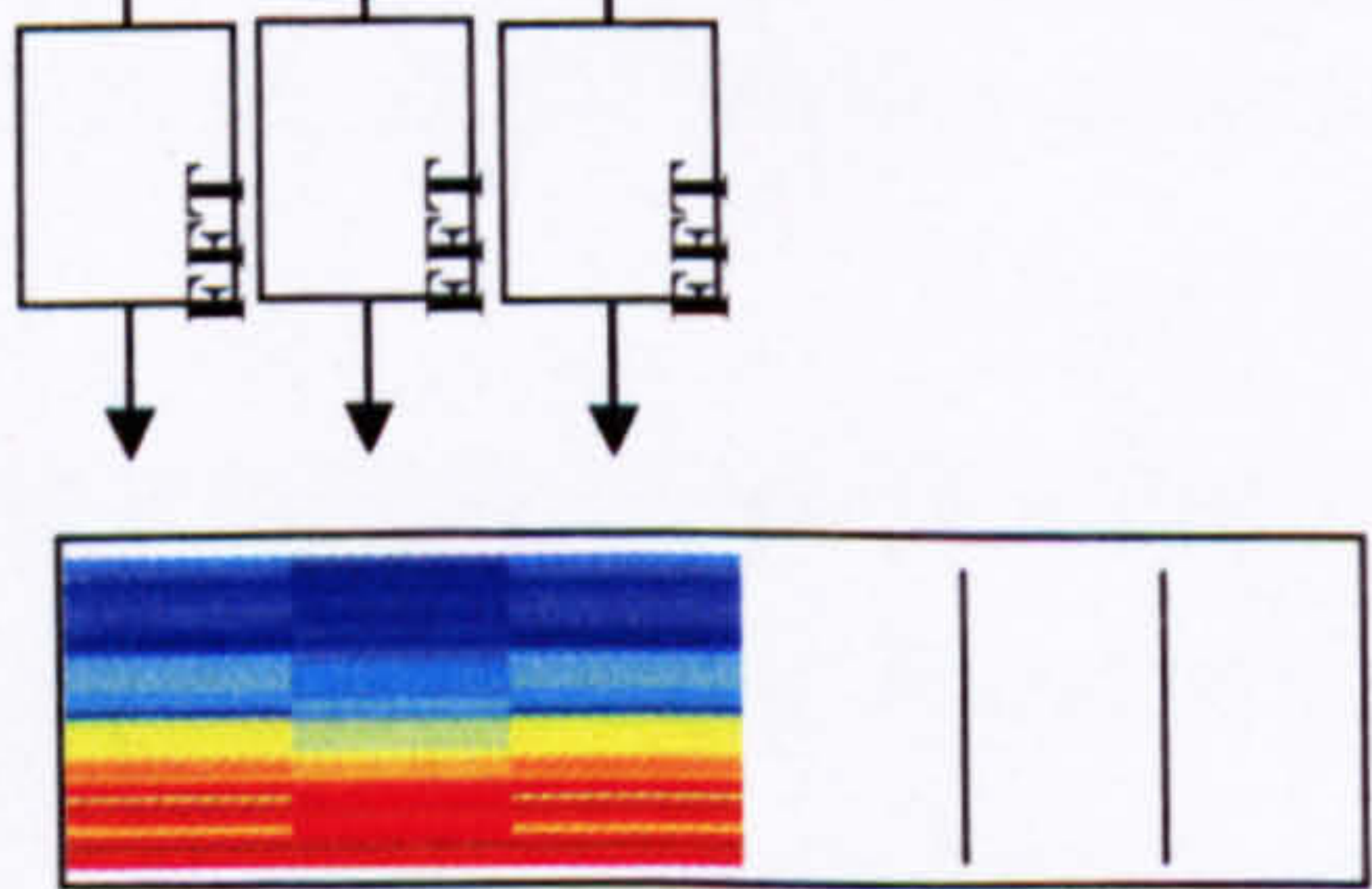
The coherence in time gives the time dependent coherence estimate versus time using a sliding window technique. The information is displayed as an image where the colourmap takes values from one to the maximum coherence value (that will be  $<1$ ) in order to optimise the colourscale representation. Since coherence is sensitive to variance, longer segments than for the spectrogram are required in order to decrease it. As a result of the longer segments, the time resolution is usually not very good.

In the same way phase can be plotted in time in order to derive the time dependent phase estimates versus time. The same principles also apply for the time dependent cumulant density. However cumulant density is a time domain parameter giving the correlation between two signals as a function of time, instead of frequency unlike power, coherence and phase that are frequency domain parameters. Thus the produced image will be time versus time rather than frequency versus time.





Estimate calculation for each pooled segment produced



Flexion time dependent estimate across subjects and trials

**Fig. 4.3** The figure illustrates the procedure for producing the pooled spectrogram from the move-hold sequence time series data. A sample of an EMG recording for three subjects is represented. The data is firstly divided into equal length disjoint sections. The time corresponding sections for each trial for all subjects are pooled to produce a matrix of elements, representing the length of a period. The pooled periodogram for each of these sections is constructed, and represented as a one dimensional image. A series of individual periodogram estimate images is used to produce the spectral representation of a complete period.



## **4.4 SPECIAL TOPICS.**

Most of the analytical methods used in this thesis are standard statistical analysis techniques already used by other researchers for physiological signal processing (Halliday and Rosenberg 1999). Original features were also introduced in the form of small or more extensive modifications of already existing methods. These methods served the better analysis of data collected in this thesis. However these techniques will hopefully find more general applications. For that reason and in order to help the reader follow the results sections these techniques are going to be presented.

### **4.4.1 Pooled time dependent estimates**

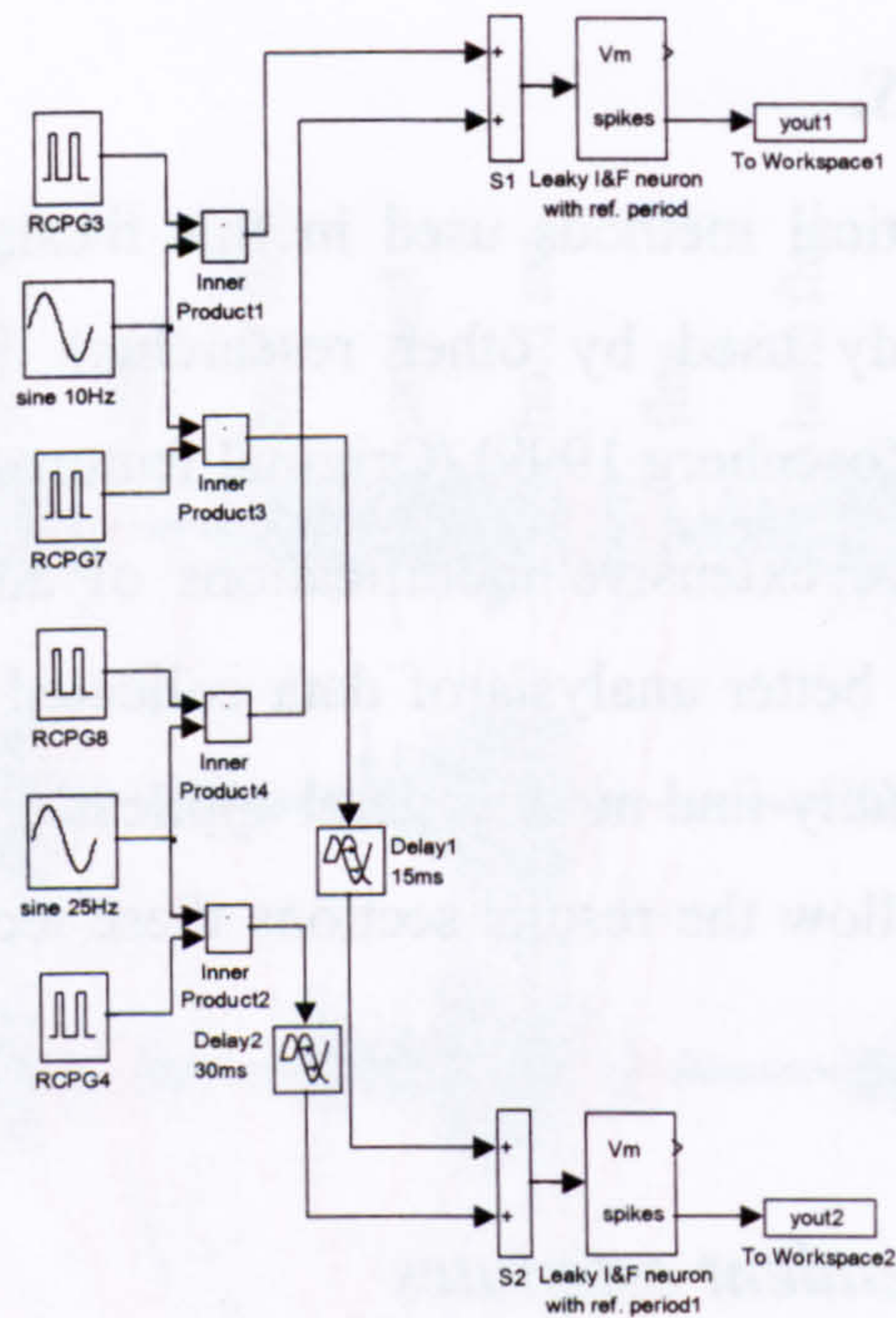
This method extends the spectrogram method and the other time dependent estimates. The aim was to find the time dependent characteristics of frequency estimates in time, across a number of recurring trials for a group of subjects, as a single estimate. This method was applied on the data from the move hold sequence.

The first step requires that the data for the 9 subjects is reorganised. The move hold data record (for a single channel) is composed of 21 trials for each subject. Each cycle contained movement flexion, posture flexion, movement extension, posture extension phases. Each trial contained  $2105 \times 4$  points (2105 ms was the duration of each phase). The point process that set off the audio cues which instructed the subjects to move or hold, are contained in the data record and used as triggering signals. The data were reorganised using as transition points the trigger signals that indicated the start of a phase resulting to a table containing  $21 \times 9$  rows and  $2105 \times 4$  columns.

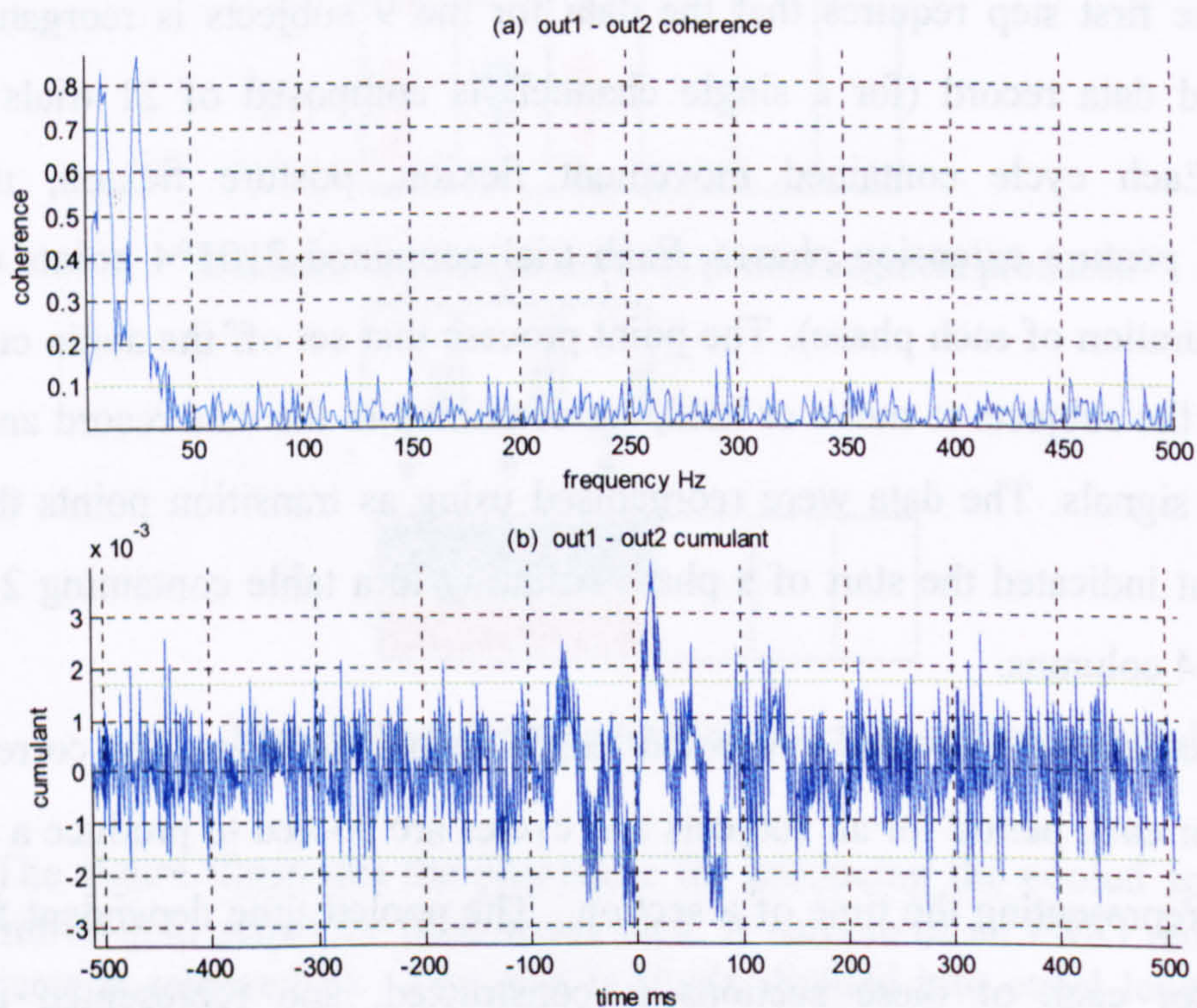
The data were divided into equal length disjoint sections. The corresponding sections for each period for all subjects and cycles are pooled to produce a matrix of elements, representing the time of a section. The pooled time dependent frequency estimate for each of these sections is constructed, and represented as a one dimensional image. A series of individual periodogram estimate images is used to produce the time dependent representation of the estimate in a complete period across subjects and cycles.

Fig. 4.3 shows schematically the realisation of the above described method.





**Fig. 4.4** The figure demonstrates a neuronal network. The inputs are Poisson processes (20 processes of 20ms mean interval each) modulated by two sinusoidal waveforms of 10Hz and 25Hz. Transport delay1 (15ms) and transport delay2 (30ms) were introduced.



**Fig. 4.5** (a) illustrates the coherence between the outputs of the simulation in Fig. 4.4. The coherence peaks at 10 and 25 Hz corresponding to the common oscillator generators can be identified. (b) shows the related cumulant plot where no clear rhythmic activity or delay information can be identified.



#### 4.4.2 Cumulant components

Coherence in different frequency bands may be the result of different physiological mechanisms with different delay characteristics. This results in complicated cumulant plots that are influenced by coupling in more than one frequency bands. The aim is to analyse the cumulant plots into relation to distinct frequency components, and thereby simplify interpretation of how different frequencies contribute to multiplexed physiological signals.

As it was shown earlier the Fourier transform of a segment of length  $T$  from a time series,  $x$ , is written as  $d_x^T(\lambda_j) \approx \sum_{t=0}^{T-1} e^{-i\lambda_j t} x_t$  where the Fourier frequencies are given by  $\lambda_j = 2\pi j/T$ , for  $j = 0, \dots, T/2$ . This defines a range for  $\lambda_j$  of  $(0, \pi)$ , where  $\pi$  corresponds to the Nyquist frequency decomposing the segment of  $x(t)$  into constituent frequency components is performed, highlighting distinct periodic components in the data (Brillinger 1983). The cross-spectrum estimate a time series  $x$  and  $y$  of length  $T$  is defined as  $I_{xy}^T(\lambda_j) = \frac{1}{2\pi T} d_x^T(\lambda_j) \overline{d_y^T(\lambda_j)}$ . The result will be a vector of length  $T/2$  the  $j$  element of which contains the complex product of the decomposed into  $\lambda_j = 2\pi j/T$  constituent frequency component  $x$  and  $y$  time series.

The second order cumulant density function between processes  $x$  and  $y$  is defined as  $q_{xy}(u) = \int_{-\pi}^{\pi} f_{xy}(\lambda) e^{i\lambda u} d\lambda$  which can be estimated by the following expression  $\hat{q}_{xy}(u) = \frac{2\pi}{T} \sum_{|j| \leq T/2b} \hat{f}_{xy}(\lambda_j) e^{i\lambda_j u}$  where  $\lambda_j = 2\pi j/T$  are the Fourier frequencies, and  $b$  is the desired time domain bin width ( $b \geq 1.0$ ), a value of  $b=1.0$  results in a time domain estimate with the same temporal resolution as the sampling rate of the two signals. If for the last expression instead of  $\lambda_j = 2\pi j/T$ , for  $j = 0, \dots, T/2$ ,  $\lambda_j = 2\pi j/T$ , for  $0 < \alpha \dots \beta < T/2$  is used then the cumulant density for the specific range of frequencies  $\alpha \dots \beta$  will be obtained.

In practice the cumulant estimate is the inverse Fourier transform of the cross-spectrum vector. So if instead of the inverse Fourier transform of the whole



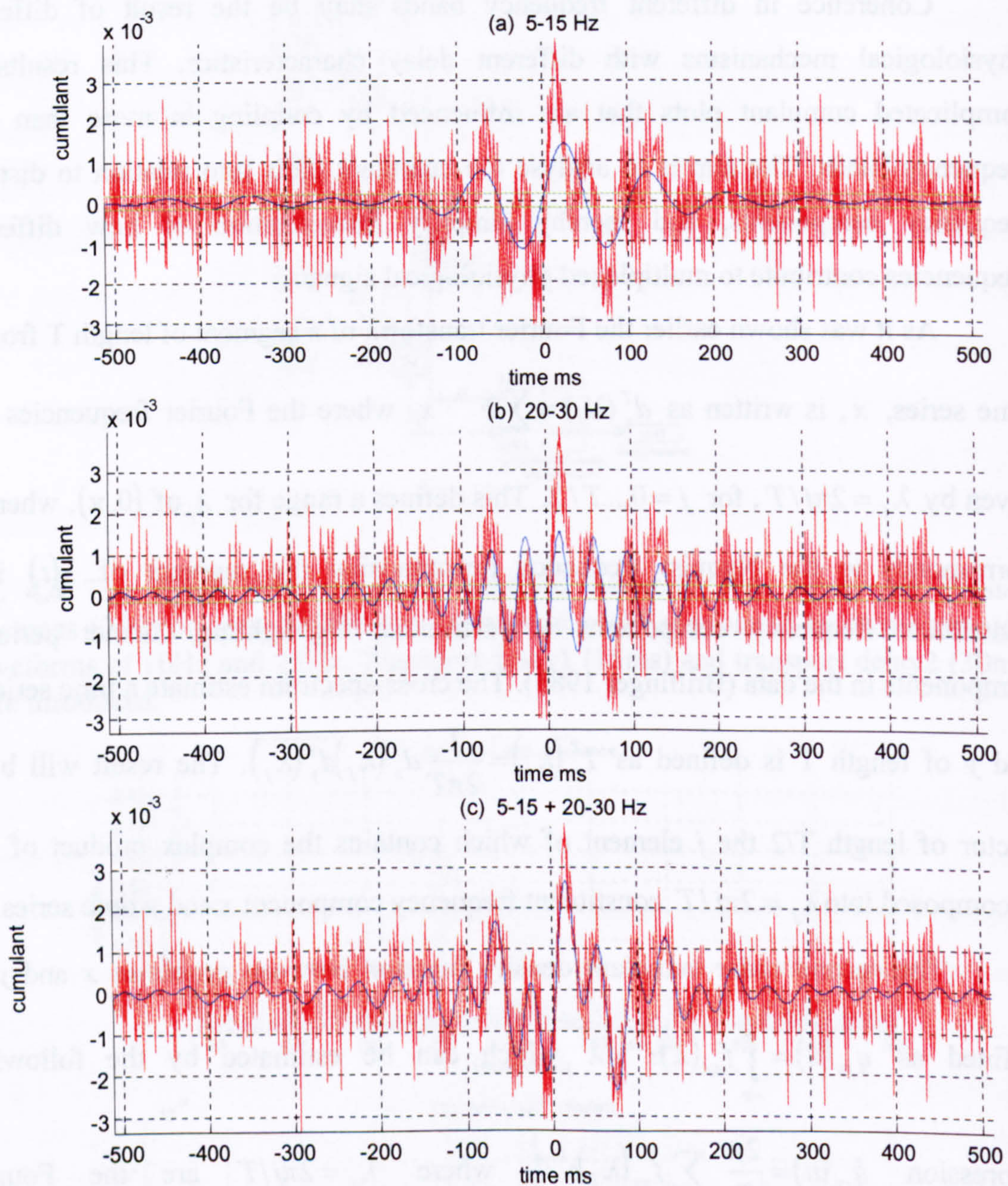


**Fig. 4.6** (a) demonstrates the 5-15Hz and (b) the 20-30Hz cumulant component with their confidence limits overlaying the original cumulant plot (red). Clear rhythmic activity can be identified in both cases. The central features at 15ms and 30ms correspond to the delays introduced in the simulation model in Fig. 4.4. (c) shows the addition of the two components which closely matches the shape of the original plot.



vector, the transform of only a segment is performed by zeroing the remaining elements. By doing this the cumulant density is then estimated only for the specific frequencies.

The practical value of the above method is demonstrated in Fig. 4.4, Fig. 4.5 and Fig. 4.6. Fig. 4.4 shows a simulation of a simple neuronal network where two independent inputs are introduced (according to the simulation cell model that will be presented later in Analytical Methods 4.4.4). Both are Poisson processes that are modulated by sinusoidal signals, the first at 10 Hz and the second one at 25 Hz. Different time delays for each input have also been introduced for the second neuron. The delay for the first input is 25 ms while for the first is 15 ms.

The coherence plot in Fig. 4.5a shows clearly two peaks corresponding to the 10 and 20Hz frequencies. The cumulant plot however (Fig. 4.5b) even though it appears to contain oscillatory features from the combined influence of the two oscillatory inputs, these are not easily interpreted. The cumulant estimate is hardly over the confidence limit indicating common oscillatory input. Furthermore no information on the delays is identifiable.

In Fig. 4.6 two cumulant components can be seen, one from 8-12Hz (Fig. 4.6a) and the second one 23-27 Hz (Fig. 4.6b). The oscillatory shape indicating the common input frequency can be seen. Figure Fig. 4.6a distance between main peak and side peaks indicates 10Hz while Fig. 4.6b shows 25Hz. The cumulant features are clearly statistically significant for both plots. The distance of the central peak-feature from zero time for each plot also indicates the delay for the corresponding input. The 5-15 Hz plot delay is 15 ms and the 20-30 gives 30ms delay; extremely close to the actual model values.

### ***4.4.3 Phase estimate of out of phase synchronised signals***

Phase estimate is a useful tool on its own and in combination with coherence and cumulant estimates. The most important information that it provided was delay between signals. The theoretical model for the interpretation of phase was described earlier. During the analysis of the experimental data it was noticed that phase calculation methodology did not behave well when there was out of phase synchronisation between rectified EMG signals (usually indicated by a negative



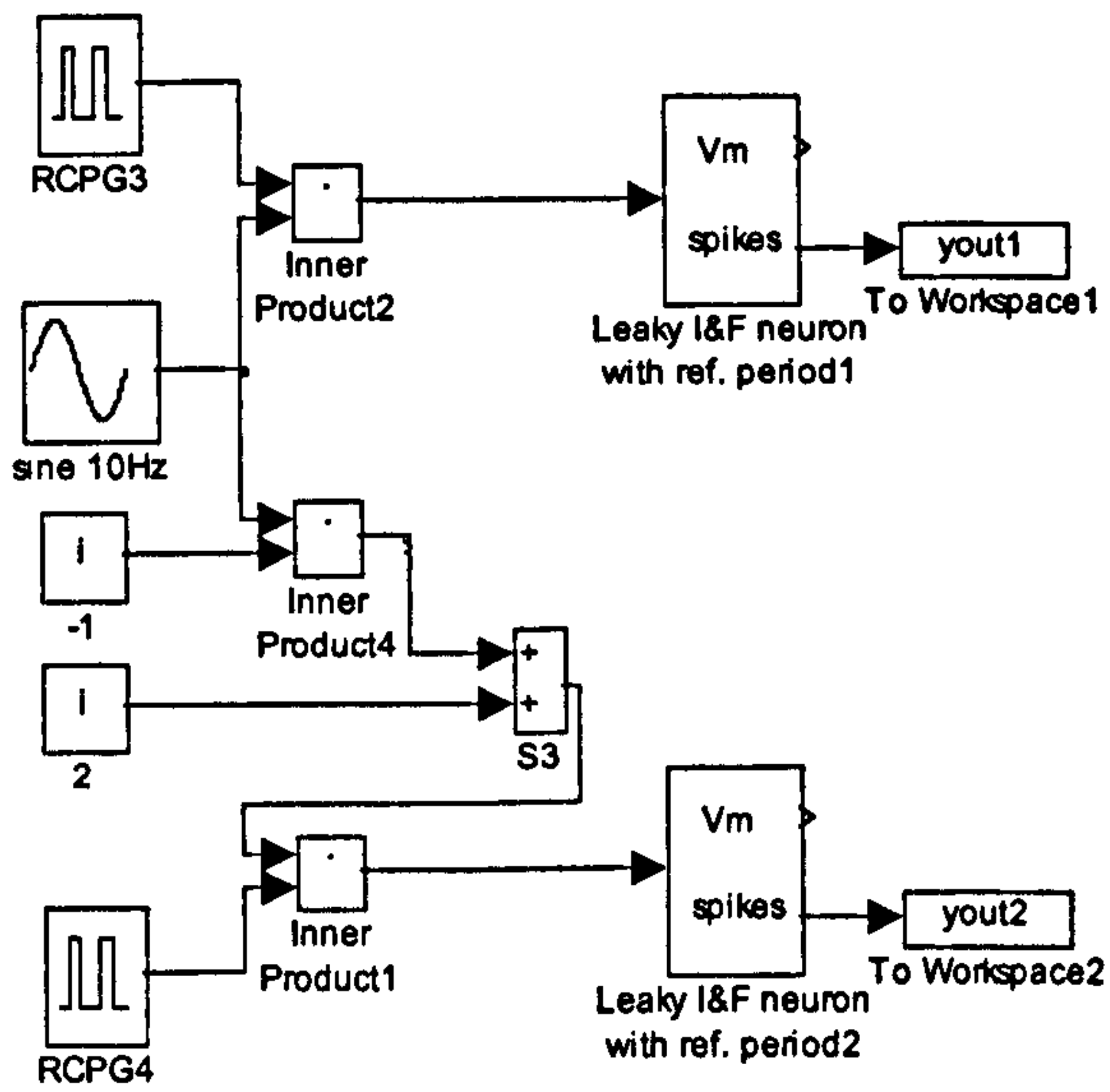


**Fig. 4.7** The figure demonstrates a neuronal network simulation model. The inputs are two Poisson processes (20 processes of 20 ms mean interval each) modulated by the same sinusoidal waveform of 10 Hz. The first Poisson process is modulated by the raw oscillatory waveform with the second modulated by the inverted oscillatory input. This results in an out of phase synchronisation demonstrated in Fig. 4.8



trough feature and oscillatory cumulant features). The phase was inconsistent with continuous over  $\pi$  jumps, and could not be interpreted with the model described earlier.

The solution that was given was the inversion of one of the two signals. In this way the out of phase synchronisation was converted to in phase synchronisation. Logically the delay does not change by the inversion of one of the two signals; only the in or out of phase nature of synchronisation changes. This can be explained by the fact that the cross-spectrum of  $x$  and  $y$  time series is the same as for  $x$  and  $-y$ . The phase however is affected by the signs of the real and imaginary parts of  $\hat{f}_{xy}(\lambda)$  which determine in which quadrant the arctangent falls. This resulted to a different phase estimate, which can be interpreted and derive the delay.

In order to support the above methodology, data from a simulation study will be analysed according to the simulation cell model that will be presented later in this chapter in 4.4.4. Fig. 4.7 demonstrates a simulation neuronal network where two neurons receive two independent Poisson processes. The first process is modulated by a sinusoidal signal and the second by the inverted sinusoidal signal used to modulate the first input. In this way we achieved out of phase synchronisation. This is obvious by the oscillatory cumulant shape and particularly the prominent trough in time zero (Fig. 4.8a). By introducing a delay for the second input the trough moves accordingly. Its displacement indicates the introduced delay. The phase presented in Fig. 4.8 has a form difficult to interpret as mentioned earlier.

Producing the same estimates after the inversion of the second output the differences are obvious. The cumulant plot in Fig. 4.8b shows in phase synchronisation. The cumulant derived delay has not changed. Most importantly the phase estimate is more comprehensive. By calculating the phase (Fig. 4.8d) using, it closely matches the actual delay introduced in the simulation model.

#### ***4.4.4 Simulation cell model***

In this section the simplified cell models are going to be presented and in particular integrate and fire neurons and Poisson spike processes. These models allowed the construction of simple neuronal models and examine the effect of different inputs, oscillatory and non oscillatory in the frequency characteristics of the



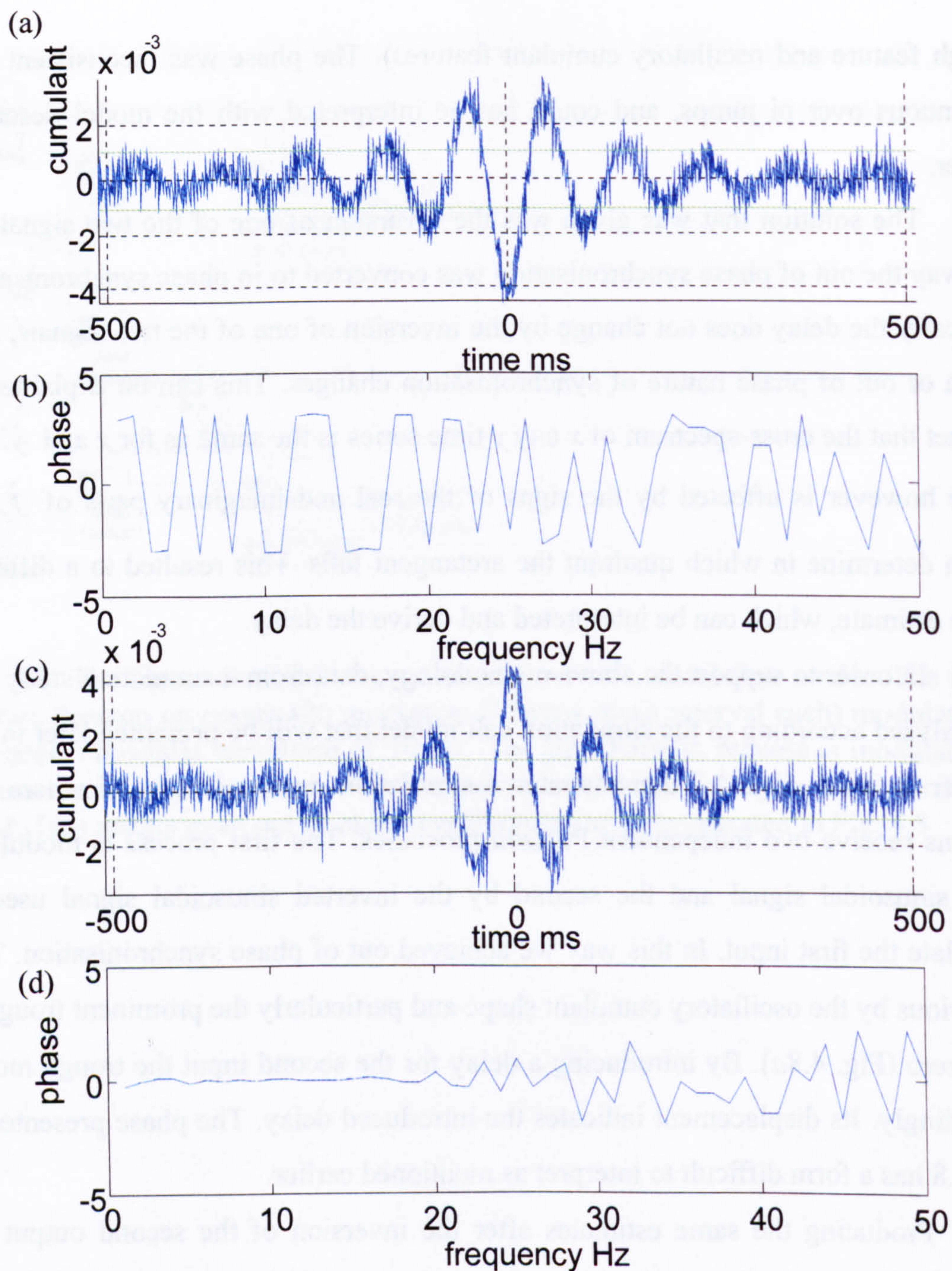


**Fig. 4.8** The cumulant plot in (a) reveals out of phase synchronisation for the outputs of the neuronal network in Fig. 4.7 indicated by the central trough. The corresponding phase plot (b) can not be interpreted according to the theoretical model presented in 4.2.3. However with the inversion of the second signal, the synchronisation becomes in phase as is indicated by the central peak in the cumulant plot (c). The phase (d) has a more regular form and can be used for the calculation of the phase which for this case is close to zero since no delay has been introduced in the simulation model.



outputs. The models do not attempt to resemble in function any biophysical properties of specific neurons, but simplified general properties of nerve cells, such as refractoriness, spike train variability or bursting. The short description of the models will follow. The models used are coded in MATLAB and SIMULINK and are freely available (Koch and Segev 1998).

#### ***4.4.4.1 Leaky Integrate and fire neuron with refractory period***

The “integrate and fire neuron” is a simple model that assumes that the neuron integrates its inputs and generates a spike when a fixed voltage threshold is reached. A more realistic behaviour is obtained by the introduction of a leak term in the dynamics of the subthreshold membrane voltage:

$$C_m \frac{dV_m}{dt} = I(t) - \frac{V_m}{R_m}, \quad \text{Eq. 4.23}$$

where  $I(t)$  is the input current, integrated to yield the membrane voltage  $V_m(t)$ . The constant  $C_m$  represents the capacity of the model cell. The leak term  $\frac{V_m}{R_m}$  is characterized by the resistance to current flowing out of the cell,  $R_m$ . A spike is generated each time that  $V_m(t)$  reaches the threshold  $V_{th}$  and the membrane is reset to zero immediately after the spike (Koch and Segev 1998).

In real neurons, the dynamic firing range is limited because of the biophysical properties of the neurons and more specifically the ionic membrane conductances responsible for the action potential generation. Sodium channels need to recover from inactivation between two action potentials and there may be an after hyperpolarisation. This feature can be implemented in simple terms by shunting off all input current for a fixed time after spike generation (Koch and Segev 1998).

#### ***4.4.4.2 Poisson processes***

While some neurons fire regularly many neurons show irregular firing in response to injected subthreshold currents. A simulated irregular response to constant current often used is called Poisson spike train. The resulting spike train is highly



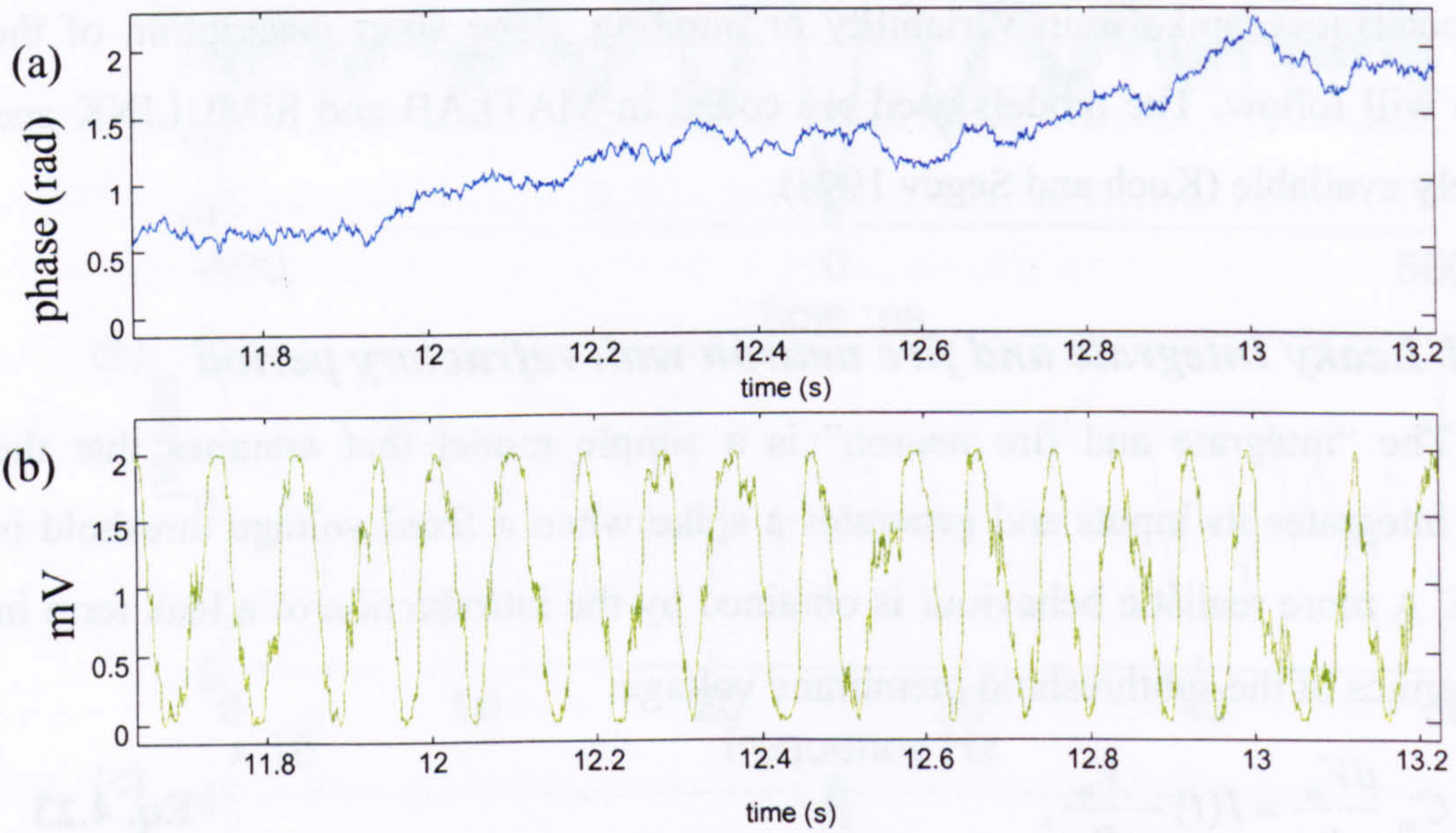


**Fig. 4.9** The figure demonstrates the random walk of the phase shift and the resulting generated signal. The Gaussian distribution used for the generation of the random phase shift step is 0.03 with mean 0. The base frequency of the generated is 10 Hz.

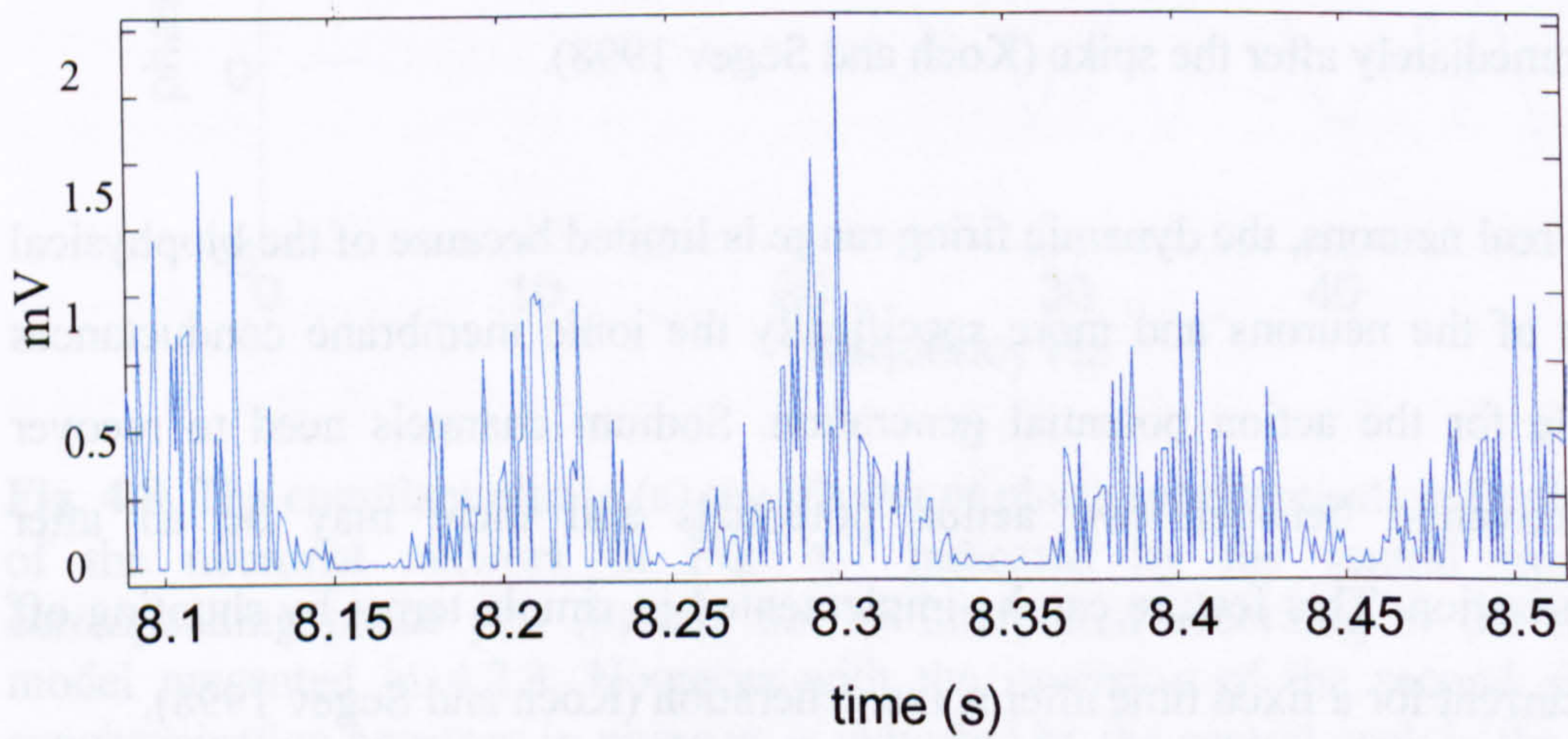


**Fig. 4.10** The figure demonstrates a Poisson process modulated by a variable sinusoidal waveform of 10 Hz.



variable because every spike is generated randomly, independently of other spikes. The interspike interval distribution is exponential with probability density

$$p(1/\bar{t})e^{-t/\bar{t}} \quad \text{Eq. 4.24}$$

where  $\bar{t}$  is the mean interspike interval (Koch and Segev 1998).

#### 4.4.4.3 Variable sinusoidal waveform.

Often in simulation of physiological neuronal networks, there is the need for an oscillatory input. Oscillations are intrinsic in physiological systems. However their nature differs significantly from a generated sinusoidal waveform, which is often used. These waveforms do not resemble the attributes of physiological signals since they have fixed frequency, phase and amplitude. The variable sinusoidal waveforms were used as inputs, instead of clear sinusoidal inputs in neuronal model simulations presented in 4.4.2 and 4.4.3 in order to obtain simulation results that will be closer to the physiological equivalent systems.

The sinusoidal waveform generator used in the present study had a variable phase, in order to simulate better the wider distribution in frequency content of physiological signals. The phase followed a random walk with step Gaussian distribution with zero mean and a standard deviation of 0.3 . Fig. 4.8 a shows an instance of the phase. Fig. 4.9b shows the resulting modulated sinusoidal waveform.

In pseudo code every 1ms step of the simulation procedure will be:

$$p(t) = p(t - 1) + \text{normrnd}(\mu, \sigma); \quad \text{Eq. 4.25}$$

$$x(t) = a * \sin(2 * \pi * fs * t + p(t)); \quad \text{Eq. 4.26}$$

where  $t$  is the time step,  $p$  is the phase,  $fs$  is the central sinus frequency and *normrand* generates normal numbers with mean  $\mu$  and standard deviation  $\sigma$ .

#### 4.4.5 Construction of bipolar EEG montages

Multichannel recordings are used to determine the distribution of potential changes over a large area of the scalp. The use of differential amplifiers makes necessary the use of multiple differential electrode recording combinations to arrive at an estimate of the activity a single electrode site. A montage consists of a combination of derivations (pairs of electrode inputs 1 and 2 of a channel of a



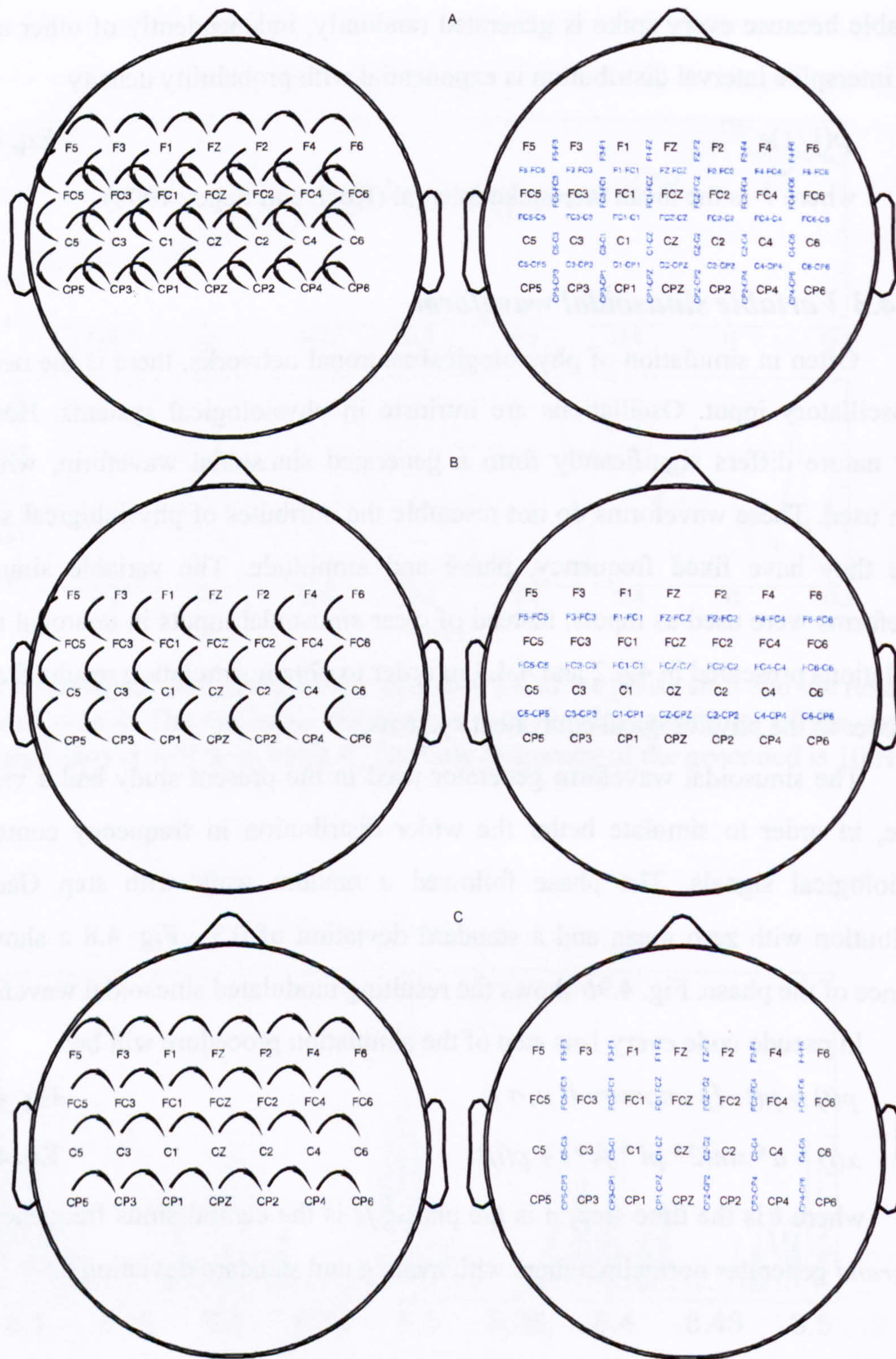


**Fig. 4.11** The three different bipolar montages used; the combined vertical-horizontal (A), the vertical montage (B) and the horizontal montage (C). The vertical montage consisted of pairs of adjacent electrodes on the vertical axis (anterior-posterior), while the horizontal montage consisted of adjacent electrodes on the horizontal axis (contralateral to ipsilateral) looking down at the top of the head. The combined montage integrates both vertical and horizontal montages.



differential amplifier). Different montages are in fact spatial filters with different characteristics.

Monopolar montage consists of a series of derivations where the input 2 for all 28 channels was the joint ear reference. Monopolar (common electrode reference) montages contain widespread potentials that have similar amplitudes and phases.

The bipolar montages consist of adjacent pairs of the 28 electrodes used in the experimental setup. Since the EEG was recorded as monopolar EEG with common joint ear reference, the bipolar montages were used by subtracting the corresponding pair of monopolar channels:

$$Bip(A,B)=V_A-V_B=V_A-V_B-V_R+V_R=(V_A-V_R)-(V_B-V_R)=Mon(A)-Mon(B) \quad \text{Eq.4.27}$$

where  $V_A$ ,  $V_B$  and  $V_R$  are the potentials for electrodes A, B and Reference respectively.

The bipolar montages act as spatial filters and remove widespread potentials with similar amplitudes and phases from the recordings. Bipolar electrodes are considered the best for analysing low to medium amplitude waveforms that are highly localised (Fish 2002).

Three different bipolar montages were used; the combined vertical-horizontal (Fig. 4.11A), the vertical montage (Fig. 4.11B) and the horizontal montage (Fig. 4.11C). The vertical montage consisted of pairs of adjacent electrodes on the vertical axis (anterior to posterior), while the horizontal montage consisted of adjacent electrodes on the horizontal axis (contralateral to ipsilateral) looking down at the top of the head. The combined montage integrates both vertical and horizontal montages.

#### ***4.4.6 Topographic maps of cortical and corticomuscular activity***

The “topoplot” function from “EEGLAB” Matlab toolbox (<http://sccn.ucsd.edu/eeglab/>) was used to visualise scalp data. A topographic map of a scalp data field in a 2-D circular view (looking down at the top of the head) was plotted using interpolation on a fine cartesian grid (Delorme and Makeig 2004). The scalp data were monopolar and bipolar EEG power, EEG\EMG corticomuscular coherence and EEG\EMG corticomuscular coupling.



## 4.5 ANALYTICAL METHODS SOURCES OF ERROR

**Fourier transform assumption of stationarity.** The finite Fourier transform assumes the examined signals are stationary (signals have constant frequency content over time). EEG and EMG signals are non-stationary which means that their frequency content changes over time. Using time-frequency techniques the signal is divided into small enough segments where the signal contained in these segments can be assumed to be stationary. The violation of this assumption is potential source of error. This errors can be quantitatively evaluated in comparison with other methods that are known to perform well with non-stationary signals like Wavelet transform methods. This was not within the scope of this thesis.

**Fourier transform assumption of linearity.** The methods used in this thesis follow an approach of spectral estimation procedures based on the finite Fourier transform, a set of frequency domain measures for characterising linear interactions between these signals. However the behaviour of neurophysiological systems is more complex and often non linear interactions may be present which can not adequately be described by linear models. The error introduced could be evaluated with methods that are known to perform well with non linear interactions, like for example the Hilbert transform. However this was not within the scope of this thesis.

**Pooling of data.** Pooled estimates (Amjad et al. 1997) give results calculated over available data from all subjects and trials, giving a summarised population result rather than results for trials and subjects separately. Pooling introduces a form of error since it is recognised that significant intersubject variability in corticomuscular coherence has been observed (Kilner et al. 1999), thus presentation of summarised data sets ignores individual differences. Within the framework of this thesis, the primary aim was to examine the typical population movement related behaviour that can be considered significant for the entire population group studied.

**Fourier transform time-frequency resolution.** With TFT one cannot know the exact time-frequency representation of a signal, i.e., one cannot know what



spectral components exist at what instances of times. What one can know are the time intervals in which certain band of frequencies exist, which is a resolution problem. This fact whose roots go back to what is known as the Heisenberg Uncertainty Principle, originally applied to the momentum and location of moving particles, can be applied to time-frequency information of a signal.

A window of infinite length, as with FT, gives perfect frequency resolution, but no time information. In order to obtain the stationarity, a short enough window is needed in which the signal is stationary. The narrower the window is, the better the time resolution, and better the assumption of stationarity, but poorer the frequency resolution:

Therefore narrow window results in good time resolution but poor frequency resolution while wide window results in good frequency resolution but poor time resolution.

*Non windowed FFT segments.* One problem with FFT based spectral estimates is that the duration of the signals is finite. Applying the FFT method to finite-duration sequences can produce inadequate results because of "spectral leakage," due primarily to the periodic extension assumption underlying DFT.

The effect occurs when the finite duration of the signal does not result in a sequence that contains a whole number of periods. In FFT analysis, "windows" are frequency weighting functions applied to the time domain data to reduce the spectral leakage associated with finite-duration time signals. Windows are smoothing functions that peak in the middle frequencies and decrease to zero at the edges, thus reducing the effects of the discontinuities as a result of finite duration. Non windowed segments have been used for the analysis in the present thesis. The reason is the calculation of the confidence intervals assumes non-windowed segments. As a result spectral leakage can be considered as a source of error. The spectrum for example will not be the actual spectrum of the original signal, but will be a smeared version with energy at one frequency leaked out into all the other frequencies. The result is more broad spectral features.



***Harmonics.*** Features in the frequency domain estimates can be enhanced or be the result of harmonics belonging to other neurogenic frequency features or harmonics of environmental interference. Therefore harmonics can introduce an error since spectral and coherence features may exceed the confidence intervals without statistically significant synchronisation. However this should have not affect the considerably since most features were very strong and appeared to be independent in the frequency as well as in the spatial domain.